



**Universität für Bodenkultur Wien**  
University of Natural Resources  
and Life Sciences, Vienna

# Doctoral Dissertation

## Process and material features influencing piezoresistive wood adhesives

submitted by

Dipl.-Ing. (FH) Christoph WINKLER, M.Sc.

in partial fulfilment of the requirements for the academic degree

**Doktor der Bodenkultur (Dr.nat.techn.)**

Vienna, October 2021

Supervisor:

Univ.-Prof. i.R. Dipl.-Ing. Dr.nat.techn. Dr.h.c. Alfred Teischinger  
Institute of Wood Technology and Renewable Materials  
Department of Material Sciences and Process Engineering (MAP)

# **Process and material features influencing piezoresistive wood adhesives**

## **Einfluss von Prozesstechnik und Materialeigenschaften auf piezoresistive Holzklebstoffe**

DISSERTATION

for obtaining a doctoral degree

at the University of Natural Resources and Life Sciences Vienna  
Institute of Wood Technology and Renewable Materials

Submitted by  
Dipl.-Ing. (FH) Christoph WINKLER, M.Sc.

Vienna, October 2021

Supervisor / Advisors:  
Univ.-Prof. i.R. Dipl.-Ing. Dr.nat.techn. Dr.h.c. Alfred Teischinger  
Univ.-Prof. Dipl.-Ing. Dr. Johannes Konnerth  
Prof. Dr.-Ing. Ulrich Schwarz

© Copyright by Christoph Winkler

All Rights Reserved

No part of this volume may be reproduced, stored in a retrieval system or transmitted in any form or by any means, electronic, mechanical, photocopying, recording or otherwise, without the prior written permission of the publishers.

## AFFIDAVIT

I hereby declare that I have authored this dissertation independently, and that I have not used any assistance other than that which is permitted. The work contained herein is my own except where explicitly stated otherwise. All ideas taken in wording or in basic content from unpublished sources or from published literature are duly identified and cited, and the precise references included. Any contribution from colleagues is explicitly stated in the authorship statement of the published papers.

I further declare that this dissertation has not been submitted, in whole or in part, in the same or a similar form, to any other educational institution as part of the requirements for an academic degree.

I hereby confirm that I am familiar with the standards of Scientific Integrity and with the guidelines of Good Scientific Practice, and that this work fully complies with these standards and guidelines.

Berlin, 15.10.2021

Christoph WINKLER (*manu propria*)



*'I never learned from a man who agreed with me.'*  
– Robert A. Heinlein –

*... which goes for woman equally  
This thesis is dedicated  
to my wife Julianne*

## SUMMARY

The use of piezoresistive adhesive bond lines in timber construction offers various advantages over classic sensors and is intended as an option to monitor structural timber components during operation and to detect damage due to changes in the conditions of use or extreme climatic events at an early stage. While the basic feasibility of the concept of piezoresistive polymers on wood bonds could already be shown experimentally in preliminary laboratory tests, the measurements showed low sensitivities and unknown deviations from the expected result. As scientific studies on the relevant influencing variables due to the materials and process parameters used are partially lacking, the production of piezoresistive wood bonds has so far been based on subjective experience.

This thesis systematically deals, for the first time, with different material- and process-specific influencing variables on the piezoresistive properties of piezoresistive wood bonds and presents the currently available fundamental theoretical inputs from other development fields. The aim was to provide a basis for understanding piezoresistive wood adhesives and thereby a foundation for future research in addition to creating development efforts.

For this purpose, electrically conductive adhesives based on polyurethane polymers and various carbon allotropes were produced, and their adhesive strengths and electrical and piezoresistive properties were initially investigated in an experimental design. The influencing factors adhesive, filler type and concentration, dispersion technique, adhesive application technique, glue spread, pressure, press time and press temperature during manufacture as well as thermal postcuring of the bond were analysed. The results showed that increased piezoresistive sensitivity can only be achieved with low filler concentrations and that low press temperatures favour this. The reduction of high instabilities of the piezoresistive reaction (electrical drift, low reproducibility and increased base resistance after loading) which accompanied high sensitivities could be achieved through higher filler concentrations, increased glue spread, longer pressing times and thermal postcuring. The results also show that, despite high filler concentrations, the minimum requirement of 10 MPa when testing the tensile shear strength according to EN 302-1 (A1) can be achieved.

In a further step, piezoresistive wood bonds were investigated using impedance spectroscopy as an alternative to resistance measurement under direct current. It could be shown that, depending on the frequency, a significantly increased signal-to-noise ratio compared to classical resistance measurements with the help of impedance spectroscopy was possible.

Finally, various piezoresistive adhesive connections were examined under transverse tension, shear, pressure and tension in scaled test specimens, including the combination in several two-meter-long glulam beams. A material-based model could be derived from the different high sensitivities and the direction of the change in resistance, which

enables both a qualitative estimation of the relative sensitivity and can explain inverse piezoresistivity in anisotropic materials.

**Keywords:** *carbon black, engineered wood, monitoring, piezoresistivity, polyurethane prepolymer*

## ZUSAMMENFASSUNG

Die Nutzung von piezoresistiven Klebschichten im Holzbau bietet verschiedene Vorteile gegenüber klassischen Sensoren und ist als Option gedacht, strukturelle Holzbauteile im Betrieb zu überwachen und Schäden durch Änderung der Nutzungsbedingungen oder klimatischer Extremereignisse frühzeitig zu erkennen. Während eine grundsätzliche Umsetzbarkeit des Konzeptes von piezoresistiven Polymeren auf Holzklebungen in vereinfachten Laborversuchen schon experimentell gezeigt werden konnte, wiesen die Messungen niedrige Sensitivitäten und unbekannte Abweichungen vom erwarteten Ergebnis auf. Wissenschaftliche Untersuchungen zu den relevanten Einflussgrößen durch eingesetzte Materialien sowie Prozessparameter fehlten vollständig und die Herstellung der piezoresistiven Holzklebungen basiert bislang auf subjektiven Erfahrungen.

Die vorgelegte Thesis befasst sich erstmalig systematisch mit verschiedenen material- und prozessspezifischen Einflussgrößen auf die piezoresistiven Eigenschaften und legt die aktuell verfügbaren theoretischen Grundlagen aus anderen Entwicklungsfeldern dar. Ziel war es, eine Grundlage für das Verständnis von piezoresistiven Holzklebstoffen zu schaffen und die Basis für zukünftige Forschungs- und Entwicklungsbemühungen zu schaffen.

Dazu wurden elektrisch leitfähige Klebstoffe auf Basis von Polyurethan-Polymeren und verschiedenen Kohlenstoffallotropen hergestellt und die Klebefestigkeiten sowie die elektrischen und piezoresistiven Eigenschaften zunächst in einem experimentellen Design untersucht. Analysiert wurden die Einflussfaktoren Klebstoff, Füllstoffart und -konzentration, Dispersionstechnik, Klebstoffauftragstechnik und -menge, Pressdruck, -zeit und -temperatur bei der Herstellung sowie eine thermische Nachbehandlung der Klebung. Die Ergebnisse zeigten, dass eine erhöhte piezoresistive Sensitivität nur durch geringe Füllstoffkonzentrationen erreicht werden kann und niedrige Presstemperaturen diese begünstigen. Die bei hohen Sensitivitäten gleichzeitig auftretenden hohen Instabilitäten der piezoresistiven Reaktion (elektrischen Drift, geringe Reproduzierbarkeit und erhöhter Basiswiderstand nach Belastung) konnten durch höhere Füllstoffkonzentrationen, erhöhte Klebstoffauftragsmengen, längere Presszeiten und eine thermische Nachbehandlung gesenkt werden. Die Ergebnisse zeigen weiterhin, dass trotz hoher Füllstoffkonzentrationen die Mindestanforderung von 10 MPa bei Prüfung der Zugscherfestigkeit nach EN 302-1 (A1) erreicht werden kann.

In einem weiteren Schritt wurden piezoresistive Holzklebungen alternativ zur Widerstandsmessung unter Gleichspannung mittels Impedanzspektroskopie untersucht. Es konnte gezeigt werden, dass frequenzabhängig ein wesentlich erhöhtes Signal-Rausch-Verhältnis gegenüber klassischen Widerstandsmessungen mit Hilfe der Impedanzspektroskopie möglich war.

Abschließend wurden verschiedene piezoresistiver Klebeverbindungen unter Querkzug, Schub, Druck und Zug in skalierten Prüfkörpern untersucht, inklusive der Kombination in mehreren zwei Meter langen Brettschichtholzträgern. Aus den unterschiedlich hohen Sensitivitäten und den Richtung der Widerstandsänderung konnte ein materialbasiertes Modell abgeleitet werden, dass sowohl eine qualitative Abschätzung der relativen Sensitivität ermöglicht sowie inverse Piezoresistivität in anisotropen Materialien erklären kann.

**Keywords:** *Leitfähigkeitsruß, Brettschichtholz, Bauwerksüberwachung, Piezoresistivität, Polyurethan-Prepolymer*

## ACKNOWLEDGEMENTS

This dissertation summarises the output of my scientific work in the field of multifunctional wood adhesives at the Eberswalde University for Sustainable Development (HNEE) in cooperation with the University of Natural Resources and Life Sciences, Vienna. This work would not have been possible without discussions and the resulting support and advice of several people, whom I would like to thank at this point.

My special thanks go to my supervisor and my support team. In particular, I would like to thank Univ.-Prof. i.R. Dipl.-Ing. Dr.nat.techn. Dr.h.c. Alfred Teischinger and Prof. Dr.-Ing. Ulrich Schwarz for their confidence in my independent scientific work and their support for my stay and exchange at the University of Natural Resources and Life Sciences in Vienna. Tulln on the Danube and Vienna remain unforgettable for me. Mr Schwarz, without your many years of support since I was studying towards my diploma in Eberswalde and the discussions about the world outside of academic education, I would never have landed at this point! Univ.-Prof. Dipl.-Ing. Dr. Johannes Konnerth was an incredibly valuable source of scientific work and reflection, which often challenged and motivated me. I can count myself lucky to have had you on my support team. Thank you, Johannes!

Of course, this work would not have been possible without the joint work with my research group and other colleagues outside the HNEE and their help and the exchanges with them. Jesco Schäfer, Christopher Jager, Johannes Gibcke, Christian Müller, Michael Günther, Björn Christen and Markus Jahreis — thank you for the discussions, conversations, and the willingness to work towards a common goal, even if some of the paths initially led away from the target.

I would like to thank my colleagues at the Westphalian University of Applied Sciences, Prof. Klaus-Uwe Koch, Ingo Schollmeyer, and Steven Konopka for the joint work in the preparation for and joint work the SmartTimbA research project. Recklinghausen and barbecues simply belong together.

The research project SmartTimbA, from which many of the results in this dissertation were derived and which hopefully will be continued in future, was financially supported by the German Government within the scope of the ‘Nachwachsende Rohstoffe’ program (FNR, BMEL) under Grant 22005018. I would like to take this opportunity to thank Ms. Hermann and Mr. Winkelmann for their support with funding. The successful application for this long-term project was the last ‘spark’ that made my dissertation possible with enriching collaborations and without financial concerns.

I would like to thank Jowat SE for the countless adhesive samples for the production of the electrically conductive polyurethane prepolymers — both before and during the project.

Finally, I would like to express my deepest thanks to my wife Juliane. I would not have made it without your constant support and encouragement during the intensive work phases.

# TABLE OF CONTENT

<b>1</b>	<b>Introduction .....</b>	<b>1</b>
1.1	Background of the thesis.....	1
1.2	Research questions, hypotheses, and objective .....	3
<b>2</b>	<b>Theoretical background .....</b>	<b>5</b>
2.1	Electrically conductive (wood) adhesives .....	5
2.1.1	Electrically conductive filler networks .....	5
2.1.2	Electrically conductive fillers.....	6
2.1.3	Interactions between fillers and polymers.....	8
2.1.4	Polymeric and (wood) adhesive matrices.....	10
2.2	Piezoresistive polymers .....	12
2.2.1	Piezoresistivity.....	12
2.2.2	Sensor characteristics .....	14
2.3	Manufacturing influences .....	15
2.3.1	Dispersion.....	15
2.3.2	Assembly processing.....	19
2.3.3	Post curing.....	20
2.4	Wood as an adherend .....	21
2.4.1	Wood and engineered wood.....	21
2.4.2	Electrical properties.....	23
2.4.3	Moisture influence.....	25
<b>3</b>	<b>Systematic Approach .....</b>	<b>27</b>
3.1	Systematic approach and overview .....	27
3.2	Applied Methods.....	28
3.2.1	Tensile shear test.....	28
3.2.2	Nanoindentation.....	29
3.2.3	Rheology.....	29
3.2.4	Resistance measurements .....	29
3.2.5	Impedance spectroscopy .....	30
3.2.6	Piezoresistive measurements .....	33
<b>4</b>	<b>Main investigations .....</b>	<b>34</b>
	Corrigenda.....	35
	Paper I .....	37
	Paper II .....	38
	Paper III.....	39
	Paper IV.....	40
	Paper V .....	41
<b>5</b>	<b>Main Findings and Discussion.....</b>	<b>42</b>



5.1	Piezoresistivity without reduction of bond strength.....	42
5.2	Influence of process parameters.....	44
5.3	Further improvement of piezoresistive properties .....	50
5.4	Improvements by impedance spectroscopy.....	52
5.5	Distinguishing stress by piezoresistive reactions.....	53
<b>6</b>	<b>Conclusion.....</b>	<b>55</b>
<b>7</b>	<b>Potential for future research and development.....</b>	<b>57</b>
	<b>References .....</b>	<b>61</b>
	<b>Additional Publications and other Contributions .....</b>	<b>79</b>
	<b>Nomenclature .....</b>	<b>82</b>
	<b>List of Tables.....</b>	<b>83</b>
	<b>List of Figures .....</b>	<b>84</b>

# 1 INTRODUCTION

The use of timber in building and civil engineering applications has a long history. Especially the development of reliable engineered timber from glued wood products (for example glued laminated timber (GLT) and cross-laminated timber (CLT)) has accelerated the development of timber constructions, starting with the first GLT patented by Otto Hetzer in 1906 [1]. The bonding of several wood lamellas to a finished product decouples the wood product from the dimensions of a tree and offers freedom of design and implementation [2]. Additionally, the use of engineered wood products such as GLT and CLT decrease the natural variability of their mechanical properties and enhances the predictability of their performance. This is due to a homogenisation effect resulting from adhesive bonding and grading single timber pieces to a bigger member [3], which, for example, leads to higher characteristic strength values of engineered timber compared to solid wood and brings the naturally grown material closer to man-made materials such as concrete or steel.

Timber buildings can reach lifespans of more than a hundred years, and they seldom need to be demolished due to degradation of their main structure [4]. However, despite these positive aspects, timber constructions are still underrepresented among new constructions. The primary reasons for the underrepresented use of timber constructions are:

- a negative perception of timber due to decay, form instability, and sound transmission as well as the risk-averse planning of developers [5],
- damaged trust resulting from sensational construction collapses as seen at Bad Reichenhall [6],
- the need for professional knowledge and skill in timber engineering, which is not necessarily beneficial for the professional status of the engineer or architect [5] and require new concepts of architectural and engineering designs [7],
- a higher risk potential compared to other materials, resulting for example in higher partial safety factor  $\gamma_M$  and lower modification factors  $k_{mod}$  compared to man-made construction materials such as steel [8], even with the appropriate wood protection.

## 1.1 Background of the thesis

Many of the concerns regarding timber construction are related to the moisture, temperature, and time-dependent changes of the material properties of timber. Timber constructions are also more vulnerable to human error in designing and operating a building. For example, the change in indoor climate due to re-utilization can result in structural damage through cracks and delamination due to uneven shrinkage [9].

Consequently, regular inspections of timber constructions are used to evaluate the risk potential [10], leading to higher service costs compared to other construction materials. Maintenance is an essential requirement for durable and long-lasting buildings and can be supported by monitoring [4,11]. The reason for this is that monitoring – over assessment – offers time-dependent information, including the strain rate, load duration, and load history, which cumulatively affects the structural load resistance of timber elements [12].

Continuous structural health monitoring (SHM) is thus more beneficial for timber than for other construction materials. As a consequence, SHM can support and extend the applicability of engineered timber, for example, in multi-story buildings and bridges. SHM has been investigated by different research groups and projects [13–17], especially regarding the wood moisture content (WMC). Reports and reviews on research activities with nanosized materials for timber assessment and monitoring are also available, which support the need for monitoring techniques [18,19].

On the other hand, SHM in timber engineering lacks efficiency. For effective monitoring, a large number of sensors are necessary to measure the wood moisture, temperature, and strain on several spots. Furthermore, the integration of sensors into timber structures is expensive due to the need for specialised staff or a high degree of automatization.

Accordingly, one option to support the use of monitoring in timber engineering is to reduce the manufacturing costs of engineered timber with integrated sensors [19]. Conductive adhesives that are produced using electrically conductive fillers offer new possibilities in this regard, as they are not only used as a coupling medium for wood moisture measurements [20] but can also exhibit piezoresistivity like other electrically conductive polymers [21]. Additionally, adhesive bond lines are not separated from the material as other discrete sensors are, as they are embedded into the structure on the level of a composite material. Finally, the use of piezoresistive adhesives in timber construction would offer the possibility to also assess and monitor the deformation of a timber structure. According to the overview of Palma and Steiger [17], this would open a digital possibility for in-situ deformation measurements.

Despite the intense research on the use of the piezoresistive properties of electrically conductive filled polymers, applications are generally based on well-defined films or bulks of nanocomposite (polymers with integrated nanofillers) and smooth surfaces on which the polymeric sensor is applied [22–31].

The transferal of this functional concept of additional piezoresistive properties to wood adhesives and engineered timber is not yet well investigated. Several screening studies by the author have shown a measurable resistance change in laboratory-scale experiments with changes in stress/strain (piezoresistive reaction), moisture, and fatigue [32–36]. Nonetheless, the resulting piezoresistive reaction was not fully predictable. Electrically conductive adhesives with piezoresistive behaviour that are applied to

engineered wood either showed several unexpected piezoresistive reactions — or none at all. The theoretical background from other fields indicated the potential impact of material selection (wood, adhesive, or electrically conductive filler) and the production parameters of the liquid adhesive in addition to the manufacturing of the piezoresistive composite.

So far, these findings from other nanocomposites and influencing process parameters are not easily applied to electrically conductive wood adhesives for engineered timber, and their use often results in different possible outcomes. For example, the increase of clamping pressure can result in thinner bond lines (higher resistance due to less cross-section), but also less porosity of foaming adhesives resulting from lower resistance due to fewer pores in the adhesive.

## **1.2 Research questions, hypotheses, and objective**

Despite the contradictory theoretical results to date, it is assumed that a better understanding of the interactions in processing electrically conductive wood adhesives and the influences of the adherends can enhance the predictability of the manufactured piezoresistive bond line of engineered wood.

The following research questions (RQ) were derived from the theoretical background:

- RQ1: Does the integration of electrically conductive nanofillers decrease the bond strength of wood bonds (section 2.1.3)?
- RQ2: What are the main influencing factors in the manufacturing process of piezoresistive wood bonds regarding the electrical resistance and piezoresistivity of electrically conductive wood bonds (section 2.3)?
- RQ3: Which further options after manufacturing exist to increase the piezoresistive sensitivity (sections 2.2.2, 2.3.3)?
- RQ4: Can additional information of resistance measurements under alternating current improve the usability of piezoresistive wood bonds (section 3.2.5)?
- RQ5: Can different stresses in engineered wood be distinguished by the piezoresistive reaction, and what is the piezoresistive reaction to shear stress (section 2.2.1)?

From the research questions, the following four working hypotheses (H) were derived:

- H1: An addition of piezoresistive properties to the bond line in engineered timber – without reducing the strength of manufactured wood bonds – is possible by the integration of electrically conductive filler without reducing the strength of manufactured wood bonds.

- H2: A decrease in electrical resistance and an increase in the piezoresistive properties of electrically conductive bond lines in wood can be achieved by the proper selection of ECF type and concentration, together with a suitable dispersion and assembly process.
- H3: The sensitivity of piezoresistive wood bonds can be increased after manufacturing by thermal postcuring.
- H4: The signal quality of piezoresistive bond lines is frequency dependent and offers higher reliability than resistance measurements based on direct current.
- H5: The kind of stress in dry engineered wood (tension, compression, shear) can be distinguished by the direction (positive, negative) and extent (sensitivity) of the piezoresistive reaction in the piezoresistive bond line.

Therefore, the overall objective of this thesis is to prove that by understanding the influences resulting from the manufacturing process and materials used, the resulting piezoresistivity of the cured adhesive can be utilized and increased to measure strain in dry, engineered timber.

## 2 THEORETICAL BACKGROUND

### 2.1 Electrically conductive (wood) adhesives

#### 2.1.1 Electrically conductive filler networks

To generate piezoresistivity and thereby strain-sensing properties in polymeric adhesives, an electrically conductive composite material needs to be created. This objective is achieved by incorporating a continuous electrically conductive network structure into an insulating polymeric matrix consisting of electrically conductive filler (ECF) particles. This principle needs to be distinguished from intrinsically conductive polymers that are also applicable as sensors [37].

Generally, spatial dispersion, which is the statistical chance of electrically conductive path building, increases with increasing ECF concentration and homogeneity by interconnecting the ECF. This transition from the pure adhesive (insulating) to the saturation plateau of the filler (conducting) follows a so-called percolation curve [21,38–40] based on the percolation theory [41,42]. More precisely, it follows an electrical percolation curve that distinguishes it from rheological percolation [43,44]. In rheological percolation, the measured percolation is a mechanical network derived from both the polymer and ECFs [45]. The electrical percolation is characterized by a decreasing resistivity (or increasing conductivity) of several magnitudes when the first electrically conducting paths are formed. Before and after this, a relatively small change in resistivity is typically observed, which represents the gradual establishment of new electrically conducting paths. The singular point at which the volume fraction of ECF  $\Phi$  generates a transition from insulation to a conducting polymer is called the percolation threshold and is termed  $\Phi_C$  (critical volume fraction). An experimentally and theoretically established power law is often used to describe the electrical percolation in electrical conductive polymer composites that are close to the percolation threshold [46]:

$$\sigma \approx \sigma_0(\Phi - \Phi_C)^t \quad \text{I}$$

where  $\sigma$  is the predicted conductivity of the polymer composite,  $\sigma_0$  is a factor based on the individual EFC conductivity [47] and/or its contact resistance and the network topology of percolation clusters [48],  $\Phi$  is the ECF volume fraction,  $\Phi_C$  is the percolation threshold and  $t$  is a critical exponent that depends on the dimensionality system with  $t \approx 1.33$  for two dimensions and  $t \approx 2$  for three dimensions.

While the description of electrically conductive polymer composites by percolation theory is based on the varying interconnections between the ECFs in a random system [49], in some polymer composites this connection can be interrupted by thin polymeric layers. The percolation model for electrically conducting polymer composites has

therefore also been extended by quantum mechanical tunnelling which can overcome the thin polymer barrier [50] and is also known as the tunnel-percolation-model [51].

From the model-based factors  $\sigma_0$  and  $t$  of the power law, it becomes apparent that the percolation behaviour and threshold depend on several attributes of the ECF and the polymer.

Consequently, a large variety of different percolation thresholds has been reported over time, ranging from 0.0025 % to 3 % for carbon nanotubes (CNTs) and 1.5 % to 30 % for carbon black (CB) [52–58]. The determination of the percolation threshold of specific ECF/polymer systems is still an experimental step, although several influencing factors from ECFs and polymers have been identified.

### **2.1.2 Electrically conductive fillers**

A significant amount of literature on ECFs for enhancing the electrical conductivity of polymers can already be found, and research activities have recently been accelerated by the application of new nanosized ECFs such as CNTs due to their outstanding electrical [59] and mechanical properties [60]. Although the use of the term ‘nano’ in publications regarding polymeric fillers is constantly increasing, as shown in the Institute for Scientific Information (ISI) Web of Science database when searching for the term ‘nano filler’, the primary particles of industrialised and traditional ECFs such as CB also offer nanosized dimensions of 1–100 nm [61,62]. Several reviews that give an overview of singular ECF types in different polymer matrices, different ECFs in a singular polymer type, or more general approaches can be found in the literature [40,63–67]. These reviews show that the prominent ECF types for rendering polymers antistatic or electrically conductive are carbon allotropes such as CB; single wall, double wall, and multiwall carbon nanotubes (SWNT, DWNT, MWNT); fullerenes, carbon (nano)fibres, graphene, graphite; and silver, copper, and metal-coated particles. Of these, (nano)silver and silver-coated metals are the predominantly used ECFs in adhesives for an electrically conductive joining alternative to soldering [68,69] with concentrations of 70 wt% and more ECFs. The development of adhesives with improved electrical and mechanical properties was proposed by Wehnert et al. [55] by the addition of CNTs. CNTs have also been used as a filler for adhesives to detect defects in aluminium single lap joints [70]. Additionally, piezoresistivity in nanocomposites is commonly achieved using carbon-based allotropes.

The desired lower percolation thresholds resulting from the selection of a given ECF type are generally achievable through higher aspect ratios of the ECF [46,47,67,71] or the use of highly structured ECFs such as conductive CB [72,73]. Fig. 1 illustrates this principle using the structures of CB and CNTs that were used in this work.

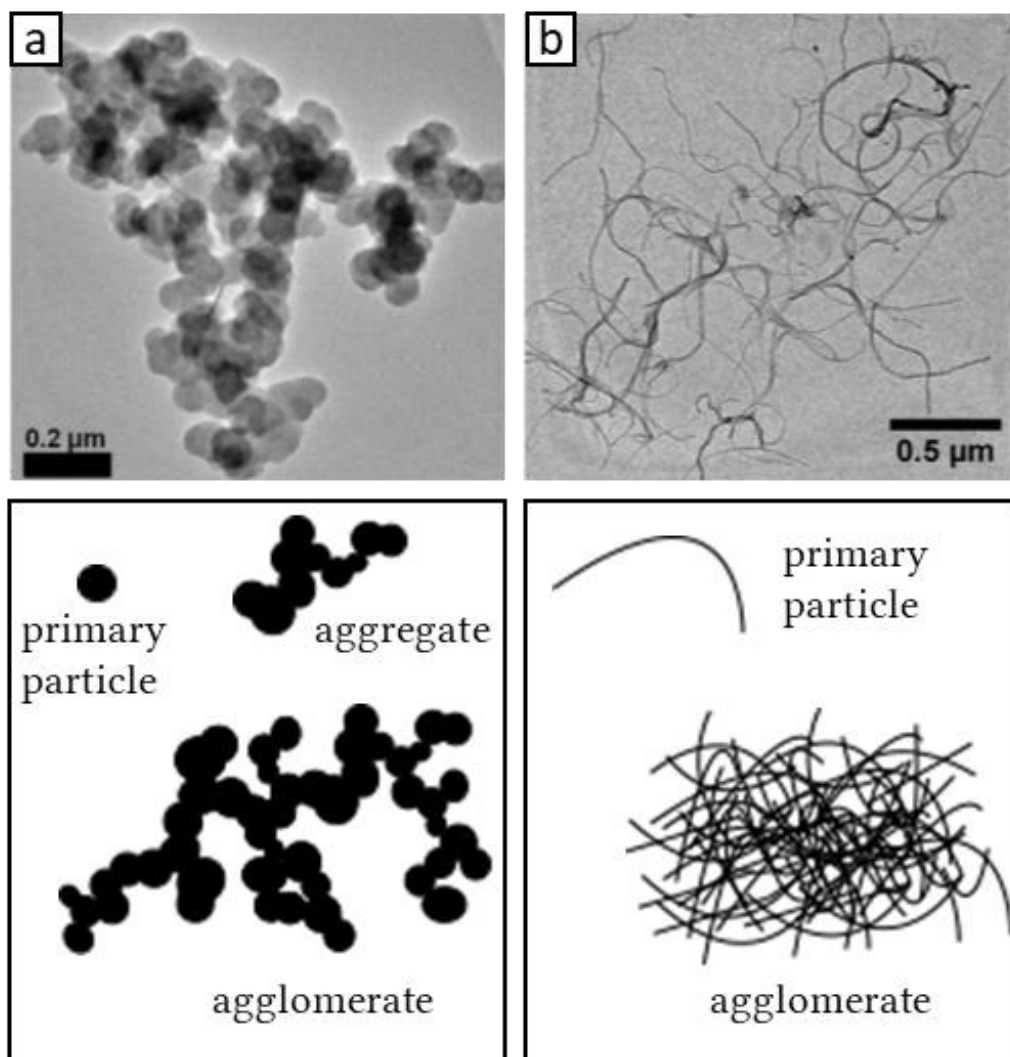


Fig. 1 Illustrations of highly structured carbon black and multi-walled nanotubes with a high aspect ratio according to electron micrographs. (a) Ketjenblack® EC-600JD (Akzonobel) with a specific surface area of  $1,400 \text{ m}^2/\text{g}$ , and (b) Nanocyl® 7000 (Nanocyl Belgium) with an aspect ratio of 10–1,000 m/m. The images were reproduced and adapted from [74] together with the terms of particle morphology used in subsequent sections of the text.

Highly structured ECFs consist of three-dimensional structures with a maximised specific surface area. The specific surface area includes the outer surface and the surface of voids in the ECF. Carbon blacks, for instance, are available with non-exclusive specific surface area values ranging from  $41 \text{ m}^2/\text{g}$  [75] to  $1,400 \text{ m}^2/\text{g}$  [74]. High values such as  $1,400 \text{ m}^2/\text{g}$  are reached through a high void volume in the primary particles [76] and the ramified CB agglomerates (Fig. 1). Further information on the properties and manufacturing methods of CB and CNTs have been summarised in several other publications [61,72,77,78].



As the terms aggregate and agglomerate are often used interchangeably in the literature, a brief clarification based on the work of others is provided here [72,79,80]. Primary particles are single particles that are not further separable. In the case of CB, the primary particles are spherical, while CNTs feature a fibre-like shape. ‘Aggregates’ is the term used for the smallest CB structures, which consist of primary particles grown together with a common crystalline structure [80], thereby fulfilling the criteria of Nichols et al. [79]. In the case of CNTs, the term aggregate is not applicable. Due to their high surface to volume ratio, van-der-Waals forces act between the primary particles/aggregates, thereby resulting in the assembly of larger numbers of particles into agglomerates. Agglomerates are characterized by the fact that their constituent particles can be separated through the input of energy such as shearing.

In contrast to the three-dimensional structure of CB aggregates, ECFs such as carbonous fibres with a high aspect ratio (ratio of length to diameter) yield a one-dimensional structure. Fibres thus generally offer lower percolation thresholds than one- or two-dimensional fillers.

By combining different ECFs with a two- and three-dimensional morphology, the electrically conductive network can be formed with smaller concentrations of ECF, as polymeric gaps are closed by the differently structured fillers [81–85].

Additionally, the intrinsic resistivity of the ECF itself can influence the resistivity of the nanocomposite made from an insulating polymer and ECF. For example, carbon fibres and CNTs exhibit distinct lower electrical resistivity compared to CB (around three decades) [63].

On the other hand, the high conductivity of the ECF does not always ensure a high conductivity of the nanocomposite. Generally, it can be said that extractable ions such as sodium, chlorine, or potassium and the corrosivity of the filler material can be detrimental to the nanocomposite [86]. Especially metal fillers – apart from silver and gold (coated) particles – bring major drawbacks to the composite as electrically non-conductive but thermodynamically more stable oxide layers are formed [63].

Therefore, ECFs with a high structure/aspect ratio, high conductivity, and low amounts of extractables are favoured for rendering insulating polymers conductive.

### **2.1.3 Interactions between fillers and polymers**

A change in the mechanical properties of the nanocomposite can be expected depending on the interaction of the introduced ECF with the polymer. Efficient stress transfer and a strong interfacial bond between filler and polymer are necessary for good mechanical properties [87,88]. A weakening of the material is expected in the case of weak chemical or physical interactions, which decreases the strength and fracture strain of the nanocomposite. Thus, depending on the type and strength of the interaction – either none at all, physical or chemical – the mechanical properties of the nanocomposite are strengthened or weakened [87,89].

The effect of decreasing mechanical properties through filler integration was not only reported in reference books [90] but also in numerous experimental studies, e.g. for shear strength in silver-based ECFs [82,91]. Studies with carbon allotropes also reported a decrease of tensile strength, fracture strength, and fracture strain through the integration of CB, CNTs, and other allotropes [92–96], which correlates with the cohesive strength of adhesives [92]. The decrease in strength results from defects in the composite structure incorporated by the filler if no bond between filler and polymer exists [97]. In this case, the weak interfacial strength between filler and polymer can act as a fracture hotspot.

On the other hand, fibrous and plate-like fillers have the potential to increase the fracture toughness of nanocomposites due to crack bridging, crack deflection, and crack pinning [98] of the polymer and filler that are bonded. Consequently, the positive effects reported for filler integration of nanocomposites included the increase of Young's modulus [93], fracture toughness, and lap shear strength [98]. Furthermore, an increasing or decreasing tensile shear strength with increasing filler concentration was reported and ascribed to agglomerates at higher filler concentrations [98] that introduce defects and stress concentrations [99].

As a result, if the agglomerates are sufficiently reduced, the changes in mechanical properties of the nanocomposite mainly depend on the surface chemistry of the filler and polymer used.

Since the invention of vulcanized car tires, CB has been used as a mechanical reinforcement of elastomers although, according to Robertson and Hardman [100], the mechanism behind the interaction between CB and rubber is not fully understood. Some of the aspects discussed for the mechanism of interaction include physical adsorption by van-der-Waals forces between CB and rubber and covalent bonds between CB and polymers that are driven by free radicals and the CB as an efficient radical acceptor [87,100]. Furthermore, CB also interacts with rubber by increasing the crosslinking near the filler particles [100].

On the other hand, the interfacial interactions of CNTs are primarily based on van-der-Waals forces and cannot efficiently transfer stress between the filler and polymer [99].

Therefore, ECFs with compatible surface chemistry to the polymer are favourable, as physical and covalent chemical bonds between the ECF and polymers offer better mechanical coupling of the filler-polymer system. Compatible surface chemistry also enhances the dispersibility of the filler, as outlined in section 2.3.1.

Finally, all wood adhesives are typically designed to have greater strength than the bonded wood. This was confirmed in daily practice [101] and leads to intact adhesive bond lines while cracks are initiated in the wood [102]. As a result, the described potential decrease of mechanical properties of the bond by residues of agglomerates is questionable.

#### 2.1.4 Polymeric and (wood) adhesive matrices

The second component of the nanocomposite – the adhesive polymer – functions as an insulating matrix to embed the ECF network. In their review, Mutiso and Winey [46] indicate that because the polymeric matrix alters the filler distribution and network geometry, the impact of the polymer on the electrical properties is difficult to isolate. They also conclude that the impact of the electrical properties of the polymer is negligible and that the selection should thus only be based on the desired nonelectrical properties [46]. Thus, various factors must be taken into account when selecting suitable adhesives as a matrix for electrically conductive adhesives including [63,77,86,103]:

- long-term behaviour (storage time, embrittling, moisture uptake)
- variability of properties
- curing behaviour (expanding, shrinking, foaming)
- mechanical resistance
- surface tension/chemistry and polarity of the polymer
- viscosity/ molecular weight
- barrier characteristics, as permeability to moisture or oxygen can alter the electrical conductivity
- chemical structure, as filler can only be distributed in the amorphous part of polymers.

Of the above aspects, the favourable curing behaviour is discussed differently in the literature. While adhesive shrinkage during the curing process helps to draw the ECFs closer together [86], Brunner mentioned that ECF networks are built around the gaseous bubbles [104]. This phenomenon of ECF network building around bubbles was dealt with by other researchers under the concept of ‘segregated structures for polymer systems with a high amount of pores’ [105] and can help to decrease the percolation threshold.

Wood adhesives are not systematically investigated in the context of electrically conductive adhesives. With the addressed application in mind, only adhesives for structural applications will be discussed in this work.

The European market for wood adhesives for structural applications is divided into five different adhesive systems. The two adhesives from polycondensation reactions are melamine-urea-formaldehyde (MUF) adhesives and phenol-resorcin-formaldehyde (PRF) adhesives. While MUF comprises a major part of the market, PRF is mostly used in special or high-end applications. The third kind of polycondensation adhesive, namely urea-formaldehyde (UF) resins, is not suitable for use in structural applications due to their poor water resistance [106]. Adhesives based on polyaddition reactions are one-component polyurethane prepolymers (1C-PUR) and epoxy resins (EP). While 1C-PUR covers the second-largest market share and over 65% of all cross-laminated-timber (CLT)

producing lines [107], EPs are only used for glued-in rods, metal-wood joining, and repairing purposes due to their high prices compared to other structural wood adhesives. The final type of adhesive used in manufacturing structurally engineered wood is the emulsion-polymer-isocyanates (EPI) that combine simultaneous physical hardening, film formation, and chemical curing due to the reaction of isocyanate with active hydrogen groups. Further information regarding the different adhesive systems and their reaction mechanisms can be found in the literature [108–113].

In terms of processing (dispersion, mixing, application, curing) and ageing, all adhesives for structural timber bonding offer favourable and unfavourable characteristics for creating piezoresistive bond lines.

Two-component adhesives (MUF, PRF, EPI, and EP) are less favourable than one-component systems (1C-PUR) as they need the development and control of two dispersion processes. The mixing step of the two components also brings another variable into the process, thus increasing the possibility of introducing more variability in the cured adhesive. Furthermore, EPI comes as a dispersed system, which makes it difficult to disperse additional filler into the first component without interfering with the dispersion of the polymer in water and thereby raising the challenge of development. The curing of polycondensation adhesives changes the adhesive polymer to a rigid and brittle state. Under ageing conditions, the stress due to swelling and shrinking of the adherend can then lead to further embrittlement of these rigid bond lines, which has been shown for urea-formaldehyde (UF) adhesives by Raknes [114] and Hass et al. [115]. This characteristic is highly unfavourable for adhesive bond lines that need to sense the behaviour of the GLT as the embrittlement would be measured as damage, although without any real damage to the GLT component.

On the other hand, polycondensation adhesives (MUF, PRF) typically consist of water and a solid content of around 50–70%, which – together with the polycondensation reaction – leads to curing shrinkage. As mentioned, shrinkage can help to draw the ECF network closer together and is therefore favourable for manufacturing electrically conductive adhesives. Additionally, polycondensation adhesives are available with low viscosity, which are favourable for the integration of ECF as wetting becomes easier

The absence of a mixing step is a process-related advantage of using 1C-PUR, as only one component is involved. Furthermore, the possibility of using polyurethane chemistry to adjust the curing time and mechanical properties can be applied to adapt the adhesive for the piezoresistive function. Based on theoretical assumptions, polyurethane can help to decrease the necessary concentration of ECF as dispersed filler can only be distributed in the amorphous part of the polymer [77] and polyurethanes are semi-crystalline in nature [116].

On the other hand, due to their prepolymerized polyols, 1C-PUR have higher viscosities than all other wood adhesives which potentially leads to inferior wetting of the filler compared to low viscosity MUF adhesives. Polyurethane prepolymers foam due

to their curing reaction, which could be unfavourable for forming electrically conductive networks. Lastly, the manufacturing of 1C-PUR modified with ECFs requires an inert environment.

## 2.2 Piezoresistive polymers

### 2.2.1 Piezoresistivity

Piezoresistivity describes an electromechanical effect in which electrical resistivity changes with strain [117] and the term partly originates from the Greek word  $\pi\acute{\epsilon}\zeta\omega$  (to squeeze). The applicable state of the art for piezoresistive adhesives is mainly derived from piezoresistive polymers and nanocomposites. Adhesives filled with ECF (mostly CNTs) have mainly been investigated for their damage sensing potential [118–122] where the strain sensing as a result of piezoresistive characteristics in the elastic regime of the adhesive plays a minor role, or none at all. The state of the art in the piezoresistivity of polymers was therefore used for the theoretical background of this thesis

In cured polymers and polymer-based composites filled with ECFs, piezoresistivity results from changes in the ECF network embedded in the insulating polymer matrix. Through straining the nanocomposite, four different contributions to the piezoresistive effect are reported near and after the percolation threshold. These are the:

- I change of intrinsic electrical resistance in the ECF, which was especially shown for CNTs [30,123,124],
- II change in contact resistance between ECFs or the complete loss of contact [30,124,125],
- III change in distance between ECFs due to microstrain in the insulating polymer layer between the ECFs, which leads to a change in the tunnelling resistance [30,124–128]
- IV change of microcapacitors formed through the Maxwell-Wagner-Sillars polarisation at the ECF-polymer interface [129,130].

For illustrative purposes, Fig. 2 visualizes the different effects that contribute to piezoresistivity using the examples of CB aggregates as the ECF.

The extent of piezoresistivity, i.e. the sensing effectiveness or sensitivity (section 2.2.2) is commonly described by the gauge factor (GF) [131], which is defined as:

$$GF = \frac{\Delta R}{R} / \frac{\Delta l}{l} \quad \text{II}$$

where  $\Delta R/R$  is the change in resistance with strain  $\Delta l/l$  in the measurement direction.

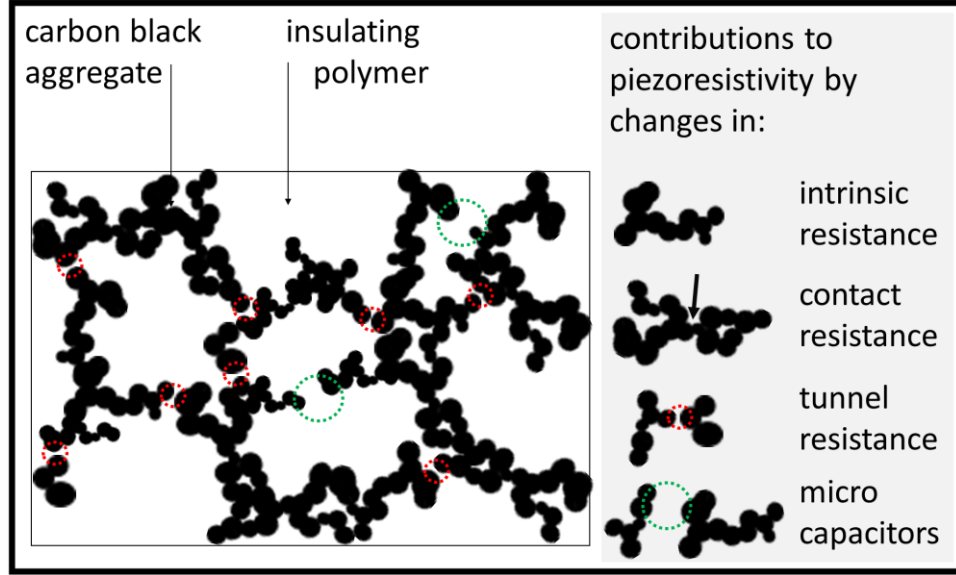


Fig. 2 Scheme of a network of carbon black aggregates together with the changes in electrical resistance and capacity from which piezoresistivity originates in nanocomposites.

By definition, piezoresistivity is a strain-dependent change in resistivity and not the resistance of material as such [131]. Thus, the fractional change in resistance  $\Delta R/R$  in equation II is defined as:

$$\frac{\Delta R}{R} = \frac{\Delta \rho}{\rho} + \frac{\Delta l}{l} * (1 + \nu_1 + \nu_2) \quad \text{III}$$

where  $\Delta \rho/\rho$  is the fractional change of specific volume resistivity,  $\Delta l/l$  the strain in measuring direction, and  $\nu_1$  and  $\nu_2$  the Poisson's ratios in the two transverse directions of the strain. According to the standard convention, the tension strain is positive and the compression strain negative. Therefore, based on the convention and equation III it follows that the piezoresistivity is positive if a material's specific resistivity increases with tension strain and decreases with compression strain.

In contrast, piezoresistivity under shear stress is not covered by this definition and – as far as is known by the author – has also not been investigated for piezoresistive nanocomposites. The only results for piezoresistivity under shear stress were published by the author for a lap-joint tension shear sample that reacted with increasing resistance [32].

It has been shown that sensitivity depends on filler concentration, filler type, and the level of strain. Several experimental studies found an increase in piezoresistive sensitivity with lower filler concentration of CNTs and CB near the percolation threshold [25,30,123,125,126,132–134]. On the other hand, higher filler concentrations enhance the reproducibility of the piezoresistive sensitivity and are better suited for practical applications [125,134,135]. Several reports indicated higher fluctuations/noise

of the piezoresistivity of CNT nanocomposites when a critical filler concentration is exceeded [25,126].

Differences in piezoresistivity according to filler type were found in a study by Wichmann et al. [128] which showed a higher sensitivity of CB compared to MWNTs that was attributed to the filler geometry. Additionally, the piezoresistivity of the CB-based nanocomposite followed a function that could be sectioned in different strain-dependent regimes such as those reported by others [127,136]. At low strain values in the elastic regime of the polymer, a linear or slightly non-linear relationship between resistance and strain can typically be observed [127,128,137]. From a modelling perspective, the tunnelling mechanisms have the most influence at low strains, while the change or breakup of inter particle contact only has a minor impact [126]. This break up of contacts becomes more important in plastic deformations of the polymer and result in a non-linear piezoresistivity.

Apart from the widely understood functional principle of piezoresistivity in nanocomposites, the following features are still discussed and were partly observed by the author in earlier studies:

- Changes in conductivity [32,52,134,138] and piezoresistivity [138–140] with repeated or cyclic load have been observed. They are generally attributed to changes in the ECF network or irreversible changes due to straining in the plastic region [141,142].
- A resistance drift (change of resistance with time) has been observed [138,143]. Wang and Ding [143] allocated the resistance drift to the polymeric material creep. Zhang et al. [138] used cyclic loading in their experiments and showed the resistance drift from a stabilizing effect as it reaches a plateau after several load cycles.
- An inversion of the piezoresistivity at high strain together with hysteresis at cyclic loading was observed by Bilotti et al. [144], but not further analysed regarding the working principle behind this behaviour.

### 2.2.2 Sensor characteristics

In addition to the general concept of piezoresistivity as a measurable change in electrical material properties, the main investigations used specific sensor characteristics. As a result of numerous sensor types and principles, standard definitions are absent in sensor engineering [145]. The following characteristics were thus used to describe the capabilities of the piezoresistive bond lines as a sensor [145]:

- Sensitivity is the ratio of sensor output to the change in the value to be measured. Thus, the sensitivity defines the amplitude of the resistance change at a given strain. As it was not always possible to measure strain in the measuring direction, the relative change in resistance  $\Delta R/R$  was given with respect to the applied stress in MPa.

- Repeatability is a statistical characteristic and describes the ability of a sensor to produce the same output when the same input is applied to it. A lack of repeatability generally occurs due to random fluctuations in environmental inputs or operator errors. In Paper III, the inverse property, namely the variability, was used to provide comparable results for the different instability characteristics (variability, drift, baseline instability) of the piezoresistive bond line.
- Drift describes a systematic deviation that changes continuously in one direction.
- Baseline stability describes the inability of a sensor element to exhibit the same sensor output after excitation. Similarly to the repeatability, the inverse property – the baseline instability – was used in the main investigations.

The extents of the variability, drift and baseline instability were used to summarise the instability of the piezoresistive bond lines as a sensor and were further defined as instability characteristics. Therefore, high stability characteristics indicate high repeatability, high baseline stability, and low drift.

## **2.3 Manufacturing influences**

The manufacturing steps of GLT, particularly the application of adhesive, assembly pressing, and post-treatment are geared towards the strength of GLT and the bonding strength. They thus do not consider the optimisation of an additional sensor function in the nanocomposite adhesive layer. On the other hand, various influences on the processing and manufacturing of these materials have been identified from the literature on nanocomposites. Unfortunately, not all of those process influences are applicable to the later-described investigations, as different kinds of polymers (thermosets, thermoplasts) and processing techniques (extruding, etc.) were used. As the use of piezoresistive wood adhesives in engineered wood is a new application in the field of nanocomposites, the following overview (Fig. 3) shows the relevant process steps of manufacturing—from the delivered materials to the electrically conductive wood bond.

### **2.3.1 Dispersion**

To ensure dust protection in the working area, electrically conductive (nano)particles are produced and mostly delivered as powder or ‘pelletized’ beads [146]. Under delivery conditions, the ECF particles are therefore agglomerated and need to be homogenously dispersed. Dispersion is especially important for CNTs that are supplied in the form of agglomerated and entangled bundles. In addition to entanglement, the high aspect ratio and surface area of CNTs result in strong inter-particular van-der-Waals forces.



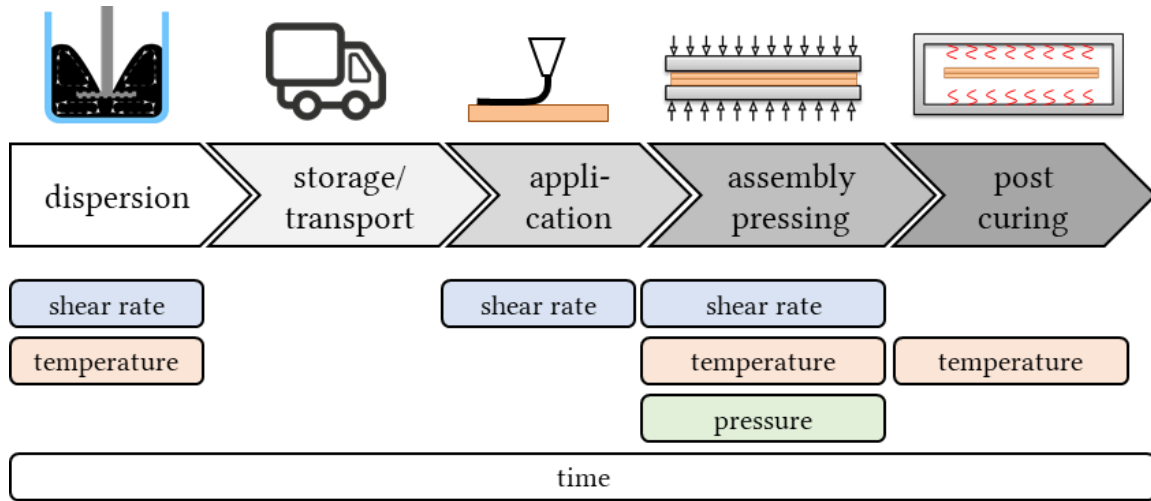


Fig. 3 Overview of the manufacturing steps of a piezoresistive bond line with the assigned influencing parameters shear rate, temperature, pressure, and time.

Therefore, research and development on suitable dispersion techniques for CNTs were of major concern for a long period. The most frequently mentioned dispersion techniques for the dispersion of nanoparticles are 3-roll-mills, ultrasonication, and mechanical stirring, although techniques such as ball milling, shear mixing with an Ultra-Turrax, microfluidizers, and dual asymmetric centrifuges have also been used [53–55,147–153]. Techniques such as extruding were generally used for incorporating ECFs in thermoplasts [154]. Depending on the working principle of the technique used, the energy density introduced into the system can vary and thereby also damage the filler. An example of this is ultrasonication, which can shorten, fracture, or disorder the carbonous structures of particles, thereby leading to reduced electrical conductivity [150,155–157].

Overviews of the different dispersion techniques and their effects for producing nanocomposites for CNTs are provided in Ma et al. [156] and Atif and Inam [99], while the efficacy of different techniques is compared in Schilde et al. [158]. Based on these literature findings and the author's own experiences with ultrasonication, calendaring, and shear mixing, different criteria for the dispersion of nanoparticles are summarised in Table 1.

The mixing process, which is generally called 'dispersion' after the second step, is characterized by three steps for incorporating the solid filler particles into a liquid phase, i.e. into the polymer matrix [77]:

1. Filler wetting: wetting of the filler by polymer and penetration of the filler into voids within aggregates and agglomerates.
2. Dispersion: the break-up of agglomerates and separation of the aggregates/primary particles from the agglomerates.

3. Distribution: separation and homogenous distribution of the aggregates/primary particles inside the polymeric matrix.

Table 1 Dispersion techniques and criteria for their use in producing nanocomposites.

Technique	Criteria			
	Description	Suitable polymers	Impact on filler	Availability
Ultrasonification	high-frequency sound waves create cavitation, resulting in local high shear rates	soluble polymers, low viscosity polymers	damages CNTs	easy operation, laboratory to industrial scale
Calendering	gaps down to 5 $\mu\text{m}$ between three rolls create high shear forces	low to high viscosity polymers	potential alignment	limited scalability, elaborate cleaning process
Shear mixing	Stirring at high rotational speed induces fluid shear flow	soluble polymers, low to medium viscosity polymers		easy operation, laboratory to industrial scale
Ball milling	grinding by balls in a mill, deagglomerates the filler	low viscosity polymer or powder	damages CNTs	easy operation, elaborate cleaning, laboratory to industrial scale
Extrusion	two screws rotating at high speed create a shear flow	thermoplastics	potential alignment	Elaborate cleaning, laboratory to industrial scale

The wetting of filler with polymer is associated with physical and chemical interactions that lead to the combined properties of the filler and polymer matrix. As CNTs are generally inert towards polymers, chemical surface modification is a common method to improve their compatibility and dispersibility within the polymer. The corresponding process is known as functionalisation, as new functional groups are created on the surface of the filler. Although dispersibility and interfacial interactions are generally improved, functionalisation also has disadvantages for nanocomposites. Functionalisation is related to an increase of the percolation threshold [124] and can damage the structure of CNTs [159], which decreases their conductivity and mechanical properties. Literature that reviews functionalisation methods can be found elsewhere [99,156,160].

After filler wetting, the step of dispersion is necessary to deagglomerate the filler by ‘chipping’ primary particles/aggregates from the surface of the agglomerate or breaking the whole agglomerate into smaller agglomerates. Researchers have shown that the dispersion does not need to separate all primary particles, aggregates, and agglomerates to achieve electrical conductivity by building an ECF network. Agglomerated ECF

structures in the polymeric matrix can show higher conductivity than perfectly and homogeneously separated and dispersed primary particles [161,162], as outlined in Fig. 4 for CB aggregates. Similar sketches were shown for fibrous particles in related literature [161–163]. The separated aggregates can be isolated from each other with increasing homogenisation and dispersion (Fig. 4d). With better-isolated ECF particles, fewer agglomerate residues lead to less degradation of the mechanical properties (Fig. 4Y), as described in section 2.1.3. Conversely, in ideally homogenous dispersions, higher concentrations of filler are necessary to reach a percolated – and therefore conductive – network (Fig. 4X).

In the last step, the dispersed ECFs need to be homogeneously distributed over the adhesive matrix.

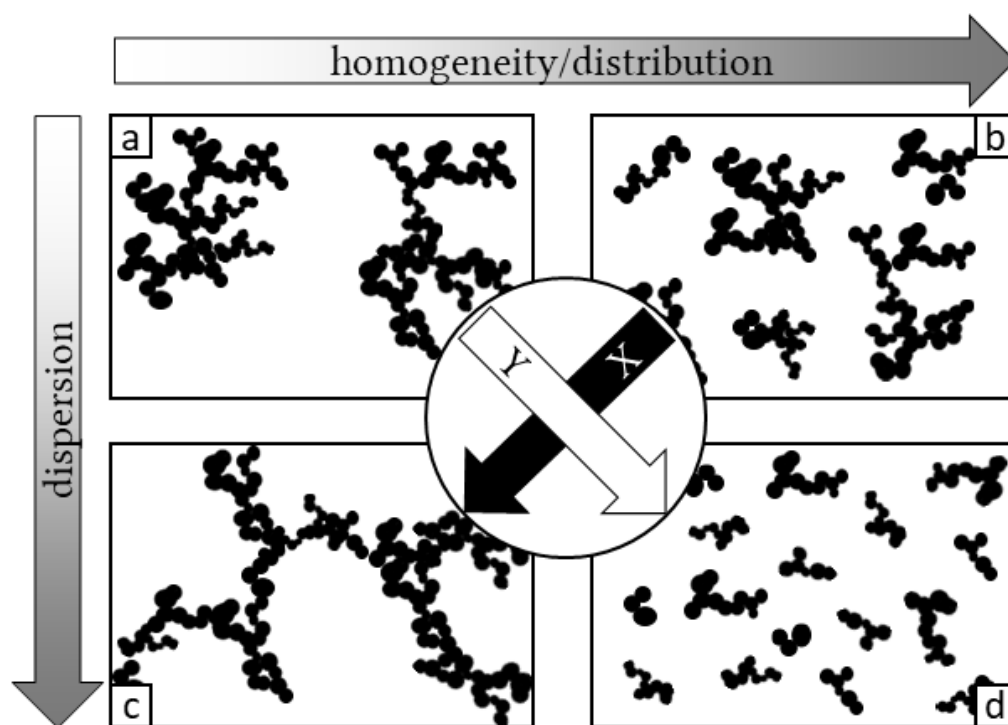


Fig. 4 Effect of carbon black aggregate dispersion and homogenisation inside an insulating polymeric matrix with (a) no dispersion and low homogenisation, (b) low dispersion and high homogenisation, (c) high dispersion and low homogenisation, and (d) high dispersion and high homogenisation. The X-direction gives a percolation threshold at lower filler concentration, while the Y-direction gives less mechanical degradation by fewer agglomerates.

The direct mixing of the final liquid nanocomposite is preferred to the use of master batches due to the narrow window of ECF concentration where the percolation threshold occurs [73]. The master batch and the dilutant feature high differences in viscosity. Furthermore, the master batch needs a much higher filler concentration, which

is often not achievable due to increased viscosity. At the very least, the dilution of the master batch requires high accuracy of dosing and a second mixing step, which would in fact lead to a two-component system.

Thus, the quality of master batches is difficult to control [73], as was confirmed by the author's work in which no particle analysing systems were able to visually penetrate the nanocomposite. The methods to analyse and describe the dispersed state of nanosized particles are still under investigation and are generally only applicable to small areas of interest that do not represent the whole composite [161]. Methods for particle size distributions based on light sources, such as laser diffraction analysis, are hindered by the intransparency of the nanocomposites based on carbon allotropes in their original form with high filler concentrations. The generally used approach for bypassing the problem by diluting the final dispersion for more transparency is not suitable in this context. With lower viscosity, the dispersion state can be changed due to the higher mobility of the particles and shear flow can also alter the dispersion state during assembly processing.

### **2.3.2 Assembly processing**

During the application of the adhesive to the timber and the assembly pressing, two different parameters can influence the percolated ECF network, namely shear rate and temperature.

The influence is based on the rebuilding of agglomerates by thermodynamics (lower viscosity and temperature) and kinetics (stirring, shear rate). The 'reagglomeration' is also described by the concept of flocculation from the colloid theory. The dispersed particles and aggregates build up new structures of particles by diffusion in hot polymeric systems, contributing to a new network that can result in fractal structures [164]. This flocculation was reported as a second percolation threshold for nanocomposites [38] and can be induced by flow with a low shear rate and under higher temperatures [163]. It is important to note that low shearing forces need to be applied to induce the flocculation as, without these, only low agglomeration due to Brownian motion is expected. Brownian motion is the term used to refer to the random motion of particles in colloid suspensions, i.e. dispersions of solid particles in liquids. The shear deformation helps to overcome the repulsive forces between particles and aggregates and accelerate the agglomeration/flocculation process, which was shown by Schöler et al. [164].

Accordingly, lower temperatures and higher shear rates will therefore increase the electrical resistance of the nanocomposite as shown by Hu et al. [30].

A significant influence is also expected from the time in which shear deformation is applied [165,166]. In her dissertation, Heintz [163] showed that an equilibrium state of dispersion and, therefore, a certain conductivity, is reached after a time, depending on the shear rate and filler concentration. The equilibrium was reached faster with higher

filler concentrations and higher shear rates. Skipa et al. [167] also showed that filler structures are more rapidly destroyed than they are built up, thereby indicating that the shear history can influence the ECF network [168].

Even in resting liquid adhesives (for example during curing), a higher temperature can change the dispersion state. Although temperature decreases the overall viscosity, a local shear rate can be induced by diffusion and convection processes [169] as well as motion from bubbles (for example the CO<sub>2</sub>-bubbles during 1C-PUR crosslinking), thereby leading to local variations of electrical resistivity as shown by Heintz using optical microscopy [163].

The second influence of shear deformation can emerge during liquid processing, especially at high shear rates. Fibrous fillers with high aspect ratios can be aligned according to the shear flow, leading to anisotropic network formation and, therefore, to anisotropic resistivity in the nanocomposite. While this effect is typical in high shear processes such as extrusion, fibre spinning, or injection moulding [46], similar effects for high flow nozzles are also plausible.

Additionally, the clamping pressure (referred to as ‘pressure’ in this dissertation) and press temperature need to be considered. It can generally be assumed that higher pressure results in thinner bond lines as higher adhesive penetration is expected. This further correlates with higher assembly temperatures that decrease the viscosity of the adhesive, resulting in more penetration into the wood adherend. While thinner – but not starved – bond lines in wood are associated with higher bonding strength, a thin bond line can over proportionally decrease the initial resistivity. Hernández-López et al. [170] showed that the thickness and initial resistivity of nanocomposites are not linearly correlated although, on the other hand, an increase of pressure results in less porosity of foaming adhesives such as 1C-PUR and therefore lowers resistance due to fewer pores in the adhesive.

Consequently, as shown in the assembly processing overview in Fig. 3, pressure, temperature, and shear deformation as well as their history can therefore influence the particle network during the application of the liquid adhesive and assembly pressing.

### **2.3.3 Post curing**

Thermal post-curing after manufacturing is used as a technique to increase the electrical conductivity and shear strength of electrically conductive adhesives [164] but has a different relevance depending on the matrix polymer. For example, thermoplasts are reduced in viscosity, which enables the percolated filler network to reallocate and form flocculated structures [168]. In thermosetting adhesives such as epoxy adhesives, thermal post-curing can reduce residual stresses [171] and increase the cross-linking density [172]. Apart from epoxy adhesives, only polyurethane-based adhesives were investigated concerning the impact of post-curing. However, the results regarding the impact of thermal post-curing on polyurethane adhesives vary. Bitomsky et al. reported

that post-curing can help to fully cure the adhesive [116] by increasing the final turnover of crosslinking from around 90% to 99%, while on the other hand Richter et al. [173] reported a decrease in the creep of 1C-PURs (with one exception) in the test series.

Therefore, it remains unclear whether post-curing can be used to enhance the electrical, mechanical, or piezoresistive properties of wood adhesives.

## 2.4 Wood as an adherend

The following sections focus on wood as an engineering material that serves as the stress-transferring adherend of piezoresistive wood bonds.

### 2.4.1 Wood and engineered wood

Wood is a naturally derived material that shows heterogenous and anisotropic properties. Heterogeneity in terms of density is found in the hierarchical structure of wood on both the macroscopic and microscopic levels due to its growth features (juvenile wood, knots, etc.), annual rings, porosity, and cellular structure (see Fig. 5).

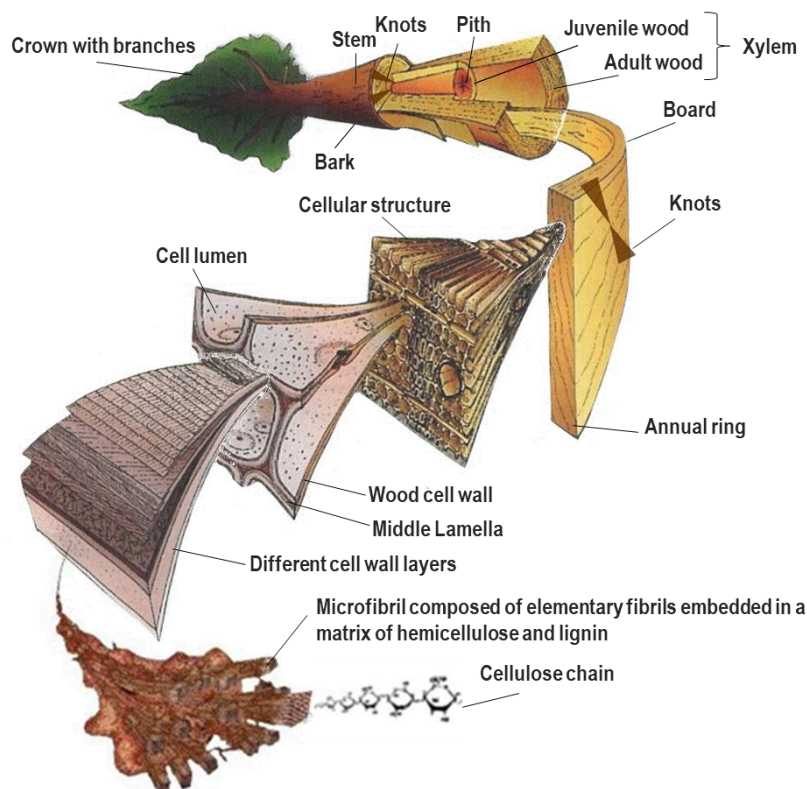


Fig. 5 Scheme of the hierarchical structure of coniferous wood with features leading to heterogenous density. The original design was taken from Harrington [174] and slightly changed and extended by Teischinger [3].

Additionally, variations in terms of structure and properties are not only found between different wood species, but also with the region of growth and with the environmental influences over the lifetime of a tree. Thus, variations in properties can be expected within a given tree, and among trees of the same or different species [175]. As a consequence, high variations are expected in test results involving wood as a tested material.

Due to the mechanical requirements of a living tree, the structure of wood is also anisotropic or, more precisely, circularly orthotropic. The mechanical properties of wood are therefore orthotropic, providing the highest strength and Young's modulus in the fibre direction (see Fig. 6).

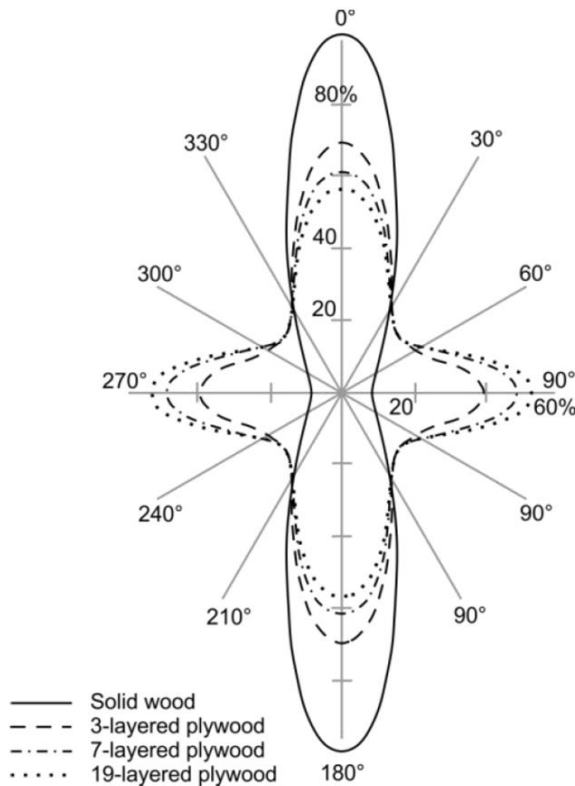


Fig. 6 Polar diagram of Young's modulus of solid wood and different plywood structures according to Keylwerth [176], modified by Baensch [177].

Additionally, wood shows viscoelastic behaviour as, in addition to the instantaneous elastic deformation in reaction to stress, the wood undergoes a time-dependent deformation [178]. This additional deformation under constant stress is characterized by creep [179] and typically decreases with time. The viscoelasticity of wood also depends on the structure/fibre direction as well as on the WMC and temperature [179].

Engineered wood is the logical consequence of these material behaviours, as the material can be homogenised and reduced in terms of the variability of its properties. Due to low vocabulary standardisation, the terms ‘engineered wood’ and ‘engineered timber’ are often used interchangeably. For this reason, the term ‘engineered wood’ is used in the cumulative thesis while ‘engineered timber’ was partly used in the main investigations.

The orthotropic behaviour can also be engineered by combining various layers of different fibre directions to reduce the orthotropic differences (see also Fig. 6). By cutting the naturally grown wood into smaller units and bonding them into standardised products, their dimensional limitations can be overcome. In this way, better predictability and thereby a higher characteristic strength for civil engineering purposes can be achieved. Because adhesives are always used for preparing engineered wood, the opportunity arises for using these adhesives as sensors.

Although the layered structure of wood with a repeated adhesive layer makes engineered wood especially suitable for the integration of adhesive-based sensors during production, wood also features some disadvantages for the integration of multifunctional bond lines.

This includes the fact that the porous structure of wood leads to diffuse structures of the adhesive in the bond line between wood adherends [180], which is dependent on the diameter of pores (vessels and cell lumina) near the bond line [181].

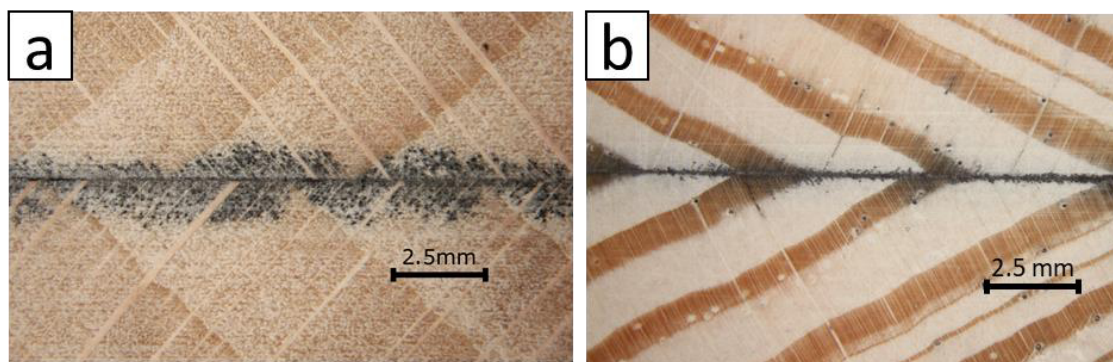


Fig. 7 Cross-section of an electrically conductive bond line between two adherends from beech (*Fagus sylvatica* L.) (a) and pine (*Pinus sylvestris* L.) (b)

Furthermore, the properties of wood – especially its electrical properties – are moisture-dependent.

#### 2.4.2 Electrical properties

In terms of its electrical properties, wood is regarded as a passive electrotechnical material concerning piezoresistive wood bonds. Therefore, GLT is simplified through the parallel use of passive electrotechnical material with an active sensor material in



between [182]. As no further modelling of the electrotechnical properties of wood or the piezoresistive adhesive was conducted in this thesis, this section concentrates on the influences resulting from the electrical properties of wood. Contributions to the modelling of electrical equivalent circuits involving wood and the relevant instrumentation were made, among others, by Katz and Miller [183], Skaar [184], Tiitta [185], Zelinka et al. [186] and Torgovnikov [187].

Under direct current (DC), wood exhibits a DC resistance, which is described by the general equation for DC resistance:

$$R = \rho \frac{l}{A} \quad \text{IV}$$

where  $R$  is the measured resistance,  $l$  is the travelling distance of current (commonly the distance between electrodes), and  $A$  is the cross-section of the resistor. The resistivity  $\rho$  is the specific electrical resistance adjusted for the geometric factor of resistance, and thus a material-specific value.

As the WMC is the main influencing factor for DC resistivity in wood, the resistivity is commonly used as an indirect property to measure the WMC, which ranges between  $10^3$  for wood at the fibre saturation point and  $10^{16} \Omega\text{m}$  for oven-dried wood with a linear relationship [188]. Other material-dependent influences are the temperature (decreasing resistivity with increasing temperature), grain angle, water-soluble salts, wood species, wood structure, and density [179,189,190]. The experimental variables that influence DC resistance measurements in wood were summarised by Vermaas [190]. These include the applied voltage, period of measurement, electrodes and their material, and the pressure for proper electrode contact. Thus, depending on the WMC, wood can be the ideal adherend for piezoresistive adhesives as it is an isolator in a dry state but a semiconductor in a wet state, thereby contributing to the measurement to a greater extent than piezoresistivity.

On the other hand, the contribution of the wood adherend to the overall measured resistance increases with higher resistance of the bond line, which raises the need for electrically conductive adhesives with low specific resistance values.

At least the passive electrotechnical properties of wood need to be separated from the only active electrotechnical property of wood, namely the piezoelectricity. The piezoelectricity of wood has been reviewed and investigated by several working groups and researchers [191–195]. Piezoelectricity describes the effect of an electric polarization proportional to strain, which can be found in non-centric crystals and similar structures [196]. In wood, piezoelectricity is allocated in the crystalline structure of cellulose [194]. The characteristic value to define piezoresistivity in wood is the piezoelectric modulus, which describes the relative charge separation to the applied force. Higher piezoresistive moduli are measured with increasing WMC [193] and in certain wood species [193] as well as according to the fibre orientation and temperature [194]. The highest piezoelectric modulus is measured in shear deformation. Due to the slight deformability

of wood, the technical relevance of piezoelectricity is still low. However, this has recently been enhanced together with the piezoelectric output by partly degrading the wood structure [197].

Although the piezoelectric effect may influence the piezoresistive effect of the adhesive bond line, it was out of the scope of this work to take the effect into account.

The electrical properties of the wood adherend are assumed as being insulating or at least as having a much higher resistivity than the electrically conductive bond line when tested under a standard climate of 20°C and 65% relative humidity (20/65), which results in a WMC of approximately 11.5 %.

### 2.4.3 Moisture influence

During its lifetime, the main influences on wood result from the change in its WMC due to cyclic and random climate changes (day/night, seasonal, prolonged meteorological events). The adsorption and desorption of moisture from the surrounding humidity is a result of the hygroscopic properties of wood. Depending on the exposure time of dry wood to high humidity, the WMC is gradually distributed over the cross-section of wood, as the moisture firstly increases in the outer region of the cross-section. Upon drying, the process is reversed and the outer layer of the cross-section experiences a reduction in WMC and shrinks, later followed by the core (see Fig. 8). Internal stresses are built up as a result of this gradient upon drying [198,199], which results in the formation of cracks, even in absence of external loads [200].

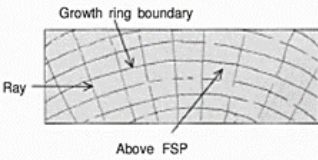
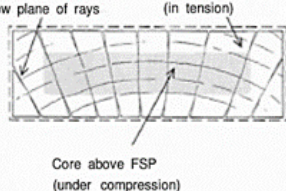
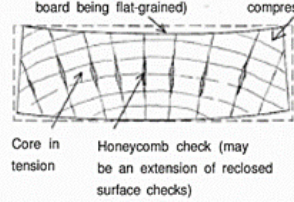
Drying stage	I	II	III
Moisture condition	Above fiber saturation point (FSP) throughout: Drying begins with loss of free water from surfaces.	Shell now below FSP, core still above FSP. Core moisture migrates outward to the shell.	Below FSP throughout, eventually reaches uniformly low EMC.
			
Stress condition	Stress-free	Shell tries to shrink, thus it is in tension across surfaces. Drying sets shell in oversized condition. Shell (in tension) squeezes core into compression.	Core now trying to shrink away from oversized shell. Core develops tension, pulls shell into compression.
Defects	Defect-free	Surface may check; core may collapse as shown.	Interior is case-hardened; if severe, core may honeycomb as shown.

Fig. 8 Example of a moisture gradient resulting from internal stresses in the drying stage and the subsequent potential for crack growth [201].

In addition to these dimensional changes and the resulting stress, the WMC also influences the mechanical and rheological properties of wood [179,184,202]. The strength and stiffness (Young's modulus) decrease with increasing WMC. Higher WMC are generally expected near the bond line, which acts as a diffusion barrier [203]. As a consequence, the piezoresistive bond line will be influenced by a:

- change in dimensions through swelling and shrinking
- decrease in strength/stiffness with increasing WMC

Accordingly, the strain in the bond line will increase over proportionally to the moisture due to increases in the dimension (swelling) and lower stiffness. The piezoresistive reaction will thus increase due to higher strain near the bond line.

Moisture is also known to influence the mechanical properties of the cured adhesive bond line due to water sorption [204]. For example, 1C-PUR decreases in tensile shear strength (TSS), Young's modulus, and elastic modulus by nanoindentation ( $E_r$ , measured in situ in the bond line) [205–207]. Furthermore, high moisture content can decrease the fatigue strength of 1C-PUR compared to PRF [208], which in a dry state shows superior fatigue properties to PRF due to the ductile behaviour.

A changing or high WMC thus not only influences the electrical properties of the wood adherend as a parallel electrical resistor to the bond line but also influences the mechanical properties of the bond line itself. However, it is unclear whether the water sorption of the polymeric adhesive changes the electrical property of the bond line. Under ageing conditions, 1C-PUR (temperature, humidity) was not found to chemically degrade and the wood layer of the wood bond thus remains the reference to determine life expectancy [209].

This influence of WMC is supported by the failure analysis of timber construction in Germany [210,211]. According to the reports, the main failure in timber structures is caused by a cyclic load of moisture and temperature which leads to drying cracks and therefore to a weakening of the timber structure. This phenomenon originates from high transversal tension stress and planning.

Due to the significant influence of the WMC, it was planned to test piezoresistive wood bonds under dry conditions to minimize the influence of higher WMC. Investigations that consider wood with different WMC will form part of future investigations.

### 3 SYSTEMATIC APPROACH

#### 3.1 Systematic approach and overview

In previous preliminary studies, although the concept of piezoresistive polymers was successfully applied to certain wood bonds, it showed some unexpected (or no) piezoresistive reactions in other test series. The literature study of other fields and applications facilitated an assessment to identify several potentially influencing factors on the piezoresistive reaction of the bond line in terms of process and material. Based on the presented theoretical background, the isolation of the most relevant influencing factors on the piezoresistivity of electrically conductive wood bonds became the basis of this thesis. By understanding the various influences, a more reproducible manufacturing approach was made possible, thereby advancing the application of this concept to timber engineering. Therefore, the thesis was approached using a systematic and iterative experimental research design to isolate the most influencing factors.

First of all, based on the literature review and previous research experience, the material variables were reduced by focussing on one adhesive type in addition to carbon allotropes for ECF. Out of the typical wood adhesive types, 1C-PUR was chosen based on the following criteria:

- 1C-PUR consists of only one component, which reduces the development time of the dispersion and the influence from the mixing of two components,
- all preliminary studies on wood adhesives as matrix polymers showed the most consistent and reliable results for 1C-PUR with various carbon allotropes,
- 1C-PURs are widely used structural adhesives in engineered wood, especially for the increasing market share of CLT,
- in contrast to MUF and PRF, they are free of volatile organic compounds (VOCs), which are increasingly regulated
- 1C-PURs do not need thermal energy for curing, making them well suited for future applications.

The selection of moisture-curing 1C-PUR for the manufacturing of piezoresistive adhesives brought higher requirements of the processing route along with it, as dispersions needed to be executed under inert conditions to limit the influence of crosslinking during the dispersion step. This requirement was challenging to fulfil for open systems such as the 3-roll-mill, which according to the literature was shown to be very effective for fibrous ECF such as CNTs and was previously used in this project. On the other hand, shear mixing techniques such as high-speed rotating dissolvers are easy to upscale compared to techniques such as calendering. An implementation involving large quantities at an industrial scale can therefore be achieved with less effort. The production of small amounts of dispersion with a dissolver under inert conditions

became possible with the progression in the development of a laboratory-sized dissolver technique.

The first experiments could therefore be realised with small amounts of adhesive in the dissolver whereby the influence of different dispersion batches could be excluded. The first experiments involved the validation of the influence from filler integration on the mechanical properties of the modified adhesive and the influence of post-curing as an optional treatment for increasing the mechanical and electrical properties of the bond line, resulting in Paper I.

With increasing confidence in the handling of the manufacturing process, the experiments were extended to a wide variety of process parameters ranging from adhesive preparation to manufacturing. Paper II and Paper III show the results of the process influence on the mechanical, electrical, and piezoresistive properties that were based on an experimental design with reduced parameters.

By including the knowledge on the important process influences, piezoresistive bond lines were investigated using impedance spectroscopy as an optional measuring technique (Paper IV) and by upscaling sample sizes with regard to the piezoresistive reaction (Paper V).

In conjunction with this work, the advancement and adaptation of methods to characterize the electrical and piezoresistive properties of electrically conductive wood bonds, for which no previous standardisation existed, was undertaken. The methods are described in detail in Paper II and Paper III.

## **3.2 Applied Methods**

### **3.2.1 Tensile shear test**

Tensile shear tests according to EN 302-1 in a dry state (condition A1) [212] were used as a rapid method for analysing the strength of manufactured wood bonds. The TSS value mostly reflects the strength of the adherend and not the adhesive itself [213], as high wood failure percentages (WFP) indicate a failure in the wood adherend. WFP is usually estimated in 10% increments by visual inspection. In contrast to common 1C-PURs, which are translucent and therefore often hard to recognize, the modified adhesives are black and easy to distinguish from the wood adherend. As a consequence, TSS reflects a correct bonding process, but not the adhesive strength. On the other hand, significant decreases in the wood failure percentage would indicate a decrease in the cohesive adhesive strength. In EN 302-1, the general agreement on a strength threshold of 10 MPa for dry wood bonds is defined, which is used for accreditation of structural applications.

### 3.2.2 Nanoindentation

Nanoindentation is a commonly used technique to study mechanical properties at the micro- and nanoscale. The method utilises small indenter tips that differ in their geometry. For polymers, the Berkovich tip – a three-sided pyramid – is commonly used. Basically, nanoindentation is a variation of the classical indentation test for hardness. Owing to the indenter size, the method is suited for in-situ analysis of the mechanical properties in adhesive bond lines (usually in the range of 30–100  $\mu\text{m}$ ), which has been described in depth by Konnerth et al. [214,215].

From the load-displacement, mechanical properties such as Young's modulus, hardness, and creep can be calculated. The method can therefore provide information on the process influences on the in-situ mechanical properties of the adhesive bond lines.

### 3.2.3 Rheology

Rheology deals with the flow of matter and covers a range of methods for determining the viscoelastic properties of fluids. It can also be used for the analysis of solid materials. While rheology and rheometric measurements are nowadays mainly associated with the flow properties of liquids [216], the rheology of wood was already studied in 1961 by Kollmann [217], who described the heterogenic mechanical properties by using mechanically equivalent circuit diagrams of springs and dampers. Modern rheology offers a wide range of methods to analyse fluids, and the transition of fluids, to viscoelastic solids, thereby overlapping with the dynamic mechanical analysis in this point. Additionally, modification of the instrumentation can also facilitate combinations of methods and the inclusion of interacting surfaces, as shown by the author [218–220]. In this work, only rheometric measurements of liquid adhesives were used to characterise and distinguish the 1C-PUR used (Paper II).

### 3.2.4 Resistance measurements

Resistance measurements under direct current comprise the predominantly used method to characterize electrically conductive nanocomposites. They measure the ohmic resistance of a material and are influenced by the inductivity and capacities of the device under test (DUT). For DC resistance measurements up to 1 G $\Omega$ , digital multimeters (DMM) offer a good trade-off for resistance measurements by working with a known constant current source to calculate the ohmic resistance from the resulting voltage.

Due to their main application area, standards for testing setups are available for electrically conductive adhesives (ECAs). Typical methods to analyse the volume resistivity of electrically conductive adhesive films are, for example, described in the American standard MIL-STD-883E [221]. However, this and similar methods are highly vulnerable to the applied film thickness and the surface roughness of the applied film of

the electrically conductive adhesive [222] and they are therefore hardly applicable to wood bonds. The bond line is neither geometrically defined nor properly represented by a one-sided applied coating on a wood surface. As proposed for other application areas [104], measurements should be done in situ, and include both adherends and adhesives that were cured according to their datasheet.

A setup was thus developed to measure the in-situ resistance of the bond line between two wood adherends, as described in Paper II, Figure 3. It utilised spring-loaded contacts in a measuring frame and conductive silver paste on the end faces of wood bonds. In this configuration, a stable resistance was measurable. Attempts to contact the bond line with conductive silver paste on the plane parallel to the bond line (similar to the standard or film-based setups) led to higher variations in DC resistance. Another influence resulted from the preparation of the end face, as sanded surfaces showed higher variations when compared to cut surfaces [223].

For contacting the specimen, the two-probe and the four-probe methods are available, and both were used in different studies in the scope of this work. For the sake of comparison between different results, the methods were not mixed. The four-probe method is usually known to provide the most precise results for resistance measurements, excluding the cabling and contact resistance of the specimen-electrode interface [131]. On the other hand, two-probe measurements are easier to implement and give reliable results at a higher level of resistance [224], which was the case for all the adhesives under investigation. Regarding the potential influence of contact resistance in two-probe measurements, a conductive silver paste was used in all cases to reduce or eliminate the contact resistance. Additionally, a sub-sample selection was compared using two-probe and four-probe measurements over time to evaluate the noise from the measurements. Similar to other investigations, the two-probe method was only applied if the four-probe method showed a negligible influence due to contact resistance [22,26]. These terms change if the specimen is additionally stressed, which is the case in the piezoresistive measurements that are shown in the corresponding method.

### **3.2.5 Impedance spectroscopy**

Impedance spectroscopy describes a non-destructive measuring technique to characterize the complex electrical impedance of electrode-sample systems over a range of frequencies. Depending on the application field, frequency-dependent impedance measurements are also applied as electrochemical impedance spectroscopy (EIS) to liquid and battery systems or dielectric analysis (DEA) for DUTs with high impedances such as the curing of insulating polymers.

Compared to DC resistance measurements, the impedance is measured if the supply voltage alternates resulting in an alternating current (AC). The applied sinusoidal voltage of the impedance spectrometer to the DUT is in phase with the current if the

DUT only induces ohmic resistance (see Fig. 9a). With further influence from the electrical properties of the DUT, including cabling and contact, the resulting current will be phase shifted.

In complex values, the impedance can be written as:

$$Z = Z' + i Z'' \quad \text{V}$$

where  $Z'$  is the real part and  $Z''$  is the imaginary part of  $Z$ . If represented as a vector (see Fig. 9b), the absolute magnitude of impedance  $Z$  is:

$$|Z| = \sqrt{Z'^2 + Z''^2} \quad \text{VI}$$

From this representation, the phase angle  $\varphi$  can be defined as:

$$\tan \theta = \frac{Z''}{Z'} \quad \text{VII}$$

together with the real and imaginary part  $\text{Re}(Z)$  and  $\text{Im}(Z)$  as:

$$\text{Re}(Z) = Z' = |Z| \cos \theta \quad \text{VIII}$$

$$\text{Im}(Z) = Z'' = |Z| \sin \theta \quad \text{IX}$$

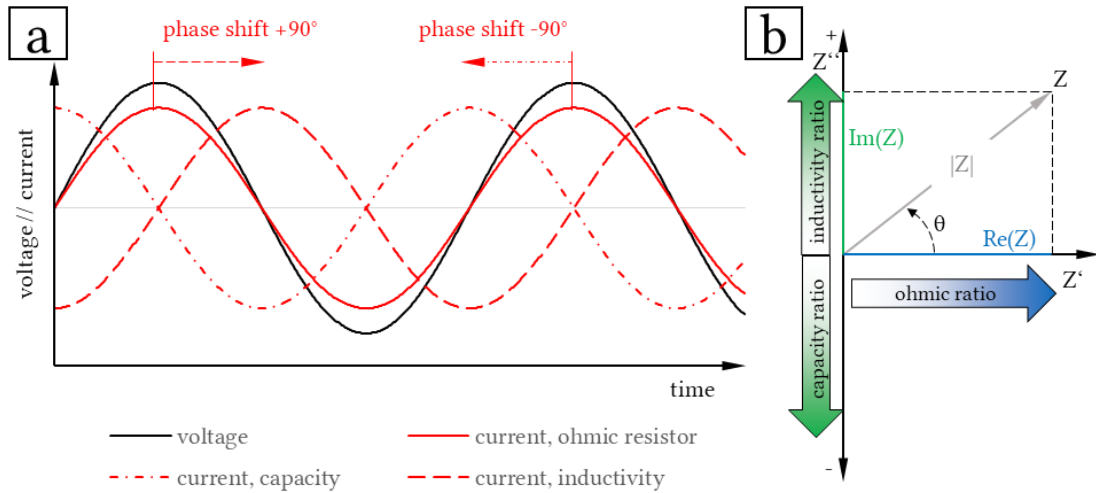


Fig. 9 (a) Alternating voltage waveform for an applied potential and the resulting sinusoidal current under the influence of ohmic resistance, capacity, and inductivity, and (b) complex representation of impedance in vector format.

The imaginary part is the combined measurement of capacity and inductivity in the same DUT. Therefore,  $\text{Im}(Z)$  increases or decreases depending on the ratio of both, as shown in Fig. 9b.



The real part describes the amount of dissipated energy as thermal energy in the sample, while the imaginary part is a measure of the stored energy [225,226]. A connection between DC resistance measurements and impedance spectroscopy can be found in the plateau regimes of frequency-dependent plots (see Fig. 10), where the impedance is independent of the frequency [137].

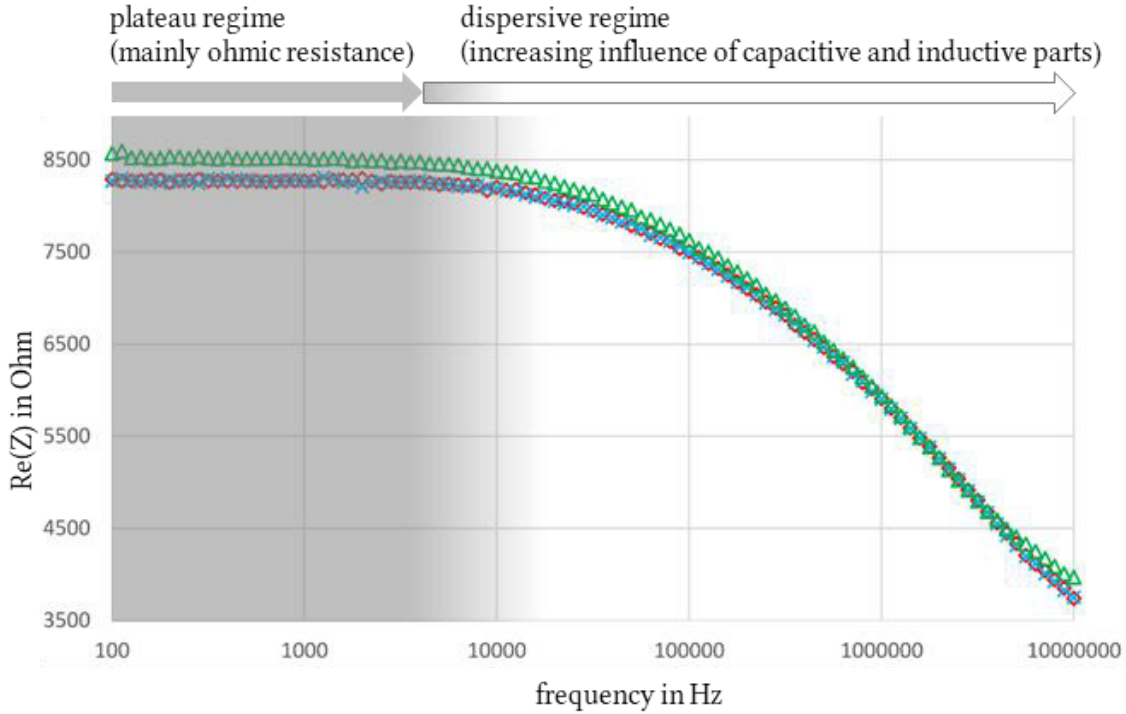


Fig. 10 Plateau and dispersive regimes of the real part in impedance spectroscopic measurements of electrically conductive adhesives.

The piezoresistive effect in nanocomposites occurs in four different changes of the material (section 2.2). The first three changes (intrinsic filler properties, contact changes of filler particles, tunnelling resistance) are measurable by DC measurements or in the real part of impedance measurements. On the other hand, the changes in microcapacitors become detectable in the imaginary part of impedance measurements together with a change in capacity from insulating polymer layers between the separated ECF particles. This made impedance spectroscopy a promising measuring technique compared to DC resistance as the piezoresistive mechanisms can be potentially measured in different frequency ranges [129,130].

The practical challenges concerning impedance measurements are especially found in the measurement setup. Without proper shielding [227], parasitic electromagnetic fields from the surroundings (power supplies, electric cables, etc.) add noise or resonance peaks [228,229]. The measuring setup in Paper IV was developed to consider these challenges.

### 3.2.6 Piezoresistive measurements

In Paper III to Paper V, combinations of mechanically-induced stress and resistance-based measurements (DC resistance and impedance spectroscopy) on piezoresistive adhesive bond lines were reported, which can be summarized as piezoresistive measurements. Piezoresistivity measurements are widely reported in the context of nanocomposites for strain sensing and also for some adhesives für damage detection. Unfortunately, these setups did not apply to the piezoresistive measurements of wood bonds, as these setups use:

- defined film specimens and are not inserted between two adherends [24–26,29,30,124,135],
- the electrical conductive adherends as electrodes [118]
- polymers, which can be produced without adherends or do not change their structure due to adherend material [133].

No specific standard that could be adapted to the task at hand was available or reported by others. Therefore, different test setups and methods were developed within the scope of this thesis as described in Paper III to Paper V. Especially the geometrical isolation of the electrical contact from mechanical strain was focussed to counteract the influence of change in contact resistance on the microscopic level as was shown for the compression between electrodes and surface micro-roughness [230,231].

## 4 MAIN INVESTIGATIONS

List of peer-reviewed papers:

- Paper I**            Winkler C, Schwarz U, Konnerth J. Effect of thermal post curing on the micro- and macromechanical properties of polyurethane for wood bonding. Appl Adhes Sci 2018;6(1)
- Paper II**            Winkler C, Konnerth J, Gibcke J, Schäfer J, Schwarz U. Influence of polymer/filler composition and processing on the properties of multifunctional adhesive wood bonds from polyurethane prepolymers I: mechanical and electrical properties. J Adhesion 2020;96(1-4):165–84
- Paper III**            Winkler C, Schäfer J, Jager C, Konnerth J, Schwarz U. Influence of polymer/filler composition and processing on the properties of multifunctional adhesive wood bonds from polyurethane prepolymers II: electrical sensitivity in compression. J Adhesion 2020;96(1-4):185–206
- Paper IV**            Schäfer J, Jager C, Schwarz U, Winkler C. Improving the usability of piezoresistive bond lines in wood by using impedance measurements. Wood Sci Technol 2021;55(4):937–54
- Paper V**            Winkler C, Haase S, Schwarz U, Jahreis M. Piezoresistive bond lines for timber construction monitoring—experimental scale-up. Wood Sci Technol 2021;55(5):1379–400

## Corrigenda

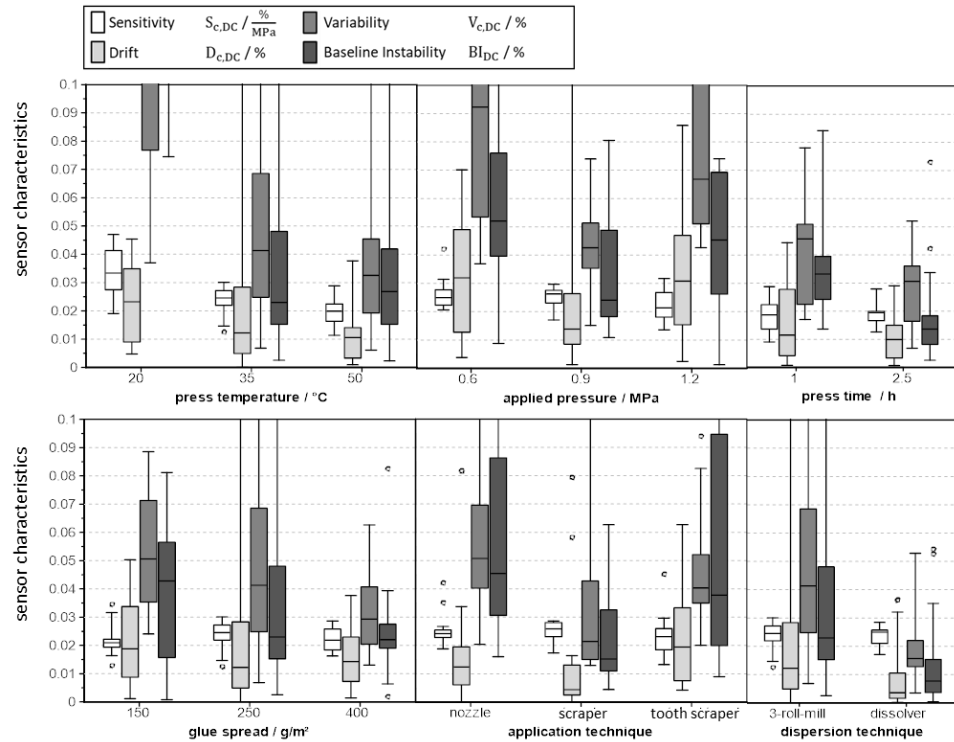
Paper I, Page 6, line 7-10

*Delete:* Indentation creep  $C_{IT}$  was calculated according to the test bench of CSM Instruments from the change in indentation depth during the holding segment, where the applied load remains constant (see Fig. 3) as described in a previous study [18].

*Insert:* Indentation creep  $C_{IT}$  was calculated according to the test bench of CSM Instruments [XX]<sup>1</sup> from the change in indentation depth during the holding segment, where the applied load remains constant (see Fig. 3).

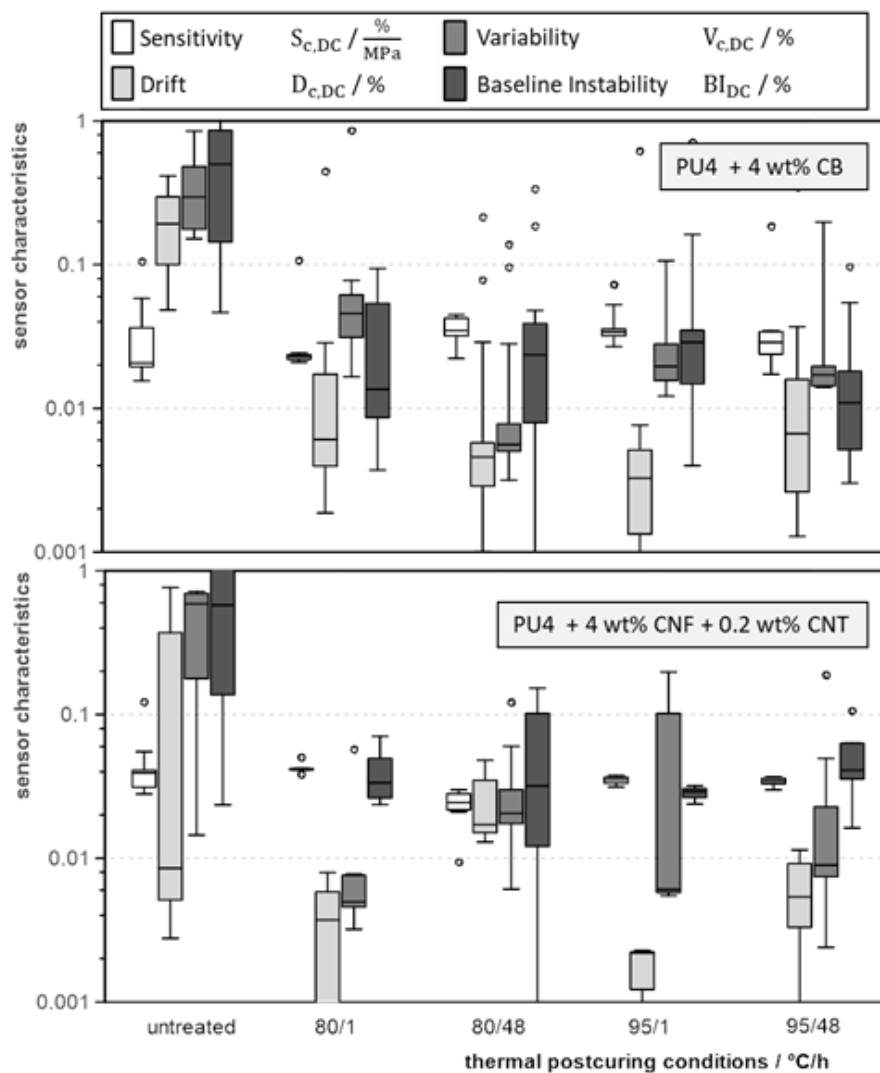
Paper III, Figure 11

*Replace with:*



<sup>1</sup> CSM Instruments. Applications Bulletin No. 18: Overview of mechanical testing standards; 2002.

Replace with:



## **Effect of thermal post curing on the micro- and macromechanical properties of polyurethane for wood bonding**

Christoph Winkler<sup>1,2</sup>, Ulrich Schwarz<sup>1</sup> and Johannes Konnerth<sup>2</sup>

<sup>1</sup> University of Applied Sciences Eberswalde, Faculty of Wood Engineering, Eberswalde, Germany

<sup>2</sup> BOKU - University of Natural Resources and Life Sciences, Institute of Wood Technology and Renewable Materials, Vienna, Austria

### **Declaration of author contributions**

Winkler, Schwarz and Konnerth jointly designed the experiment. Winkler prepared all adhesives, samples and tested lap-joints, Winkler performed the nanoindentation experiments under guidance of Konnerth. All authors jointly evaluated the results, discussed them and contributed to the manuscript. Writing and editing of the final manuscript was done by Winkler. All authors read and approved the final manuscript.

RESEARCH

Open Access



# Effect of thermal postcuring on the micro- and macromechanical properties of polyurethane for wood bonding

Christoph Winkler<sup>1,2</sup>, Ulrich Schwarz<sup>1</sup> and Johannes Konnerth<sup>2\*</sup>

\*Correspondence:  
johannes.konnerth@boku.  
ac.at

<sup>2</sup> Institute of Wood  
Technology and Renewable  
Materials, BOKU-University  
of Natural Resources and Life  
Sciences, Vienna, Austria  
Full list of author information  
is available at the end of the  
article

## Abstract

The optimization of mechanical properties of adhesive bonds is of interest especially in structural applications. Besides transferring stresses, bondlines can also provide additional functionality, such as measuring deformations in structural timber applications by electrically conductive adhesives. This study investigates the influence of a thermal postcure treatment of polyurethane bonded wood joints. Bonded beech wooden samples were manufactured with three adhesives—a commercial one-component polyurethane for structural laminated timber and two modified ones, filled with electrically conductive particles. Adhesive bonds were subjected to a subsequent postcuring at 80 and 95 °C for 1 and 48 h, respectively. Mechanical properties of the bonds were studied on the macroscopic level by tensile shear tests and the properties of the cured adhesive on the microscopic level by nanoindentation. As a result, the tensile shear strength slightly dropped with addition of filler, while all specimens still fulfilled the requirement of EN 302-1 in dry condition. Nanoindentation revealed minor decreases in mechanical properties of the cured adhesive with postcuring time for two adhesives and a different reaction of carbon black filled polyurethane, as the creep factor decreases with the thermal postcure.

**Keywords:** Polyurethane prepolymer, Carbon black, Carbon nanofibers, Carbon nanotubes, Thermal postcure, Mechanical properties of adhesives, Nanoindentation, Wood adhesives

## Introduction

The importance of mechanical properties of adhesives is evident, as the bond has to transfer mechanical stresses from one adherend to the other. When the adhesive is used for further functions like deformation measurements in structural timber, mechanical properties of the bondline will become even more important as the stiffness and creep of the adhesive polymer influences the sensor properties.

One approach to use the adhesive bondline as a sensor, is in providing the adhesive electrical conductivity [1, 2]. Such adhesives are produced by dispersing electrically conductive fillers into the electrically insulating adhesive matrix. With a sufficient dispersion quality they exhibit a strain-dependent electrical resistance change similar to a strain gauge.

One-component polyurethane prepolymers (1C-PUR), such as those used frequently for structural wood bonding, consist of relatively high molecular weight polyols with a stoichiometric excess of isocyanates. The crosslinking to form the polymeric adhesive film is effected by the reaction of the isocyanate with water, which is supplied to the adhesive film as air and wood moisture [3]. In the cross-linked prepolymer urethane bonds (present in prepolymer macromolecules, as a result of the reaction with alcohol groups) are found in addition to urea bonds (reaction of isocyanate with water).

A change in mechanical properties can be achieved by further cross-linking of the polymeric structure, which leads to higher strength, elastic modulus and creep resistances [4]. For polyurethanes, the linear polyurethane macromolecules needs to be converted into a three-dimensional structure with an elastomeric or duromeric character [5, 6] by forming allophanate and biuret bonds from the reaction of urethane and urea bonds with free isocyanates. The occurrence of this chemical reaction depends mainly on the temperature, which ensures the necessary reaction energy of the active hydrogen at the nitrogen in the urethane bond.

Literature indicates a range of different temperatures necessary to start forming allophanates and biuretes between 80 and 140 °C [4–8].

Additionally, the crosslinking by forming of allophanates and biuretes is sometimes reported as reversible [7] and increases with temperature and time [8]. Below 60 °C this crosslinking is very slow, but in bulk at high temperatures such as 145 °C it can also reach a conversion of 10% of all nitrogen-containing groups [8].

Thermal postcuring of samples bonded with polyurethane has been investigated by different authors and showed no obvious positive or negative effect: Bitomski et al. [9] reported of a 2-component polyurethane adhesive in which a thermal post-treatment at 80 °C resulted in increased peel strength. Additionally, a heat treatment at 60 °C after 7 days of curing at 20 °C indicated by IR spectroscopic that the converting of monomers to a certain state of equilibrium can be accelerated again. Richter et al. [10] investigated the temperature-dependent creep of seven different 1C-PUR by combining results from thermomechanical analysis (TMA), creep under temperature, load and analysis of chemical composition by carbon-13 nuclear magnetic resonance spectroscopy (<sup>13</sup>C-NMR). In addition, they applied a thermal postcuring of 80 °C for 4 h and showed that out of all the tested adhesives, only one showed an improvement in creep resistance after postcuring, while all others deteriorated. They concluded that the heat treatment has no positive effect on 1C-PUR in contrast to epoxy resins.

Difficult for the application of postcuring on wood adhesive bonds is that high temperatures can degrade the wood substrate, but for postcuring a relative high temperature is necessary. Small physical changes start with the emission of extractives at temperatures of around 40 °C [11]. Degradation starts with the hydrolysis of hemicellulosis in small amounts at 80 °C, followed by degradation of cellulose at 100 °C [11]. Thermal degradation of moisture-cured polyurethanes has also been reported to start at temperatures higher than 120 °C [12].

From the state of the art it is unclear whether an improvement of polyurethane by postcuring is possible and furthermore at which temperatures such a postcuring can effect the mechanical properties of the corresponding adhesive.



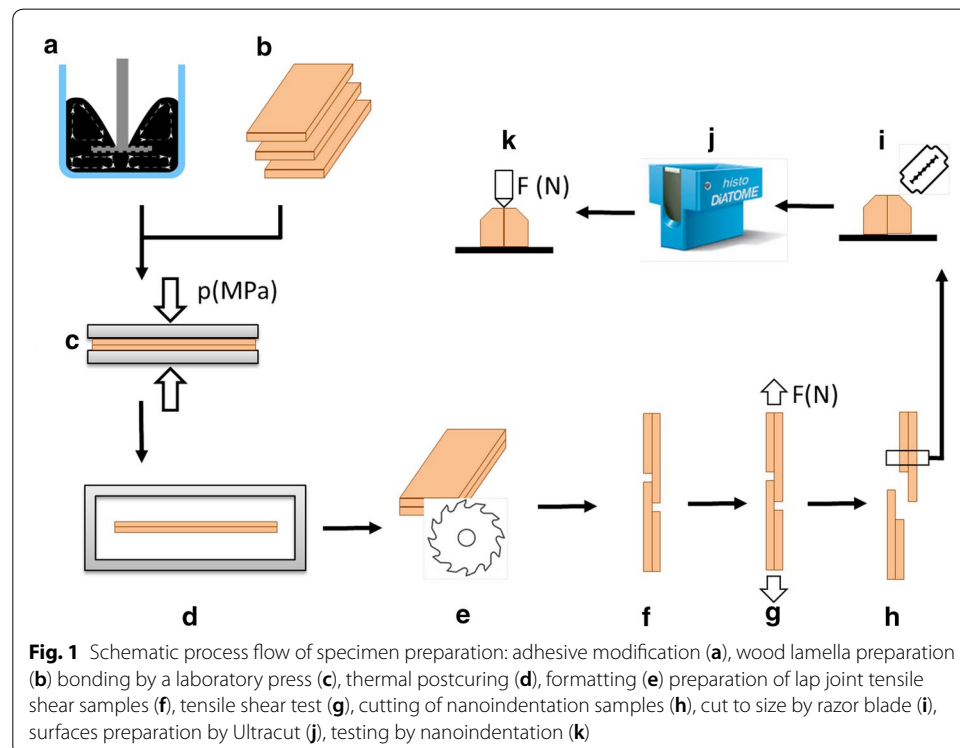
The aim of the present study is to examine the hypothesis that subsequent heat treatment of polyurethane-based conductive wood adhesive joints (postcuring) improves the mechanical properties (strength, stiffness, hardness, creep resistance) of the bond, respectively the adhesive.

For this, lap joint tensile shear tests were used for investigating macromechanical properties and nanoindentation for micromechanical properties. As adhesives a commercial one-component polyurethane prepolymer was used and two variations from the same, each mixed with electrically conductive fillers.

## Methods/experimental

### Preparation

The process flow to produce adhesive bond specimens for micro- and macromechanical testing is illustrated in Fig. 1. Specimen preparation started by manufacturing different adhesives by dispersing electrically conductive fillers. Based on a commercial 1C-PUR adhesive (Jowapur 686.60, Jowat SE, Detmold, Germany), two additional modified 1C-PUR were produced by adding conductive particles into the adhesive, resulting in three different adhesives. The final modified adhesives are composed of the mentioned 1C-PUR with 4 wt% carbon black (Ketchenblack EC300J, Akzo Nobel Functional Chemicals B.V., Arnhem, The Netherlands), further named 1C-PUR-CB, and with a mixture of 2 wt% carbon nanofibers (PR-25-XT-HHT, Pyrograf Products Inc., Cedarville, USA) as well as 0.2 wt% carbon nanotubes (NC7000, Nanocyl S.A., Sambreville, Belgium), further named 1C-PUR-CNFT. The amount and composition of filler was determined in preliminary tests with the aim to find dispersions with sufficient processability and a low



electrical resistance of the bondline. Table 1 summarizes the relevant measurements of electrical resistance and the quantitative evaluation of the processability. The DC electrical resistance was measured with a digital multimeter (NI PXI 4071, National Instruments Germany GmbH, Munich, Germany) on bondlines with the dimensions of 20 mm (width), 55 mm (length) and around 0.1 mm (thickness). Due to the variability of wood bondlines (see also) the resistivity could be calculated reliable.

The manufacturing process of the conductive adhesives covered the following steps. First, the electrically conductive fillers have been dried at 103.5 °C for 24 h to reduce the overall moisture in the dispersion process of a moisture curing 1C-PUR. Afterwards, a dispersion container has been prefilled with argon to further reduce the amount of moisture in the dispersion process. Laboratory sized sample amounts of 40 g were produced by a miniaturized dispersing technique. The dispersion technique used a cooled laboratory container, a Ø25 mm dissolver disc (VMA Getzmann GmbH, Reichshof, Germany) and a rotational frequency of 15,000 rpm, which was adjusted with changing viscosity to maintain the doughnut effect according to manufacturer recommendations.

Clear, defect-free wood lamellas of beech wood (*fagus sylvatica* L.) were selected and prepared according to EN 302-1 [13]. The bulk density of the beech substrate was  $648 \pm 11 \text{ kg m}^{-3}$  at an equilibrium wood moisture content of  $10.8 \pm 0.2\%$ . The lamellas were bonded in pairs at 1.0 MPa and 30 °C in a laboratory press for 1.5 h according to the datasheet of Jowapur 686.60. After conditioning in standard climate (20 °C, 65% relative humidity) for 7 days, the two-layered lamellas were postcured at different conditions, as shown in Table 2.

Due to the expected thermal degradation of the wood adherend at excessive temperature, as outlined in the introduction, postcure temperatures were selected to be 80 °C and 95°. In order to prevent wood from dimensional changes as a result of loss or uptake of moisture, humidity has been selected according to the extended Keylwerth-chart of Böhner [14] to maintain the equilibrium wood moisture of beech constant (82% relative humidity at 80 °C; 85% at 95 °C). At these postcuring conditions no mechanical stress due to moisture induced swelling and shrinkage movements of the wood substrate in the bondline is expected.

Subsequent to the thermal treatment all lamellas were conditioned for 7 days at standard climate and lap-joint tensile shear specimens were manufactured according to EN 302-1 (Fig. 1f), resulting in 10–15 bonded specimens with dimensions of  $150 \times 20 \times 10 \text{ mm}^3$  for each postcure parameter. From the tested tensile shear specimen nanoindentation samples were cut from intact parts, where no damage due to testing or clamping was visible. Bonded by Epoxy resin on metal disks, the samples were cut to size

**Table 1 Results of preliminary tests to evaluate two different suitable dispersions of electrical conductive fillers with in component polyurethane (1C-PUR)**

Adhesive	1C-PUR							
	CNF		CNT		CNF/CNT		CB	
Filler in wt%	2	3	0.25	0.5	1	2/0.2	3	4
Processability	Good	Good	Good	Moderate	Poor	Good	Good	Moderate
Resistance [ $\Omega$ ]	1.2M	200k	4M	50k	19k	20k	1M	34k

**Table 2 Thermal postcure parameters and resulting terminology for the specimen series, made from 2-layered beech lamellas, bonded by one-component polyurethane (1C-PUR), mixed with carbon nanofibers/carbon nanotubes (CNFT) or carbon black (CB)**

Adhesive	Temperature/relative humidity (°C/%)	Postcure time (h)	Terminology
1C-PUR	–	–	PU
	80/82	1	PU-80/1
		48	PU-80/48
	95/85	1	PU-95/1
		48	PU-95/48
1C-PUR-CNFT	–	–	CNFT
	80/82	1	CNFT-80/1
		48	CNFT-80/48
	95/85	1	CNFT-95/1
		48	CNFT-95/48
1C-PUR-CB	–	–	CB
	80/82	1	CB-80/1
		48	CB-80/48
	95/85	1	CB-95/1
		48	CB-95/48

by a razor blade. Smooth surface was achieved by using a Leica Ultracut-R microtome (Leica, Ultracut R, Wetzlar, Germany) equipped with a Diatome Histo diamond knife (Diatome, Histo, Nidau, Switzerland).

#### **Tensile shear strength**

Macromechanical properties of polyurethane bonded wood were characterised by tensile shear tests. Specimen dimensions are specified in EN 302-1 [13], the shear area was  $20 \times 10 \text{ mm}^2$ . A universal testing machine (Zwick/Roell Z020, load cell 20kN, Ulm, Germany) was used to carry out the tests according to EN 302-1 with a cross head speed of 1 mm/min. Tensile shear strength was calculated from the maximum force at shear failure divided by the overlapping area of the lap joint. The failure zone was analysed visually for percentage of wood failure. Corresponding wood failure amount was noted in 10% steps.

#### **Nanoindentation**

Characterisation of the micromechanical bondline properties was done by nanoindentation. All nanoindentation experiments were carried out by a Hysitron TriboIndenter system (Hysitron, Minneapolis, MN), equipped with a Berkovich type indenter (three-sided pyramid diamond). From each series, two to four specimens have been prepared for nanoindentation according to the described method in 2.1 and were clamped magnetically to the nanoindenter sample stage. Each specimen was characterized by at least 20 indents in the region of the bondline, giving 40–80 measurements for each series, which is known as representative from previous studies [15, 16]. Figure 2 shows the evenly distributed indents on one sample bondline. The experiments were performed in load controlled mode, using a preforce of 2  $\mu\text{N}$  and a three segment load ramp, which is shown in

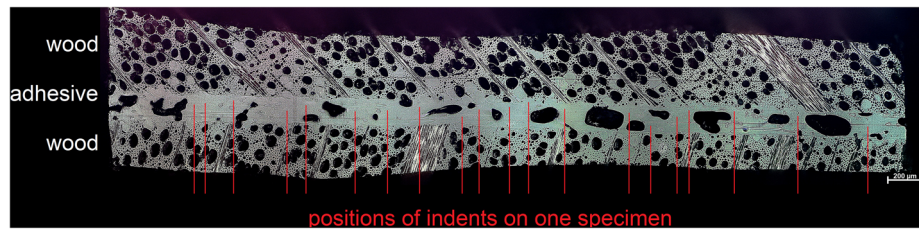


**Fig. 2** Overview of an exemplary adhesive bondline between wooden adherends, prepared for nanoindentation. Red lines point to selected indent positions within the bondline

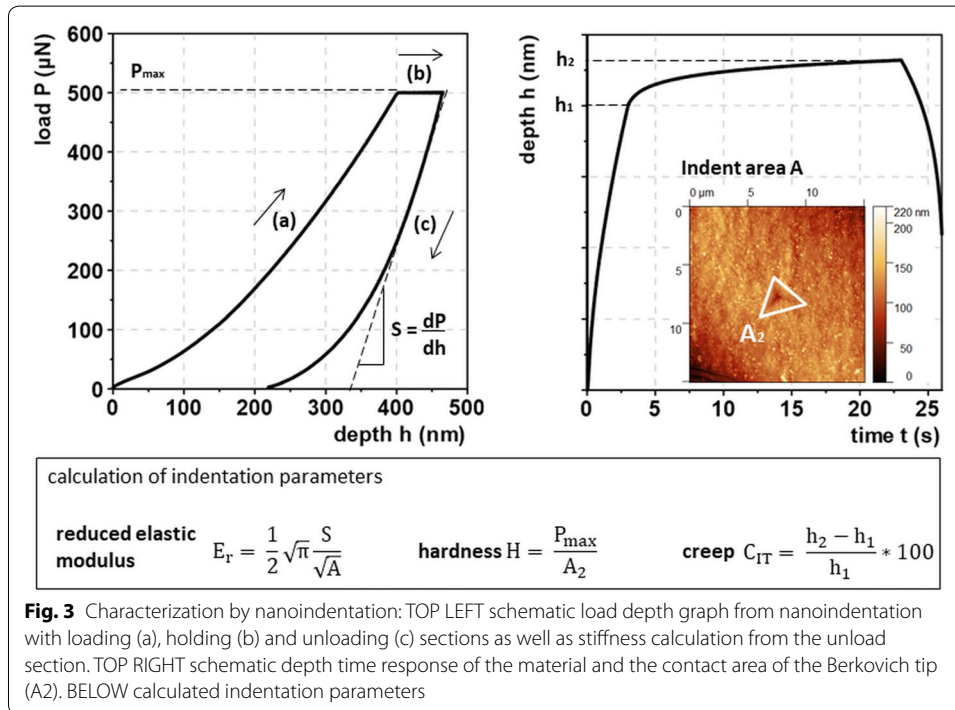
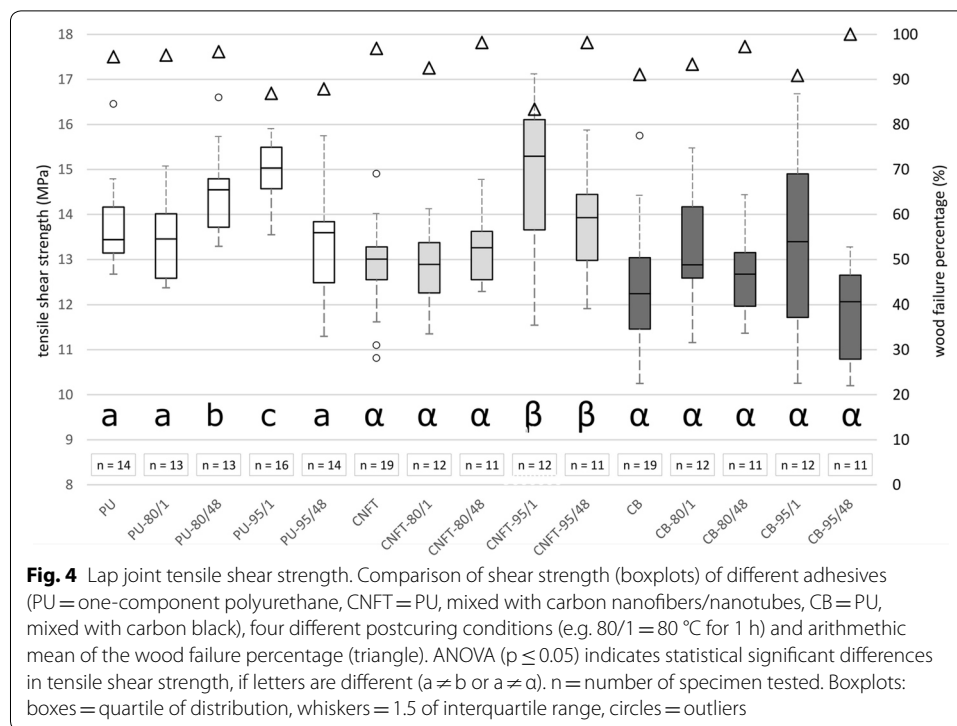


**Fig. 3** After reaching preforce, the maximum testing force of 500  $\mu\text{N}$  has been reached in 3 s, was held for 20 s and was linearly released within 3 s.

The load-depth curve was analysed using the Oliver and Pharr method [17], resulting in reduced elastic modulus and hardness of the bondline. The reduced elastic modulus  $E_r$  was calculated from the measured unloading stiffness ( $S$ ) (see Fig. 3). Hardness ( $H_{\text{Bondline}}$ ) was calculated by dividing the maximum load by the contact area at the end of the holding segment (see Fig. 3). Indentation creep  $C_{IT}$  was calculated according to the test bench of CSM Instruments from the change in indentation depth during the holding segment, where the applied load remains constant (see Fig. 3) as described in a previous study [18].



## Results and discussion

### Lap joint tensile shear strength

On the macroscopic level tensile shear strength of lap joint specimens was measured to characterise probable changes due to thermal postcuring as shown in Figure 4. A one-way analysis of variance (ANOVA,  $p \leq 0.05$ ) was used to statistically evaluate the postcuring effect on the tensile shear strength.

All specimens, untreated and thermal postcured, show higher tensile shear strength values than 10 MPa thus fulfilling the requirements for structural wood bonding according to EN 302-1 in dry condition (A1 treatment). Additionally, all specimens show a high mean wood failure percentage of 80–100%, implicating a good bonding quality.

Comparing the different non-treated adhesives (PU vs. CNFT vs. CB, see Table 2), both adhesives filled with particles show significantly lower tensile shear strength than the unfilled polyurethane. The type of filler did not show significant differences.

Within the group of PU the thermal postcure leads to no differences for 80/1 (80 °C for 1 h) and 95/48, but at a longer treatment of 48 h at 80 °C the tensile shear strength increases significantly (ANOVA,  $p \leq 0.05$ ). The highest value of tensile shear strength is reached at 95/1.

Within the group of CNFT significant increases in tensile shear strength were only measured for treatments at 95 °C.

Within the group of CB differences in tensile shear strength can be recognized, but they seem to be neither systematic nor statistically significant.

Overall, the presented dataset indicates significant higher tensile shear strength values for PU-80/48, PU-95/1, CNFT-95/1 and CNFT-95/48. Therefore, no systematic

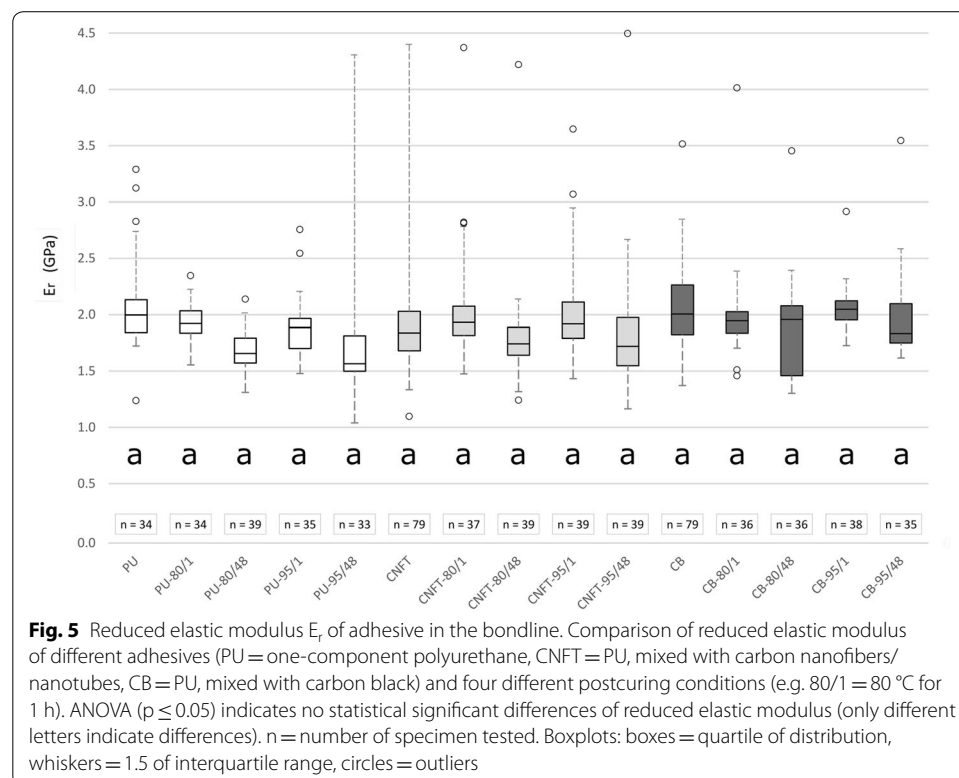
effect of thermal postcure on the lap joint tensile shear strength is evident. As no significant decrease for any postcure treatment for all three adhesives can be measured, it can be stated that this range of postcuring parameters didn't damage the wood adhesive bond. Based on the high wood failure percentage, the data set mainly reflects the shear strength of the wood adherend [18]. Thus no distinct conclusion can be drawn regarding the thermal postcuring effect on the adhesive.

The decrease in tensile shear strength with filler concentration has been reported in literature [19] already and is regarded as one of the drawbacks of electrically conductive fillers. As the wood failure percentage indicates that failure happens mostly in the wood adherend and in the wood-adhesive interphase, it's indicated that the incorporation of the filler doesn't seem to impact the bond strength of glued wooden samples according to EN 302-1 like in other applications.

### Micromechanical properties of adhesive by nanoindentation

Nanoindentation experiments were used to characterise the mechanical properties of the bondline on the microscopic level. Figure 5 shows the reduced elastic modulus ( $E_r$ ), Fig. 6 the hardness ( $H_{\text{Bondline}}$ ) and Fig. 7 the creep factor ( $C_{\text{IT}}$ ).

The non-treated adhesives (PU, CNFT and CB) show measured values of 2GPa ( $E_r$ ) and 0.11GPa ( $H_{\text{Bondline}}$ ) and are therefore in the range of usual one-component polyurethane prepolymers [20]. The investigated filler contents reveal no statistical significant difference (ANOVA,  $p \leq 0.05$ ) of  $E_r$  and  $H_{\text{Bondline}}$ , only the creep factor ( $C_{\text{IT}}$ ) increases slightly, but significant.



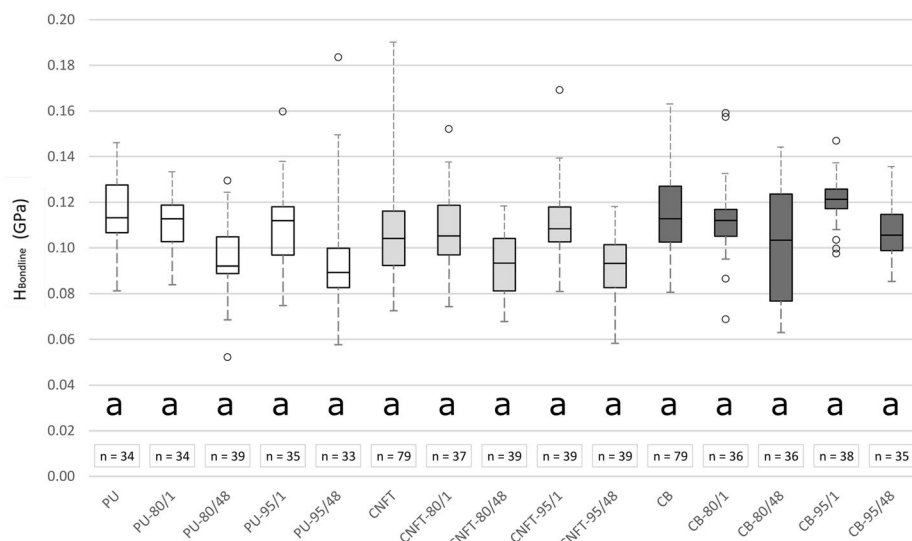


**Fig. 6** Hardness of adhesive in the bondline ( $H_{\text{Bondline}}$ ). Comparison of  $H_{\text{Bondline}}$  of different adhesives (PU = one-component polyurethane, CNFT = PU, mixed with carbon nanofibers/nanotubes, CB = PU, mixed with carbon black) and four different postcuring conditions (e.g. 80/1 = 80 °C for 1 h). ANOVA ( $p \leq 0.05$ ) indicates no statistical significant differences of reduced elastic modulus (only different letters indicate differences).  $n$  = number of specimen tested. Boxplots: boxes = quartile of distribution, whiskers = 1.5 of interquartile range, circles = outliers

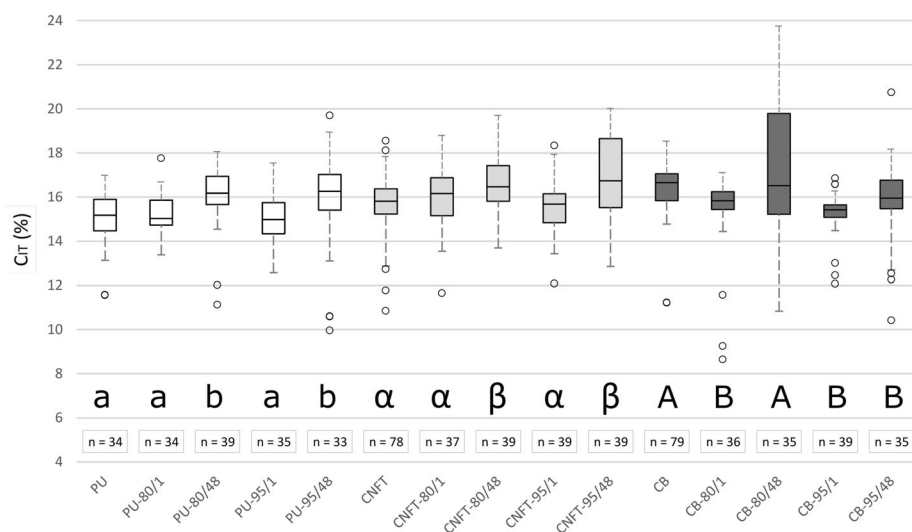
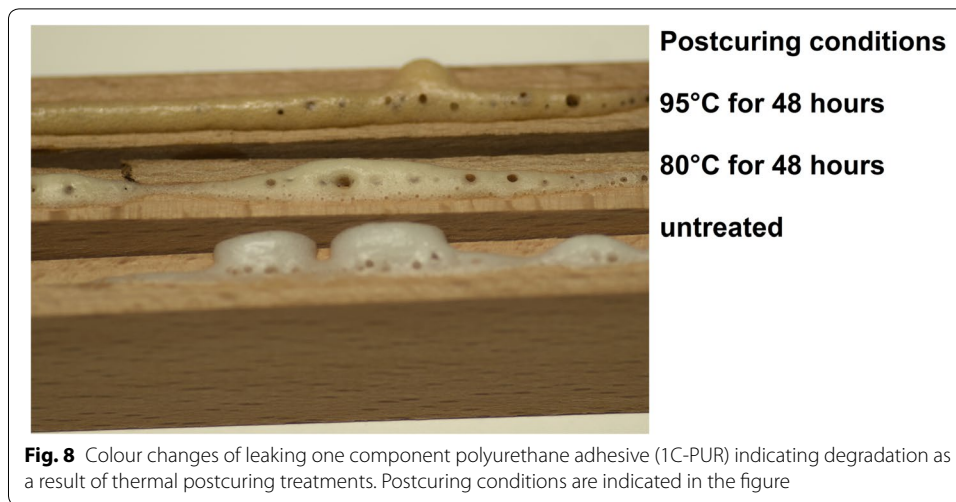


**Fig. 7** Creep factor  $C_{IT}$  of adhesive in the bondline. Comparison of creep factor of different adhesives (PU = one-component polyurethane, CNFT = PU, mixed with carbon nanofibers/nanotubes, CB = PU, mixed with carbon black), four different postcuring conditions (e.g. 80/1 = 80 °C for 1 h) and arithmetic mean of the wood failure percentage (triangle). ANOVA ( $p \leq 0.05$ ) indicates statistical significant differences of creep factor, if letters are different ( $a \neq b$  or  $a \neq \alpha$  or  $a \neq A$ ).  $n$  = number of specimen tested. Boxplots: boxes = quartile of distribution, whiskers = 1.5 of interquartile range, circles = outliers

The measurements reveal a different effect of the thermal postcure on PU and CNFT versus CB. A systematic effect of postcuring time was found for PU and CNFT, deteriorating the mechanical properties (decrease of  $E_r$  and  $H_{\text{Bondline}}$ , increase of  $C_{IT}$ ). In





contrast CB shows no systematic effect and partly improves his mechanical properties (decrease of  $C_{IT}$ ).

Within the groups of PU and CNFT all measured properties ( $E_r$ ,  $H_{\text{Bondline}}$  and  $C_{IT}$ ) change systematically with thermal postcuring time, but differences are only significant for the creep factor (ANOVA,  $p \leq 0.05$ ). While no difference is visible when thermally postcured for 1 h, a longer postcuring of 48 h results in a decrease of  $E_r$  and  $H_{\text{Bondline}}$  (− 10 to − 20.3%) and in an increase of  $C_{IT}$  (+ 2 to + 8.5%).

Within the group of CB no significant change of  $E_r$  and  $H_{\text{Bondline}}$  is indicated, but a significant decrease of  $C_{IT}$  (− 5 to − 7.5%) for three of four thermal postcuring conditions (ANOVA,  $p \leq 0.05$ ). Only the treatment of 80 °C for 48 h shows no significant difference.

Additionally, a significant difference between the creep factor of all adhesives (PU vs. CNFT vs. CB) was found. The creep factor changes with the filler material, with an arithmetic mean of 15% for PU, 15.7% for CNFT and 16.4% for CB.

Comparing the results of PU and CNFT, the decrease in  $E_r$  and  $H_{\text{Bondline}}$  together with the significant increase in creep factor indicates that the polyurethane bondline became softer, even after reconditioning to 20 °C for 7 days. While other studies showed a softening of polyurethane adhesive bondlines with increasing testing temperature [21, 22], the remaining decrease of properties after reconditioning is obvious. A possible reason could be the postcuring condition, which also included high humidity. While the equilibrium wood moisture of beech was hold constant, the high humidity could have supported the polyurethane degradation by oxidation or hydrolysis [23]. Indication for degradation by oxidation is a darker color, which was visible at the foamed polyurethane in the bondline of the series PU-80/48 and PU-95/48 (Fig. 8). As the oxidative degradation enhances with the amount of surface, the color of foamed polyurethane can't be alone used to prove this assumption.

As carbon black filled polyurethane (CB) didn't decrease in  $E_r$  and  $H_{\text{Bondline}}$ , but partly increases in  $C_{IT}$ , the filler seems to have a stabilizing effect on the adhesive.

The stabilizing effect of carbon black could be attributed to chemical interaction between carbon black with polyurethane or other mechanisms. However, the type of



interaction was not addressed within the frame of this study, but will be a topic of further work.

## Conclusion

Several conclusions can be drawn from the results:

1. One-component polyurethane prepolymers (1C-PUR) with different filler was successfully produced and reached tensile shear strength values between 10.2 and 16.4 MPa. Through addition of electrically conductive filler the tensile shear strength of the 1C-PUR significantly decreased without breaking the requirements of EN 302-1 in dry (A1) condition.
2. The applied postcuring leads to higher tensile shear strength for single treatment conditions, but in no case to a decrease. However, a systematic trend was not measurable.
3. Based on nanoindentation measurements of the bondline, a slight, but insignificant decrease of  $E_r$  and  $H_{\text{Bondline}}$  for two adhesives (PU and CNFT) was measurable for thermal postcuring times of 48 h. The creep factor of these adhesives increases significantly for thermal postcuring times of 48 h.
4. Carbon black filled polyurethane prepolymers (CB) differs from PU and CNFT in their response to the thermal postcuring and exhibit a stabilizing effect.

## Abbreviations

1C-PUR: one-component polyurethane prepolymer; TMA: thermomechanical analysis;  $^{13}\text{C}$ -NMR: carbon-13 nuclear magnetic resonance; 1C-PUR-CB: one-component polyurethane prepolymer, filled with 4 wt% carbon black; 1C-PUR-CNFT: one-component polyurethane prepolymer, filled with 2 wt% carbon nanofibers and 0.2 wt% carbon nanotubes; ANOVA: analysis of variance; PU: further abbreviation of 1C-PUR to include process parameters in the abbreviation; CB: further abbreviation of 1C-PUR-CB to include process parameters in the abbreviation; CNFT: further abbreviation of 1C-PUR-CNFT to include process parameters in the abbreviation;  $C_T$ : creep factor;  $E_r$ : reduced elastic modulus;  $H_{\text{Bondline}}$ : hardness of the bondline.

## Authors' contributions

CW, US and JK jointly designed the experiment. CW prepared all adhesives, samples and tested lap-joints, CW and JK performed nanoindentation experiments. All authors jointly evaluated the results, discussed them and contributed to the manuscript. All authors read and approved the final manuscript.

## Author details

<sup>1</sup> Faculty of Wood Engineering, University of Applied Sciences Eberswalde, Eberswalde, Germany. <sup>2</sup> Institute of Wood Technology and Renewable Materials, BOKU-University of Natural Resources and Life Sciences, Vienna, Austria.

## Acknowledgements

We would like to thank Prof. Klaus-Uwe Koch (Westfälische Hochschule, Germany) for valuable discussion regarding the laboratory sized dissolver technique.

## Competing interests

The authors declare that they have no competing interests.

## Availability of data and materials

All relevant data are presented in the manuscript, if needed additional information may be made available upon request.

## Funding

No funding was received.

## Publisher's Note

Springer Nature remains neutral with regard to jurisdictional claims in published maps and institutional affiliations.

Received: 11 October 2018 Accepted: 27 October 2018

Published online: 10 November 2018

**References**

- Winkler C, Schwarz U. Characterization of adhesively bonded wood structures by electrical modification of the bonding system. In: Vienna University of Technology, Austria, editor. WCTE 2016: proceedings. Vienna: Vienna University of Technology; 2016.
- Kang I, Schulz MJ, Kim JH, et al. A carbon nanotube strain sensor for structural health monitoring. *Smart Mater Struct*. 2006;15:737–48.
- Habenicht G. Kleben: Grundlagen, Technologien, Anwendungen, 6. aktualisierte ed. Berlin: Springer; 2009.
- Pocius AV, Chaudhury M, editors. Adhesion science and engineering—2: surfaces, chemistry and applications. Amsterdam: Elsevier Science; 2002.
- Randall DJ, Lee S. The polyurethanes book [Huntsman Polyurethanes]. New York: John Wiley & Sons, [Everberg, Belgium]; 2002.
- Stepanski H, Leimenstoll M. Polyurethan-Klebstoffe: Unterschiede und Gemeinsamkeiten, 1. Aufl. 2016. essentials. Wiesbaden: Springer Fachmedien Wiesbaden; Imprint Springer Vieweg; 2016.
- Ionescu M. Chemistry and technology of polyols for polyurethanes. Shrewsbury: Smithers Rapra; 2005.
- Delebecq E, Pascault J-P, Boutevin B, et al. On the versatility of urethane/urea bonds: reversibility, blocked isocyanate, and non-isocyanate polyurethane. *Chem Rev*. 2013;113(1):80–118. <https://doi.org/10.1021/cr300195n>.
- Bitomsky P, Krieger A, Nies C, et al. Polyurethane adhesives: influence of curing on dynamics and property changes with time. In: EURADH—11th European adhesion conference; 2016.
- Richter K, Pizzi A, Despres A. Thermal stability of structural one-component polyurethane adhesives for wood—structure-property relationship. *J Appl Polym Sci*. 2006;102(6):5698–707. <https://doi.org/10.1002/app.25084>.
- Navi P, Sandberg D. Thermo-hydro-mechanical processing of wood. 1st ed. Lausanne: EPFL Press; CRC Press; 2012.
- Chattopadhyay DK, Sreedhar B, Raju KVS. Thermal stability of chemically crosslinked moisture-cured polyurethane coatings. *J Appl Polym Sci*. 2005;95(6):1509–18. <https://doi.org/10.1002/app.21404>.
- EN 302-1. Adhesives for load bearing timber structures – Test methods. Part 1: Determination of longitudinal tensile shear strength. Vienna: Austrian Standards Institute; 2013.
- Böhner G. Überlegungen und Ergänzungen zum Keywerth-Diagramm. *Holz als Roh- und Werkstoff*. 1996;54:73–9.
- Konnerth J, Stöckel F, Müller U, et al. Elastic properties of adhesive polymers. III. Adhesive polymer films under dry and wet conditions characterized by means of nanoindentation. *J Appl Polym Sci*. 2010. <https://doi.org/10.1002/app.32342>.
- Konnerth J, Jäger A, Eberhardsteiner J, et al. Elastic properties of adhesive polymers. II. Polymer films and bond lines by means of nanoindentation. *J Appl Polym Sci*. 2006;102(2):1234–9. <https://doi.org/10.1002/app.24427>.
- Oliver WC, Pharr GM. An improved technique for determining hardness and elastic modulus using load and displacement sensing indentation experiments. *J Mater Res*. 1992;7(06):1564–83. <https://doi.org/10.1557/JMR.1992.1564>.
- Konnerth J, Gindl W, Harm M, et al. Comparing dry bond strength of spruce and beech wood glued with different adhesives by means of scarf- and lap joint testing method. *Eur J Wood Wood Prod*. 2006;64(4):269–71. <https://doi.org/10.1007/s00107-006-0104-1>.
- Novák I, Krupa I, Chodák I. Relation between electrical and mechanical properties in polyurethane/carbon black adhesives. *J Mater Sci Lett*. 2002;21(13):1039–41. <https://doi.org/10.1023/A:1016073010528>.
- Stoeckel F, Konnerth J, Gindl-Altmutter W. Mechanical properties of adhesives for bonding wood—a review. *Int J Adhes Adhes*. 2013;45:32–41. <https://doi.org/10.1016/j.jadhadh.2013.03.013>.
- Konnerth J, Gindl W. Observation of the influence of temperature on the mechanical properties of wood adhesives by nanoindentation. *Holzforschung*. 2008;62(6):71. <https://doi.org/10.1515/HF.2008.108>.
- Na B, Pizzi A, Delmotte L, et al. One-component polyurethane adhesives for green wood gluing: structure and temperature-dependent creep. *J Appl Polym Sci*. 2005;96(4):1231–43. <https://doi.org/10.1002/app.21529>.
- Quye A, Williamson C, editors. Plastics: Collecting and conserving. Edinburgh: NMS; 1999.

**Submit your manuscript to a SpringerOpen<sup>®</sup> journal and benefit from:**

- Convenient online submission
- Rigorous peer review
- Open access: articles freely available online
- High visibility within the field
- Retaining the copyright to your article

---

Submit your next manuscript at ► [springeropen.com](https://www.springeropen.com)

**Influence of polymer/filler composition and processing on the properties of multifunctional adhesive wood bonds from polyurethane prepolymers I: mechanical and electrical properties**

Christoph Winkler<sup>1,2</sup>, Johannes Konnerth<sup>2</sup>, Johannes Gibcke<sup>1</sup>, Jesco Schäfer<sup>1</sup> and Ulrich Schwarz<sup>1</sup>

<sup>1</sup> University of Applied Sciences Eberswalde, Faculty of Wood Engineering, Eberswalde, Germany



<sup>2</sup> BOKU - University of Natural Resources and Life Sciences, Institute of Wood Technology and Renewable Materials, Vienna, Austria

**Declaration of author contributions**

Winkler conceptualized and designed the experiment. Sample preparation was done by Gibcke and Schäfer under the guidance of Winkler. Lap shear tests were carried out by Gibcke, DC resistance measurements by Schäfer. Data have been evaluated and discussed by all, statistical analysis was done by Winkler under the guidance of Konnerth. Writing and editing of the final manuscript was done by Winkler. Funding acquisition of the financial support leading to this publication was done by Winkler and Schwarz. All authors read and approved the final manuscript.



# Influence of polymer/filler composition and processing on the properties of multifunctional adhesive wood bonds from polyurethane prepolymers I: mechanical and electrical properties

Christoph Winkler <sup>a,b</sup>, Johannes Konnerth <sup>b</sup>, Johannes Gibcke<sup>a</sup>, Jesco Schäfer<sup>a</sup>, and Ulrich Schwarz<sup>a</sup>

<sup>a</sup>Faculty of Wood Engineering, University of Applied Sciences Eberswalde, Eberswalde, Germany;

<sup>b</sup>Department of Material Sciences and Process Engineering (MAP), University of Natural Resources and Life Sciences, Vienna, Austria

## ABSTRACT

Multifunctional adhesives out of a polymer matrix and electrically conductive fillers are known to typically decrease in bond strength with increasing filler content, while the electrical resistance drops extensively at the percolation threshold. Three experiments have focused on different aspects of the production of electrically conductive adhesive wood bonds, experiment I with a variation of the adhesive components, experiment II is varying the process parameters in the bonding process, and experiment III is investigating a thermal postcuring effect. Tensile shear strength (EN 302–1, requirement for structural wood bonding dry condition (A1 treatment)) and electrical resistography under direct current (DC measurements) of the bondline was used to identify major influences on tensile shear strength and the formation of the electrically conductive network. The results show high differences due to the adhesive polymer selection, the filler type and some of the process parameters. As an example, it was revealed that the bond strength of multifunctional adhesive wood joints can be increased by integrating increasing contents of carbon nanotubes in polyurethane prepolymers, if the polymers do not contain fibrous fillers before the dispersion.

## ARTICLE HISTORY

Received 30 July 2019


Accepted 2 August 2019

## KEYWORDS

Conductive adhesives; adhesives for wood; adhesives with nanoparticles; polyurethane; wood; civil engineering

## 1. Introduction

Multifunctional adhesives, consisting of a base polymer and a functional – in this case electrically conductive – filler, enhance the functionality of adhesive bondlines by inducing a strain-dependent electrical resistance. Examples for sensor applications based on conductively filled polymers in literature are predominantly applied to artificial and well-defined materials and surfaces.<sup>[1–6]</sup> In the field of wood bonding, in contrast, the production of multifunctional bondlines can be

**CONTACT** Christoph Winkler  [Christoph.Winkler@hnee.de](mailto:Christoph.Winkler@hnee.de)  Eberswalde University for Sustainable Development, Alfred-Möller-Strasse 1, Eberswalde 16225, Germany

Color versions of one or more of the figures in the article can be found online at [www.tandfonline.com/gadh](http://www.tandfonline.com/gadh).

© 2019 Taylor & Francis Group, LLC

difficult due to the high variation of wood properties as well as the geometrically not defined bondline due to the penetration zone. Regardless of these challenges, it was shown with different studies that strain-dependent relative changes of DC resistance in wooden bondlines can be measured.<sup>[7–9]</sup> While these results reflect the possibility of electrically sensitive wooden bondlines, the influences on the bondline properties due to manufacturing processes are unknown and can only be estimated from other fields of application and adhesives.

The gradual filling with electrically conductive filler particles into an insulating polymer matrix will decrease the resistivity of the new composite as a new conductive network is formed by interconnection between the particles. The transition follows a non-linear, so-called percolation curve<sup>[10–12]</sup> and depends mainly on dispersion technique, polymer and filler type.<sup>[13–17]</sup> Within similar polymers, the rheology has been found as one major influence on the dispersion quality<sup>[18]</sup> as well as the decision for the best applicable dispersion technique.<sup>[19]</sup> Sanli et al.<sup>[20]</sup> reported that with increasing filler content, the reproducibility and practical applicability is increasing. A well-known downside of increasing filler content is the decrease in bonding strength<sup>[21,22]</sup>, which can be attributed to a poor dispersion and therefore residues of agglomerates<sup>[23,24]</sup>, but can be counteracted by using fiber-shaped fillers like carbon nanotubes (CNT) as they help fiberbridging of cracks.<sup>[25,26]</sup> During manufacturing, press parameters like temperature, pressure and time can be of great influence on mechanical properties and the conductivity of the bondline.<sup>[27,28]</sup> After manufacturing, thermal postcuring is a widely used technique to enhance the mechanical, but also the electrical properties of electrically conductive adhesives.<sup>[29]</sup> In contrast, a preliminary study using wood as a substrate indicated no significant decrease in bond strength of multifunctional adhesives, when using carbon black as filler.<sup>[30]</sup>

Based on these findings and theory, an experimental setup has been developed to achieve an overview on mechanical, electrical and sensitivity properties of electrically conductive bondlines from one-component polyurethanes for structural wood bonding. Three experiments have focused on different aspects of the production of electrically conductive adhesive wood bonds, experiment I with a variation of the adhesive components, experiment II varying the process parameters in the bonding process, and experiment III investigating a thermal postcuring effect. Although three different aspects were in focus, the same preparation method of the samples has been used to make the data comparable for analysis.

Comprising data from these three experiments within this work will give an overview of the main influencing parameters for the production of electrically conductive and sensitive wood bondlines. Part I will show the mechanical and electrical properties, while Part II will focus on electrical sensitivity due to compression stresses.

## 2. Material and methods

### 2.1. Preparation

The process to produce all test specimens for mechanical and electrical testing is illustrated in Figure 1, the different parameters used for manufacturing are listed in Table 1.

Specimen preparation started by providing the adhesives by dispersing electrically conductive fillers. Experiment I used five different polyurethane prepolymer

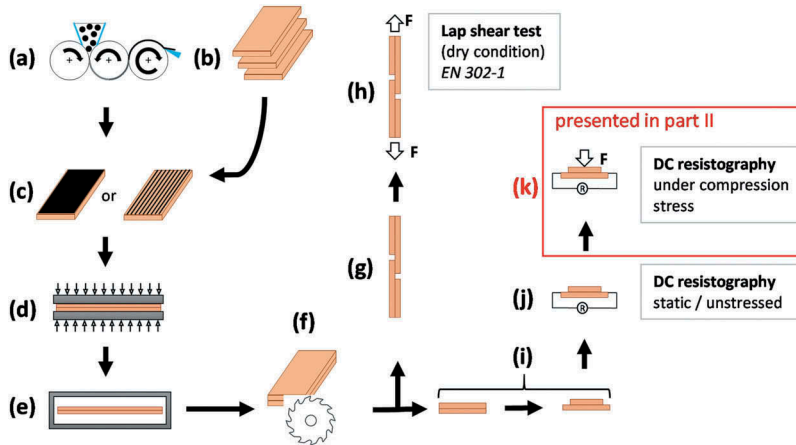


**Figure 1.** Schematic process of specimen preparation and testing: filler dispersing (a), wood lamella preparation (b), adhesive application (c), bonding by a laboratory press (d), thermal postcuring, see also<sup>[4]</sup> (e), formatting (f) preparation of lab joint tensile shear samples (g), tensile shear test (h), preparation of electrical test samples (i), DC resistography (j), DC resistography under load (k).

**Table 1.** Variables of the experiments (superscript indicated the process step according to Figure 1) and their parameters. Bold printed parameters have been held constant while varying other variables in the same experiment. Abbreviations: PU1 to PU5 polyurethane prepolymer one to five according to Table 2, CB carbon black, CNT carbon nanotubes, CNFT mixture of carbon fibers and carbon nanotubes, see also Winkler et al.<sup>[31]</sup>.

Variables	Experiment I (polymer, filler and filler content)	Experiment II (manufacturing process)	Experiment III (effect of thermal postcuring)
Polymer <sup>(a)</sup>	PU1; PU2; PU3; PU4; PU5	PU4	see <sup>[31]</sup>
Filler type <sup>(a)</sup>	CB; CNT	CB	CNFT; CB
Filler content <sup>(a)</sup> in wt%	0–7 (CB); 0–3 (CNT)	4	2 + 0.2; 4
Dispersion technique <sup>(a)</sup>	<b>3-roll-mill</b>	<b>3-roll-mill</b> ; dissolver nozzle; <b>scraper</b> ;	<b>dissolver</b>
Application technique <sup>(c)</sup>	<b>tooth scraper</b>	tooth scraper	<b>scraper</b>
Glue spread <sup>(c)</sup> in g/m <sup>2</sup>	<b>250</b>	150; <b>250</b> ; 400	<b>250</b>
Pressure <sup>(d)</sup> in MPa	<b>1</b>	0.6; <b>0.9</b> ; 1.2	<b>1</b>
Press time <sup>(d)</sup> in h <sup>1</sup>	<b>1</b>	1; <b>2.5</b>	<b>1.5</b>
Press temperature <sup>(d)</sup> in °C	<b>50</b>	20; <b>35</b> ; 50	<b>30</b>
Thermal postcuring <sup>(e)</sup> in °C/h	<b>untreated</b>	untreated	untreated; 80/1; 80/48; 95/1; 95/48

adhesives (1C-PUR), further named PU1 to PU5, which are currently in use or under research for bonding structural timber. All were modified by dispersing two different fillers with increasing contents. The properties of the used one component polyurethane adhesives (1C-PUR) are listed in Table 2. For deeper understanding of the process relevant rheology of the polymers, shear rate dependent viscosities for all unmodified 1C-PUR have been measured by a rheometer (MCR502, Anton Paar Germany, Ostfildern/Germany), equipped with a plate/plate system, diameter 25 mm and a gap of 1 mm (see Figure 2). The table shows uniform properties with differences mainly in viscosity and fiber content (fibers are sometimes used in 1C-PUR adhesives for structural applications).

Used fillers have been conductive carbon black (Ketchenblack EC300J, Akzo Nobel Functional Chemicals B.V., Arnhem/The Netherlands), further labeled CB and carbon nanotubes (NC7000, Nanocyl S.A., Sambreville/Belgium), further labeled CNT. Only experiment III on the thermal postcuring effect used a mixture of 2wt% carbon nanofibers (PR-25-Xt-HHT, Pyrograf Products Inc.,

**Table 2.** Used polyurethane prepolymers (PU) and properties based on data sheets and viscosity measurements. <sup>(a)</sup> At 20 rpm and 20°C with a plate/plate measurement system, Ø25mm, gap 1 mm. <sup>(b)</sup> At 20°C and 12% wood moisture content.

Property	PU1	PU2	PU3	PU4	PU5
Viscosity in mPa·s <sup>(a)</sup>	9'000	2'700	15'000	10'500	7'000
Density in g/cm <sup>3</sup>	1.16	1.1	1.15	1.15	1.15
contains fibers	-	yes	yes	yes	-
Open time in min	70	60	45	45	45
Pressure in MPa	0.6–1.0	0.6–0.8	0.8–1.2	0.6–1.0	0.6–1.0
Glue spread in g/m <sup>2</sup>	140–180	200+	200–300	150–250	150–250
Press time in h <sup>(b)</sup>	3	3	2.25	2.25	2.25
Press temperature in °C	>20	>20	>20	>20	>20

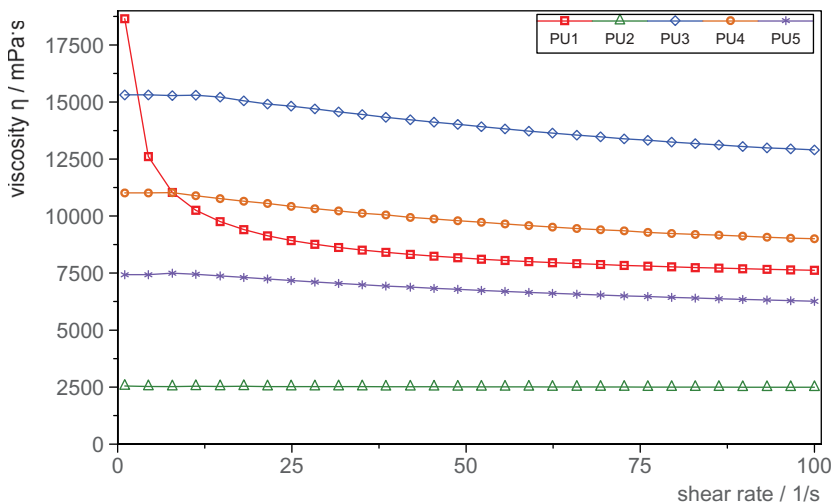


**Figure 2.** Viscosity vs. shear rate of the used polyurethane prepolymers.

Cedarville, USA) and 0.2wt% carbon nanotubes (NC7000, Nanocyl S.A., Sambreville/Belgium), which will be further named CNFT and is described in Winkler et al.<sup>[31]</sup>

Conductive adhesives have been manufactured, covering the following steps. First, the electrically conductive fillers have been dried at 103.5°C for 24 h to reduce the overall moisture during the dispersion process of these moisture curing 1C-PUR. The dispersion was achieved with a 3-roll mill (Exakt 50 Klassik, Exakt Advanced Technologies GmbH, Norderstedt/Germany), using three iterations with decreasing gap sizes. The first iteration used gap sizes of 180 µm (first gap) and 60 µm (second gap), the second iteration 120 µm/40 µm and the last iteration 60 µm/25 µm. The second used dispersion process used a dissolver technique (Table 1), which has been described earlier in Winkler et al.<sup>[31]</sup>

Clear, defect-free wood lamellas of beech wood (*Fagus Sylvatica* L.) were selected and prepared according to EN 302–1.<sup>[32]</sup> The bulk density and the equilibrium wood moisture content of the beech substrate varied due to two sets of wood used. Wood lamellas from experiment I featured a bulk density of  $617 \pm 28 \text{ kg/m}^3$  and a wood moisture content of  $13.2 \pm 1.3\%$  and was used for investigating the variation of polymer, filler and filler content. Wood lamellas from experiment II had a bulk density of  $710 \pm 15 \text{ kg/m}^3$  and a wood moisture content of  $11.5 \pm 0.7\%$ . Samples for postcuring (experiment III), which are covered in Winkler et al.<sup>[31]</sup>, featured a bulk density of  $648 \pm 11 \text{ kg/m}^3$  and a wood moisture content of  $10.8 \pm 0.2\%$ .

The lamellas were manufactured in pairs in a laboratory press with different parameters according to Table 1. Details on postcuring of the lamellas are described in.<sup>[31]</sup> After conditioning in standard climate (20°C, 65% relative humidity) for at least 7 days, all samples have been prepared for testing. Lap joint tensile shear samples and electrical test samples were cut from the same lamella.

The three experiments consisted of a total of 82 series of samples and each series consisted of at least 10 to 15 samples. Most factors have been tested with at least three parameters to evaluate non-linear influences. Samples have been randomized in the test procedure.

## 2.2. Lap joint testing

Mechanical properties of the bonding process were characterized by tensile shear tests on lap joint specimen (EN 302–1), which are used to verify the requirements for structural wood bonding in dry condition (A1 treatment). Specimen dimensions are given in EN 302–1<sup>[32]</sup>, the shear area was  $20 \times 10 \text{ mm}^2$ . A universal testing machine (Zwick/Roell Type 1484, load cell 200 kN, Ulm, Germany) was used to carry out the tests according to EN 302–1 with a cross head speed of five mm/min to ensure a test duration of 30 to 90 s. Tensile shear strength was calculated from the maximum force at shear failure divided by the



overlapping area of the lap joint. The failure zone was analyzed visually for the percentage of wood failure. Corresponding wood failure amount was noted in 10% steps.

### 2.3. DC resistography

DC electrical resistance has been measured with a digital multimeter (NI PXI 4071, National Instruments GmbH, Munich/Germany) on bondlines with dimensions of 20 mm width, 60 mm length and a thickness of 0.05–0.2 mm at climate conditions of 21°C/37% rH. The variation of wood bondline thickness is estimated from microscopy images, using a selection of 20 specimens and shows that thickness varies in width and length, which is attributed to the material structure of wood. Due to the vessel system present in wood, the adhesive is distributed deep into the wood adherend/adherends (see Figure 3a), which is limiting the calculation of resistivity from the DC resistance. In order to perform electrical measurements, electrical contact was realized by applying silver conductive paste (L204N, Ferro GmbH, Hanau/Germany) on the end faces, which was dried for at least 24 h and electrodes were pressed on with springs (see Figure 3b).

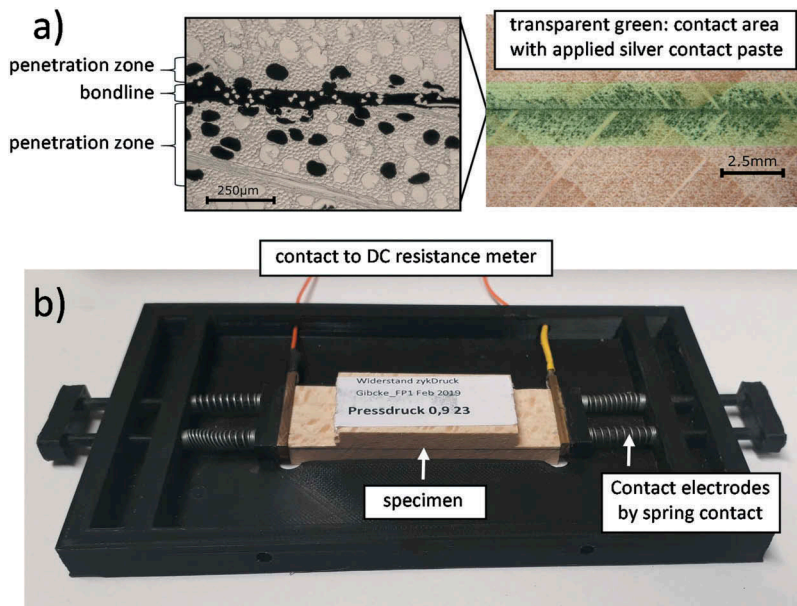


**Figure 3.** Setup for DC resistography. (a) Cross-section of the electrically conductive bondline in beech wood with adhesive penetration zone and the area, where silver contact paste has been applied. (b) Test setup for DC resistography with a frame and two spring-loaded electrodes on the end face of the specimen.

### 3. Results and discussion

#### 3.1. Experiment I: polymer, filler and filler content

The lap joint tensile shear strength under dry conditions (TSS) as well as the DC resistance ( $R_{DC}$ ) from the five polyurethane groups (PU1 to PU5, modified by two different electrically conductive fillers with increasing filler contents) are shown in Figures 4–8. Each group is described by two diagrams, one for the TSS and one for  $R_{DC}$ . Both parameters refer to the filler content displayed on the x-axis. Boxplots for TSS show the data distribution of each series of samples, additionally the minimum requirement of 10 MPa from the EN 302–1 is indicated as a dotted line in each diagram. Wood failure percentage in the same

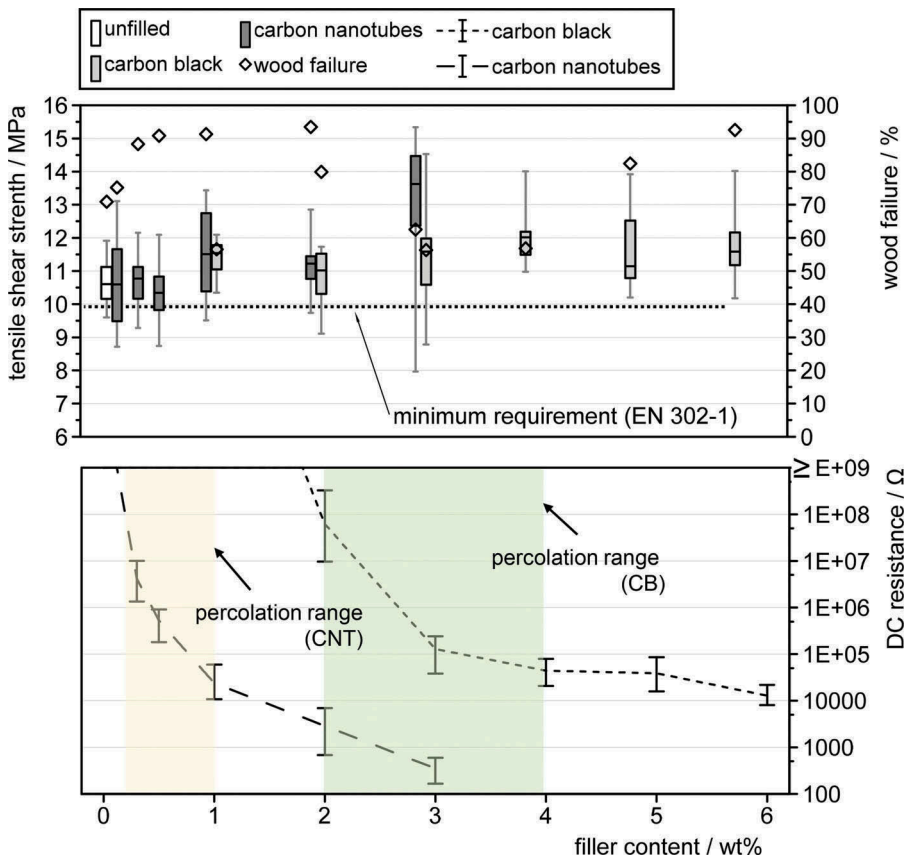


**Figure 4.** Comparison of lap joint tensile shear strength, wood failure (both upper diagram) and DC resistance (lower diagram) of PU1, filled with a varying weight content of electrically conductive filler. Boxplots: boxes = quartile of distribution, whiskers = maximal and minimal values. DC resistance: whiskers are minimal to maximal values, the dotted line connects the mean values to estimate the percolation curve, yellow and green transparent zones estimate the range of filler content, where percolation occurs.

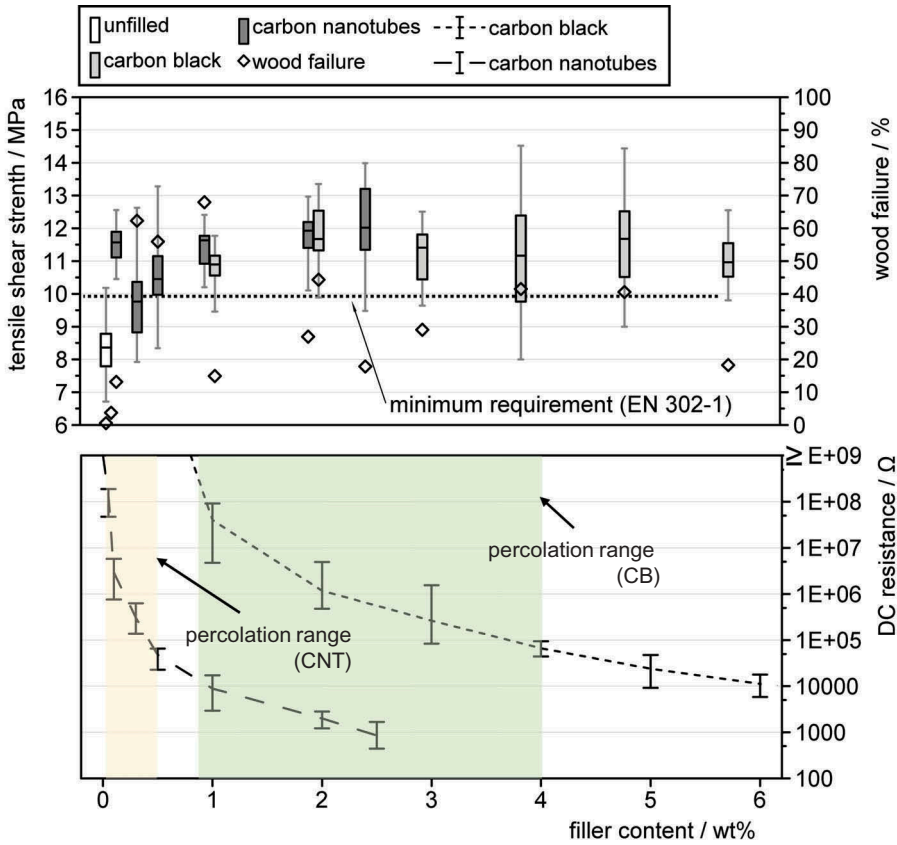


**Figure 5.** Comparison of lap joint tensile shear strength, wood failure (both upper diagram) and DC resistance (lower diagram) of PU2, filled with a varying weight content of electrically conductive filler. Boxplots: boxes = quartile of distribution, whiskers = maximal and minimal values. DC resistance: whiskers are minimal to maximal values, the dotted line connects the mean values to estimate the percolation curve, yellow and green transparent zones estimate the range of filler content, where percolation occurs.

diagram indicates if failure happens in the bondline or in the wood adherend. The  $R_{DC}$  diagrams visualize the electrical percolation of the filler with the change of DC resistance over the filler content (percolation curves).

From the percolation curves, it is obviously not suitable to give a certain value for the percolation threshold. Therefore, the description of the percolation threshold is done by a span of critical filler content  $\Phi_c$ , where the electrical percolation occurs. The span of  $\Phi_c$  has been defined by  $10^8$  to  $10^5$  Ohm and reflects the highest relative drop of DC resistance relative to the filler content. Additionally, it reflects a practical aspect of electrically conductive adhesive joints in wood. Higher DC resistances of  $10^8$  equal a resistivity in the range of  $1.7 \cdot 10^3$  to  $6.7 \cdot 10^3 \Omega m$  (based on a bondline thickness of 0.05 to 0.2 mm), which is the resistivity of wood at fiber saturation point.<sup>[33]</sup> As a resistivity of three decades lower than the resistivity of

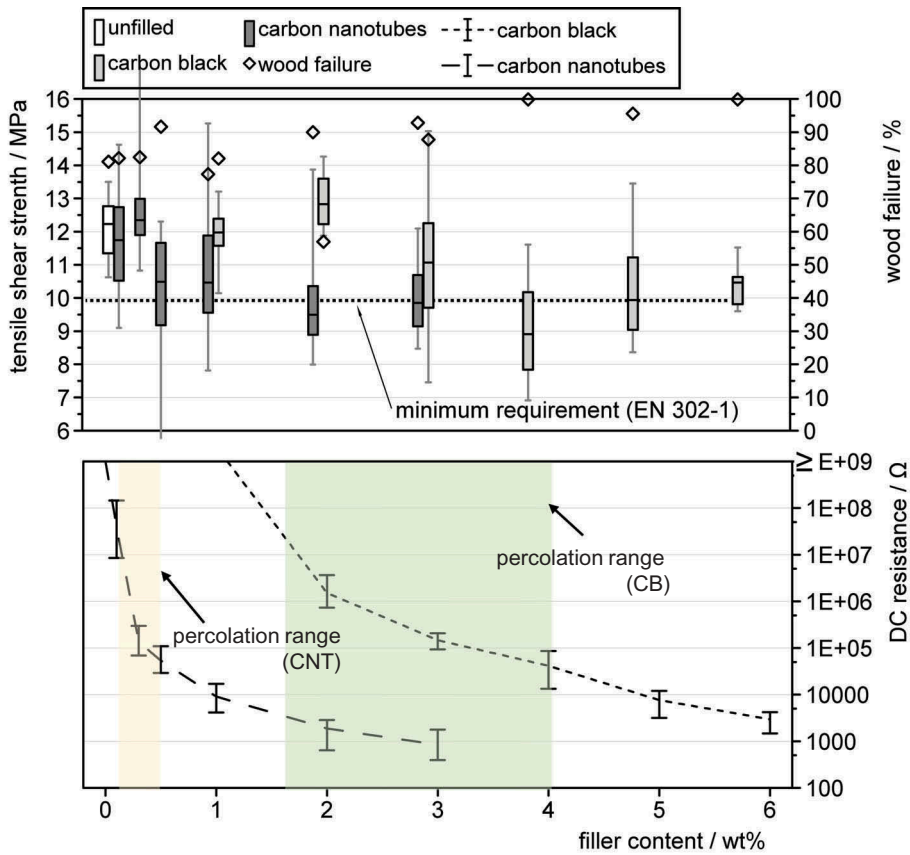


**Figure 6.** Comparison of lap joint tensile shear strength, wood failure (both upper diagram) and DC resistance (lower diagram) of PU3, filled with a varying weight content of electrically conductive filler. Boxplots: boxes = quartile of distribution, whiskers = maximal and minimal values. DC resistance: whiskers are minimal to maximal values, the dotted line connects the mean values to estimate the percolation curve, yellow and green transparent zones estimate the range of filler content, where percolation occurs.

wood at fiber saturation point is necessary to distinguish strain from moisture influence,  $10^5$  Ohm represents a practical lower DC resistance limit of  $\Phi_c$ .

This range of  $\Phi_c$  as well as the DC resistance after percolation  $R_{DC,PT}$  at 4 wt% for CB and 2 wt% for CNT are summarized in Table 3. The DC resistance at 4 wt% and 2 wt%, respectively has been chosen due to good processability of the adhesives at this filler content.

As expected PU1, PU3, PU4 and PU5 clearly surpass the TSS requirement of 10 MPa for structural wood bonding according to EN 302-1 in dry condition (A1 treatment), only PU2 fails to reach it. No unmodified adhesive gives a measurable DC resistance, confirming an insulating character of the polymer.

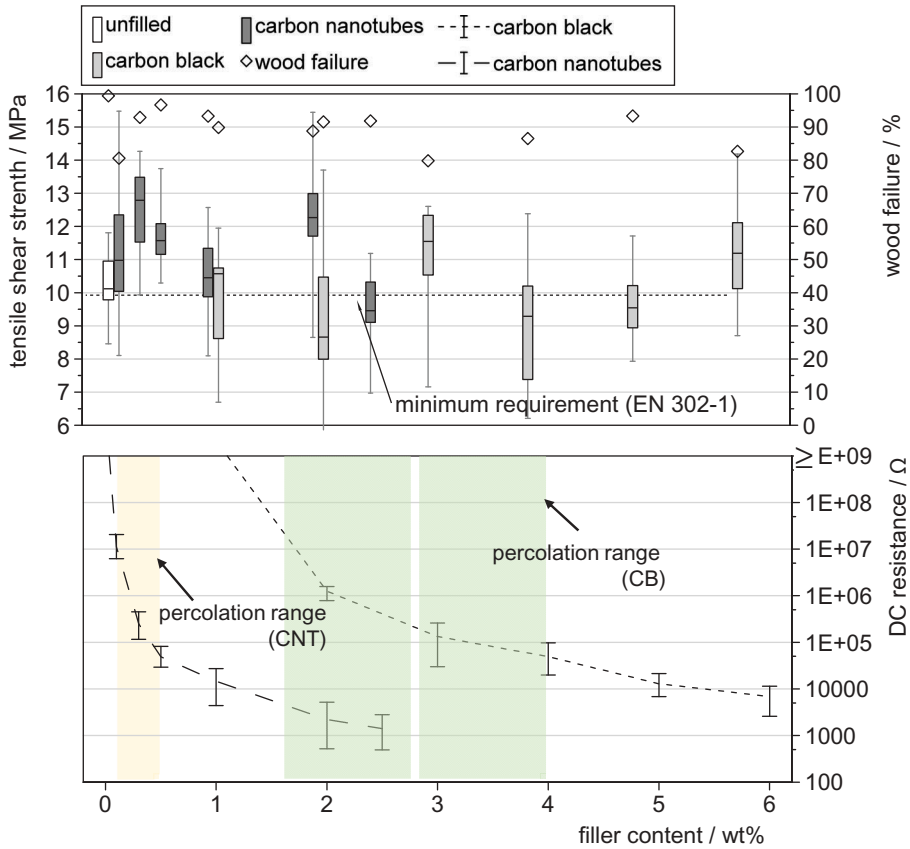


**Figure 7.** Comparison of lap joint tensile shear strength, wood failure (both upper diagram) and DC resistance (lower diagram) of PU4, filled with a varying weight content of electrically conductive filler. Boxplots: boxes = quartile of distribution, whiskers = maximal and minimal values. DC resistance: whiskers are minimal to maximal values, the dotted line connects the mean values to estimate the percolation curve, yellow and green transparent zones estimate the range of filler content, where percolation occurs.

With increasing filler content, similarities between adhesive properties are recognizable. All  $R_{DC}$  measurements follow – as expected from literature – a nonlinear curve with increasing filler content (percolation curve), indicating the formation of a conductive network with low DC resistance at a specific critical filler content  $\Phi_c$ . All 1C-PUR's filled with CNT reach a lower absolute  $R_{DC,PT}$  of at least one decade compared to 1C-PUR's filled with CB (around 2 k $\Omega$  for CNT compared to around 45 k $\Omega$  for CB, see Table 3). This observation is coherent with theory as lower bondline resistance of polyurethanes filled with CNTs can be found in the overall higher conductivity of CNTs, which has been published by Marinho et al.<sup>[34]</sup> for the used fillers. Additionally, all 1C-PUR's filled with CNTs reach an overall lower  $\Phi_c$ , which is also covered by theory as the percolation threshold decreases with an increasing aspect ratio of the filler.<sup>[35,36]</sup>

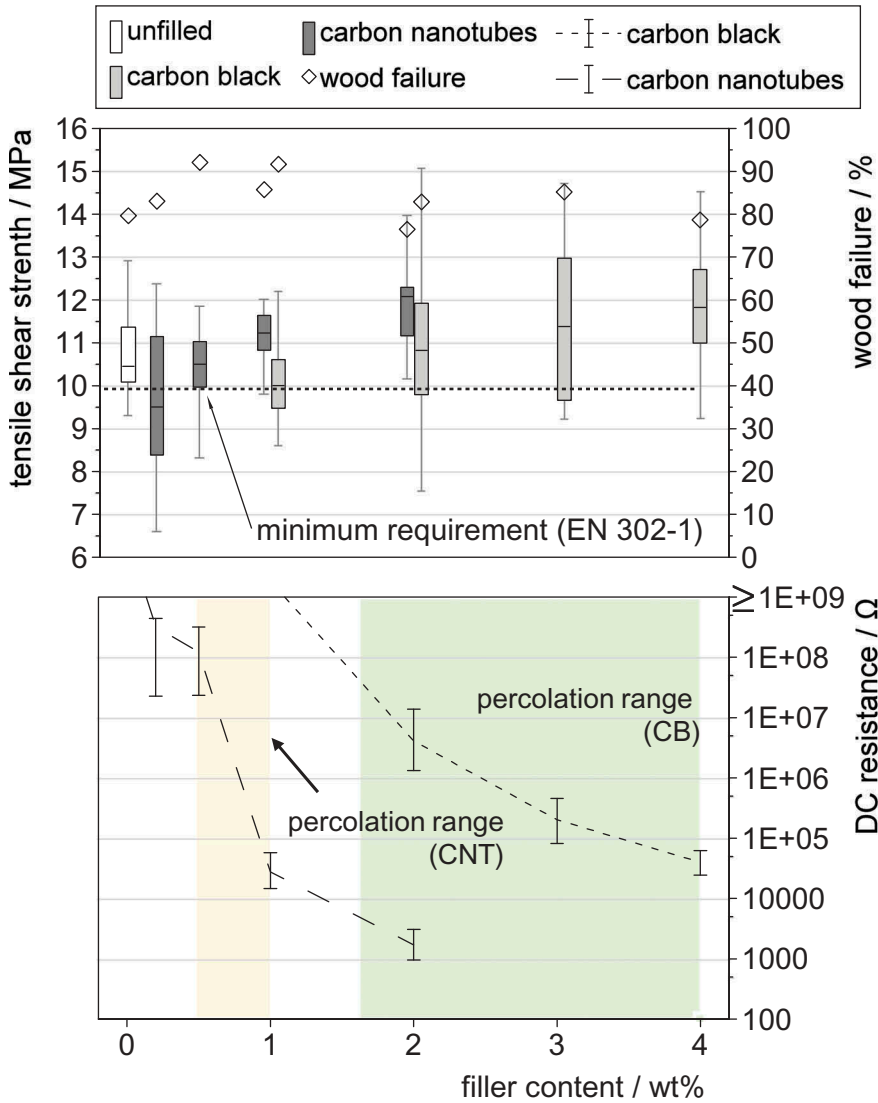


**Figure 8.** Comparison of lap joint tensile shear strength, wood failure (both upper diagram) and DC resistance (lower diagram) of PU5, filled with a varying weight content of electrically conductive filler. Boxplots: boxes = quartile of distribution, whiskers = maximal and minimal values. DC resistance: whiskers are minimal to maximal values, the dotted line connects the mean values to estimate the percolation curve, yellow and green transparent zones estimate the range of filler content, where percolation occurs.

Differences in  $R_{DC,PT}$  due to differences in adhesive polymers cannot be found. Noticeable, the percolation threshold of 1C-PUR filled with CB is not as distinct as when CNTs are used as filler and can therefore only be described by a wider range of filler addition (Table 3). These differences are mainly not described in the literature as percolation thresholds are derived from mathematical fits with statistical power laws and given as a specific value. Chanklin<sup>[37]</sup> describes the

**Table 3.** Properties of the electrically conductive bondlines with variation of filler content.  $\Phi_c$  is the critical filler content, in which the percolation occurs (percolation threshold).  $R_{DC,PT}$  gives the DC resistance at the filler content, which is processable and higher than the percolation threshold (4 wt% for carbon black (CB) and 2 wt% for carbon nanotubes (CNT)).

Property		PU1	PU2	PU3	PU4	PU5
$\Phi_c$ in wt%	CB	2.0–4.0	<1.0–4.0	<2.0–4.0	<2.0–4.0	<2.0–4.0
	CNT	>0.1–1.0	0.05–0.5	<0.1–0.5	<0.1–0.5	0.5–1.0
$R_{DC,PT}$ in k $\Omega$	CB	44 +/- 18	66 +/- 16	41 +/- 22	49 +/- 22	40 +/- 12
	CNT	2.9 +/- 1.8	2.0 +/- 0.5	1.9 +/- 0.7	2.2 +/- 1.5	1.7 +/- 0.6

same difference in Nylon, filled with CB and CNTs, and explains it with the characteristics of the conducting filler. The last similarity in most groups – except PU2 – is the overall high mean wood failure percentage of all sample series, which implies a good bonding quality.

Differences in the five adhesive groups are recognizable for the filler types as well as their response of TSS with increasing filler content.

PU1 and PU5 show no systematic effect of CB filler content on TSS but a trend of increasing TSS with increasing CNT content as filler material. Both adhesives show a higher  $\Phi_c$  for CNTs as filler to reach a DC resistance of 50 k $\Omega$ m. PU1 exhibits as the only tested adhesive a measurable higher minimum  $\Phi_c$  for CB filler (see Table 3).

PU2 with addition of filler obviously helps to fulfill the requirements of EN 302–1 by increasing the overall TSS over 10 MPa, but shows no systematic effect on TSS with increasing filler content. A possible explanation for this effect is that PU2 has a low viscosity without filler (Table 2). This could lead to a bondline starvation due to excessive adhesive penetration into the wood adherend, which decreases with filler content and therefore better bonding properties are reached.<sup>[38]</sup> Nonetheless, the low mean wood failure percentage of all samples implicates a comparably lower bonding quality compared to the other adhesives. Measured critical minimum filler content  $\Phi_c$  is lower than all other 1C-PURs, both for CB and CNT as filler.

PU3 shows a clear decrease in TSS starting with 3 wt% CB, which stays constant until the last filler content of 6 wt%. Additionally, the decrease of TSS with rising filler content leads to TSS below the requirements of 10 MPa at around 0.5 wt% CNT. Critical filler content  $\Phi_c$  is similar with PU4, both for CB and CNT as filler.

PU4 at last shows a high variation of TSS with increasing the filler content, both for CB and CNTs as filler. At different filler contents, the adhesive bond performs below the requirement of 10 MPa, but no systematic trend can be recognized.

With these observations, four types of response to increasing filler content could be identified in different 1C-PURs for structural wood bonding. Compared with literature, only PU3 shows a similar trend of strength (in this case TSS) and DC



resistance at a critical filler content, where percolation occurs (3 wt% for CB, 0.5 wt% for CNT). Lap joint tensile shear tests typically reflect the shear strength of the wood adherend, if the overall wood failure is high.<sup>[39]</sup> Therefore, only data from PU2 show that a decrease in adhesive strength with increasing filler content can be avoided by choosing the right polymer.

The lower critical filler content  $\Phi_c$  for PU2, PU3 and PU4 is only achieved by 1C-PUR's, which contains fibrous fillers before dispersing the conductive filler (Table 3). While no analytical evidence can be given, explanations for this phenomenon could be that (a) the fibers act as mixing elements or (b) due to fiber content the relative filler content referred to the polymer mass is higher, which gives a lower  $\Phi_c$ . Since PU1 and PU5 shows an increasing TSS with dispersed CNTs without containing fibers in the adhesive formulation, the absence of fibers seems to be a positive aspect in formulating conductive 1C-PURs with good bonding qualities.

Conclusions, which can be drawn from the data, are that the formulation of 1C-PUR has a strong influence on the usability as polymer for the electrically conductive formulation, even though that all adhesives are designed to pass the same tests for structural wood bonding and show similar process requirements. Additionally, even at high filler content, where the highly filled adhesive is paste-like, no tested 1C-PUR lost its ability to bond wood.

### 3.2. Experiment II: influence of manufacturing process

Figure 9 shows the TSS, wood failure percentage and the  $R_{DC}$  of all varied process parameters as groups of boxplots, based on the same scale for comparability.

A one-way analysis of variance (ANOVA,  $p \leq 0.05$ ) was used to statistically evaluate the significance of process parameters on TSS and  $R_{DC}$ . Press temperature, applied pressure and glue spread did not show any significant differences in TSS, while application by nozzle, longer press time and the dispersion technique by 3-roll mill give a significant higher TSS (ANOVA,  $p \leq 0.05$ ).  $R_{DC}$  shows significant decrease with less applied pressure during manufacturing, a low glue spread rate, the application by nozzle as well as the dispersion by dissolver technique (ANOVA,  $p \leq 0.05$ ).

A lower  $R_{DC}$  at no decrease of TSS for less applied pressure can be attributed to a thicker bondline, as in contrast high pressure is going to increase the penetration of the adhesive into the adherend. Therefore, the electrically conductive bondline with less penetration will provide a larger cross-section of multifunctional adhesive.

Extended time of pressure in the manufacturing resulted in significantly higher TSS and lower  $R_{DC}$ . It is expected that foaming of 1C-PUR will be suppressed, and therefore a less porous bondline will be the product.

The compared application techniques show the difference between industrial application by parallel nozzles, while scrapers and tooth scrapers are used



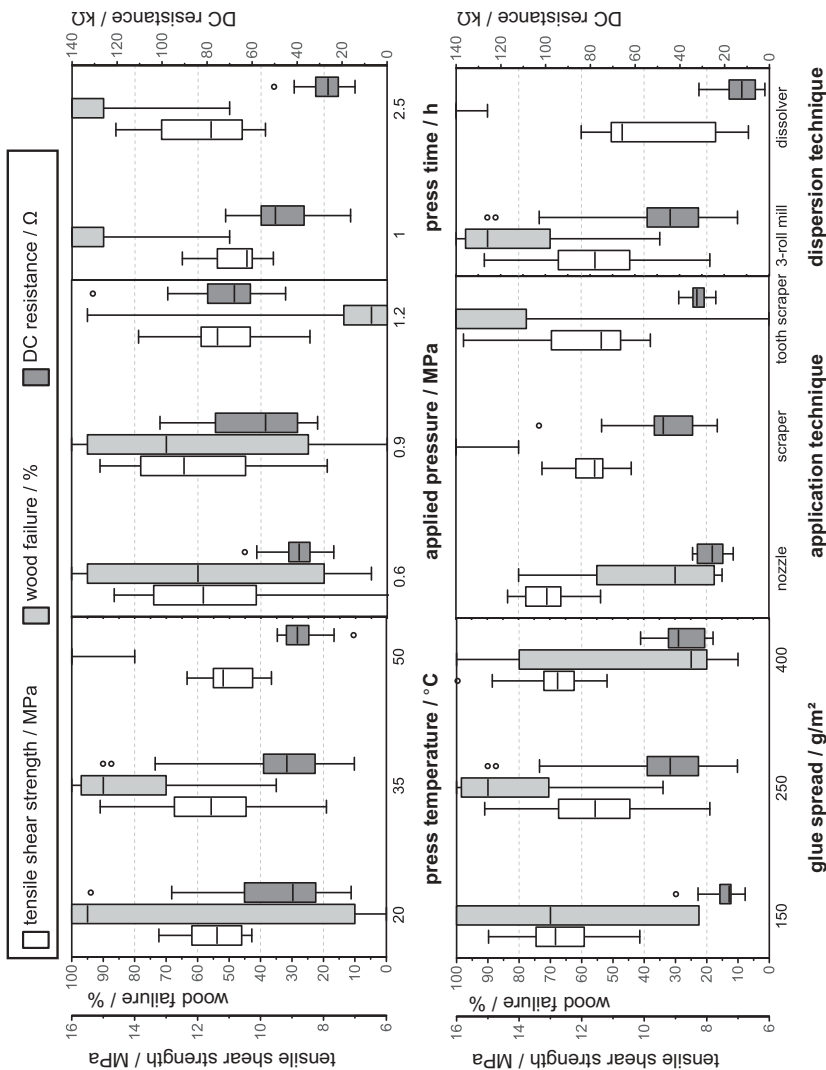


**Figure 9.** Comparison of lap joint shear strength, wood failure and DC resistance of PU4, filled with a 4 wt% of carbon black filler, manufactured with varying process-related parameters. Boxplots: boxes = quartile of distribution, whiskers = 1.5 of interquartile range, circles = outliers.

typically in laboratory as well as for manually manufactured specimens. With parallel nozzles, the adhesive is applied in parallel strings on the wood surface and will be spread by pressing the lamellas together. In the first place, scraper and tooth scraper application will spread the adhesive over the whole area of the lamella before a second lamella is pressed on top. Therefore, the adhesive from (toothed) scraper application has a higher risk to produce an uneven penetration of adhesive as the applied adhesive is pressed on the first lamella for equal spread with the scraper. The use of notched scraper reduces this inequality as pressure on the liquid adhesive is only applied at the teeth. Thus, theoretical influences are supported by the experimental results as application by nozzle results in significant higher TSS (bonding quality) and reduced  $R_{DC}$  due to a more equal spread of the adhesive.

No final explanation can be given for the significant lower  $R_{DC}$  due to lower glue spread. One possible explanation could be the higher shear rate due to the use of a scraper and less adhesive. But even as it is known that shear rates could influence the dynamics of electrical network formations<sup>[40]</sup>, the difference seems to be too small for applying this theory.

The different dispersion quality of 3-roll mills and dissolver have been discussed in the literature, showing that dissolver produces less shear rate and therefore a reduced quality of dispersion, referring to the separation of primary nanoparticles.<sup>[19]</sup> It is also known that an electrical percolated network from less dispersed agglomerates indicates lower DC resistance than a well-dispersed network from separated particles.<sup>[41]</sup> Thus, it appears that the experimental data – showing a lower TSS and also lower  $R_{DC}$  for dissolver dispersed filler – supports the assumption that the dispersion technique in experiment II gives a lower quality dispersion, where agglomerates decrease the overall bond quality.

It should be noted that even if for all phenomena logical explanations could be given by the knowledge of material behavior and processing, no experimental evidence is possible. As explained before, the evaluation of wood bondline thickness cannot technically be done for all specimen due to thickness variation in width and length. The only possibility known to evaluate the assumptions would be tomography images of all the samples.

### **3.3. Experiment III: influence of thermal postcuring**

Results from mechanical characterization considering thermal postcuring have already been published in Winkler et al.<sup>[31]</sup> It could be shown that the applied postcuring lead to partly higher tensile shear strength values for single treatment conditions and in no case to a decrease, but without a systematic trend in the change. DC resistance measurements, in contrast, show an influence of thermal postcuring. Figure 10 displays  $R_{DC}$  for untreated and all postcuring condition for CB and CNFT filled 1C-PUR. All thermal postcuring treatments show a reduction of variation. Additionally, a lower  $R_{DC}$  can be recognized for some

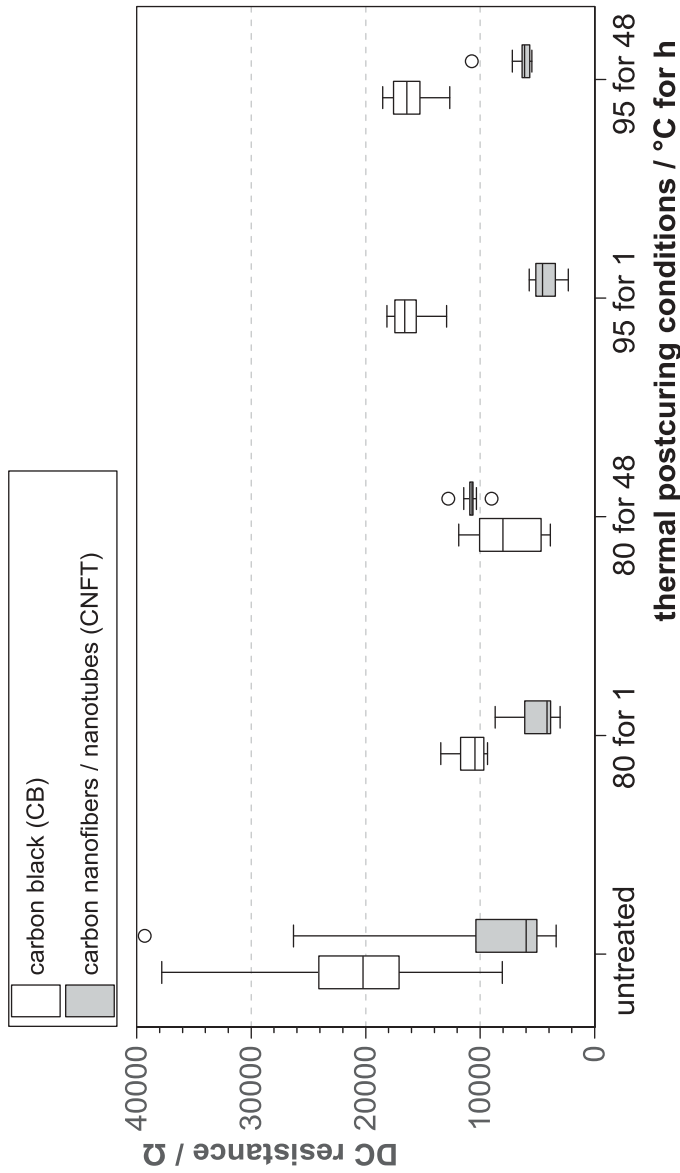


**Figure 10.** Comparison of DC resistance of two sets PU4, one filled with a 4 wt% of carbon black (CB), the other with 2wt% carbon nanotubes and 0.2wt% carbon nanotubes and four different postcuring conditions (e.g. 80/ $^{\circ}\text{C}$  for 1 h) as well as an untreated reference. Boxplots: boxes = quartile of distribution, whiskers = 1.5 of interquartile range, circles = outliers.

treatment. The reduction of  $R_{DC}$  is only statistically significant for a treatment of 80°C at one or 48 h (ANOVA,  $p \leq 0.05$ ).

Therefore, it can be assumed that thermal postcuring has a similar effect compared to other (silver filled) conductive adhesives, where a postcuring leads to lower DC resistance, which can be attributed to shrinkage and hence the relative increase of the particle volume fraction.<sup>[15]</sup>

#### 4. Conclusion

Several variables have been tested in three experiments to identify process influences on the manufacturing of electrically conductive bondlines in wood, ranging from the materials for the modified adhesives to the manufacturing parameters of bonded wooden lamellas. Based on the desired properties (i.e. high tensile shear strength, low bondline resistance and low percolation threshold) different process-related factors have been discussed. The following conclusions can be drawn from the results:

- (1) Carbon nanotubes lower the percolation threshold and overall DC resistance of the bondline compared to carbon black as filler.
- (2) The formulation of 1C-PUR has shown to be of importance for the reaching of bond strength (EN 302–1). The latter has shown to be effected by filler type and content.
- (3) The presence of fibrous filler in 1C-PUR before dispersion can lower the percolation threshold, 1C-PUR without them increase in bond strength with CNTs as filler.
- (4) Thermal postcuring of wood bonds from 1C-PUR, filled with electrically conductive nanoparticles, reduces the variation of DC resistance of the bondlines and in some cases also the DC resistance.
- (5) The elongation of press time and the adhesive application by parallel nozzles gives higher bond strengths as well as lower DC resistance of the bondline
- (6) Less applied pressure and less glue spread also results in lower DC resistance of the bondline without affecting the bond quality
- (7) Dispersion by dissolver results lower DC resistance of the bondline and lower bond strength than the dispersion by 3-roll mills.

#### Funding

This work was supported by the German Government within the “Nachwachsende Rohstoffe” program (FNR, BMEL) [22005018].

## ORCID

Christoph Winkler  <http://orcid.org/0000-0002-0444-4309>

Johannes Konnerth  <http://orcid.org/0000-0003-3826-8566>

## References

- [1] Li, C.; Thostenson, E. T.; Chou, T.-W. Sensors and Actuators Based on Carbon Nanotubes and Their Composites: A Review. *Compos. Sci. Technol.* **2008**, *68*, 1227–1249. DOI: [10.1016/j.compscitech.2008.01.006](https://doi.org/10.1016/j.compscitech.2008.01.006).
- [2] Wichmann, M. H. G.; Buschhorn, S. T.; Böger, L.; Adelung, R.; Schulte, K. Direction Sensitive Bending Sensors Based on Multi-wall Carbon Nanotube/epoxy Nanocomposites. *Nanotechnology*. **2008**, *19*(475503). DOI: [10.1088/0957-4484/19/47/475503](https://doi.org/10.1088/0957-4484/19/47/475503).
- [3] Loyola, B. R.; Zhao, Y.; Loh, K. J.; La Saponara, V. The Electrical Response of Carbon Nanotube-based Thin Film Sensors Subjected to Mechanical and Environmental Effects. *Smart Mater. Struct.* **2013**, *22*, 025010. DOI: [10.1088/0964-1726/22/2/025010](https://doi.org/10.1088/0964-1726/22/2/025010).
- [4] Sanli, A.; Benchirouf, A.; Müller, C.; Kanoun, O. Piezoresistive Performance Characterization of Strain Sensitive Multi-walled Carbon Nanotube-epoxy Nanocomposites. *Sensors Actuat. A-Phys.* **2017**, *254*, 61–68. DOI: [10.1016/j.sna.2016.12.011](https://doi.org/10.1016/j.sna.2016.12.011).
- [5] Bautista-Quijano, J. R.; Avilés, F.; Cauich-Rodriguez, J. V. Sensing of Large Strain Using Multiwall Carbon Nanotube/segmented Polyurethane Composites. *J. Appl. Polym. Sci.* **2013**, *130*, 375–382. DOI: [10.1002/app.39177](https://doi.org/10.1002/app.39177).
- [6] Zhang, R.; Baxendale, M.; Peijs, T. Universal Resistivity–strain Dependence of Carbon Nanotube/polymer Composites. *Phys. Rev. B.* **2007**, *76*, 195433. DOI: [10.1103/PhysRevB.76.195433](https://doi.org/10.1103/PhysRevB.76.195433).
- [7] Winkler, C.; Schwarz, U. *Materials and Joints in Timber Structures*; Dordrecht, Rilem-Bookseries: 381–394. **2014**; Vol. 9.
- [8] Winkler, C.; Schwarz, U. Wood Adhesives for Non-Destructive Structural Monitoring. 19th World Conference on Non-Destructive Testing. Munich. **2016**, *158*, 1–8.
- [9] Myslicki, S.; Winkler, C.; Gelinski, N.; Schwarz, U.; Walther, F. *Fatigue 2017: 7th International Conference on Durability and Fatigue*. **2017**, 446–455.
- [10] Hu N, Fukunaga H, Atobe S, Liu Y, Li J. Piezoresistive Strain Sensors Made from Carbon Nanotubes Based Polymer Nanocomposites. *Sensors*. **2011**, *11*, 10691–10723. DOI: [10.3390/s111110691](https://doi.org/10.3390/s111110691).
- [11] Kovacs, J. Z.; Velagala, B. S.; Schulte, K.; Bauhofer, W. Two Percolation Thresholds in Carbon Nanotube Epoxy Composites. *Compos. Sci. Technol.* **2007**, *67*, 922–928. DOI: [10.1016/j.compscitech.2006.02.037](https://doi.org/10.1016/j.compscitech.2006.02.037).
- [12] Bauhofer, W.; Kovacs, J. Z. A Review and Analysis of Electrical Percolation in Carbon Nanotube Polymer Composites. *Compos. Sci. Technol.* **2009**, *69*, 1486–1498. DOI: [10.1016/j.compscitech.2008.06.018](https://doi.org/10.1016/j.compscitech.2008.06.018).
- [13] Davidson, T.; *Functional Fillers for Plastics*; 2nd; Wiley-VCH: Weinheim, Germany, **2010**; pp 351–368.
- [14] Wehnert, F.; Langer, M.; Kaspar, J.; Jansen, I. *EURADH - 10th European Adhesion Conference*, **2014**, 63–67.
- [15] Petrie, E. M.; Electrically and Thermally Conductive Adhesive Formulation: Online, 18.05.2018.
- [16] Thostenson, E. T.; Chou, T.-W. Processing-structure-multi-functional Property Relationship in Carbon Nanotube/epoxy Composites. *Carbon*. **2006**, *44*, 3022–3029. DOI: [10.1016/j.carbon.2006.05.014](https://doi.org/10.1016/j.carbon.2006.05.014).

- [17] Lakdawala, K.; Salovey, R. Rheology of Polymers Containing Carbon Black. *Polym. Eng. Sci.* **1987**, *27*, 1035–1042. DOI: [10.1002/\(ISSN\)1548-2634](https://doi.org/10.1002/(ISSN)1548-2634).
- [18] Skipa, T.; Lellinger, D.; Böhm, W.; Saphiannikova, M.; Alig, I. Influence of Shear Deformation on Carbon Nanotube Networks in Polycarbonate Melts: Interplay between Build-up and Destruction of Agglomerates. *Polymer*. **2010**, *51*, 201–210. DOI: [10.1016/j.polymer.2009.11.047](https://doi.org/10.1016/j.polymer.2009.11.047).
- [19] Schilde, C.; Mages-Sauter, C.; Kwade, A.; Schuchmann, H. P. Efficiency of Different Dispersing Devices for Dispersing Nanosized Silica and Alumina. *Powder Technol.* **2011**, *207*, 353–361. DOI: [10.1016/j.powtec.2010.11.019](https://doi.org/10.1016/j.powtec.2010.11.019).
- [20] Sanli, A.; Müller, C.; Kanoun, O.; Elibol, C.; Wagner, M. F.-X. Piezoresistive Characterization of Multi-walled Carbon Nanotube-epoxy Based Flexible Strain Sensitive Films by Impedance spectroscopy. *Compos. Sci. Technol.* **2015**, *122*, 18–26. DOI: [10.1016/j.compscitech.2015.11.012](https://doi.org/10.1016/j.compscitech.2015.11.012).
- [21] Schulte, K.; Gojny, F. H.; Wichmann, M. H. G.; Sumfleth, J.; Fiedler, B. Polymere Nanoverbundwerkstoffe: Chancen, Risiken und Potenzial zur Verbesserung der mechanischen und physikalischen Eigenschaften. *Materialwiss. Werkst.* **2006**, *37*, 698–703. DOI: [10.1002/\(ISSN\)1521-4052](https://doi.org/10.1002/(ISSN)1521-4052).
- [22] Novák, I.; Krupa, I.; Chodák, I. *J. Mater. Sci. Lett.* **2002**, *21*, 1039–1041. DOI: [10.1023/A:1016073010528](https://doi.org/10.1023/A:1016073010528).
- [23] Gojny, F. H.; Wichmann, M. H. G.; Köpke, U.; Fiedler, B.; Schulte, K. Carbon Nanotube-reinforced Epoxy-composites: Enhanced Stiffness and Fracture Toughness at Low Nanotube Content. *Compos. Sci. Technol.* **2004**, *64*, 2363–2371. DOI: [10.1016/j.compscitech.2004.04.002](https://doi.org/10.1016/j.compscitech.2004.04.002).
- [24] Karger-Kocsis, J.; *Nano- and Micromechanics of Polymer Blends and Composites*; Carl Hanser Verlag: München, Germany, **2009**; pp 425–470.
- [25] Tjong, S. C.; *Nano- and Micromechanics of Polymer Blends and Composites*; Carl Hanser Verlag: München, Germany, **2009**; pp 341–375.
- [26] Wehnert, F.; Pötschke, P.; Jansen, I. Hotmelts with Improved Properties by Integration of Carbon Nanotubes. *Int. J. Adhes. Adhes.* **2015**, *62*, 63–68. DOI: [10.1016/j.ijadhadh.2015.06.014](https://doi.org/10.1016/j.ijadhadh.2015.06.014).
- [27] Wu, G.; Asai, S.; Zhang, C.; Miura, T.; Sumita, M. A Delay of Percolation Time in Carbon-black-filled Conductive Polymer Composites. *J. Appl. Phys.* **2000**, *88*, 1480. DOI: [10.1063/1.373843](https://doi.org/10.1063/1.373843).
- [28] Barth, N.; Schilde, C.; Kwade, A. *Chem.-Ing.-Tech.* **2012**, *84*, 328–334. DOI: [10.1002/cite.201100193](https://doi.org/10.1002/cite.201100193).
- [29] Ho, L.-N.; Nishikawa, H. Influence of Post-curing and Coupling Agents on Polyurethane Based Copper Filled Electrically Conductive Adhesives. *J. Mater. Sci.-Mater. EL*. **2013**, *24*, 2077–2081. DOI: [10.1007/s10854-012-1059-0](https://doi.org/10.1007/s10854-012-1059-0).
- [30] Winkler, C.; Schwarz, U. *EURADH - 11th European Adhesion Conference*, **2016**, 90–93.
- [31] Winkler, C.; Schwarz, U.; Konnerth, J. Effect of Thermal Postcuring on the Micro- and Macromechanical Properties of Polyurethane for Wood Bonding. *Appl. Adhes. Sci.* **2018**, *6*(737). DOI: [10.1186/s40563-018-0106-3](https://doi.org/10.1186/s40563-018-0106-3).
- [32] EN 302-1: Adhesives for load-bearing timber structures. Test methods. Determination of longitudinal tensile shear strength (April 2013).
- [33] Ross, R. J.; *Wood Handbook - Wood as an Engineering Material*; Centennial ed: Madison, WI, **2010**.
- [34] Marinho, B.; Ghislandi, M.; Tkalya, E.; Koning, C. E.; With, G. *Powder Technol.* **2012**, *221*, 351–358. DOI: [10.1016/j.powtec.2012.01.024](https://doi.org/10.1016/j.powtec.2012.01.024).

- [35] Gurunathan, T.; Rao, C. R. K.; Narayan, R.; Raju, K. V. S. N. Polyurethane Conductive Blends and Composites: Synthesis and Applications Perspective. *J. Mater. Sci.* **2013**, *48*, 67–80. DOI: [10.1007/s10853-012-6658-x](https://doi.org/10.1007/s10853-012-6658-x).
- [36] Hwang, S.-H.; Bang, D. S.; Yoon, K. H.; Park, Y.-B. *Smart Materials and Structures Based on Carbon Nanotube Composites*; INTECH Open Access Publisher, London, **2011**.
- [37] Chanklin, W.;. *Electrical Properties Study of Carbon Fillers in Polymer Nanocomposites*; New Brunswick, **2016**.
- [38] Habenicht, G.;. *Kleben. Grundlagen, Technologien, Anwendungen*, 6th ed.; Springer: Berlin, **2009**.
- [39] Konnerth, J.; Gindl, W.; Harm, M.; Müller, U. Comparing dry bond strength of spruce and beech wood glued with different adhesives by means of scarf- and lap joint testing method. *Eur. J. Wood Wood Prod.* **2006**, *64*, 269–271. DOI: [10.1007/s00107-006-0104-1](https://doi.org/10.1007/s00107-006-0104-1).
- [40] Zhang, R.; Dowden, A.; Deng, H.; Baxendale, M.; Peijs, T. Conductive network formation in the melt of carbon nanotube/thermoplastic polyurethane composite, *Compos. Sci. Technol.* **2009**, *69*, 1499–1504.
- [41] Buschhorn, S. T.; Wichmann, M. H. G.; Sumfleth, J.; Schulte, K.; Pegel, S.; Kasaliwal, G. R.; Villmow, T.; Krause, B.; Göldel, A.; Pötschke, P. Charakterisierung der Dispersionsgüte von Carbon Nanotubes in Polymer-Nanokompositen. *Chem.-Ing.-Tech.* **2011**, *83*, 767–781. DOI: [10.1002/cite.v83.6](https://doi.org/10.1002/cite.v83.6).

**Influence of polymer/filler composition and processing on the properties of multifunctional adhesive wood bonds from polyurethane prepolymers II: electrical sensitivity in compression**

Christoph Winkler<sup>1,2</sup>, Jesco Schäfer<sup>1</sup>, Christopher Jager<sup>1</sup>, Johannes Konnerth<sup>2</sup> and Ulrich Schwarz<sup>1</sup>

<sup>1</sup> University of Applied Sciences Eberswalde, Faculty of Wood Engineering, Eberswalde, Germany

<sup>2</sup> BOKU - University of Natural Resources and Life Sciences, Institute of Wood Technology and Renewable Materials, Vienna, Austria



**Declaration of author contributions**

Winkler conceptualized and designed the experiment. Combined DC resistance measurements under load were carried out by Schäfer under the guidance of Winkler. Jager wrote the code to evaluate the data set according to the given sensor characteristics by Winkler. Data have been evaluated and discussed by all. Writing and editing of the final manuscript was done by Winkler. Funding acquisition of the financial support leading to this publication was done by Winkler and Schwarz. All authors read and approved the final manuscript.





# Influence of polymer/filler composition and processing on the properties of multifunctional adhesive wood bonds from polyurethane prepolymers II: electrical sensitivity in compression

Christoph Winkler <sup>a,b</sup>, Jesco Schäfer<sup>a</sup>, Christopher Jäger<sup>a</sup>, Johannes Konnerth <sup>b</sup>, and Ulrich Schwarz<sup>a</sup>

<sup>a</sup>Faculty of Wood Engineering, University of Applied Sciences Eberswalde, Eberswalde, Germany;

<sup>b</sup>Department of Material Sciences and Process Engineering (MAP), University of Natural Resources and Life Sciences, Vienna, Austria

## ABSTRACT

Electrically conductive fillers enhance the functionality of adhesive bondlines by inducing a strain-dependent electrical resistance. Applied as sensor elements in engineered timber, these multifunctional adhesive bondlines are influenced by a lot of process parameters, including the dispersion process, manufacturing parameters and postcuring conditions. Additionally, the sensitivity of these sensor elements is counteracted by instabilities of the piezoresistivity. A setup and analysing method of the piezoresistive response have been developed, which includes sensitivity as well as instability effects. With this setup, the quality of the piezoresistive bondline has been assessed by three experiments, varying 10 influencing factors. The piezoresistive response was investigated in compression perpendicular to the bondline. It was shown that the electrical sensitivity in compression and stability of the piezoresistive bondline can be influenced by polymer formulation, filler type, filler content as well as the press temperature, glue spread, dispersion technique and thermal postcuring.

## ARTICLE HISTORY

Received 30 July 2019



Accepted 2 August 2019

## KEYWORDS

Conductive adhesives; adhesives for wood; piezoresistivity; signal stability; adhesives with nanoparticles; civil engineering

## 1. Introduction

Electrically conductive fillers are considered suitable to enhance the functionality of polymers, making them to piezoresistive sensor elements. In other words, these nanocomposite materials show a strain-dependent change of electrical resistance and can therefore be utilized for a new class of directly attachable strain sensors.<sup>[1,2]</sup> While in the last years carbon nanotubes (CNT) have been the most prominent filler class for these composite polymers, carbon black (CB) is still under research<sup>[3–5]</sup>, same as various other fillers, among them carbon nanofibers.<sup>[6–8]</sup>

**CONTACT** Christoph Winkler  [Christoph.Winkler@hnee.de](mailto:Christoph.Winkler@hnee.de)  Faculty of Wood Engineering, University of Applied Sciences Eberswalde, Alfred-Möller-Strasse 1, Eberswalde 16225, Germany

Color versions of one or more of the figures in the article can be found online at [www.tandfonline.com/gadh](http://www.tandfonline.com/gadh).

This article has been republished with minor changes. These changes do not impact the academic content of the article.

© 2019 Taylor & Francis Group, LLC

By dispersing electrically conductive fillers into an insulating polymer matrix, an electrically conductive network can be formed throughout the material. With increasing content, the electrical resistance is following a so-called percolation curve.<sup>[9]</sup> The mechanical strength of the material typically decreases with increasing filler content<sup>[10]</sup> and additionally strain sensitivity is generated. Consequently, polymer based adhesives with multifunctionality have been reported<sup>[11,12]</sup> and multifunctional bondlines for timber constructions were investigated.<sup>[13–15]</sup> In order to evaluate the suitability of multifunctional adhesive bondlines as sensor elements in timber structures, a broad variety of influencing factors is needed to be considered, ranging from polymer/filler composition and dispersion to the process parameters for bonding. While influences of process parameters on the mechanical and electrical properties of adhesive bondlines in beech have been reported and discussed in our prior study<sup>[16]</sup>, piezoresistivity wasn't discussed yet.

So far, the piezoresistive effect of CNT-filled polymers is not fundamentally understood<sup>[17]</sup>, but significant progress has been made. Under tensile load, the piezoresistivity is attributed to three working mechanisms<sup>[18]</sup>, (1) the change of tunneling resistance between particles, which are isolated by the surrounding polymer, (2) variations of conducting network by change of contact points and (3) the piezoresistive effect of carbon nanotubes themselves.

Thus, the piezoelectric sensitivity, which is defined as the relative change of resistance with applied strain, decreases with an increasing filler content of CNT<sup>[18–20]</sup> as well as CB<sup>[21]</sup> due to the distinct influence of tunneling with lower filler content. Although this correlation prefers polymers with lower filler content, higher filled composites will increase the reproducibility and are therefore more suitable for practical applications.<sup>[18]</sup>

Beyond this theoretical knowledge, experimental results regarding the use of nanocomposites as sensors are mainly based on bulk samples<sup>[22,23]</sup> or in form of, coatings, typically applied on well-defined surfaces.<sup>[24]</sup> Integrating such multifunctionality in wood adhesive bondlines is more challenging as the bondline is lacking of defined geometric dimension. During fabrication the adhesive penetrates the adherents, making the cross section of the bondline diffuse and therefore not reproducible regarding their geometrical dimensions.<sup>[25]</sup>

Even studies on reproducible materials often report instability effects, which are adverse to the intended use of multifunctional polymers as sensor. Changes in conductivity with loading cycles is a typical effect of instability, published e.g. by Zhao et al.<sup>[26]</sup> Instability in the form of resistance creep has been reported by Wang and Ding<sup>[27]</sup> for CB-filled silicones, showing that higher filler contents tend to reduce the overall creep of the resistance and a higher Young's modulus of the polymer matrix can decrease the resistance creep. Creep under load, also reported by Abu-Abdeen et al.<sup>[28]</sup>, can therefore be traced back to the viscoelastic character of polymers. Repeatability has shown to increase with mass content of CNT, reaching a better reproducibility of the piezoresistive change when reaching a limit beyond the percolation threshold.<sup>[29]</sup>

From own experiments, the authors also knew about instabilities in multifunctional wood bondlines, including creep of resistance and change of resistance after applying loads. Based on these observations a setup has been developed for a faster evaluation of influences derived from processing multifunctional bonds in layered wood, considering the bonding quality, the electrical properties of the bondline as well as the suitability for piezoresistive measurements.

Three different experiments are focusing on different aspects of the sensitive bondline production, experiment I is varying the adhesive components, experiment II is varying the process parameters in the bonding process and experiment III is investigating a possible impact of a thermal postcuring. The same preparation method of the specimen for compression sensitivity tests has been used for all experiments. Mechanical and electrical properties of the bonds with various parameters has been shown in Part I<sup>[16]</sup>, the compression sensitivity together with an evaluation of stability parameters will be presented in the present Part II.

## 2. Material and methods

### 2.1. Preparation and experimental setup

The preparation of the glued-in-pairs wood lamellas has been described in a previous paper.<sup>[16]</sup> The wood lamellas have been manufactured with different material combinations and process parameters, which are also described in detail in Winkler et al.<sup>[16]</sup>, and summarized in Table 1.

Adhesives have been prepared from five different one-component polyurethane prepolymers (1C-PUR) intended for use in structural timber bonding (PU1 to PU5). Fillers to achieve conductivity have been carbon black (Ketchenblack EC300J, Akzo Nobel Functional Chemicals B.V., Arnhem/The Netherlands), further labeled CB and carbon nanotubes (NC7000, Nanocyl S.A., Sambreville/Belgium), further labeled CNT. In experiment III, a combination of 2wt% carbon nanofibers (PR-25-XT-HHT, Pyrograf Products Inc., Cedarville, USA) and 0.2wt% carbon nanotubes (NC7000, Nanocyl S.A., Sambreville/Belgium) has been used, in the text labeled with CNFT.

Compression tests with the force perpendicular to the bondline have been chosen to evaluate the influence of the process on the piezoresistive effect. The specimen for the test have been cut from the specimen for DC resistography, described in Winkler et al.<sup>[16]</sup>, with a total of 10 to 15 samples for each parameter.

Figure 1 shows details of the test specimen (1), the strain distribution in the specimen (2), and the test setup for evaluation of the electrical sensitivity in compression (3).

The specimen had dimensions of 60 mm length, 20 mm width and 10 mm height, the glued joint was located in the middle between two lamellas of

**Table 1.** Variables of the experiments and their parameters. Bold printed parameters have been held constant while varying other variables in the same experiment. Abbreviations: PU1 to PU5 polyurethan prepolymer one to five, according to.<sup>[16]</sup> CB carbon black, CNT carbon nanotubes, CNFT mixture of carbon fibers and carbon nanotubes, see also.<sup>[28]</sup>

Variables	Experiment I (polymer, filler and filler content)	Experiment II (manufacturing process)	Experiment III (effect of thermal postcuring)
Polymer	PU1; PU2; PU3; PU4; PU5	PU4	see <sup>[30]</sup>
Filler type	CB; CNT	CB	CNFT; CB
Filler content in wt%	0–7 (CB); 0–3 (CNT)	4	2 + 0.2; 4
Dispersion technique	<b>3-roll-mill</b>	<b>3-roll-mill</b> ; dissolver	<b>dissolver</b>
Application technique	<b>tooth scraper</b>	nozzle; <b>scraper</b> ; tooth scraper	<b>scraper</b>
Glue spread in g/m <sup>2</sup>	<b>250</b>	150; <b>250</b> ; 400	<b>250</b>
Pressure in MPa	<b>1</b>	0.6; <b>0.9</b> ; 1.2	<b>1</b>
Press time in h <sup>1</sup>	<b>1</b>	1; <b>2.5</b>	<b>1.5</b>
Press temperature in °C	<b>50</b>	20; <b>35</b> ; 50	<b>30</b>
Thermal postcuring in °C/h	<b>untreated</b>	Untreated	untreated; 80/1; 80/48; 95/1; 95/48

5 mm thickness. The compression area on the glue joint has been reduced by cutting in two notches with dimensions of 10 mm length, 20 mm width and 4.5 mm height. The glued joint was thus intact over the entire length of 60mm, but only exposed to compressive forces in the area of 40mm length and 20mm width. The strain distribution in the specimen has been measured by digital image correlation (Aramis 3D, 5M cameras, GOM GmbH, Braunschweig/Germany) up to a stress level of 9 MPa to ensure that no strain is directly applied to the electrical contact as this would influence the measurement more than the piezoresistive response. As intended, the electrical contact points on the end face of the test specimens have not been stressed mechanically with this specimen preparation, as can be seen from the strain distribution in [Figure 1 \(2\)](#). Electrical contact to the bondline was realised by applying silver conductive paste (L204N, Ferro GmbH, Hanau/Germany) on the end faces, drying it for at least 24 hours. The electrodes were pressed on with springs ([Figure 1 \(7\)](#)). The frame with spring-loaded contacts is shown in detail in Winkler et al.<sup>[16]</sup>

A universal testing machine (Zwick/Roell Type 1484, load cell 200kN, Ulm, Germany) was used to apply compressive stress perpendicular to the bondline, and DC resistance has been measured with a digital multimeter (NI PXI 4071, National Instruments GmbH, Munich/Germany) at a sample rate of 7.5 Hz. All tests were performed at climate conditions of 21/37 (21°C/37% rH).

## 2.2. Piezoresistivity and stability

[Figure 2](#) displays the method to derive sensitivity and stability characteristics related to the use of the bondline as the sensor element. The upper diagram

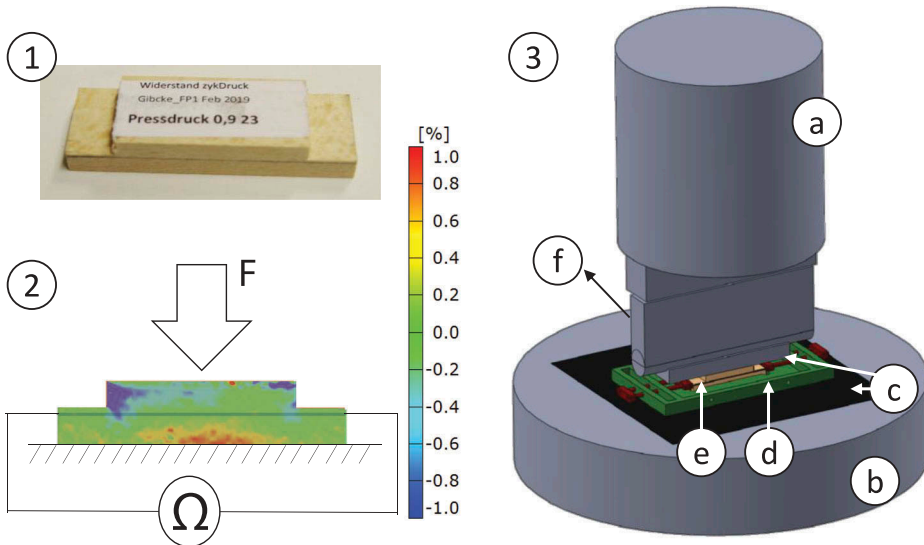


**Figure 1.** Details of test setup for DC resistography under compression load. (1) wood adhesive bond specimen. (2) simplified test setup indicating load direction, DC resistography connection and measured strain distribution in load direction at 8MPa compression stress (3) test setup with testing tools for support and load application (a-b), electrical insulation (c), frame with spring-loaded contact electrodes (d), specimen (e) and connection to DC resistance meter (f).

displays the mechanical load profile applied in each test, the middle diagram is an exemplary DC resistance output – corresponding to the piezoresistive response – and the box below the diagrams displays the calculation of the sensor characteristics.

Measured DC resistance has been recorded at a sample rate of 7.5 Hz and the raw signal (green) smoothed for further calculations (brown). Raw data have been filtered using a LOWESS algorithm (Locally Weighted Scatterplot Smoothing), which is based on a local linear estimation (time frame = 6.8 s).<sup>[31]</sup> Each test consists out of 4 sections with:

Section I, where the specimen remains unstressed.

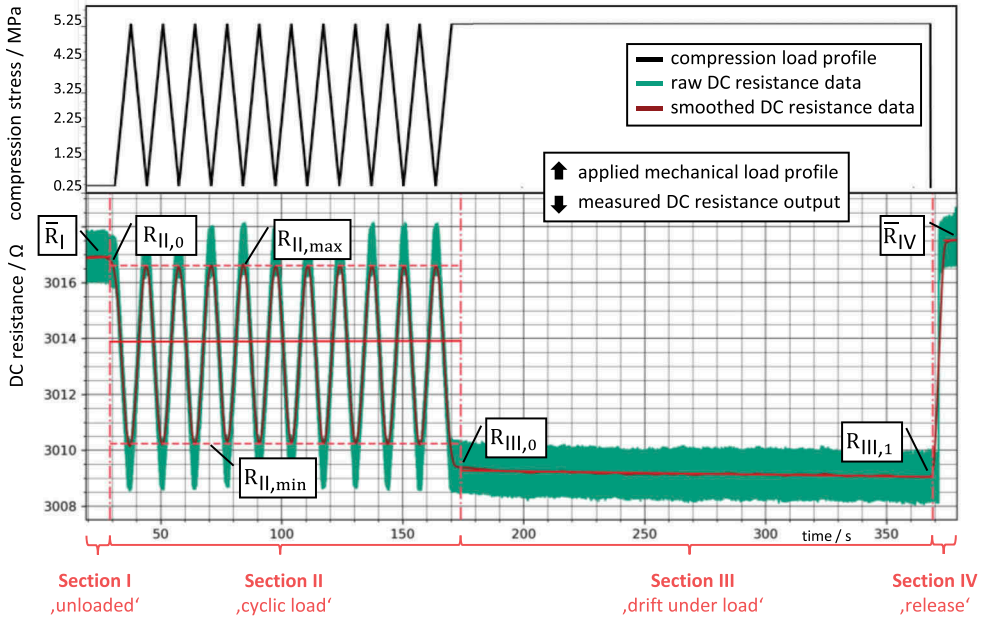
Section II, in which a cyclic load over 10 cycles has been applied, changing from a basic load of 0.25 MPa to 5.25 MPa within 10 seconds (stress-controlled mode with a speed of 1 MPa/s). 5.25 MPa has been chosen due to the maximum compression strength of beech perpendicular to the grain reported to be 7–11 MPa.<sup>[32,33]</sup>

Section III, which is characterized by a uniform compression load of 5.25 MPa.

Section IV, where the specimen was unloaded again.

The sensor characteristics are derived from the smoothed DC resistance output according to Figure 2 and are defined as follows:

Sensitivity describes the ratio of sensor output to the change in the value to be measured.<sup>[34]</sup> Typically, the sensitivity of nanocomposite strain sensors is given by a gauge factor, which represents the change ratio of resistance



calculation of sensor characteristics:

**Sensitivity:** relative change of DC resistance under compression load in %/MPa

$$S_{c,DC} = \frac{|\overline{R_{II,max}} - \overline{R_{II,min}}|}{R_{II,0} * 5} * 100$$

**Variability:** relative change of DC resistance under repeated loading in %

$$V_{c,DC} = \frac{\max(R_{II,max}) - \min(R_{II,max})}{\min(R_{II,max})} * 100$$

**Drift:** relative change DC resistance under compression load in %

$$D_{c,DC} = \frac{R_{III,1} - R_{III,0}}{R_{III,0}} * 100$$

**Baseline Instability:** relative change of DC resistance baseline in %

$$BI_{DC} = \frac{\overline{R_{IV}} * \overline{R_I}}{\overline{R_I}} * 100$$

**Figure 2.** Measuring sequence to characterise the sensitive properties. Applied mechanical load profile (upper diagram) and an example for a sensitive output signal from DC resistography (lower diagram). Indicated values in the measured DC resistance curve are used to calculate sensor characteristics (formulas indicated in the box).

$\Delta R/R_0$ , where  $R_0$  is the initial resistance, per applied strain in percent. In adhesive bondlines of around 20–200  $\mu\text{m}$  thickness, compressive strains are technically not measurable for a large number of samples. Thus the sensitivity  $S_{c,DC}$  is represented by  $\Delta R/R_0$  per applied stress in MPa.  $\Delta R/R_0$  equals the calculation of  $S_{c,DC}$  in the box without the divisor 5, which derives from the amplitude 5 MPa of the cyclic load.

Variability defines the incapability of a sensor to produce the same output when the same input is applied to it. In this work,  $V_{c,DC}$  was calculated by the relative deviation of the resistance measured at 5.25 MPa.

Drift describes a systematic deviation that changes continuously in one direction. In other publications, resistance creep is used equally. As creep is typically mechanically induced, the more sensor related term drift or drift response will be used. Drift  $D_{c,DC}$  was calculated by the relative DC resistance change under constant load in section III.

As last parameter, baseline instability describes the incapability of a sensor element to exhibit the same sensor output after excitation. In these experiments, baseline instability  $BI_{DC}$  results out of the relative change of the bondline DC resistance after and before applying the load.

### 3. Results and discussion

#### 3.1. Data evaluation

All calculated characteristics related to stability – variability, drift, and baseline instability – need to be lower than the sensitivity as they represent adverse effects on the quality of the sensitive bondline. With a high percentual value in these instability characteristics, changes of stress due to real events can't be distinguished from the change due to instabilities.

Thus, instability characteristics are compared to a normalised sensitivity. Normalising the sensitivity means that sensitivity was related to one unit of stress (%/MPa). By calculating all sensor characteristics as described, they became comparable among each other, as all describe a relative change in percent. Thus, the quality of the electrically conductive bondline for a sensor can be evaluated from four boxplots. [Figure 3](#) displays three examples to explain this data interpretation.

Examples a) to c) include on the left side four boxplots describing all four characteristics of one test series – at the examples of PU1, filled with 6 wt% carbon black (CB) – and on the right side a diagram of the piezoresistivity of one sample from this series. While the diagrams show differences in single measurements, the whole series of measurements can be described with the four boxplots on the left side.

The measurement presented in [Figure 3\(a\)](#) represents data from bondlines made out of PU1, filled with 6 wt% CB. The results of sensitivity  $S_{c,DC}$  is around one decade higher than the Drift  $D_{c,DC}$ .  $S_{c,DC}$  is also higher than repeatability as well as baseline stability. Therefore, the bondline as sensor element is considered to be stable, stresses can be measured even at low levels and the bondline can be considered as qualified for sensing stresses.

The measurement presented in [Figure 3\(b\)](#) – data from bondlines made of PU2, filled with 5 wt% CB – shows that all instability characteristics are clearly higher than the sensitivity, which is also visible from the diagram. Therefore, this distribution of characteristics is unfavorable for sensor elements. Still, some samples show lower instability effects than the sensitivity, which offers possibilities for optimization.



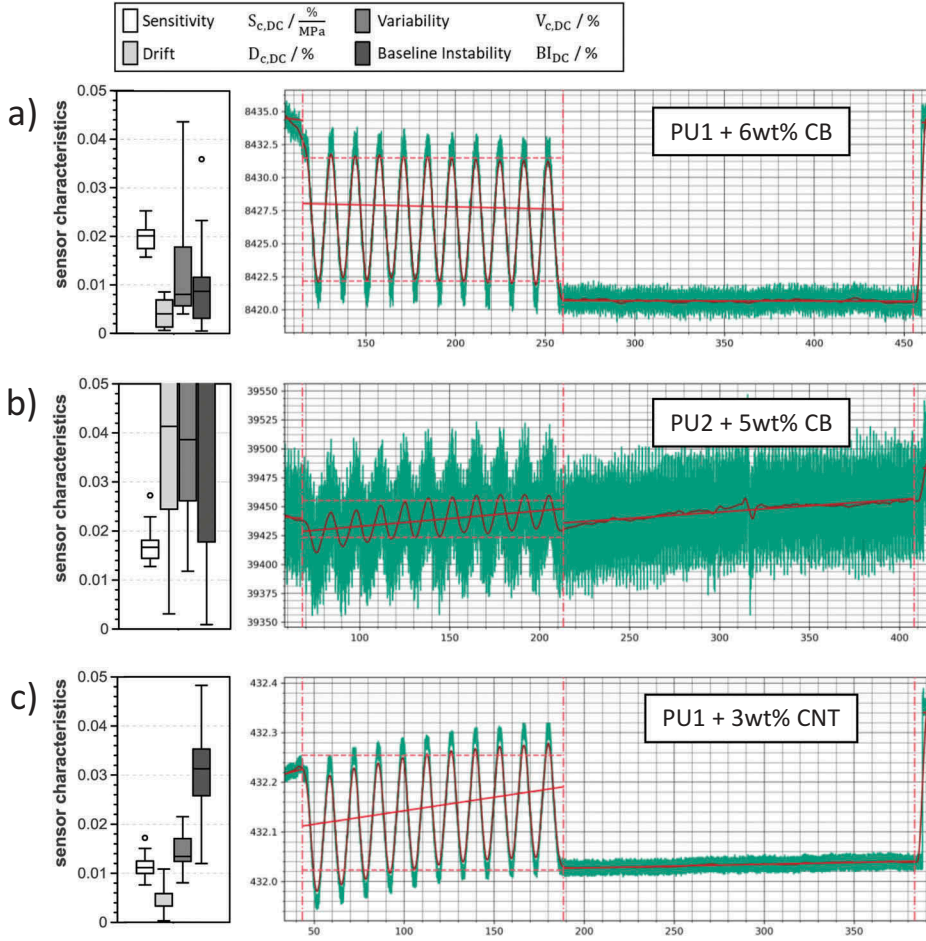


**Figure 3.** Sensor output signal and calculated sensor characteristics of three exemplarily displayed measurements (a-c); (left) boxplots describing the sensor characteristics. (right) examples from the test series indicated in the right upper corner graph.

The measurement presented in Figure 3(c) – data from bondlines made of PU1, filled with 6 wt% CB – results in a sensitivity  $S_{c,DC}$ , which is higher than the resistance drift under constant load  $D_{c,DC}$ , but due to changes in the resistance with loading cycles, the repeatability show a high deviation as well as the baseline DC resistance is not reproducible, thus unstable.

Similar to all boxplots is that high deviation of the data implies a high variation in the sensor element properties. Regarding a measuring system analysis, this represents non-reproducible sensor elements.

Thus, when interpreting data to analyse influences due to process parameters, not only the single characteristics and statistically significant changes need to be considered. Additionally, the reduction of data deviation can be interpreted as evidence for better quality in applications.



Some instabilities in the nanocomposites may result that the signal can't be processed. Figure 4 illustrates two test results, which couldn't be analysed. The first one exhibit some irreversible changes in the nanocomposite bondline, which can be attributed to the destruction of existing conductive networks. The second diagram displays a high deviation in the filtered signal, which is one decade higher (0.2 %) than the sensitivity of the bondline (0.02%).

### 3.2. Polymer, filler and filler content

Polymer, filler type and filler content have been varied in experiment I. The resulting data are shown in Figures 5–9, one for each polyurethane prepolymer.

Each Figure displays the data in groups of four boxplots for the different filler contents, the first boxplot representing sensitivity  $S_{c,DC}$ , the other three drift  $D_{c,DC}$ , variability  $V_{c,DC}$  and baseline instability  $BI_{DC}$ . All are referred to the left scale while using the same scale for comparability. As their variation would in some cases prevent an overview, sensitivity is used as the reference

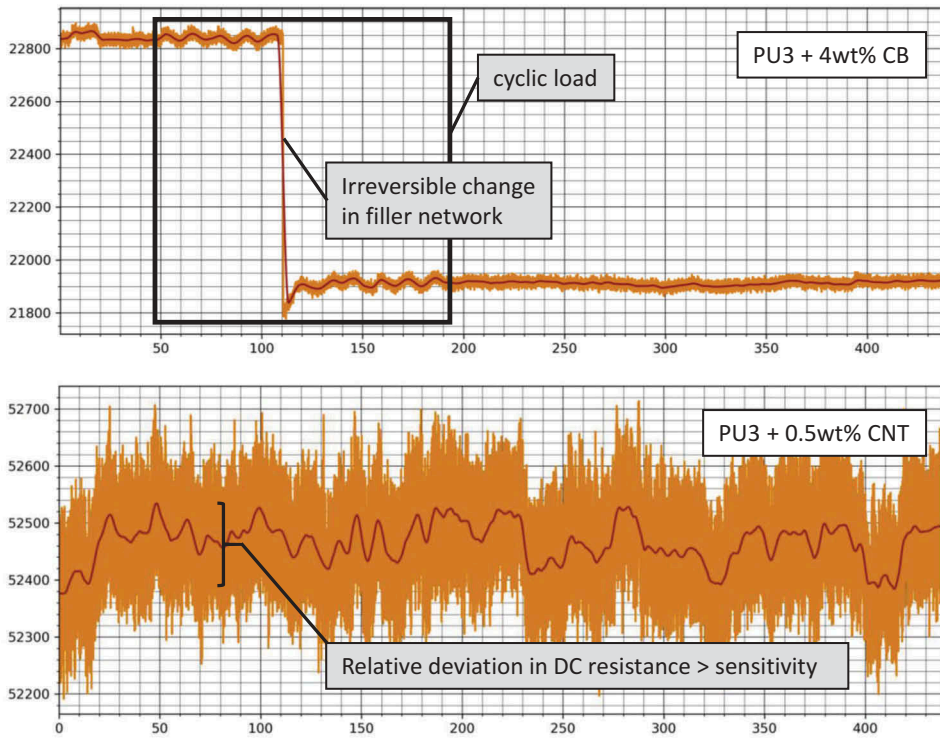


**Figure 4.** Example of a piezoresistive response indicating (top) an irreversible change in the filler network or (bottom) a high deviation in the baseline DC resistance.

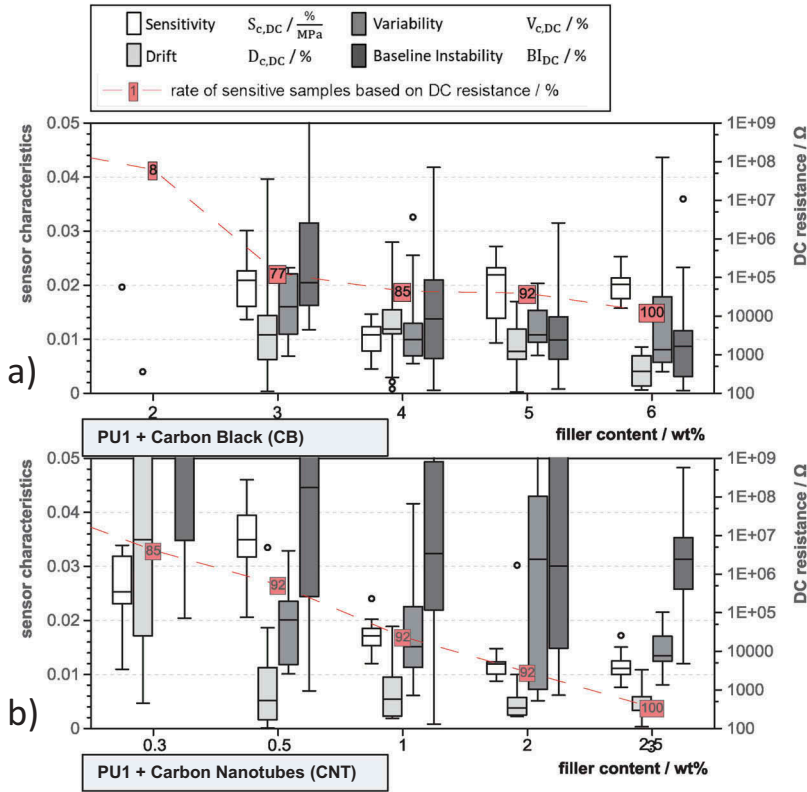


**Figure 5.** Comparison of sensor characteristics sensitivity, drift under load, variability and baseline instability, as well as DC resistance of PU1, filled with a varying weight content of electrically conductive filler ((a) carbon black; (b) carbon nanotubes). Boxplots: boxes = quartile of distribution, whiskers = 1.5 of interquartile range, circles = outliers. Dotted red line: corresponding baseline DC resistance (right axis). Red squares: relative percentage (out of 10–15 samples), resulting in analysable signal quality.

for the scaling. Thus, in some instances, the boxplots are not fully displayed as they cover considerably higher values.

The red boxes in each diagram displays the baseline DC resistance, which has been discussed in Winkler et al.<sup>[16]</sup>, referring to the right scale. Additionally, to take into account the number of analysable signals (Figure 4) a boxed number displays the rate of samples, which has been analysable out of 12 to 15 samples.

As a general result, sensitivity  $S_{c,DC}$  could not be measured until a certain amount of filler has been reached. Comparing the necessary filler content of all nanocomposite bondlines to achieve a piezoresistive response, it is obvious that it differs with the polymer/filler composition. For carbon black filled 1C-PURs, the data show consistent results as sensitivity is achieved, starting at 3 wt% CB, only PU2 gives a piezoresistive response at 2 wt%. Comparing these data with the percolation threshold range, which has been presented in Winkler et al.<sup>[16]</sup>, it reveals that sensitivity for CB filled 1C-PURs in the shape of wood bonds

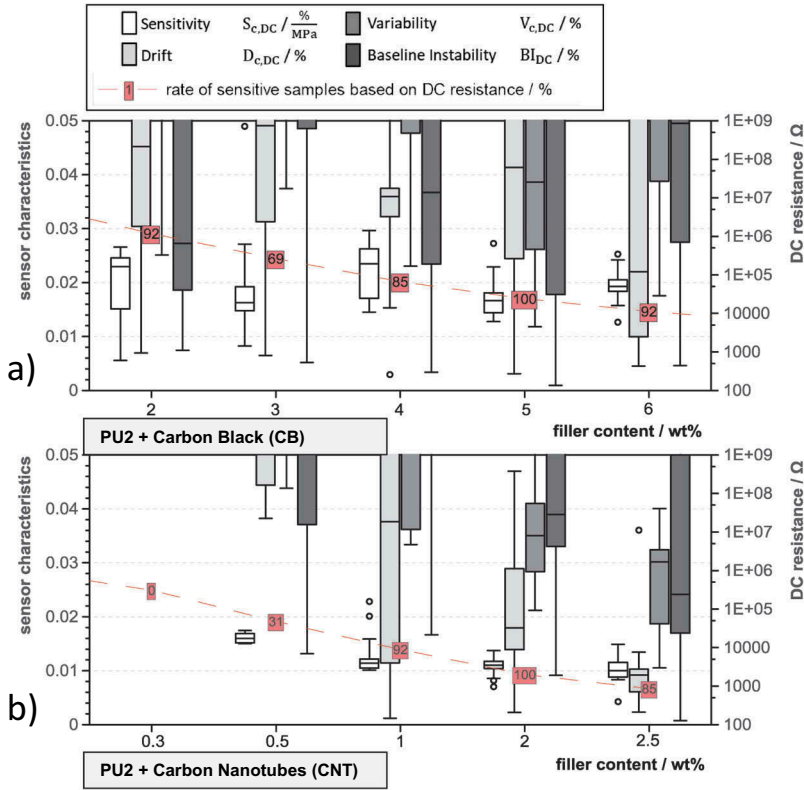


**Figure 6.** Comparison of sensor characteristics sensitivity, drift under load, variability and baseline instability, as well as DC resistance of PU2, filled with a varying weight content of electrically conductive filler ((a) carbon black; (b) carbon nanotubes). Boxplots: boxes = quartile of distribution, whiskers = 1.5 of interquartile range, circles = outliers. Dotted red line: corresponding baseline DC resistance (right axis). Red squares: relative percentage (out of 10–15 samples), resulting in analysable signal quality.

exhibits piezoresistivity after passing the critical filler content  $\Phi_c$ , which has been determined as 1 to 4 wt%. In respect to the unloaded (baseline) DC resistance of the bondline,  $10^5$  Ohm is the limit to achieve sensitivity.

Polyurethane prepolymers, filled with CNT, are non-consistent to this limit. While the critical filler content  $\Phi_c$  is one decade lower than for carbon black (in the range of 0.05 to 1 wt%)<sup>[16]</sup>, CNT-filled 1C -PURs exhibit sensitivity at filler content ranging from 0.3 wt% for PU1 to 2.5 wt% for PU3 and PU4. Additionally, the associated DC resistance limit at which the first piezoresistance can be measured, ranges from  $10^7$  Ohm for PU1 to  $10^3$  Ohm for PU3 and PU4. Thus, it must be rejected that only by reaching a specific limit of DC resistance in the bondline, a measurable piezoresistive response is achieved. By reviewing the measurements with low electrical resistance, but no measurable piezoresistivity, most of the data show a high deviation in the baseline DC resistance as shown in Figure 4. Hypothetically,

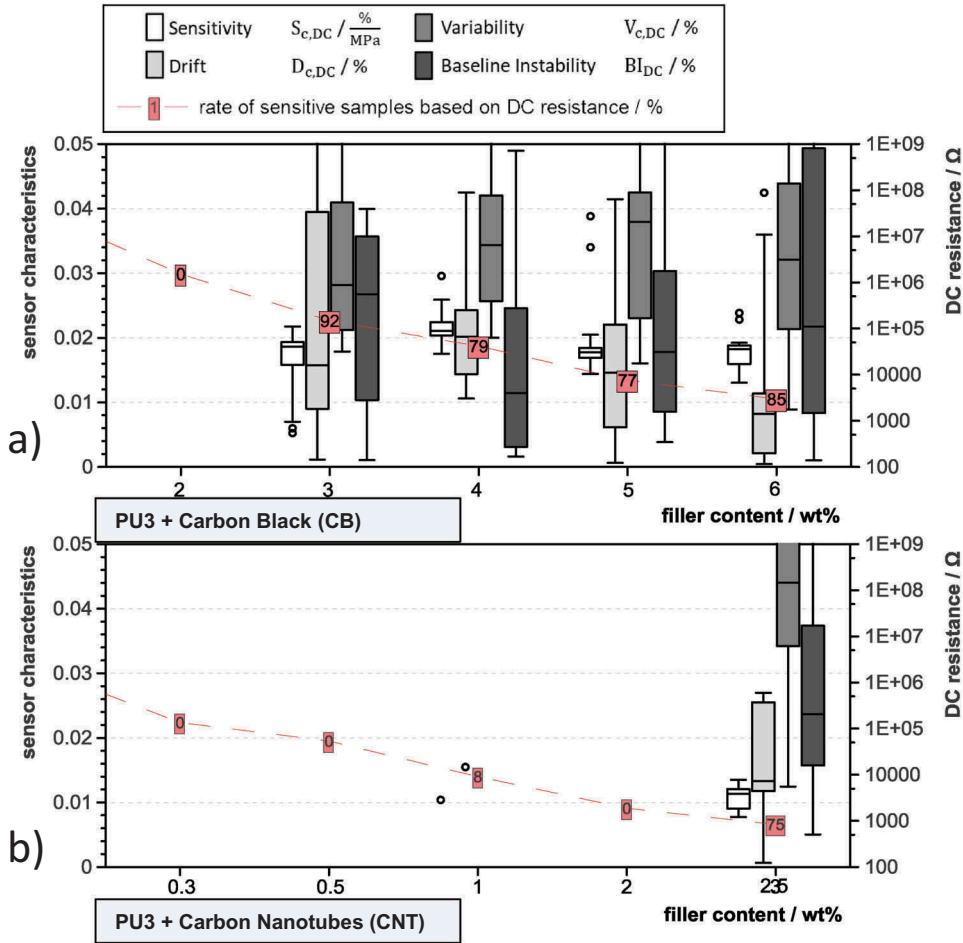


**Figure 7.** Comparison of sensor characteristics sensitivity, drift under load, variability and baseline instability, as well as DC resistance of PU3, filled with a varying weight content of electrically conductive filler ((a) carbon black; (b) carbon nanotubes). Boxplots: boxes = quartile of distribution, whiskers = 1.5 of interquartile range, circles = outliers. Dotted red line: corresponding baseline DC resistance (right axis). Red squares: relative percentage (out of 10–15 samples), resulting in analysable signal quality.

an explanation for this high deviation could be the state of dispersion.<sup>[35]</sup> With an inhomogeneous distribution of CNT-agglomerates, which are still forming a conductive network inside the insulation polymer, low resistance can be achieved without resulting in piezoresistivity.

When piezoresistivity is measurable, all measured  $S_{c,DC}$  values are lower than the instability characteristics, excluding some datasets of PU1 with a high filler content of CB or CNTs. Thus, it is obvious that piezoresistivity of the bondline doesn't qualify the same as a qualified sensor element.

With increasing filler content, no change in sensitivity  $S_{c,DC}$  can be measured with CB as filler.  $S_{c,DC}$  is measured for all 1C-PURs in the range of 0.01 to

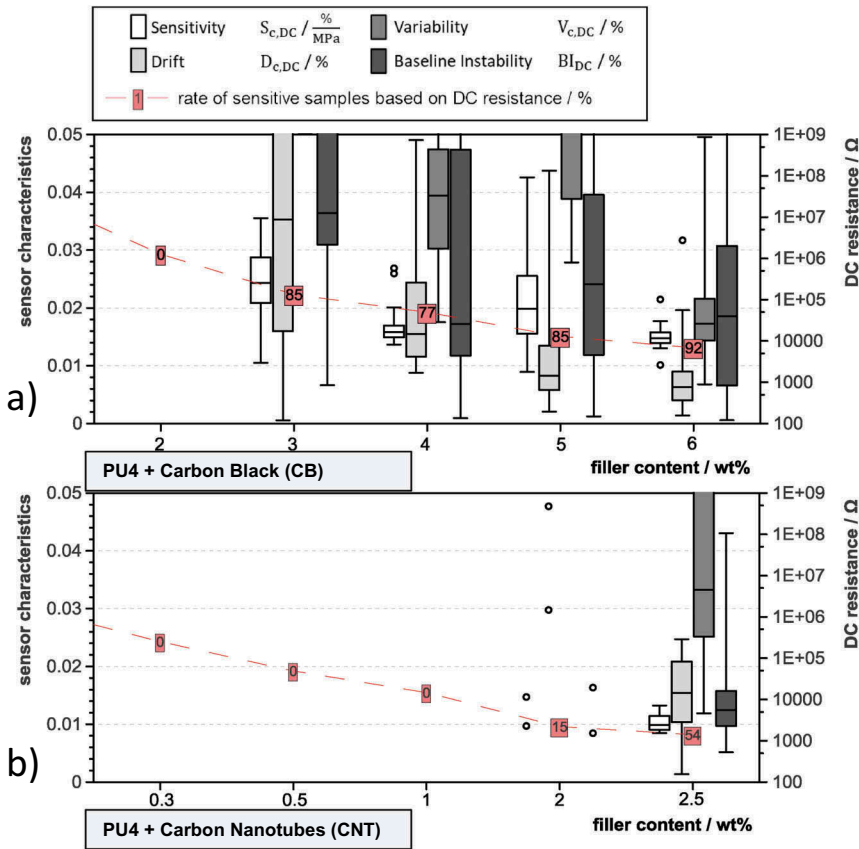


**Figure 8.** Comparison of sensor characteristics sensitivity, drift under load, variability and baseline instability, as well as DC resistance of PU4, filled with a varying weight content of electrically conductive filler ((a) carbon black; (b) carbon nanotubes). Boxplots: boxes = quartile of distribution, whiskers = 1.5 of interquartile range, circles = outliers. Dotted red line: corresponding baseline DC resistance (right axis). Red squares: relative percentage (out of 10–15 samples), resulting in analysable signal quality.

0.02%. Contrary, with increasing content of CNTs, the sensitivity decreases from 0.03 to 0.04% down to 0.01 to 0.02%. Therefore, it can be noted that results from nanocomposite research regarding carbon nanotubes can be applied to piezoresistive bondlines in wood as sensitivity decreases with increasing filler content.<sup>[18–20]</sup> Since the decreasing sensitivity is attributed to less polymer barriers between the filler particles<sup>[36]</sup> it can be assumed that the dispersion of CB in 1C-PUR leads to more direct electrical contact of particles and less polymer between them. The higher overall sensitivity of CB-filled 1C-PUR leads to the conclusion that carbon black is more suitable for piezoresistive bondlines in wood from 1C-PUR.

Resistance drift  $D_{c,DC}$  in all variations show a lower value than the variability as well as the baseline instability. Additionally,  $D_{c,DC}$  typically tends to decrease with increasing filler content as illustrated in Figure 10.

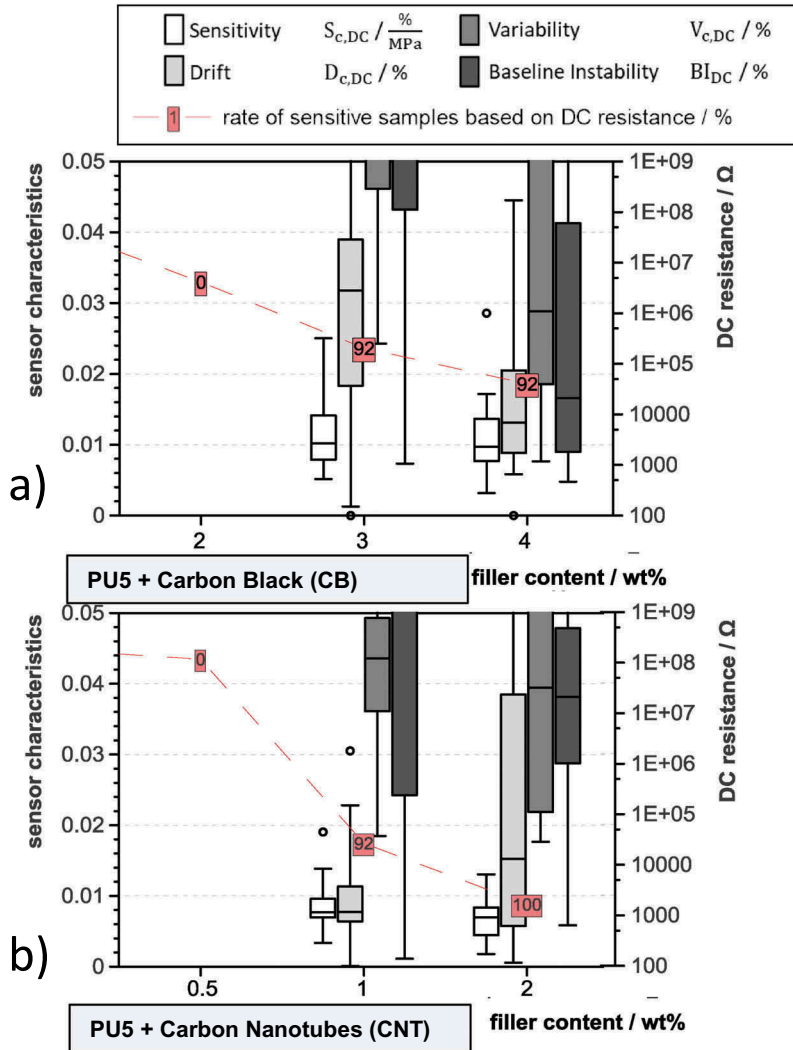


**Figure 9.** Comparison of sensor characteristics sensitivity, drift under load, variability and baseline instability, as well as DC resistance of PU5, filled with a varying weight content of electrically conductive filler ((a) carbon black; (b) carbon nanotubes). Boxplots: boxes = quartile of distribution, whiskers = 1.5 of interquartile range, circles = outliers. Dotted red line: corresponding baseline DC resistance (right axis). Red squares: relative percentage (out of 10–15 samples), resulting in analysable signal quality.

This phenomenon is in accordance with investigations by Wang and Ding<sup>[27]</sup> and is therefore also considered to be applicable for piezoresistive bondlines in wood.

It can be summarized that with higher sensitivity, carbon black gives a higher quality of piezoresistive bondlines in wood and with increasing filler content the quality becomes better as resistance drift is decreasing. It is also clear that the selection of polymer influences not only the dispersion quality

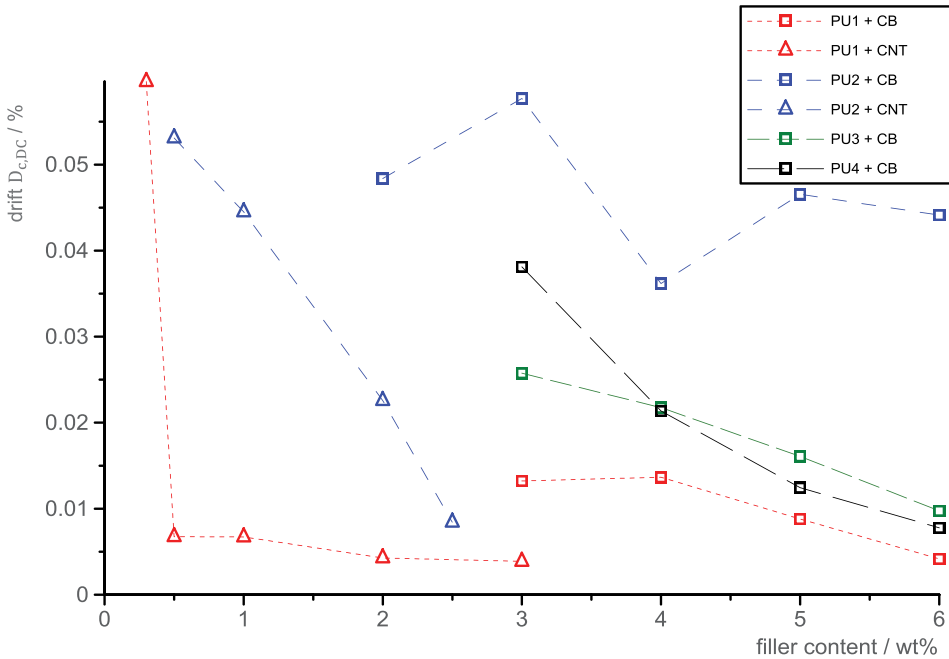


**Figure 10.** Drift in resistance  $D_{c,DC}$  under load with increasing content of electrically conductive filler. PU1 to PU4 refer to the different polymers. CB = carbon black. CNT = carbon nanotubes.

and therefore the mechanical and electrical properties (as shown in the previous paper<sup>[16]</sup>), but also the quality as a sensor as PU1 obviously results in the best piezoresistive properties for compressive sensor elements.

### 3.3. Manufacturing process influences

Figure 11 displays sensitivity and instability characteristics of all varied process parameters in experiemnt II in the same manner as described before. A one-way analysis of variance (ANOVA,  $p \leq 0.05$ ) was used to statistically evaluate the significance of process parameters on the sensor characteristics.

Except for the variation of press temperature, all process parameters as well as their variations, result in a constant sensitivity  $S_{c,DC}$  of 0.015 to 0.03%. With lower press temperature, a trend to higher  $S_{c,DC}$  can be observed, resulting in a significant higher  $S_{c,DC}$  (ANOVA,  $p \leq 0.05$ ) of 0.03 to 0.04% at a pressing temperature of 20°C. As discussed earlier, higher sensitivity originates from more polymer barriers between the filler particles. While this phenomenon acts on the molecular level, another, not yet explained reason for enhanced compression sensitivity could be the structure of bondlines from polyurethane prepolymers on the microscopic level. 1C-PUR cures under forming carbon dioxide ( $CO_2$ ) and thus will create a foamed structure of the bondline. Under compression, a higher amount of gas inclusions in the conductive polymer



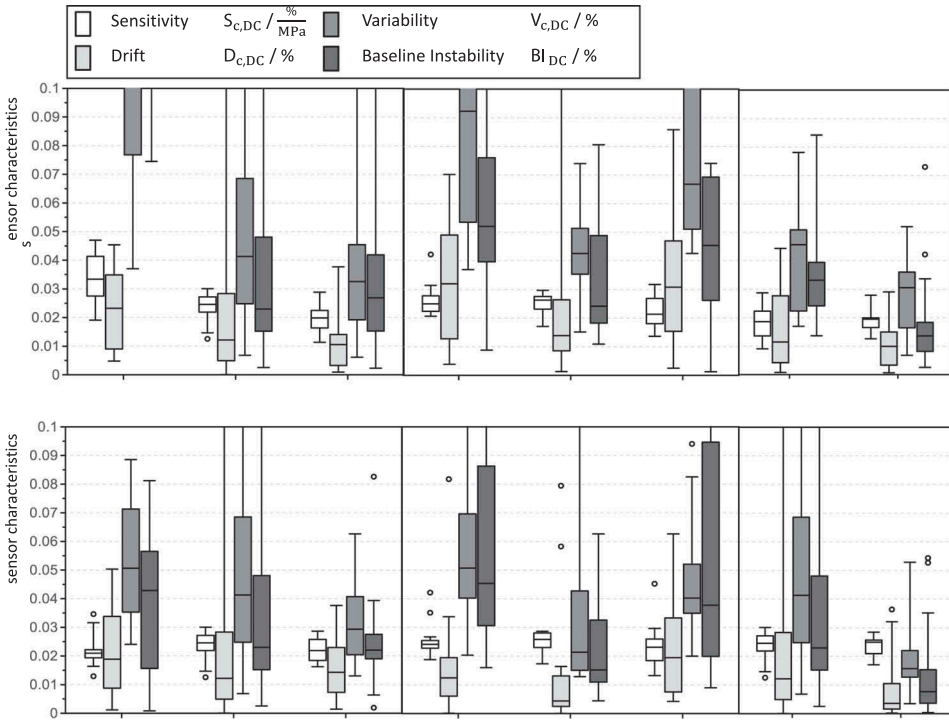


**Figure 11.** Comparison of sensitivity, resistance, drift under load, variability and baseline instability of piezoresistive wood bonds from PU4, filled with a 4 wt% of carbon black (CB), manufactured with varying process parameters. Boxplots: boxes = quartile of distribution, whiskers = 1.5 of interquartile range, circles = outliers.

would increase the amplitude of the resistance change (in this case, the piezoresistive sensitivity). With increasing temperature,  $\text{CO}_2$  can escape easier from liquids due to coalescence and/or Ostwald ripening<sup>[37]</sup>, thus a higher porosity structure of the bondline would be the consequence of less press temperature. With decreasing bondline porosity, the stability of the electrically conductive filler network and therefore the DC resistance of the bondline should decrease and shows less deviation. As measurements of all instability characteristics decrease with increasing press temperature, it can therefore be hypothesized that a higher porosity in the bondline gives higher sensitivity, but less stability of the piezoresistivity.

Regarding the influence of process parameters on the instability characteristics, applied pressure and the application technique showed no impact. With increasing pressure time and glue spread as well as by using the dissolver for dispersing, the all instability characteristics decrease slightly and are reduced in variation, while the sensitivity stays constant. As discussed in Winkler et al.<sup>[16]</sup>, a longer application of pressure in the manufacturing will give a less porous bondline. With increasing glue spread, the adhesive will be more homogeneously distributed over the adherend area.



Consequently, a less porous bondline as well as a more homogenous distribution would increase the stability of the filler network.<sup>[38]</sup>

Dispersions by dissolver causes less separation of agglomerates than the 3-roll mill.<sup>[39]</sup> To what extent the less dispersion quality is responsible for the higher stability of the piezoresistive response can not be fully explained.

### 3.4. Thermal postcuring influences

Figure 12 compares all sensor characteristics of two sets of thermally post-cured multifunctional bondlines, both differentiable by the kind of dispersed filler (CB and CNFT).

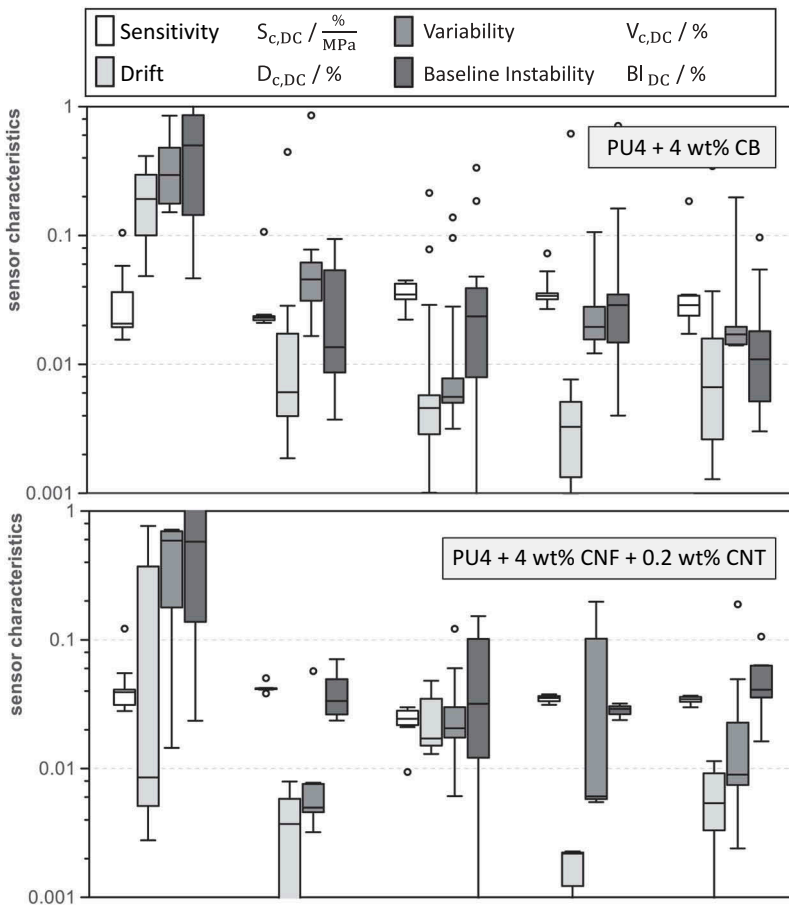


**Figure 12.** Comparison of sensitivity, resistance, drift under load, variability and baseline instability of two sets PU4, TOP filled with a 4 wt% of carbon black (CB), or BELOW filled with 2 wt% carbon nanofibers and 0.2 wt% carbon nanotubes (CNFT) and four different postcuring conditions (e.g. 80/1 = 80°C for 1 hour) as well as one untreated reference. Boxplots: boxes = quartile of distribution, whiskers = 1.5 of interquartile range, circles = outliers.

Both datasets show no distinct influence of thermal postcuring on the sensitivity, which has measurable values of 0.02 to 0.03%/MPa for all treatments. On the contrary, both datasets show that with thermal postcuring all instability effects decrease. Except for  $D_{c,DC}$  of 1C-PUR filled with CNFT, no instability effect results in a systematic trend due to postcuring temperature or time. In case of 1C-PUR filled with CNFT,  $D_{c,DC}$  decreases with thermal postcuring of one hour, but increases again with a longer treatment at 48 hours. Other studies indicated that the mechanical behavior of the polymer matrix influenced the stability and sensitivity of nanocomposites.<sup>[30]</sup> As creep data from micromechanical characterisation by nanoindentation has been available for the same sets of samples<sup>[40]</sup>, these datasets were compared, finding no correlation. Consequently, no effect of the polymer creep behavior on the resistance drift can be approved. Nonetheless, resistance drift of bondlines of 1C-PUR filled with carbon nanoparticles can obviously be reduced by thermal postcuring.

#### 4. Conclusion

Multifunctional adhesive bondlines in the wood are influenced by a range of process parameters, starting with the dispersion process through to the manufacturing and postcuring conditions. Additionally, the sensitivity of these sensor elements is counteracted by instabilities of the piezoresistivity. Thus, a setup and analyses of the piezoresistive response have been developed, which includes sensitivity as well as instability effects. From this holistic observation, the quality of the piezoresistive bondline can be estimated.

The setup has been used for three experiments, varying 10 influencing factors on the piezoresistive response in compression perpendicular to the bondline. From the results, the following conclusions can be drawn:

- (1) The quality of bondlines for piezoresistive sensor application can be assessed by using four parameters, illustrating the relationship between the sensor characteristics and their variation.
- (2) Carbon black is more qualified than carbon nanotubes as a functional filler in 1C-PURs as it resulted in higher sensitivities.
- (3) Due to the lack of sensitivity by reaching a certain limit of conductivity the quality of CNT-filled 1C-PUR is inferior.
- (4) Higher filler contents are more suitable for applications as the resistance drift under load is decreasing with it.
- (5) Sensitivity and instability characteristics of the multifunctional bondlines are not connected. With constant sensitivity, the instability characteristics can be reduced with filler content as well as with manufacturing parameters.

- (6) The polymer formulation of 1C-PUR influences both the mechanical and electrical properties, as shown in Winkler et al.<sup>[16]</sup>, but also the piezoresistive quality.
- (7) Influences caused by manufacturing could be identified, which can help to produce more qualified multifunctional bondlines, reducing their instability and variation. These parameters are lower press temperature, higher glue spread, dissolver as dispersion technique and thermal postcuring.

## Acknowledgements

This work was supported by the German Government within the „Nachwachsende Rohstoffe“ program (FNR, BMEL) under Grant 22005018. We also gratefully acknowledge the help of M. Günther (University of Applied Sciences Eberswalde) with DIC measurements.

## Funding

This work was supported by the German Government within the Nachwachsende Rohstoffe program (FNR, BMEL) [22005018].

## ORCID

Christoph Winkler  <http://orcid.org/0000-0002-0444-4309>

Johannes Konnerth  <http://orcid.org/0000-0003-3826-8566>

## References

- [1] Bautista-Quijano, J. R.; Avilés, F.; Cauich-Rodriguez, J. V. Sensing of Large Strain Using Multiwall Carbon Nanotube/segmented Polyurethane Composites. *J. Appl. Polym. Sci.* **2013**, *130*, 375–382. DOI: [10.1002/app.39177](https://doi.org/10.1002/app.39177).
- [2] Kang, I.; Schulz, M. J.; Kim, J. H.; Shanov, V.; Shi, D. A Carbon Nanotube Strain Sensor for Structural Health Monitoring. *Smart Mater. Struct.* **2006**, *15*, 737–748. DOI: [10.1088/0964-1726/15/3/009](https://doi.org/10.1088/0964-1726/15/3/009).
- [3] Vadlamani, V. K.; Chalivendra, V. B.; Shukla, A.; Yang, S. Sensing of Damage in Carbon Nanotubes and Carbon Black-Embedded Epoxy under Tensile Loading. *Polym. Compos.* **2012**, *33*, 1809–1815. DOI: [10.1002/pc.v33.10](https://doi.org/10.1002/pc.v33.10).
- [4] Köckritz, T.; Wehnert, F.; Pap, J.-S.; Jansen, I. Increasing the Electrical Values of Polydimethylsiloxane by the Integration of Carbon Black and Carbon Nanotubes. A Comparison of the Effect of Different Nanoscale Fillers. *Phys. Soc. Jpn.* **2015**, *51*, 221–222.
- [5] Elhad Kassim, S. A.; Achour, M. E.; Costa, L. C.; Lahjomri, F. Prediction of the DC Electrical Conductivity of Carbon Black Filled Polymer Composites. *Polym. Bull.* **2015**, *72*, 2561–2571. DOI: [10.1007/s00289-015-1421-5](https://doi.org/10.1007/s00289-015-1421-5).
- [6] Singer, G.; Rennhofer, H.; Sinn, G.; Unterlass, M. M.; Wendrinsky, J.; Windberger, U.; Lichtenegger, H. C. Processing of Carbon Nanotubes and Carbon Nanofibers Towards

- High Performance Carbon Fiber Reinforced Polymers. *Key Eng. Mat.* **2017**, 742, 31–37. DOI: [10.4028/www.scientific.net/KEM.742](https://doi.org/10.4028/www.scientific.net/KEM.742).
- [7] Feng, L.; Xie, N.; Zhong, J. Carbon Nanofibers and Their Composites: A Review of Synthesizing, Properties and Applications. *Materials*. **2014**, 7, 3919–3945. DOI: [10.3390/ma7053919](https://doi.org/10.3390/ma7053919).
- [8] Kang, I.; Heung, Y. Y.; Kim, J. H.; Lee, J. W.; Gollapudi, R.; Subramaniam, S.; Narasimhadevara, S.; Hurd, D.; Kirikera, G. R.; Shanov, V.; et al. Introduction to Carbon Nanotube and Nanofiber Smart Materials. *Compos. Part B Eng.* **2006**, 37, 382–394. DOI: [10.1016/j.compositesb.2006.02.011](https://doi.org/10.1016/j.compositesb.2006.02.011).
- [9] Alamus; Hu, N.; Fukunaga, H.; Atobe, S.; Liu, Y.; Li, J. Piezoresistive Strain Sensors Made from Carbon Nanotubes Based Polymer Nanocomposites. *Sensors*. **2011**, 11, 10691–10723. DOI: [10.3390/s111110691](https://doi.org/10.3390/s111110691).
- [10] Novák, I.; Krupa, I.; Chodák, I. J. Relation between electrical and mechanical properties in polyurethane/carbon black adhesives. *Mat. Sci. Lett.* **2002**, 21, 1039–1041. DOI: [10.1023/A:1016073010528](https://doi.org/10.1023/A:1016073010528).
- [11] Wehnert, F.; Langer, M.; Kaspar, J.; Jansen, I. Design of Multifunctional Adhesives by the Use of Carbon Nanoparticles. *J. Adhes. Sci. Technol.* **2014**, 29, 1849–1859. DOI: [10.1080/01694243.2015.1014536](https://doi.org/10.1080/01694243.2015.1014536).
- [12] Wehnert, F.; Pötschke, P.; Jansen, I. Hotmelts with Improved Properties by Integration of Carbon Nanotubes. *Int. J. Adhes. Adhes.* **2015**, 62, 63–68. DOI: [10.1016/j.ijadhadh.2015.06.014](https://doi.org/10.1016/j.ijadhadh.2015.06.014).
- [13] Myslicki, S.; Winkler, C.; Gelinski, N.; Schwarz, U.; Walther, F. *Fatigue assessment of adhesive wood joints through physical measuring technologies Fatigue 2017: 7th International Conference on Durability and Fatigue*. Cambridge. **2017**, 446–455.
- [14] Winkler, C.; Schwarz, U. Materials and Joints in Timber Structures. *Rilem Bookseries*. **2014**, 9, 381–394.
- [15] Winkler, C.; Schwarz, U. *Wood Adhesives for Non-Destructive Structural Monitoring. 19th World Conference on Non-Destructive Testing*. Munich. **2016**, 158, 1–8.
- [16] Winkler, C.; Konnerth, J.; Gibcke, J.; Schäfer, J.; Schwarz, U. J. Influence of Polymer/Filler Composition and Processing on the Properties of Multifunctional Adhesive Wood Bonds from Polyurethane Prepolymers I: Mechanical and Electrical Properties. *Adhes.* to appear. 2019.
- [17] Kanoun, O.; Müller, C.; Benchirouf, A.; Sanli, A.; Dinh, T. N.; Al-Hamry, A.; Bu, L.; Gerlach, C.; Bouhamed, A. Flexible Carbon Nanotube Films for High Performance Strain Sensors. *Sensors*. **2014**, 14, 10042–10071. DOI: [10.3390/s140610042](https://doi.org/10.3390/s140610042).
- [18] Sanli, A.; Müller, C.; Kanoun, O.; Elibol, C.; Wagner, M. F.-X. Piezoresistive Characterization of Multi-walled Carbon Nanotube-epoxy Based Flexible Strain Sensitive Films by Impedance spectroscopy. *Compos. Sci. Technol.* **2015**, 122, 18–26. DOI: [10.1016/j.compscitech.2015.11.012](https://doi.org/10.1016/j.compscitech.2015.11.012).
- [19] Hu, N.; Karube, Y.; Arai, M.; Watanabe, T.; Yan, C.; Li, Y.; Liu, Y.; Fukunaga, H. Investigation on Sensitivity of a Polymer/carbon Nanotube Composite Strain Sensor. *Carbon*. **2010**, 48, 680–687. DOI: [10.1016/j.carbon.2009.10.012](https://doi.org/10.1016/j.carbon.2009.10.012).
- [20] Ferreira, A.; Martínez, M. T.; Ansón-Casaos, A.; Gómez-Pineda, L. E.; Vaz, F.; Lanceros-Mendez, S. Relationship between Electromechanical Response and Percolation Threshold in Carbon Nanotube/poly(vinylidene Fluoride) Composites. *Carbon*. **2013**, 61, 568–576. DOI: [10.1016/j.carbon.2013.05.038](https://doi.org/10.1016/j.carbon.2013.05.038).
- [21] Luheng, W.; Tianhuai, D.; Peng, W. Influence of Carbon Black Concentration on Piezoresistivity for Carbon-black-filled Silicone Rubber Composite. *Carbon*. **2009**, 47, 3151–3157. DOI: [10.1016/j.carbon.2009.06.050](https://doi.org/10.1016/j.carbon.2009.06.050).

- [22] Ke, K.; Pötschke, P.; Wiegand, N.; Krause, B.; Voit, B. Tuning the Network Structure in Poly(vinylidene fluoride)/Carbon Nanotube Nanocomposites Using Carbon Black: Toward Improvements of Conductivity and Piezoresistive Sensitivity. *ACS Appl. Mater. Interfaces*. **2016**, *8*, 14190–14199. DOI: [10.1021/acsami.6b03451](https://doi.org/10.1021/acsami.6b03451).
- [23] Georgousis, G.; Pandis, C.; Kalamiotis, A.; Georgiopoulos, P.; Kyritsis, A.; Kontou, E.; Pissis, P.; Micusik, M.; Czanikova, K.; Kulicek, J.; et al. Strain Sensing in Polymer/carbon Nanotube Composites by Electrical Resistance Measurement. *Compos. Part B Eng*. **2015**, *68*, 162–169. DOI: [10.1016/j.compositesb.2014.08.027](https://doi.org/10.1016/j.compositesb.2014.08.027).
- [24] Sanli, A.; Benchirouf, A.; Müller, C.; Kanoun, O. Piezoresistive Performance Characterization of Strain Sensitive Multi-walled Carbon Nanotube-epoxy Nanocomposites. *Sensors Actuat. A Phys*. **2017**, *254*, 61–68. DOI: [10.1016/j.sna.2016.12.011](https://doi.org/10.1016/j.sna.2016.12.011).
- [25] McKinley, P. E.; Ching, D. J.; Kamke, F. A.; Zauner, M.; Xiao, X. Micro X-Ray computed tomography of adhesive bonds in wood. *Wood Fibre Sci*. **2016**, *48*, 2–16.
- [26] Zhao, J.; Dai, K.; Liu, C.; Zheng, G.; Wang, B.; Liu, C.; Chen, J.; Shen, C. A Comparison between Strain Sensing Behaviors of Carbon Black/polypropylene and Carbon Nanotubes/polypropylene Electrically Conductive Composites. *Compos. Part A-Appl. S*. **2013**, *48*, 129–136. DOI: [10.1016/j.compositesa.2013.01.004](https://doi.org/10.1016/j.compositesa.2013.01.004).
- [27] Wang, P.; Ding, T. J. Creep of electrical resistance under uniaxial pressures for carbon black-silicone rubber composites. *Wood Sci*. **2010**, *45*, 3595–3601.
- [28] Abu-Abdeen, M.; Aboud, A. I.; Ramzy, G. H. *Int. J. Effect of Temperature on Creep behavior of Poly(vinylchloride) Loaded with Single Walled Carbon Nanotubes*. *Sci. Eng*. **2016**, *5*, 112–120.
- [29] Vertuccio, L.; Vittoria, V.; Guadagno, L.; Santis, F. D. C. Strain and Damage Monitoring in Carbon-nanotube-based Composite under Cyclic Strain. *Part A-Appl. S*. **2015**, *71*, 9–16. DOI: [10.1016/j.compositesa.2015.01.001](https://doi.org/10.1016/j.compositesa.2015.01.001).
- [30] Ku-Herrera, J. J.; Avilés, F. Cyclic Tension and Compression Piezoresistivity of Carbon Nanotube/vinyl Ester Composites in the Elastic and Plastic Regimes. *Carbon*. **2012**, *50*, 2592–2598. DOI: [10.1016/j.carbon.2012.02.018](https://doi.org/10.1016/j.carbon.2012.02.018).
- [31] Cleveland, W. S.; Robust Locally Weighted Regression and Smoothing Scatterplots. *J. Am. Stat. Assoc*. **1979**, *74*, 829–836. DOI: [10.1080/01621459.1979.10481038](https://doi.org/10.1080/01621459.1979.10481038).
- [32] Ross, R. J.; *Wood Handbook - Wood as an Engineering Material*; Madison, WI: Forest Products Laboratory. **2010**. Centennial ed..
- [33] Niemz, P. *Physik des Holzes und der Holzwerkstoffe*; Leinfelden-Echterdingen: DRW. **1993**.
- [34] McGrath, M. J.; Scanail, C. N. *Sensor Technologies*; Apress: Berkeley, CA, **2013**.
- [35] Buschhorn, S. T.; Wichmann, M. H. G.; Sumfleth, J.; Schulte, K.; Pegel, S.; Kasaliwal, G. R.; Villmow, T.; Krause, B.; Gödel, A.; Pötschke, P. Charakterisierung der Dispersionsgüte von Carbon Nanotubes in Polymer-Nanokompositen. *Chem. Ing. Tech*. **2011**, *83*, 767–781. DOI: [10.1002/cite.v83.6](https://doi.org/10.1002/cite.v83.6).
- [36] Wichmann, M. H. G.; Buschhorn, S. T.; Böger, L.; Adelung, R.; Schulte, K. Direction Sensitive Bending Sensors Based on Multi-wall Carbon Nanotube/epoxy Nanocomposites. *Nanotechnology*. **2008**, *19*(475503). DOI: [10.1088/0957-4484/19/47/475503](https://doi.org/10.1088/0957-4484/19/47/475503).
- [37] Lerche, D.; Sobisch, T. Direct and Accelerated Characterization of Formulation Stability. *J. Disper. Sci. Technol*. **2011**, *32*, 1799–1811. DOI: [10.1080/01932691.2011.616365](https://doi.org/10.1080/01932691.2011.616365).
- [38] Petrie, E. M.; *Electrically and Thermally Conductive Adhesive Formulation*. Paris: SpecialChem S.A. Online, 18.05.2018.

- [39] Schilde, C.; Mages-Sauter, C.; Kwade, A.; Schuchmann, H. P. Efficiency of Different Dispersing Devices for Dispersing Nanosized Silica and Alumina. *Powder Technol.* **2011**, *207*, 353–361. DOI: [10.1016/j.powtec.2010.11.019](https://doi.org/10.1016/j.powtec.2010.11.019).
- [40] Winkler, C.; Schwarz, U.; Konnerth, J. Effect of Thermal Postcuring on the Micro- and Macromechanical Properties of Polyurethane for Wood Bonding. *Appl. Adhes. Sci.* **2018**, *6*(737). DOI: [10.1186/s40563-018-0106-3](https://doi.org/10.1186/s40563-018-0106-3).

## **Improving the usability of piezoresistive bond lines in wood by impedance measurements**

Jesco Schäfer<sup>1</sup>, Christopher Jager<sup>1</sup>, Ulrich Schwarz<sup>1</sup> and Christoph Winkler<sup>1</sup>

<sup>1</sup> University of Applied Sciences Eberswalde, Faculty of Wood Engineering, Eberswalde, Germany

### **Declaration of author contributions**

Schäfer and Winkler conceptualized and designed the experiment. Sample preparation was done by Schäfer under the guidance of Winkler. Combined impedance spectroscopy under load were carried out by Schäfer. Jager wrote the code to evaluate the spectroscopic data set and developed the method of SNR ratio together with Schäfer. Data have been evaluated and discussed by all. Writing and editing of the final manuscript was done by Schäfer. Funding acquisition of the financial support leading to this publication was done by Winkler and Schwarz. All authors read and approved the final manuscript.



# Improving the usability of piezoresistive bond lines in wood by using impedance measurements

Jesco Schäfer<sup>1</sup> · Christopher Jager<sup>1</sup> · Ulrich Schwarz<sup>1</sup> · Christoph Winkler<sup>1</sup>

Received: 20 November 2020 / Accepted: 10 June 2021 / Published online: 19 June 2021  
© The Author(s) 2021

## Abstract

Various studies on wood adhesives filled with conductive fillers for future application to structural monitoring showed a piezoresistive (resistance change with strain) response of the adhesive bond lines that is measurable under direct current. The results also showed a relatively high signal noise with low sensitivity. Using impedance spectroscopy as a measurement technique, the improvements in frequency-dependent piezoresistivity over DC (Direct Current) resistography of multifunctional bonded wood were studied. Beech specimens were bonded by one-component polyurethane prepolymer (1C-PUR) filled with carbon black and tested under shear load. The quality of the piezoresistive properties was described by calculating the signal-to-noise ratio (SNR) of the measured signal. A setup-specific frequency band with optimized SNR between 100 kHz and 1 MHz could be derived from the measurements. Several frequencies showed a signal with higher quality resulting in a higher SNR. Regardless of the variations in impedance spectra for all specimens, this frequency band provided several frequencies with improved signal quality. These frequencies give a more reliable signal with lower noise compared to the signal from DC resistography.

## Introduction

The use of wood adhesives as piezoresistive (resistance change with strain) sensor elements in engineered timber has been the focus of several previous studies conducted by the research group maderawood research (Winkler et al. 2020a, b; Winkler and Schwarz 2014, 2016). In these studies, adhesive joints between two wooden adherents—the bond line—have been modified by adding electrically conductive filler. Subsequently, the change of electrical properties could be used for measuring stress/strain differences. In contrast to the present study, the past work only used

---

✉ Jesco Schäfer  
jesco.schaefer@hnee.de

<sup>1</sup> Faculty of Wood Engineering, Eberswalde University for Sustainable Development, Schicklerstraße 5, 16225 Eberswalde, Germany



resistance under direct current as the leading sensory property. The long-term objective of these adhesive-based sensor elements is to provide affordable control and monitoring insights into the health of engineered timber under strain changes due to irregular loads as well as into moisture-induced changes of the wood's material stiffness.

In 2015, it was reported that no state of the art in structural monitoring of timber construction exists (Kurz 2015), which could improve the durability of the construction and optimize maintenance. The main methods in non-destructive testing for assessment of timber structures have been summarized (Kasal and Tannert 2010; Kurz and Boller 2015), but are rarely used for long-term monitoring of structures. Several assessment techniques are in use to continuously prove public construction sites like bridges, but these assessments require ongoing investment. In contrast, monitoring methods have higher investment costs in the beginning and lower ongoing costs, while the integration of sensors into the monitored structure is needed (Adams 2007). Since the integration of discrete sensors can be very time consuming and is mostly done after production, the hurdle to use monitoring in timber constructions is still high. The utilization of the adhesive, which is generally used for production, can help at this point. The integration of the piezoresistive adhesive into the manufacturing process is easier and can be used to monitor locations inside the engineered timber element. Hence, bond lines in wood with high sensitivity (relative change with monitored stress) and reliability (small variability of the measured signal) are necessary.

The sensitivity of the sensor elements mainly originates in the compressibility differences between the filler material and the polymer, combining a theoretically dielectric polymer with electrical conductive filler material and thus creating a mostly linear and reversible change in the electrical resistance under strain (Dharap et al. 2004; Ferreira et al. 2013; Ferreira et al. 2012; Hu et al. 2008; Li et al. 2008; Luheng et al. 2009; Pham et al. 2008).

The electrical conductivity and permittivity and therefore the electrical properties of dielectric polymers filled with conductive filler particles rely on four theoretical assumptions (Bao et al. 2012; Davidson 2005; Elhad Kassim et al. 2015; Elimat et al. 2010; Li et al. 2008; Sanli et al. 2016; Xia et al. 2017), which are also relevant for the change of electrical resistance under stress (Fig. 1). The four assumptions are the intrinsic electrical resistance of a conductive particle itself (1), the contact resistance of contacting particles (2), the tunneling effect between conductive particles which are not touching (3), and micro-capacitors formed through the Maxwell–Wagner–Sillars polarization in the interfaces between conductive particles (4), if insulating polymer can be found between two conductive particles (Elimat et al. 2010; Sanli et al. 2016; Sanli and Kanoun 2020; Xia et al. 2017). The impedance measured by impedance spectroscopy for a range of frequencies can be written as  $Z = Z' + iZ''$  in the Cartesian form for each frequency, where  $Z'$  is the real part ( $\text{Re}(Z)$ ) and  $Z''$  is the imaginary part ( $\text{Im}(Z)$ ) of the impedance (Elimat et al. 2010; Sanli and Kanoun 2020). Compared to the DC-resistance the impedance for alternating current takes phase differences into account and can be carried out for different frequencies (Elimat et al. 2010; Sanli and Kanoun 2020) which gives the ability to receive more information on the electrical characteristics of the examined material.

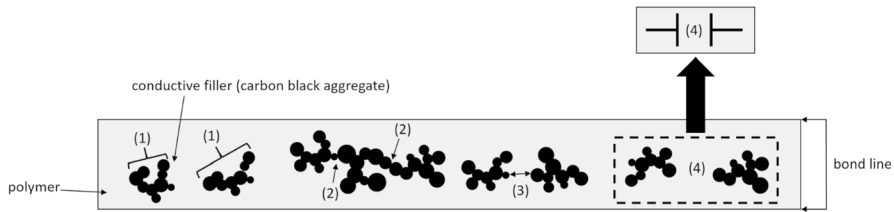


**Fig. 1** Schematic visualization of the four mechanisms theoretically responsible for the change of electrical resistance in the bond line under stress. (1) Intrinsic electrical resistance of a conductive particle/aggregate itself. (2) Contact resistance of two contacting particles/aggregates. (3) Tunneling resistance between two conductive, but not touching particles/aggregates. (4) Micro-capacitors formed through Maxwell–Wagner–Sillars polarization in the interfaces between conductive particles/aggregates. The shapes of carbon black are shown according to Chang et al. (2012) (colour figure online)

The effects (1) to (3) can be measured in the real part of the complex impedance (Xia et al. 2017), which describes the dissipation of electrical energy as thermal energy and includes all ohmic parts (Funke 1993). On the contrary, effect (4) can be measured in the imaginary part of the complex impedance (Elimat et al. 2010; Sanli et al. 2016; Sanli and Kanoun 2020; Xia et al. 2017) which describes the amount of electrical energy stored in the material containing induction and capacitance (Funke 1993).

In theory, the strain-dependent electrical resistance originates in the change of these four mechanisms, when the geometry of the polymer sample is deformed (Ferreira et al. 2013). Through the deformation of a conductive filler particle, it shows a change of its intrinsic resistance (Dharap et al. 2004; Elimat et al. 2010; Kang et al. 2006; Sanli et al. 2016; Zhang et al. 2006). In addition, the deformation of the conductive polymer could lead to changes in the mean filler distance which can separate two directly contacted particles (Park et al. 2008; Pham et al. 2008; Sanli et al. 2016; Yin et al. 2011) leading to increasing resistance. Furthermore, the change in distance between conductive particles affects the energy needed for the tunneling effect (Hu et al. 2008; Park et al. 2008; Sanli et al. 2016; Wichmann et al. 2009; Yasuoka et al. 2010; Yin et al. 2011). It also is possible that the change in distance exceeds or undercuts the maximal distance for the tunneling effect, whereby tunneling becomes possible or impossible. Therefore, the number of existing conductive paths decreases or increases. Additionally, the capacitance of the bond line can be altered through deformation by changing the distance between the particles separated through the insulating polymer matrix (Elimat et al. 2010; Sanli et al. 2016; Xia et al. 2017). These mechanisms creating the piezoresistive response can be measured in different frequency ranges between 20 Hz and 10 MHz according to the literature (Elimat et al. 2010; Xia et al. 2017). Impedance spectroscopy can be used to identify optimal frequencies with high signal quality and reliability in electrically conductive bond lines. The described mechanisms react to different applied frequency ranges in the measured signal to a varying extent (Sanli et al. 2016; Sanli and Kanoun 2020; Xia et al. 2017). Thus, this research study focuses on the piezoresistive response of bonded wood samples at various frequencies under compressive shear load as one of the critical load situations in timber engineering, for example shear load at the

end face or inclined cut of curved glulam beams. Carbon black (CB) as opposed to carbon nanotubes (CNT) was used because of its higher sensitivity based on the findings from Winkler et al. (2020a).

## Materials and methods

### Sample preparation

Figure 2 illustrates the process of producing the specimens, whereby defect-free lamellas of beechwood (*Fagus sylvatica* L.) were cut in pairs and conditioned for 14 days at 20 °C and 65% RH (20/65). Electrically conductive filler (Ketjenblack EC-300 J, Akzo Nobel Functional Chemicals B.V., Arnhem, Netherlands/Agglomerate size before dispersion 50 to 200 µm, primary aggregate size before dispersion 100 to 1000 nm, primary particle size of 30 to 50 nm according to data sheet) was dispersed into a one-component polyurethane prepolymer (Laboratory-Sample 1506-PV, Jowat, Detmold, Germany) by using a dissolver (Dispermat CV-SIP, VMA-Getzmann GMBH, Reichshof, Germany). A filler content of 4 wt% ( $\hat{=}$  25.35 vol%) was chosen, positioned at the upper limit of the percolation threshold area (2 wt% to 4 wt%) for this polymer-filler combination (Winkler et al. 2020a, 2020b) to reliably reach a usable sensitivity and at the same time a high reproducibility (Sanli et al. 2017). Based on the findings from Winkler et al. (2020b) that signal quality rises with rising amount of conductive adhesive, an amount of  $640 \pm 19.3 \text{ g/m}^2$  of electrically conductive adhesive was applied to two pairs of lamellas using a glass scraper. Afterward, the two bonded beech lamellas were pressed in a laboratory press next to each other under a pressure of 0.9 MPa for 240 min at room temperature and were then stored in standard climate (20 °C/65% RH) for approximately 14 days. Nine samples of 60 mm × 20 mm × 10 mm were cut from the center of the lamellas according to DIN EN 302-1:2013-06 and formatted into the geometry that is described in Winkler et al. (2020a). To avoid changes in the contact resistance through deformation of the specimen in the contacting area, the shear area has been reduced by cutting two notches with dimensions of 10 mm length, 20 mm width, and 4.9 mm height as shown in Fig. 3 (Chung 2020). The adhesive joint was intact

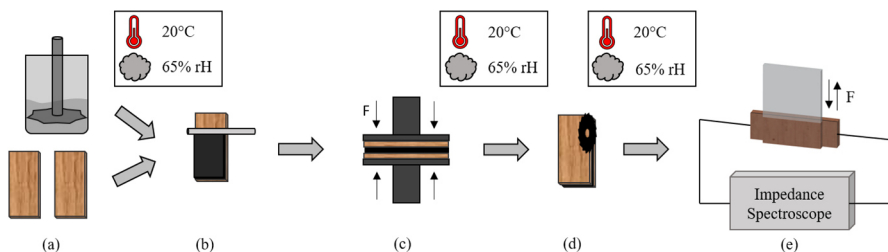


**Fig. 2** Schematic process of specimen preparation and testing: wooden lamella preparation and filler dispersion (a), application of adhesive (b), bonding by a laboratory press (c), formatting (d), impedance spectroscopy under swelling compressive shear load (e)

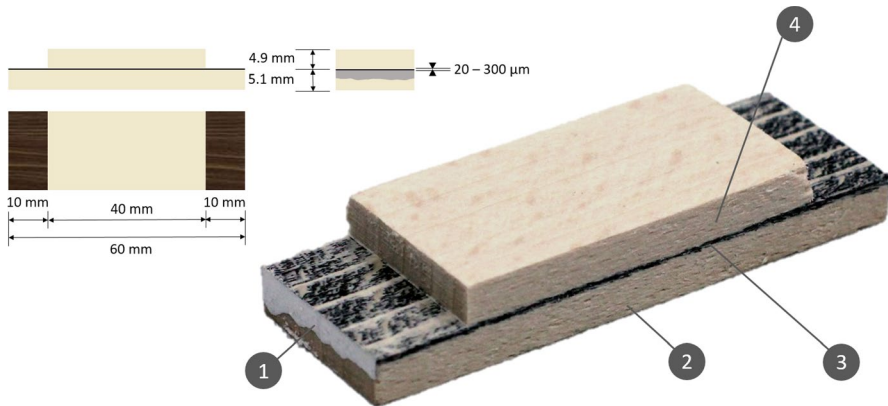


**Fig. 3** Picture of a specimen with silver conductive paint applied. 1. Silver conductive paint (contact area ring electrodes); 2. wooden layer (faces for fastening the specimen); 3. piezoresistive bond line; 4. wooden layer (application of swelling compressive load)

over the entire length of 60 mm but only subjected to compressive shear stress in an area of 40 mm × 20 mm. Finally, silver conductive paint (Leitsilber 200 N, Ferro GmbH, Hanau, Germany) was applied to the front faces of the specimens in the area of the bond line as described before (Winkler et al. 2020a, b)). Five replicas with a total outcome of 43 samples were manufactured and randomized during the test procedure.

## Measuring setup

As shown in Fig. 4, the experimental setup for testing the electrical properties under alternating current at different frequencies consisted of an impedance spectroscop (ISX-3, Sciospec Scientific Instruments GmbH, Bennewitz, Germany) (a), connected to the specimen by two spring-loaded ring electrodes (b) via BNC-Cables (c) and specimen (d)

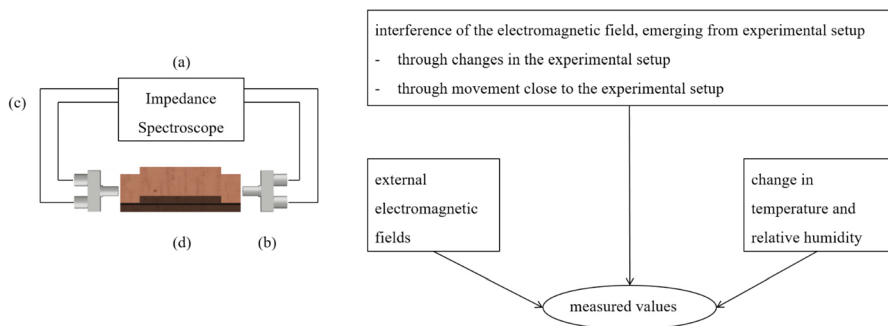


**Fig. 4** Schematic experimental setup and influences on the values from impedance spectroscopic measurements. Impedance spectroscop (a), ring electrodes (b), shielded cables (c) and specimen (d)

(RF Cable Assemblies, RG-58C/U, Pomona Electronics Inc., USA) (c). A two-probe and four-wire method was used for the measurement. In this paper, measured values (e.g., Fig. 5) from impedance spectroscopy not only include the impedance values for the measured specimens but also the impedance of the whole measuring setup including the contact resistance between silver conductive paint and bond line or rather the silver conductive paint and the electrode. As the objective is not to provide an impedance spectroscopic analysis of the composite material, the frequency-dependent relative piezoresistive change in the measurements could be characterized instead. To counteract various possible influences on the measured values of impedance spectroscopic measurements (Bulst 2017; Chung 2020; Joffe and Lock 2010), the experimental setup was modified. To minimize the influence of external electromagnetic fields on the measured values, shielded coaxial cables were used, and the exposed electrodes (b) and specimen (d) were shielded by a grounded aluminum-encased box. To avoid distortions through movement in the experimental setup, the impedance spectroscopy and the cables were fixed. Shielding ring electrodes were used to neutralize the electromagnetic field between electrodes, which could be disturbed by movements in the direct environment of the experimental setup. Through the usage of spring-loaded ring electrodes, pressure differences in the contact area between electrode and sample were minimized to keep the contact resistance as stable as possible (Chung 2020). Prior to the experiments, it was ensured that a change in pressure between electrode and silver conductive paste of the specimens does not have any influence on the measured values to avoid misleading signal changes by change in contact resistance. Through the conditioning of the specimens in the standard climate (20/65) prior to testing, the effect of the temperature and relative humidity was minimized. The actual testing was carried out under room climate conditions (20/40).

As shown in Fig. 6, this setup was used to measure impedance spectra while applying swelling shear stress to the bond line by applying pressure with a universal

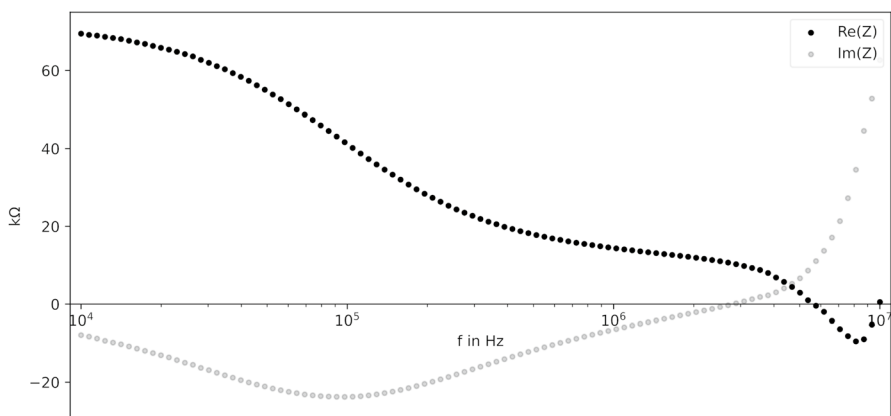


**Fig. 5** Exemplary plot of the real- and imaginary part of an impedance spectrum measured with the applied setup. The plot shows the representative characteristics for all measurements discussed in this paper

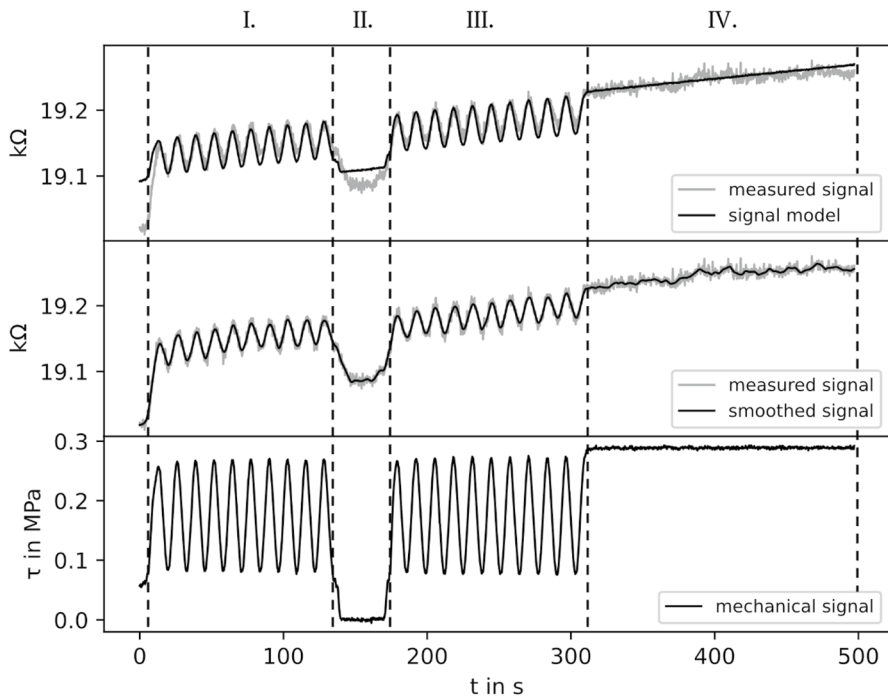


**Fig. 6** Measured signal and calculated signal model (top), measured signal and LOWESS-smoothed signal (middle) and swelling compression shear stress (bottom). Sections I to IV of the used compression shear load pattern. The spaces between measured points are interpolated

testing machine (Zwick/Roell Type 1484, load cell 200 kN, Ulm, Germany). For shear load application, a test setup was adapted from the standardized test for shear in adhesive joints (DIN EN 14,080:2013-09). As no shear test exists without any lateral stress at all, this setup includes transversal tension and transversal compression stress from a torsional moment. For simplification, the stress is labelled compression shear in the whole paper. The swelling shear load was used in earlier studies (Winkler et al. 2020b) with the intention to analyze the repeatability of the piezoresistive response. The swelling load rate of 0.1 Hz, compromising between a time-efficient testing cycle and a real load situation, ranks below the typically applied dynamic load rate, but above the quasi-static load. Typical load situations at these frequencies could be loads from wind-induced vibration as well as railroads and cars on bridges. A cyclic load over ten cycles has been applied in section I, changing from a basic load of 0.05 MPa to 0.25 MPa and back within 10 s (stress-controlled mode with a speed of 0.04 MPa/s) without leaving the elastic regime of the beech lamellas to avoid irreversible damage of the material. Section II consists of a relaxation phase for approx. 30 s. Followed by section III, which is equal to section I. Section IV was characterized by a uniform compression shear load at 0.25 MPa for 180 s. The measurements were performed at room temperature with a voltage amplitude of 500 mV over a frequency range from 10 kHz to 10 MHz with 101 log sized steps in between. The measurement range was set to 10 kOhm. For comparability, a

four-wire DC-resistance measurement was performed on all samples. A pulsed DC with an amplitude of 1000 mV with a current pulse of  $f_{\text{measure}} = 100$  ms and a break between every current pulse of  $f_{\text{breake}} = 50$  ms. To keep results comparable, the measurement setup and the environmental setting stayed the same. Only the impedance spectroscopy and the cables were replaced by a digital multimeter (NI PXI 4071, National Instruments GmbH, Munich/Germany) and aluminum foil shielded commercial 3 mm cables.

## Data analysis

The signal quality was evaluated by the signal-to-noise ratio (SNR) (Carminati 2017) calculated through Equation (1).

$$\text{SNR} = \frac{a}{\sigma_{\text{signal\_noise}}} \quad (1)$$

$a$  describes the absolute sensitivity of the signal and  $\sigma_{\text{signal\_noise}}$  the standard deviation of the measured signal noise. Based on the assumption of a linear reaction of the response signal to the applied stress in the used experimental setup, the standard deviation of the measured signal noise was calculated from the values of the actually measured signal minus the measurement signal smoothed with the locally weighted scatterplot smoothing algorithm (LOWESS-algorithm with a 5 s time frame) (Cleveland 1979). The dividend  $a$  was extracted from a nonlinear model function in the form of  $X = a * \tau + b * t^c + d$  where  $X$  is the unit of impedance value ( $\text{Re}(Z)$  or  $\text{Im}(Z)$ ) as a function of the compressive shear stress ( $\tau$ ) and time ( $t$ ), by calculating the model parameters with a nonlinear least squares fitting algorithm. As mentioned before, the constant  $a$  represents the absolute sensitivity of the signal,  $b$  represents the drift factor,  $c$  the drift exponent over time and  $d$  the constant  $Z_0$  (theoretical impedance base value) at time  $t_0$  and compressive shear stress  $\tau_0$ . For further evaluation of the results, the relative standard errors for the constants  $a$ ,  $b$ ,  $c$ , and  $d$  were calculated.

Further, a ratio  $q_{\overline{\text{SNR}}}$  between arithmetic mean SNR ( $\overline{\text{SNR}}$ ) and relative standard deviation of the SNR ( $\sigma_{\text{rel.SNR}}$ ) over all samples for each frequency was calculated by Equation (2). This calculated ratio can be used to evaluate the frequencies at which high signal quality and high reliability occur at the same time.

$$q_{\overline{\text{SNR}}} = \frac{\overline{\text{SNR}}}{\sigma_{\text{rel.SNR}}} = \frac{\overline{\text{SNR}}}{\frac{\sigma_{\overline{\text{SNR}}}}{\overline{\text{SNR}}}} = \frac{\overline{\text{SNR}}^2}{\sigma_{\overline{\text{SNR}}}} \quad (2)$$

The standard deviation of the  $\overline{\text{SNR}}$  values needed to be relativized to achieve comparability throughout all frequencies. The frequency with the maximum value for  $q_{\overline{\text{SNR}}}$  was used to compare the results of the measurement with impedance spectroscopy to the DC resistography (measuring changes in electrical resistance under direct current). The signals measured with direct current were evaluated in the same way as the impedance spectroscopic signals to compare the quality of both modes.



## Results and discussion

Figure 7 shows the  $\overline{\text{SNR}}$  and  $\sigma_{\text{rel.}\overline{\text{SNR}}}$  for each frequency over all measured samples. The real part of the complex impedance shows its highest values in the frequency band of 100 kHz to 1 MHz. These values are at least one third higher than the highest values for the imaginary part of the complex impedance, which occur in the higher frequencies above 8 MHz. The  $\sigma_{\text{rel.}\overline{\text{SNR}}}$  for the real part of the complex impedance has its lowest values in the same frequency band where the  $\overline{\text{SNR}}$  has its highest values. The imaginary part of the complex impedance,  $\sigma_{\text{rel.}\overline{\text{SNR}}}$  has its lowest values at the same frequencies, where it has its highest values for the  $\overline{\text{SNR}}$ . The strong  $\overline{\text{SNR}}$  drops at the frequencies 479 kHz and 631 kHz and the step-shaped form in the lower frequencies could depend on measurement system interferences, as reference measurements show similar shapes. Figure 7 further shows that a drop in the  $\overline{\text{SNR}}$  goes along with a rise of noise in the signal while the sensitivity shows no significant change. This shows that calculating the SNR can be used to compare the sensor characteristics for the generated impedance data in this paper.

A drift in the measured signal can be seen and has also been reported in several studies (Abu-Abdeen et al. 2016; Kang et al. 2006; Wang and Ding 2010; Winkler et al. 2020b; Zhao et al. 2013). As the specimens are composites of two viscoelastic materials—the polymer-based bond line and the wood itself—it is possible that the drift is generated by the time-dependent material creep or strain hysteresis of the polymer, the wood or both components at the same time (Abu-Abdeen et al. 2016; Hunt 1999). A time-dependent creep or hysteresis can be caused by the relaxation motion speed of the macromolecular chain segments, not matching the change rate of the applied stress (Zhao et al. 2013). These effects could lead to a drifting resistance of the bond line over time because of the contained deformation of the polymer after each loading-cycle while testing the specimen and therefore cause a drifting signal (Abu-Abdeen et al. 2016; Zhao et al. 2013). Moreover, the wooden adherents could cause a drifting signal by applying a transferred stress to the bond line

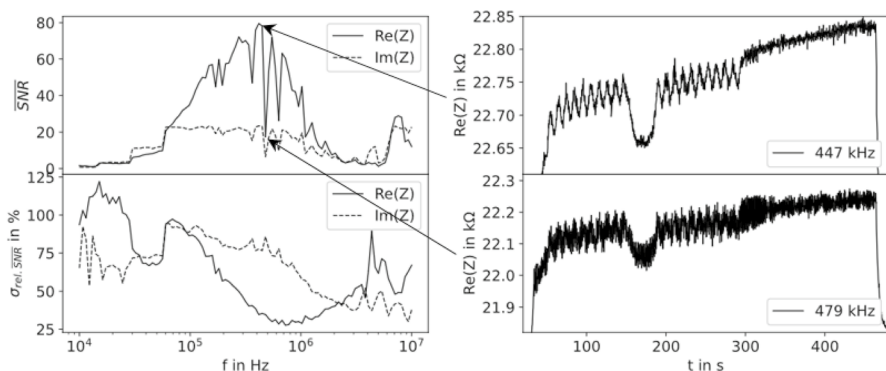


**Fig. 7** Left: Mean SNR and percental relative standard deviation of the SNR for each frequency over all samples for the real- and imaginary part of the complex impedance. Right: Examples of measured signals at two different frequencies with relatively different SNR. The spaces between measured points are interpolated



which leads to a creep or hysteresis in polymer deformation. Further, the possibility of an electrically induced signal drift (Chung 2020) must be considered, as measurements on mechanically unloaded specimens show the tendency of a drifting signal over time. Figure 8 gives an example of the relation between the strain of the specimen—measured by the traverse path sensor of the testing machine—and the change in resistance of the real part of the complex impedance over time that most of the measurements show while the gradients are varying with different specimens. The figure also shows the signal of the same specimen without mechanical load over time. The strain of the specimen shows a decent creep while keeping the signal of the stress constant in each loading-cycle (see above). The change in the real part of the complex impedance over time shows the same curve shape with a higher gradient. A positive drift also occurs in the signal of the mechanically unloaded specimen (electrically induced drift) which is relatively small compared to the drift of the mechanically loaded test. Nevertheless, the experimental results do not allow a conclusion about the possibly present quantity of material creep in each material of the composite. Further electrically induced drift seems to have an influence on the drifting signal under load at the same time. As other tests show the same creep in measurements of specimens that were not conditioned in a climate of 20 °C and 65% RH prior to testing, it is unlikely that the signal drift is caused by the change in wood moisture content during the testing process in room climate in the test procedure for these experiments. Additionally, the mean DC-resistance of the measurements is 124 kOhm with a standard deviation of 92 kOhm. Specimens produced in the same way, just without any kind of conductive filler, showed an overall resistance above 1 GOhm as also reported in Winkler et al. (2020a). Therefore, the ratio between the measured resistance with and without electrically conductive adhesive is at least 1/4000, resulting in a small part of the beechwood in the overall resistance.

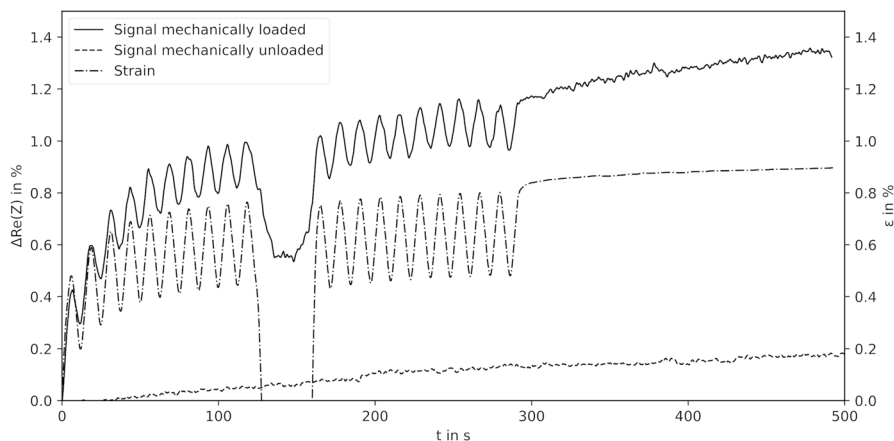


**Fig. 8** Example of the strain ( $\epsilon$ ) and the resistance change of the real part over time for a mechanically loaded and a mechanically unloaded specimen at 549 kHz. The spaces between calculated points are interpolated. For better visibility, the signal of the mechanically loaded and unloaded measurements is smoothed by a LOWESS-algorithm

The mostly lower  $\overline{\text{SNR}}$  for the imaginary part of the complex impedance means a lower change in inductive and capacitive properties of the test setup in comparison to the ohmic resistance change. Since three of the four known mechanisms of the piezoresistive response are measured in the real part of the complex impedance, a signal with higher sensitivity and lower noise in the real part of the complex impedance is most reasonable. In relation to the theory of the four mechanisms of piezoresistive response, it means that either the intrinsic change in resistance of the conductive particles or the change in contact resistance between contacting particles has the greatest impact on the piezoresistive response. This behavior fits to the conductive filler content above the percolation threshold as the arrangement of the particles changes from not contacting particles in the polymer to a larger number of direct contacts between the particles compared to a lower filler content. Thus, the described piezoresistive mechanisms (III) and (IV) are less likely to occur in the percolation network (Chung 2020).

The variation in  $\sigma_{\text{rel. SNR}}$  at different frequency bands shows that not only the value of the SNR is frequency-dependent but also the stability of the SNR values for different samples. The values for  $p$  of the real and imaginary parts of the complex impedance at all frequencies are shown in Fig. 9. The local maxima mark the frequencies, optimal for measuring the given specimens. Combining

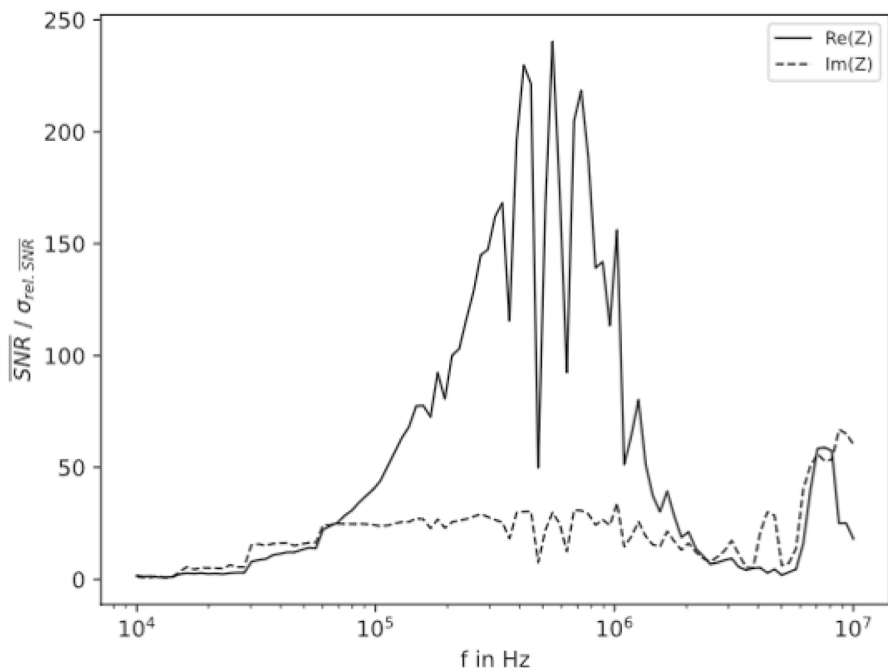


**Fig. 9** Ratio between mean SNR and mean standard deviation for each frequency over all samples for the real- and the imaginary part of the complex impedance. The spaces between calculated points are interpolated

the manufactured specimens and the used test setup, the maximum  $q_{\overline{\text{SNR}}}$  lies at 548 kHz for the real part and at 8710 kHz for the imaginary part of the complex impedance. The diagram also shows that the real part of the piezoelectric response has a nearly overall higher measurement quality compared to the imaginary part of the complex impedance for this set of samples at its best frequency. The real part of the complex impedance shows lower values for the mean relative standard error for the constants  $a$ ,  $b$ ,  $c$ , and  $d$  in the frequency bands where the real part of the complex impedance additionally has a higher  $q_{\overline{\text{SNR}}}$  in comparison to the imaginary part of the complex impedance. As a sensor signal, the real part of the complex impedance is more reliable because of the lower values for the constants. Therefore, the frequency-dependent piezoresistive response of the real part of the complex impedance with the highest value for  $q_{\overline{\text{SNR}}}$  will be used in the following comparison of the piezoresistive reaction measured by impedance spectroscopy and DC resistography. Figure 10 exemplarily shows the measurement of a specimen with DC and the measurement of the same specimen at the optimal frequency of 548 kHz with the impedance spectroscopy. Both signals are representing the overall properties of the signal characteristics for each measuring mode. The noise of the piezoelectric response measured by impedance spectroscopy at the optimal frequency is lower compared to the response of the DC-resistance measurement. Furthermore, no clear signal is visible, even in the LOWESS-algorithm smoothed curve.

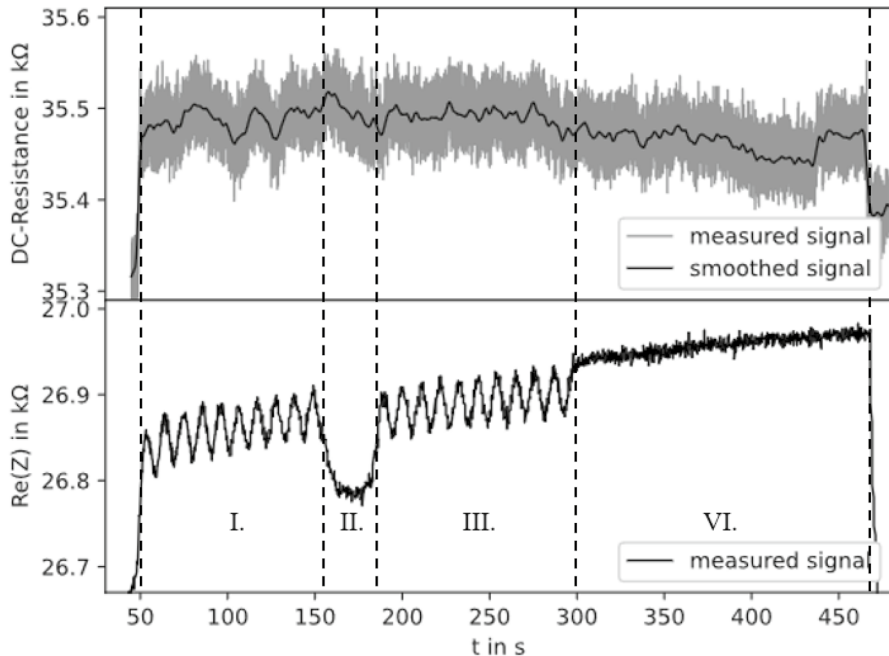


**Fig. 10** Example of a measured sample under DC and at the optimal frequency found with the impedance spectroscopy. The spaces between measured points are interpolated

Of the 43 DC measurements, 19 could not be analyzed because the algorithm was not able to extract the values for the constants  $a$ ,  $b$ ,  $c$ , and  $d$  by the nonlinear regression. With impedance spectroscopy, there was an analyzable signal for each specimen. As shown in Table 1, the SNR for the analyzable impedance spectroscopic signals is more than four times higher compared to the SNR of the signals generated with DC resistography. Furthermore, for the DC-resistance measurements, the mean relative standard noise is more than three times higher. Besides the higher SNR and the lower mean relative standard noise, the mean relative standard errors for the constants  $a$ ,  $b$ ,  $c$ , and  $d$  are significantly lower for the impedance spectroscopic measured signals, as shown in Table 1. The 19 signals from DC measurements that cannot be analyzed led to the conclusion that the received signal shows no clear structure, which means that the signal must be of low quality and is not usable as a sensor signal. Furthermore, the high mean relative standard errors for the regression parameters  $b$ ,  $c$ , and  $d$  for the DC-measurement data listed in Table 1, show that the model is not suitable for representing the measurements. In combination with the overall lower mean relative standard errors for the constants, the SNR evaluates the measurements with impedance spectroscopy as significantly higher in its quality and reliability. It should be noted that further work is needed to verify if the best frequencies defined in this paper remain the same over a long period of time or are applicable to other material combinations and specimen shapes. Further, experiments would be needed where the measuring setup used (device, cables, etc.) is changed in order to analyze the impact of the testing setup on the frequencies with the highest SNR.

Thus, changes in the real part of the complex impedance can deliver an overall higher signal quality for the present measuring setup and the specimens used. This could be due to the dominance of the dynamic effects of the conductive mechanisms in the polymer used that are affected due to the change in material stress. In the low-frequency (DC) plateau regime (Funke 1993), static effects of conductivity mechanisms play the dominant role in the conductivity of the material which is captured in the signal including the effects of the conductivity mechanisms 1 to 3 (Elimat et al. 2010; Xia et al. 2017). With rising frequency in the following dispersive regime (Funke 1993), the ratio between static and dynamic effects of the conductivity mechanisms changes, and the dynamic effects of the conductivity mechanisms (the increase in the tunneling possibility with rising frequency (Xia et al. 2017)) gain the dominant role in the signal (Elimat et al. 2010; Xia et al. 2017). With DC resistography, only static effects of the conductivity mechanisms can be measured, whereas measurements with impedance spectroscopy detect dynamic and static effects at higher frequencies at the same time.

In comparison, the practical handling of the DC-resistance measurements is less prone to failure. One reason is that external influences have a smaller impact on DC-resistance measurements compared to impedance spectroscopic measurements. Further, the handling and analysis of the data require more knowledge if measurements are carried out by impedance spectroscopy because the data volume is much higher, and the interpreter needs a wider knowledge of electrodynamic processes in the current state. Additionally, the costs for the impedance spectroscopic devices exceed the costs for DC instruments. The objective of this study was a comparison

**Table 1** Statistics for the SNR and relative standard errors from the parameter evaluation of the constants. All values are given with two significant figures according to GUM (Guide to the Expression of Uncertainty in Measurement)

	Mean SNR	Mean relative standard noise in %	Mean relative standard error a in %	Mean relative standard error b in %	Mean relative standard error c in %	Mean relative standard error d in %
DC resistography	17.00 ± 16.00	0.10 ± 0.17	6.10 ± 2.10	2100.00 ± 5700.00	2000.00 ± 5700.00	1700.00 ± 5100.00
Impedance spectroscopy	72.00 ± 22.00	0.03 ± 0.01	1.20 ± 0.24	20.00 ± 30.00	6.60 ± 3.30	0.04 ± 0.03

of different methods for measuring the piezoresistive response of the previously described multifunctional adhesives in wood, which poses some challenges to the use of piezoresistive polymers (Winkler et al. 2020a). Therefore, the present study can only give an overview of the possible gain of impedance measurement. Covering the different influences and aspects associated with piezoresistive bond lines in wood, for example the influence of moisture or density, will be part of future studies. A well-adapted setup of the measurement for later applications to buildings could also avoid the influence of external disruptive factors. This development can only be the objective of further application-related work.

## Conclusion

Overall, the results of this study suggest that the usability of electrically conductive wood bond lines for piezoresistive measurements of the engineered structure can be optimized by using frequency-dependent measurements. While with DC resistography, the piezoresistive effect was partly not measurable, the impedance spectroscopic analysis showed a distinctive piezoresistive behavior of each sample, making the technique more reliable for process integrated sensors.

The following conclusions can be drawn from the data and discussion:

- (1) Frequency-based measurements can enhance the reliability and usability of multifunctional bond lines in wood compared to DC-based resistography.
- (2) The real part of the complex impedance results in more reliable piezoresistive reactions compared to the imaginary part for the discussed data set, which is coherent with theory as the filler degree in the adhesive is above the percolation threshold and therefore the piezoresistive change is based on the assumptions 1 to 3 from the introduction (changes in intrinsic resistance, contact resistance and tunnel effects)
- (3) A method using the signal-to-noise ratio (SNR) as well as the calculated  $q_{\text{SNR}}$  was developed to evaluate the quality and reliability of the piezoresistivity of multifunctional bond lines in wood.

**Acknowledgements** This work was supported by the German Government with the “Nachwachsende Rohstoffe” program (FNR, BMEL) under Grant 22005018.

**Funding** Open Access funding enabled and organized by Projekt DEAL. This work was supported by the German Government with the “Nachwachsende Rohstoffe” program (FNR, BMEL) under Grant 22005018.

**Availability of data and material** Available upon request: jesco.schaefer@hnee.de.

**Code availability** Available upon request: jesco.schaefer@hnee.de.

**Declarations**

**Conflict of interest** On behalf of all authors, the corresponding author states that there is no conflict of interest.

**Open Access** This article is licensed under a Creative Commons Attribution 4.0 International License, which permits use, sharing, adaptation, distribution and reproduction in any medium or format, as long as you give appropriate credit to the original author(s) and the source, provide a link to the Creative Commons licence, and indicate if changes were made. The images or other third party material in this article are included in the article's Creative Commons licence, unless indicated otherwise in a credit line to the material. If material is not included in the article's Creative Commons licence and your intended use is not permitted by statutory regulation or exceeds the permitted use, you will need to obtain permission directly from the copyright holder. To view a copy of this licence, visit <http://creativecommons.org/licenses/by/4.0/>.

## References

- Abu-Abdeen M, Aboud AI, Ramzy GH (2016) Effect of temperature on creep behavior of Poly(vinyl chloride) loaded with single walled carbon nanotubes. *IJSEA* 5:112–120. <https://doi.org/10.7753/IJSEA0503.1001>
- Adams DE (2007) Health monitoring of structural materials and components: methods with applications. Wiley, Chichester, UK
- Bao WS, Meguid SA, Zhu ZH, Weng GJ (2012) Tunneling resistance and its effect on the electrical conductivity of carbon nanotube nanocomposites. *J Appl Phys* 111:93726. <https://doi.org/10.1063/1.4716010>
- Bulst M (2017) Impedance spectroscopy basics: choosing the instrumentation. In: Gruden R, Schweiger B, Pliquet U, Carminati M, Büschel P, Strunz W, Günther T, Radschun M, Bulst M, Errachid A, Danzer MA, Wagner N (eds) *Advanced School on Impedance Spectroscopy (ASIS)*. Chair for measurement and sensor technology, pp. 199–217
- Carminati M (2017) Advances in high-resolution microscale impedance sensors. *J Sens* 2017:1–15. <https://doi.org/10.1155/2017/7638389>
- Chang C-C, Su H-K, Her L-J, Lin J-H (2012) Effects of chemical dispersant and wet mechanical milling methods on conductive carbon dispersion and rate capabilities of LiFePO<sub>4</sub> batteries. *J Chinese Chem Soc* 59:1233–1237. <https://doi.org/10.1002/jccs.201200330>
- Chung DDL (2020) A critical review of piezoresistivity and its application in electrical-resistance-based strain sensing. *J Mater Sci* 55:15367–15396. <https://doi.org/10.1007/s10853-020-05099-z>
- Cleveland WS (1979) Robust locally weighted regression and smoothing scatterplots. *J Am Stat Assoc* 74:829. <https://doi.org/10.2307/2286407>
- Davidson T (2005) Conductive and Magnetic Fillers. In: Xanthos M (ed) *Functional fillers for plastics*. Wiley-VCH, Weinheim, pp 317–337
- DIN EN 14080:2013–09 (2013) Timber structures—Glued laminated timber and glued solid timber—Requirements; German version EN 14080:2013. Deutsches Institut für Normung
- DIN EN 302–1:2013–06 (2013) Adhesives for load-bearing timber structures - Test methods—Part 1: Determination of longitudinal tensile shear strength; German version EN 302–1:2013. Deutsches Institut für Normung
- Dharap P, Li Z, Nagarajaiah S, Barrera EV (2004) Nanotube film based on single-wall carbon nanotubes for strain sensing. *Nanotechnology* 15:379–382. <https://doi.org/10.1088/0957-4484/15/3/026>
- Elhad Kassim SA, Achour ME, Costa LC, Lahjomri F (2015) Prediction of the DC electrical conductivity of carbon black filled polymer composites. *Polym Bull* 72:2561–2571. <https://doi.org/10.1007/s00289-015-1421-5>
- Elimat ZM, Hamideen MS, Schulte KI, Wittich H, La Vega A, de, Wichmann M, Buschhorn S, (2010) Dielectric properties of epoxy/short carbon fiber composites. *J Mater Sci* 45:5196–5203. <https://doi.org/10.1007/s10853-010-4557-6>
- Ferreira A, Martínez MT, Ansón-Casaos A, Gómez-Pineda LE, Vaz F, Lanceros-Mendez S (2013) Relationship between electromechanical response and percolation threshold in carbon nanotube/poly(vinylidene fluoride) composites. *Carbon* 61:568–576. <https://doi.org/10.1016/j.carbon.2013.05.038>

- Ferreira A, Rocha JG, Ansón-Casaos A, Martínez MT, Vaz F, Lanceros-Mendez S (2012) Electromechanical performance of poly(vinylidene fluoride)/carbon nanotube composites for strain sensor applications. *Sens Actuators A* 178:10–16. <https://doi.org/10.1016/j.sna.2012.01.041>
- Funke K (1993) Jump relaxation in solid electrolytes. *Prog Solid State Chem* 22:111–195. [https://doi.org/10.1016/0079-6786\(93\)90002-9](https://doi.org/10.1016/0079-6786(93)90002-9)
- Hu N, Karube Y, Yan C, Masuda Z, Fukunaga H (2008) Tunneling effect in a polymer/carbon nanotube nanocomposite strain sensor. *Acta Mater* 56:2929–2936. <https://doi.org/10.1016/j.actamat.2008.02.030>
- Hunt DG (1999) A unified approach to creep of wood. *Proc R Soc Lond A* 455:4077–4095. <https://doi.org/10.1098/rspa.1999.0491>
- Joffe EB, Lock K-S (2010) *Grounds for grounding: a circuit to system handbook*. Wiley, Hoboken, New Jersey
- Kang I, Schulz MJ, Kim JH, Shanov V, Shi D (2006) A carbon nanotube strain sensor for structural health monitoring. *Smart Mater Struct* 15:737–748. <https://doi.org/10.1088/0964-1726/15/3/009>
- Kasal B, Tannert T (eds) (2010) *In Situ Assessment of Structural Timber*. State of the Art Report of the RILEM, Springer, Heidelberg
- Kurz JH (2015) Monitoring of timber structures. *J Civil Struct Health Monit* 5:97. <https://doi.org/10.1007/s13349-014-0075-6>
- Kurz JH, Boller C (2015) Some background of monitoring and NDT also useful for timber structures. *J Civil Struct Health Monit* 5:99–106. <https://doi.org/10.1007/s13349-015-0105-z>
- Li C, Thostenson ET, Chou T-W (2008) Sensors and actuators based on carbon nanotubes and their composites: a review. *Compos Sci Technol* 68:1227–1249. <https://doi.org/10.1016/j.compscitech.2008.01.006>
- Luheng W, Tianhuai D, Peng W (2009) Influence of carbon black concentration on piezoresistivity for carbon-black-filled silicone rubber composite. *Carbon* 47:3151–3157. <https://doi.org/10.1016/j.carbon.2009.06.050>
- Park M, Kim H, Youngblood JP (2008) Strain-dependent electrical resistance of multi-walled carbon nanotube/polymer composite films. *Nanotechnology* 19:55705. <https://doi.org/10.1088/0957-4484/19/05/055705>
- Pham GT, Park Y-B, Liang Z, Zhang C, Wang B (2008) Processing and modeling of conductive thermoplastic/carbon nanotube films for strain sensing. *Compos B Eng* 39:209–216. <https://doi.org/10.1016/j.compositesb.2007.02.024>
- Sanli A, Kanoun O (2020) Electrical impedance analysis of carbon nanotube/epoxy nanocomposite-based piezoresistive strain sensors under uniaxial cyclic static tensile loading. *J Compos Mater* 54:845–855. <https://doi.org/10.1177/0021998319870592>
- Sanli A, Müller C, Kanoun O, Elibol C, Wagner MF-X (2016) Piezoresistive characterization of multi-walled carbon nanotube-epoxy based flexible strain sensitive films by impedance spectroscopy. *Compos Sci Technol* 122:18–26. <https://doi.org/10.1016/j.compscitech.2015.11.012>
- Sanli A, Benchirouf A, Müller C, Kanoun O (2017) Piezoresistive performance characterization of strain sensitive multi-walled carbon nanotube-epoxy nanocomposites. *Sens Actuators A* 254:61–68. <https://doi.org/10.1016/j.sna.2016.12.011>
- Wang P, Ding T (2010) Creep of electrical resistance under uniaxial pressures for carbon black–silicone rubber composite. *J Mater Sci* 45:3595–3601. <https://doi.org/10.1007/s10853-010-4405-8>
- Wichmann MHG, Buschhorn ST, Gehrmann J, Schulte K (2009) Piezoresistive response of epoxy composites with carbon nanoparticles under tensile load. *Phys Rev B*. <https://doi.org/10.1103/PhysRevB.80.245437>
- Winkler C, Schwarz U (2014) Multifunctional wood-adhesives for structural health monitoring purposes. In: Aicher S, Reinhardt H-W, Garrecht H (eds) *Materials and joints in timber structures: recent developments of technology*; [contributions from the RILEM International Symposium on Materials and Joints in Timber Structures that was held in Stuttgart, Germany from October 8 to 10, 2013. Springer, Dordrecht, pp 381–394
- Winkler C, Schwarz U (2016) Wood Adhesives for Non-Destructive Structural Monitoring. *e-J Non-destructive Testing* 21:1–8
- Winkler C, Konnerth J, Gibcke J, Schäfer J, Schwarz U (2020a) Influence of polymer/filler composition and processing on the properties of multifunctional adhesive wood bonds from polyurethane prepolymers I: mechanical and electrical properties. *J Adhes* 96:165–184. <https://doi.org/10.1080/00218464.2019.1652601>



- Winkler C, Schäfer J, Jäger C, Konnerth J, Schwarz U (2020b) Influence of polymer/filler composition and processing on the properties of multifunctional adhesive wood bonds from polyurethane pre-polymers II: electrical sensitivity in compression. *J Adhes* 96:185–206. <https://doi.org/10.1080/00218464.2019.1652602>
- Xia X, Wang Y, Zhong Z, Weng GJ (2017) A frequency-dependent theory of electrical conductivity and dielectric permittivity for graphene-polymer nanocomposites. *Carbon* 111:221–230. <https://doi.org/10.1016/j.carbon.2016.09.078>
- Yasuoka T, Shimamura Y, Todoroki A (2010) Electrical resistance change under strain of CNF/Flexible-Epoxy Composite. *Adv Compos Mater* 19:123–138. <https://doi.org/10.1163/092430410X490446>
- Yin G, Hu N, Karube Y, Liu Y, Li Y, Fukunaga H (2011) A carbon nanotube/polymer strain sensor with linear and anti-symmetric piezoresistivity. *J Compos Mater* 45:1315–1323. <https://doi.org/10.1177/0021998310393296>
- Zhang W, Suhr J, Koratkar N (2006) Carbon nanotube/polycarbonate composites as multifunctional strain sensors. *J Nanosci Nanotechnol* 6:960–964. <https://doi.org/10.1166/jnn.2006.171>
- Zhao J, Dai K, Liu C, Zheng G, Wang B, Liu C, Chen J, Shen C (2013) A comparison between strain sensing behaviors of carbon black/polypropylene and carbon nanotubes/polypropylene electrically conductive composites. *Compos A Appl Sci Manuf* 48:129–136. <https://doi.org/10.1016/j.compositesa.2013.01.004>

**Publisher's Note** Springer Nature remains neutral with regard to jurisdictional claims in published maps and institutional affiliations.

## **Piezoresistive bond lines for timber construction monitoring – experimental scale-up**

Christoph Winkler<sup>1</sup>, Stefan Haase<sup>1</sup>, Ulrich Schwarz<sup>1</sup> and Markus Jahreis<sup>1</sup>

<sup>1</sup> University of Applied Sciences Eberswalde, Faculty of Wood Engineering, Eberswalde, Germany

### **Declaration of author contributions**

Winkler conceptualized and designed the experiment together with Haase and Jahreis. Specimen design was done by Winkler, Haase and Jahreis. Sample preparation was done by Haase (first set) and Winkler (GLT beams). Combined DC resistance measurements under load were carried out by Haase (first set) and Winkler (GLT beams). Data have been evaluated and discussed by all. The analysing of piezoresistive data and model building was carried out by Winkler. Writing and editing of the final manuscript was done by Winkler. Funding acquisition of the financial support leading to this publication was done by Winkler and Schwarz. All authors read and approved the final manuscript.



# Piezoresistive bond lines for timber construction monitoring—experimental scale-up

Christoph Winkler<sup>1,2</sup> · Stefan Haase<sup>1,2</sup> · Ulrich Schwarz<sup>1,2</sup> · Markus Jahreis<sup>1,2</sup>

Received: 15 January 2021 / Accepted: 18 May 2021 / Published online: 24 June 2021  
© The Author(s) 2021

## Abstract

Several laboratory studies and experiments have demonstrated the usability of polymer films filled with electrically conductive filler as piezoresistive material. Applied to adhesives, the glue lines of wood products can achieve multifunctional—thus bonding and piezoresistive/strain sensing—properties. Based on critical load areas in timber constructions, upscaled test setups for simplified load situations were designed, especially with regard to a stress-free electrical contact. In a second step, another upscaling was done to small glulam beams. Based on an experimental test sequence, the piezoresistive reactions as well as the behaviour until failure were analysed. The results show in all cases that a piezoresistive reaction of the multifunctionally bonded specimens was measurable, giving a difference in the extent of relative change. Additionally, measured phenomena like inverse piezoresistive reactions, electrical resistance drift and the absence of a piezoresistive reaction were discussed, based on additional strain analysis by digital image correlation. A model of macroscopic and microscopic strains influencing the piezoresistive reaction of the electrically conductive bond line in wood was used to explain all experimental results. Finally, a first scale-up of piezoresistive bond lines from laboratory samples to glulam beams was possible and successful.

## Introduction

Timber structures are particularly exposed to environmental influences and must therefore be preserved by constructive wood protection and monitored by inspection intervals. While constructive wood protection elongates the usability of the structure, inspection intervals help to prove the integrity of infrastructure, public or re-utilised buildings. From an economic viewpoint, the costs and time of

---

✉ Christoph Winkler  
christoph.winkler@hnee.de

<sup>1</sup> University of Applied Sciences Eberswalde, Eberswalde, Germany

<sup>2</sup> Hochschule für nachhaltige Entwicklung Eberswalde, Alfred-Möller-Straße 1,  
16225 Eberswalde, Germany

inspections are justified by alternative maintenance costs, protection of capital investment and assurance of safety of the inspected structures (Kasal and Tannert 2010). Due to decreasing costs of sensors and interpretation software, structural health monitoring (SHM)—the permanent integration of sensors into structures and assessing of their integrity by cyclic measurement—has become an important strategy to reduce the maintenance costs while keeping a high level of safety (Balageas et al. 2006).

In the last years, the currently available methods for assessing and monitoring timber structures non- or less destructively have been reviewed and it was shown that several sensors are usable and reliable for monitoring purposes (Koch et al. 2016; Kurz 2015; Kurz and Boller 2015; Tannert et al. 2010; Tannert and Müller 2010).

Nonetheless, the additional costs for integrating these sensors into timber structures are high due to the necessary highly specialised staff and the time-consuming installation. Usage of electrically conductive adhesives as sensory layers can help at this point. The integration of these multifunctional adhesives during the manufacturing of glulam beams, cross-laminated timber or other engineered wood products can help to decrease the production costs and integrate sensors at points inside the engineered product.

Research on adhesives with electrical conductive nanofillers (depending on the application and research area also called nanocomposites, ECA's, multifunctional adhesives, etc.) was mostly focussed on the application of cold bonding in electronic devices to replace soldering joints. Considerable investigations tried to overcome the decrease in bonding strength by the historically used silver filler with carbon allotropes like carbon nanotubes, graphene and carbon black (Han et al. 2019; Masaebi et al. 2018; Massoumi et al. 2015; Santamaria et al. 2013; Wehnert et al. 2014). Generally, electrically conductive adhesives consist of electrically conductive particles in an insulating polymeric matrix. They show as bond lines a piezoresistive effect, which generally describes a change in electrical resistance with strain. With increasing strain, the length and cross section of the electrically conductive polymer as well as the amount of conductive paths of the filler particles change.

In previous publications by the working group, this piezoresistive effect has been shown for small samples of adhesively bonded wood specimens from beech wood (*Fagus sylvatica* L.) under compression stress (Winkler et al. 2020b), under tensile and compression stresses in beams (Winkler and Schwarz 2016) as well as under pull-shear stress (Winkler and Schwarz 2016).

First of all, the later presentation of the results as positive or negative piezoresistive reaction (PR) per stress unit in this paper needs to be delimited from the scientifically defined piezoresistivity.

Piezoresistivity is typically described by the gauge factor (GF) and given by the fractional change of resistance per strain unit if the change is reversible. Mathematically described (Eq. 1), the fractional change in resistance ( $\Delta R/R$ ) of the measured material depends on the fractional change in volume resistivity ( $\Delta \rho/\rho$ ) as well as the strain ( $\Delta l/l$ ) in direction of the resistance measurement and the Poisson's ratios  $\nu_1$  and  $\nu_2$  of the material in transverse directions to the resistance measurement (Chung 2020)

$$\frac{\Delta R}{R} = \frac{\Delta \rho}{\rho} + \frac{\Delta l}{l} * (1 + \nu_1 + \nu_2) \quad (1)$$

Based on the general definition of tensile strain as positive and compressive strain as negative, the piezoresistivity/GF

$$GF = \frac{\Delta R}{R} / \frac{\Delta l}{l} \quad (2)$$

becomes positive if the fractional change in resistance ( $\Delta R/R$ ) increases/decreases according to the strain ( $\Delta l/l$ ). Thus, an increasing resistance under tensile strain as well as a decreasing resistance under compressive strain is defined as positive piezoresistivity. A reversed reaction gives a negative piezoresistivity. Finally, both definitions are only valid under the assumption that measuring direction of resistance and strain direction are aligned. Furthermore, shear strain and its resulting piezoresistivity are not defined for in-plane shearing of electrically conductive films. Theoretically, the signal at in-plane shear strain can be positive (from pull-shear-tests) or negative (from push-shear-tests) and the change in conductive paths along the electrically conductive particles will be independent of the direction; the piezoresistivity by this definition must be positive and at the same time negative. Therefore, the change in electrical resistance due to strain will be reported as PR, which in the following is defined positive for increasing resistance with applied strain and negative for decreasing resistance with strain.

Additionally, a real analysis of GF for adhesive bond lines in timber structures is only possible if the cross section of the bond line is constant, the parameters are known (thus,  $\rho$  is calculable) and the change in the cross section can be measured during deformation (thus, the Poisson's ratio  $\nu$  is calculable). It can be seen from Fig. 1 that even for laboratory specimens, it is difficult to calculate the cross section of the bond line within spruce (Fig. 1a). In other wood species the penetration into wood cells and vessels (Fig. 1b) is even higher; besides, one-component polyurethane (1C-PUR)-based adhesives show imperfection due to for example cavities from  $CO_2$ -forming (Fig. 1c).

Therefore, due to the relationship of stress and strain, the PR's in adhesive bond lines in timber will be presented stress related, keeping in mind that scientifically piezoresistivity is strain related.

Other challenges come up, when piezoresistive bond lines are applied to timber structures. Due to its grain-oriented structure, timber exhibits a strong orthotropic elasticity and due to fibre- and density-based irregularities in the macro- and microstructure also heterogeneity. Thus, the relation between strain and stress depends on the micro-, meso- and macrostructure (Oppel et al. 2016). Therefore, there are difficulties in detecting and isolating the values of stress and strain in detailed structures with strain gauges or in this case, multifunctional adhesive bond lines. For example, notches near the support of a bending beam enforce lateral tension stress to the timber/adhesive bond line. The result is a crack layer from the inner edge towards the beam. Moreover, the stress distribution shows a strong peak at the beginning and a steep decrease over the length (Franke et al.

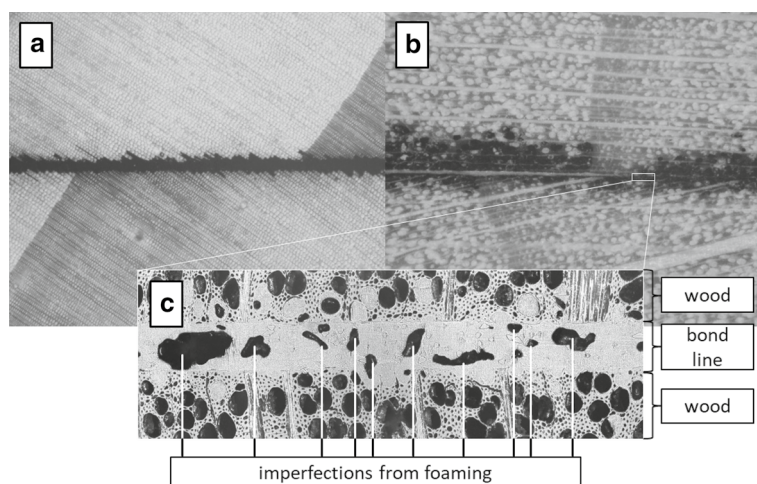


**Fig. 1** Cross section of laboratory produced multifunctional bond lines in spruce **a**, beech **b** and a highly resolved image of the cross section of a multifunctional bond line from 1C-PUR **c** with marked imperfections

2007). On the other side, shear stresses also appear at those points, leading to several overlapping stresses.

These challenges are increasing with an upscaling of structural elements, raising the question of whether the PR in the previously investigated laboratory scaled specimens are applicable to glulam beams (Winkler et al. 2020b; Winkler and Schwarz 2014).

Therefore, the objective of the experiments was to determine the feasibility of the given multifunctional bond lines under load in real situations by a first scale-up of the laboratory tests. It should answer the question, whether the change in electrical resistance of the adhesive layer—the PR—can be used in glulam beams to detect stress. According to the theory, the working hypothesis was that the piezoresistivity can be transferred to glulam beams and different stresses can be distinguished by the direction and extent of PR.

## Materials and methods

### Specimen design

Specimens were first upscaled with regard to load situations, which often occur in glulam constructions or which are prone to critical overloading. Because of the three-dimensional behaviour of a material [see Mohr–Coulomb theory (Mang and Hofstetter 2013)], it is almost impossible to create single mode tests for isolated stresses. In particular, there are no shear tests without lateral stress at all. Even if the load and support are placed in one line, there are deviation forces, bending, compression and elongation. Furthermore, the stress along a bond line is not distributed

equally. The geometry, basically the anchorage length, influences the stress distribution at the end of the bond line. There is a singularity at every end of a member or a change of material, which induces peaks in the stress distribution. With an increasing mounting length, the slenderness of the connection increases. Thus, the inhomogeneity of the stress distribution rises (Jahreis and Rautenstrauch 2016; Kästner et al. 2014). This is also comparable with the shear distribution inside a bending beam according to Filon 1903.

Thus, to investigate the PR of the multifunctional adhesive in shear mode, push-shear-tests were used, because of the low load capacity for lateral pull stress of timber.

Setups for longitudinal tension stress in tapered finger joints and transversal tension were adapted from standardised methods. In all designs, a stress-free electrical connection to the specimen as well as an electrochemically stable electrode was considered (see Fig. 2). Additional photographs with indicated features are available as online supplementary material.

The stress-free electrical connection was realised by recesses in the material or offsets between the two bonded parts, with the objective to have no strain between electrode and adhesive (mechanical decoupling), which would have distorted the

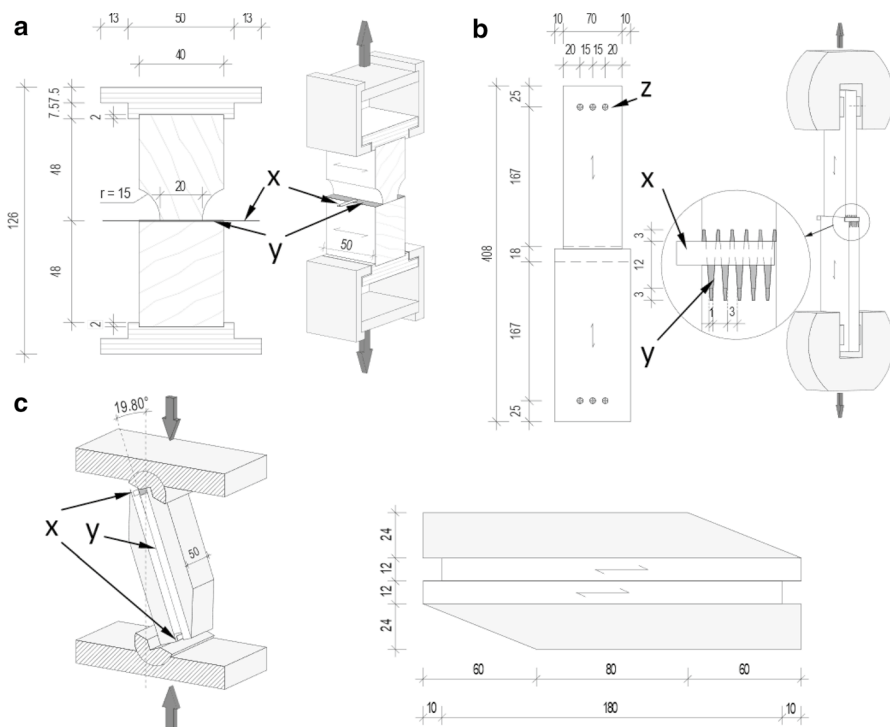


**Fig. 2** Design and dimensions of simple specimen for testing the piezoresistive reaction in transversal tension load **a**, tension load in tapered finger joints **b** and compressive shear load **c**, all with an electrode from Hilumin sheet (x) and electrically conductive adhesive (y)

PR. Electrical connection was done by sheets made from HILUMIN®, an electrolytically nickel-coated strip steel, usually applied in the battery industry.

In a second iteration, upscaling was realised by the production of two glulam beams with different isolated measurement points (Fig. 3) by partly applying electrically conductive adhesive in certain areas of stress. These measurement points were chosen with the intention of predominant transversal tension stress at a notched beam as well as shear stress, tension stress in tapered finger joints and compression stress in the second beam.

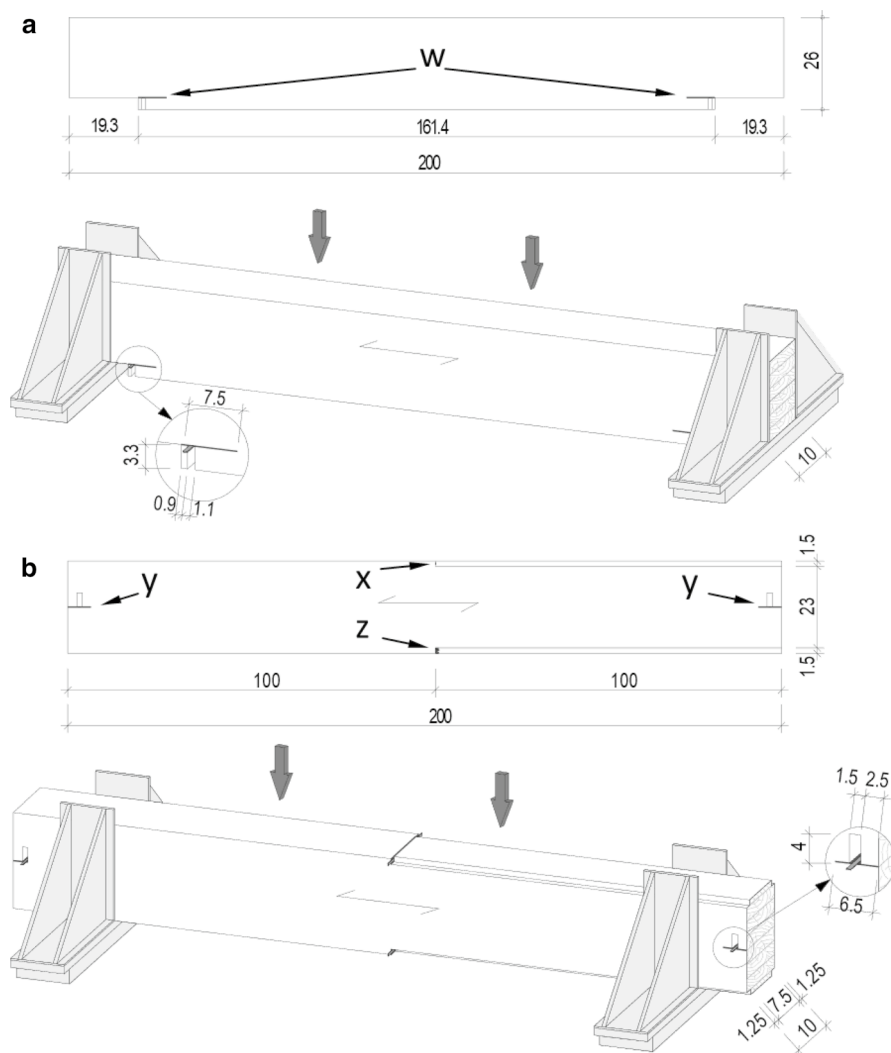


**Fig. 3** Design and dimensions of specimen for testing the piezoresistive reaction in glulam beams with electrically conductive adhesive partly applied to measure transversal tension stress (w), compression stress (x), shear stress (y) and tension stress in finger-jointed lamellas (z)



Thus, the measurements of the first set of samples were upscaled and supplemented by compression stress.

Mechanical decoupling was realised by partly removing material near the electrode by drilling (transversal tension, shear) and offsets between two lamellas (tension in tapered finger joints and compression). Additional photographs with indicated features are available as online supplementary material.

From the design of all specimens, it was found that the resistance is always measured along the adhesive bond line and stresses are applied perpendicular to this direction. Thus, and because three-dimensional experiments especially with orthotropic materials always result in several stress components, the main stress within these test settings (transversal tension, shear, tension and compression) will be used in further references.

## Sample preparation

All specimens were manufactured from spruce wood (*Picea abies* L.) of strength category C24 (according to EN 338 (EN 338, 2016)), which has been conditioned at a standard climate of 20 °C and 65% RH (20/65) until equilibrium moisture content. The different parts of the specimens were cut from the conditioned wood, planed prior to bonding and, for mechanical decoupling, prepared by drilling/cutting out parts near the electrode. Adhesive was prepared by dispersing 4 wt% carbon black (CB) (Ketjenblack EC-300 J, Akzo Nobel Functional Chemicals B.V., Arnhem, Netherlands) into a one-component polyurethane prepolymer (laboratory prototype 1506-PV, Jowat SE, Detmold, Germany) by using a dissolver (Dispermat CV-SIP, VMA-Getzmann GMBH, Reichshof, Germany). Compared to other electrically conductive nanofillers with strong agglomerates, CB only needs a good homogenisation (Köckritz et al. 2015) and, in case of moisture curing 1C-PUR, other preparations. To prevent moisture uptake during preparation, the CB was dried to equilibrium at 103.5 °C and the dispersion process was performed under argon atmosphere. A filler content of 4 wt% was chosen according to previous investigations and exceeded the percolation threshold, giving a reliable piezoresistivity and reproducibility (Winkler et al. 2020a). 400 g/m<sup>2</sup> of electrically conductive adhesive was spread on the pre-planned lamellas using a glass scraper. Electrodes, made from HILUMIN® strips with a thickness of 0.1 mm, width of 5 mm and length of 30 mm, were prefixed by a two-component epoxy resin (Bocoll 2-K-Epoxy-Reparaturharz, Boldt & Co. Vertriebs OHG, Wermelskirchen, Germany) and contacted by the liquid electrically conductive adhesive. All specimens were pressed by clamps according to the result of previous studies. These showed a minor influence of applied pressure between 0.6 and 1.2 MPa on the tensile shear strength, electrical DC resistance and piezoresistive sensitivity of piezoresistive bond lines in wood (Winkler et al. 2020a; Winkler et al. 2020b).

After 24 h of curing at room climate (20 °C / 35% RH), the electrodes were mechanically fixed by locally applying a two-component epoxy resin (Bocoll 2-K-Epoxy-Reparaturharz, Boldt & Co. Vertriebs OHG, Wermelskirchen, Germany).

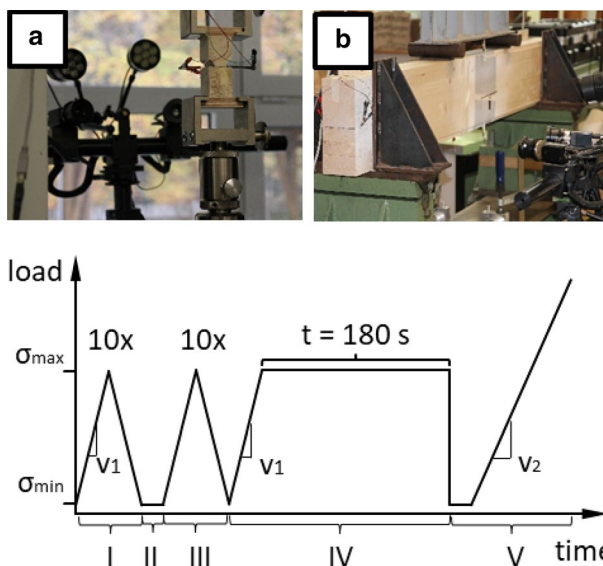


**Fig. 4** Pictures from testing the transversal tension specimen (a), glulam beam B from Fig. 3 (b) and test sequence with (I) mechanical condition phase, (II) unloading, (III) piezoresistive response, (IV) constant load and (V) load until break. The glulam beams were only tested according to phase IV, but repeating in the elastic range

**Table 1** Test parameters for all mechanical tests according to Fig. 4 of specimen defined in Figs. 2, 3

Specimen (number)	$\sigma_{\min}$ [MPa]	$\sigma_{\max}$ [MPa]	$V_1$	$V_2$ [MPa/s]	Test phases
Transversal tension ( $n=30$ )	0.1	0.6	0.2 MPa/s	0.05	I–V
Tension ( $n=18$ )	0.1	10.0	1.5 MPa/s	0.2	I–V
Push-shear ( $n=12$ )	0.15	3.15	0.2 MPa/s	0.05	I–V
Glulam beam A ( $n=1$ )	0 kN	40 kN	250 N/s	–	IV*
Glulam beam B ( $n=1$ )	0 kN	40 kN	250 N/s	–	IV*

The finger-jointed specimens were reinforced against transverse compression by adding three fully threaded screws (diameter 4 mm).

## Measuring setup

All specimens were tested according to the sequences pictured in Fig. 4. The parameters of the test sequences together with the number of specimens in each test are given in Table 1. Phase I and III are load-wise the same, but only phase III is used to characterise the piezoresistive reaction in this manuscript (see "[Piezoresistive reaction](#)" section). Phase I was introduced in the test sequence to mechanically condition the sample. Phase II ( $\sigma_{\min}$  for 20 s) was added to distinguish between phase I

and III and shows the stability of the baseline resistance. Phase IV is used to evaluate the mechanical and electrical creep under constant load. Phase V is used to analyse the behaviour until break. The beams were tested only according to phase IV. The maximum stresses in the first set of samples were derived from the strength category C24 (according to EN 338 (EN 338, 2016)) under the assumption that timber fails before the adhesive bond line.

For testing of the first set of samples, a universal testing machine (Zwick/Roell Type 1484, load cell 200 kN, Ulm, Germany) was used. The beams were loaded in a testing rack at the Eberswalde University of Applied Sciences (WPM 600 kN, WPM Leipzig, Leipzig, Germany; load cell 500 kN, A.S.T.—Angewandte Systemtechnik GmbH, Dresden, Germany).

Measurements of electrical resistance under direct current ( $R_{DC}$  measurements) were performed by a two-wire method for the first set of samples (NI PXI-4071, National Instruments GmbH, Munich, Germany) and a four-wire method for the beams, which were multiplexed to all measurement points in each beam (NI PXI-4071 and NI PXI-2527, National Instruments GmbH, Munich, Germany). Connection of the resistometer and the electrodes was realised by shielded cables and spring-loaded contacts. The measurement and analysis of the strain near the adhesive bond line were performed by digital image correlation (DIC) with two cameras (Aramis 3D, 5 M cameras, GOM GmbH, Braunschweig, Germany).

The presented data were partly smoothed (moving average, 10 points) for better understanding. In all cases, the smoothed data are specified in the legends of the graphs. The piezoresistive sensitivity—the fractional change of resistance per stress—was calculated from the smoothed data. The data from mechanical testing (load/force/traverse path/strain) were synchronised, using the timestamp of both measuring computers. Thus, the mismatch amounted to a maximum of 1 s and these timestamps were marked as synchronised time or—for clearer figures—time in the figure.

## Results and discussion

### Piezoresistive reaction

Phase III (Fig. 4) was analysed for the piezoresistivity, and the results are given in Table 2 together with the baseline resistance  $R_{BL}$ . The baseline resistance differs with type of specimen, reaching a range of around 2 to 50 kOhm. It has been shown in earlier work that the baseline resistance does not affect the sensitivity of piezoresistive bond lines in wood (Winkler et al. 2020b) after exceeding the percolation range (Winkler et al. 2020a).

The piezoresistive sensitivity under direct current  $S_{DC}$  in Table 2 represents the relative change of electrical resistance per unit stress (calculated from load divided by the cross section) or, in the case of unknown stresses in the glulam beams, the relative change of electrical resistance in respect of the maximum load, which was defined in Fig. 4. The PR shows whether the resistance under direct current is increasing (+) or decreasing (−) with increasing stress. In case

**Table 2** Results from the different load situations in simple specimens and glulam beams with baseline resistance ( $R_{BL}$ ), piezoresistive sensitivity under direct current ( $S_{DC}$ ) and the sign for the measured piezoresistivity (PR)

Specimen	$R_{BL}$ (k $\Omega$ )	$S_{DC}$ [%/MPa]	$S_{DC}$ [%/ $\sigma_{max}$ ]	PR [sign]
Transversal tension $\sigma_t$ , ( $n=30$ )	$33.7 \pm 15.6$	0.14	0.084	– (28/30); + (1/30)
Tension in finger joints $\sigma_t$ ( $n=18$ )	$2.7 \pm 0.3$	0.25	2.5	+
Push-shear $\tau_c$ ( $n=9$ )	$17.8 \pm 3.1$	0.805	2.536	+ (9/12); – (2/12)
Transversal tension $\sigma_{t,t}$ glulam ( $n=2$ )	4.7 / 4.7	–	0.15; 0.12	+
Bending-tension $\sigma_{m(t)}$ glulam ( $n=1$ )	2.2	–	0.20	+
Push-shear $\tau_c$ glulam ( $n=2$ )	17.8 / 23.8	–	0.07; 0.06	+
Bending-compression $\sigma_{m(c)}$ glulam ( $n=1$ )	7.2	–	0.39	–

of a difference in PR in the set of samples, the ratio in brackets represents the rate of samples for the given sign (+/–).

A visual overview of the PR of the first set of specimens is given in Fig. 5 with an example for each specimen. For specimens with different PR, the majority is represented.

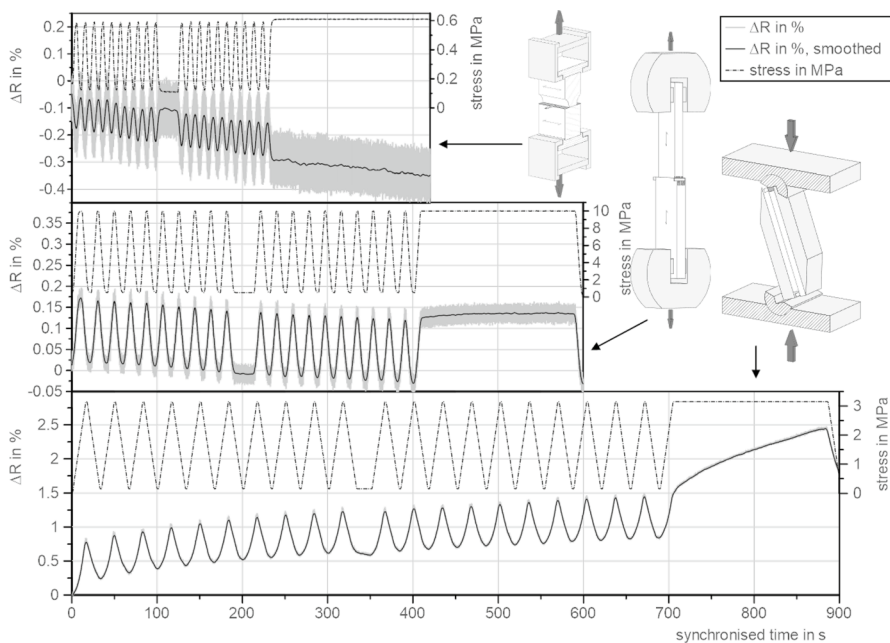


**Fig. 5** Example data from the first set of specimens, showing the piezoresistive reaction to the different stresses. The results from the tested glulam beams are visualised in Fig. 6 with all measured points in relation to the applied force in the test rack

From the set of 30 transversal tension tests, 28 specimens showed a negative PR, one a positive PR and one specimen did not show a visible reaction at all. The set of tension tests showed a consistent positive PR in all 18 samples. The set of 12 push-shear-tests showed 11 times a PR, nine times positive and two times negative.

The tests of the glulam beams (Fig. 6) result in positive PRs for all measuring points, except the bond line with compression stress. The doubled-up measurement points (transversal tension stress and shear stress) in the glulam beams show a comparable PR, but all monitored points give a different extent of PR, starting with compression load as the highest, followed by tension in tapered finger joints, transversal tension and shear with the lowest fractional change during the whole experiment of 0.06%.

Contrary to the lowest  $S_{DC}$  for shear in the glulam beam, the push-shear-tests in the first set of samples showed the highest  $S_{DC}$  compared to the other specimen, followed by the specimen in tension and transversal tension with the lowest  $S_{DC}$ .

Finally, it is visible that all samples in the first test setup show a drift in the resistance signal, which is negative for transversal tension and positive for shear with compression. For the specimen in tension, the drift is changing from negative (phase I to III) to positive (phase IV).

Even though PR could be measured in all load situations (and therefore, the hypothesis was proven positive), the following questions arose from the data set:

1. Why did some samples not show a measurable PR?
2. Why is the extent of PR different for different load situations?

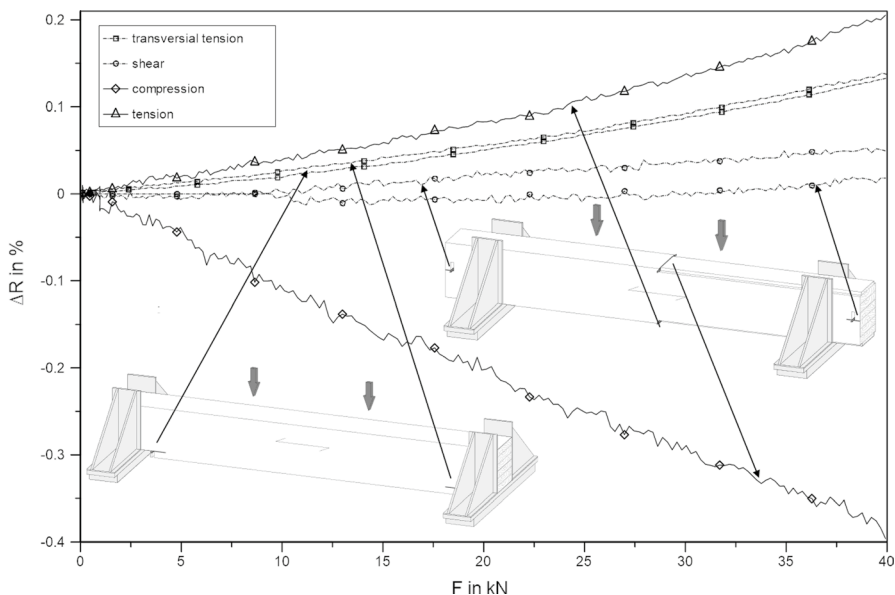


**Fig. 6** Relative change in electrical resistance as a function of test load at all measured points of the glulam beams (the marker represents every twentieth point)

3. Why is the PR in transversal tension of the first set of samples mainly positive, but negative in glulam beam testing?
4. Why did the specimens in transversal tension load and shear with compression load show inverse PR in some samples?
5. Why do most samples show a drift in electrical resistance during the measurement?

The first question is explainable by the extent of noise during the measurement. All samples with no PR show a noise of the resistance in the order of around 25%, which is several magnitudes higher than the average  $S_{DC}$  of 0.15%/MPa.

For all other questions, it is first necessary to look upon the theoretical three-dimensional stress distribution in each specimen and consider how strain and electrical resistance measurement direction are located.

## Strain analysis

Piezoresistivity and PR are influenced by the macroscopic strain ( $\Delta l/l$ ) in resistance measurement direction as well as the specific resistance of the material, which is changed by microstrains ( $\Delta\rho/\rho$ ) (see also Eq. 1).

In general, under the assumption of co-linear strain and electrical resistance measurement, the electrical resistance in

- specimens under tension increases due to the increasing conductor length ( $+\Delta l/l$ ) and distance between conducting particles, which decreases the amount of conducting paths in the material ( $+\Delta\rho/\rho$ )
- specimens under compression decreases due to the decreasing conductor length ( $-\Delta l/l$ ) and distance between conducting particles, which increases the amount of conducting paths in the material ( $-\Delta\rho/\rho$ )

Figure 7 gives a proposed model of the macroscopic and microscopic influences on the PR.

The upper part shows the theoretical stresses in the tested load situation of the first set of samples with transversal tension (a), tension in finger joints (b) and shear with compression (c) as well as the glulam beam tests with transversal tension (a'), tension in finger joints (b), shear (c') and compression (d). For a clearer diagram, the minor stresses perpendicular to the depicted area are not shown. The shown strain is the strain in direction of the resistance measurement, with compression strain negative and tension strain positive. The lower part pictures the microstructural changes, focusing on the change in specific resistance with microstrain. All strains and specific resistance changes in brackets are meant to be restricted by the structure of glulam beams. As the lamellas are bonded in layers, the transverse deformation is more restricted than in the specimen of the first set.

In addition, crucial for the understanding is the alignment of electrical resistance measurement direction with the micro shear in the bond line. On one side, if the shear is aligned with the measurement of resistance, the PR will be positive as

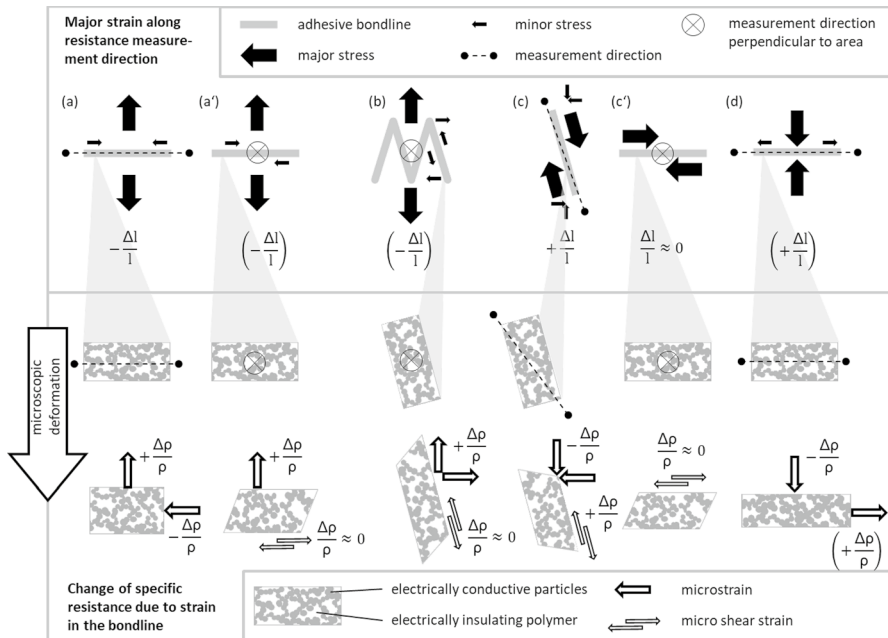


**Fig. 7** Model of strains, which influence the piezoresistive reaction of the electrically conductive bond line in wood with the tested load situations **a** transversal tension (**a'**) transversal tension in glulam beam **b** tension in finger joints **c** compression shear (**c'**) shear in glulam beam and (**d**) compression in glulam beam, with strain ( $\Delta l/l$ ) and change in specific resistance ( $\Delta \rho/\rho$ )

inter-particle distance will increase, similar to tension. On the other side, shear will not or less influence the specific resistance if the measurement direction is perpendicular to the shear field. In this case, the inter-particle distance has a lower ranked influence.

First of all, it is evident from the differentiation of  $(\Delta l/l)$  and  $(\Delta \rho/\rho)$  that the macroscopic strain cannot be the only influence on the PR, as only for the specimen in compression shear mode do the strain and PR correlate. Thus, the microstrain has an influence.

Despite the fact that the real three-dimensional strain measurement of the microstrain in the bond line is beyond the scope of this work, the model of microstrains can answer the second question and explain the differences between the extent of PR in the measurements.

As there are opposed strains in each setup, the extent of PR can be decreased by opposing strains. For example, the specimen under shear with compression (Fig. 7c) would have a positive PR from the macroscopic strain (elongation of the conductor) as well as from the microscopic strain (increasing distance between particles). The experimental results show one of the highest extents of PR for this specimen.

In addition, the strains in the shear region of the glulam beam (Fig. 7c') are proposing no or at least only small amounts of  $S_{DC}/PR$  and the experimental results show the lowest extent of  $S_{DC}$  (Table 2), partly with a negative PR (Fig. 6).

To explain the differences of PR (second question), the strain distribution was analysed by DIC as described before (see “[Measuring setup](#)”) on the surface of the transversal tension specimen in the first set as well as transversal tension in the glulam beams. With the DIC method, it was possible to measure the strain near the bond line and therefore estimate the Poisson’s ratio of the strained bond line. The different strains are visualised in Fig. 8, together with the locations of the measurement.

Mainly, the strain distribution near the bond line fitted the proposed strain model in Fig. 7.

In Fig. 8a, the measurement points for strain near the bond line of the specimen under transversal tension are shown. Figure 8a’ visualises the strain in the elastic regime of a sample with positive PR, and Fig. 8a’’ shows a sample with negative PR. Both specimens show a typical behaviour with higher strain in transversal tension (y-axis) than in lateral contraction (x-axis), thus giving no indication of the influence. On the other side, a difference is visible by the calculated Poisson’s ratio. While the specimen with positive PR gives a Poisson’s ratio  $\nu$  of  $0.65 \pm 0.05$ , the specimen with negative PR gives a  $\nu$  of  $0.82 \pm 0.01$ . These Poisson’s ratios are—contrary to the limits of  $-1$  to  $0.5$  for isotropic materials (Ting and Chen 2005)—possible and in accordance with theoretical (Mentrasti et al. 2021) and experimental literature (Kumpenza et al. 2018) on orthotropic materials like wood. This leads to the conclusion that the compression in direction of the x-axis, which is identical with the direction of the resistance measurement, is relatively higher compared to the tension perpendicular to the measurement direction. As compression-induced

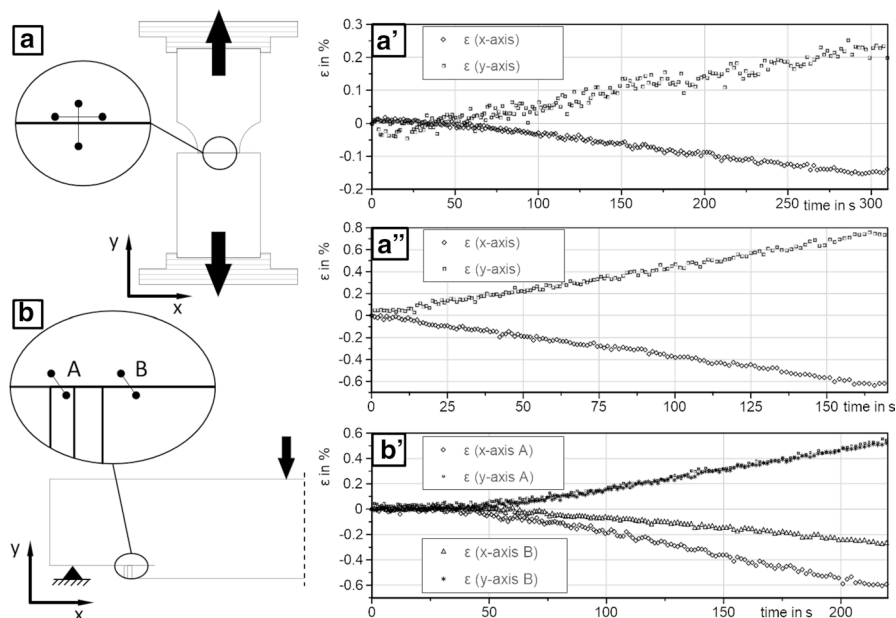


**Fig. 8** DIC measuring location at specimen from the first set **a** as well as the notched glulam beam **b** together with the calculated strain (right) of one positive (a') and one negative (a'') piezoresistive transversal tension specimen and the strain at the glulam notch (b')



PR is theoretically negative, the negative piezoresistivity in the specimen can be explained by a higher influence of compression strain. This leads to the conclusion that.

1. the majority of the tested samples of the first set exhibits higher lateral contraction compared to the transversal tension.
2. even if there are multiple stress situations while testing this specimen, the results are consistent and it is possible to detect the dominant strain with the piezoresistive bond line.

Figure 8b' also shows that transversal tension strain is not dominant in the notched glulam beam as the highest shear strain is on the same level of around 0.6%. As shear in this specimen design is supposed to not influence the PR (see Fig. 7a'), the positive PR has its origin in the transversal tension microstrain of the bond line.

### Inverse piezoresistive reaction

Three samples in all tests showed an inverse PR, from which the one from the transversal tension set was discussed and explained by strain analysis. In Fig. 9, the two samples with inverse PR of the shear with compression are shown.

Now, as the strain analysis showed that overlapping stress states can be contractionary to the PR, the resistance reaction of the two inverse samples is comprehensible. From the theory of the specimen design, a minor influence of compression stress, therefore negative PR, is possible, while the main influence—shear stress—should exhibit positive PR (see also Fig. 7).

In both specimens shown in Fig. 9, a change in PR is visible. In sample (a), the resistance increases first (positive PR) but after a certain load, the PR becomes negative (Fig. 9a'). Sample (b) starts with decreasing resistance (negative PR), but changes to an increasing resistance with higher loads (positive PR), shown in Fig. 9b'. As the PR of both samples is repeatable, an influence of damage accumulation (Myslicki et al. 2017) can be excluded as the cause of the erratic behaviour. It must be concluded that the change in piezoresistivity originates presumably from the change in the predominant strain or microstrain.

From the data set it cannot be identified why these two samples show a higher compression strain after a certain load. On the other side, it is known from wood that annual ring angle has a high influence on the stress transfer as well as the Poisson's ratio, ranging from 0.014 to 0.739 for spruce (Kumpenza et al. 2018; Niemz and Sonderegger 2017). Thus, a relatively higher influence of compressive strain at some load periods is a reasonable explanation.

### Resistance drift

In all measurements of the first set of samples, a drift in electrical resistance (RD) during the whole measurement (phase I to VI) was detectable, partly with an asymptotic trend (Fig. 10a and b). In contrast, the resistance measurements at the glulam

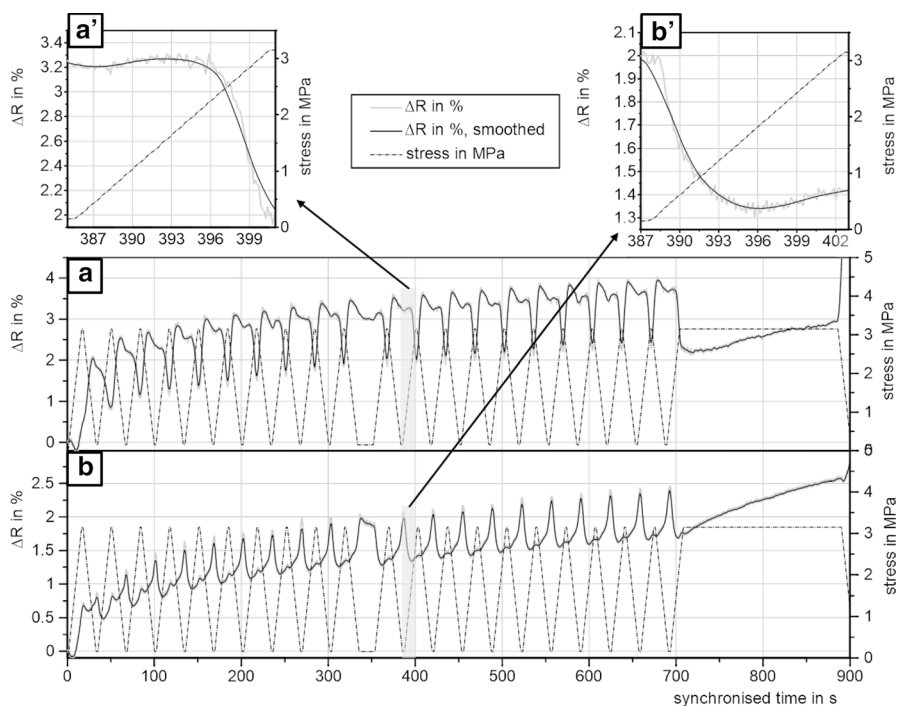


**Fig. 9** Inverse piezoresistive reaction in two samples under compression shear load (a and b) and details (a' and b')

beams did not show this RD (Fig. 10c). RD in electrically conductive polymers has also previously been reported in other studies (Abu-Abdeen et al. 2016; Kang et al. 2006; Wang and Ding 2010; Winkler et al. 2020b; Zhao et al. 2013). Possible influences along the measuring chain are the instruments, the measuring method, measuring voltage and current, the measuring cables, the contact resistances and the viscoelastic properties of the sensor (the adhesive bond line) and the stress transferring material (wood).

As all measurements on the glulam beams showed no drift, the instrument as well as the cables can be excluded as major influences as they would influence all measurements.

A reasonable explanation of the overall negative RD in the first set of samples—even in the unloaded specimens prior to the measurement (Fig. 10a and b)—is the two-probe method in the first set, which includes the contact resistance (Chung 2010). Together with the measurement method, the source voltage and current can also alter the RD, which has been investigated for voltage by Paredes-Madrid on electrically conductive filled polymers, leading to positive or negative RD (Paredes-Madrid et al. 2017). Depending on the baseline resistance (Table 2), the test current of the used instrument was 100  $\mu\text{A}$  (for  $R_{\text{BL}} \leq 10 \text{ k}\Omega$ ) and 10  $\mu\text{A}$  (for  $R_{\text{BL}} \leq 100 \text{ k}\Omega$ ). Thus, an influence from current induced heating at the contact point is unlikely, but not fully excludable.

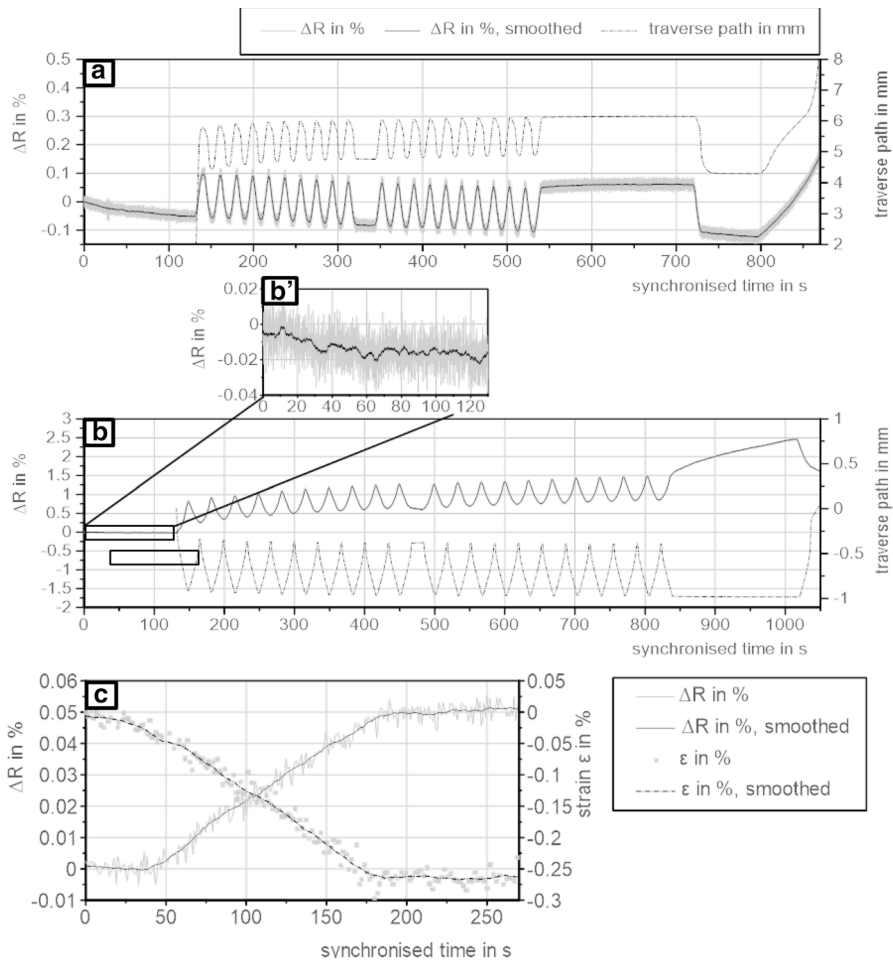


**Fig. 10** Examples of electrical resistance drift and traverse path during load-controlled testing for **a** tension in finger-jointed specimen, **b** compression shear stress and **c** electrical resistance change in one shear loaded measuring point in glulam beam b, together with the DIC measured strain

On the other hand, an additional positive drift of electrical resistance becomes visible, when the specimens are loaded. As the drift shows an asymptotic behaviour similar to creep in viscoelastic material, creep of the stress transferring wood adherend as well as the polymer of the multifunctional adhesive are possible influences. The deformation of the whole specimen was measured by the traverse path of the testing machine, but reveals only a small drift at the beginning of the test, which did not correlate with the positive drift of electrical resistance, for example in compression shear stress (Fig. 10a).

At least there are two remaining influences from measuring setup and the material, which need to be analysed with an adjusted test setup to isolate the influences and find a conclusion.

## Load until failure

The first set of specimens was partly tested until failure, which gives insight into the PR at higher stress levels and until failure. The results of load until failure are shown in Fig. 11. Figure 11a visualises the PR until failure of a specimen under shear with compression. Additionally, it represents the PR until failure of the majority of samples with positive PR. The nonlinearity presented in Fig. 11a is more distinct for specimens with higher electrical drift like the specimen under shear load. Piezoresistive measurements in the glulam beam specimen showed a linear response (see Fig. 6).

A behaviour shared by all specimens under test is a positive PR before failure, which can especially be seen in Fig. 6b and Fig. 6c, representing negative piezoresistive samples in transversal tension and shear load. The change in PR always occurs

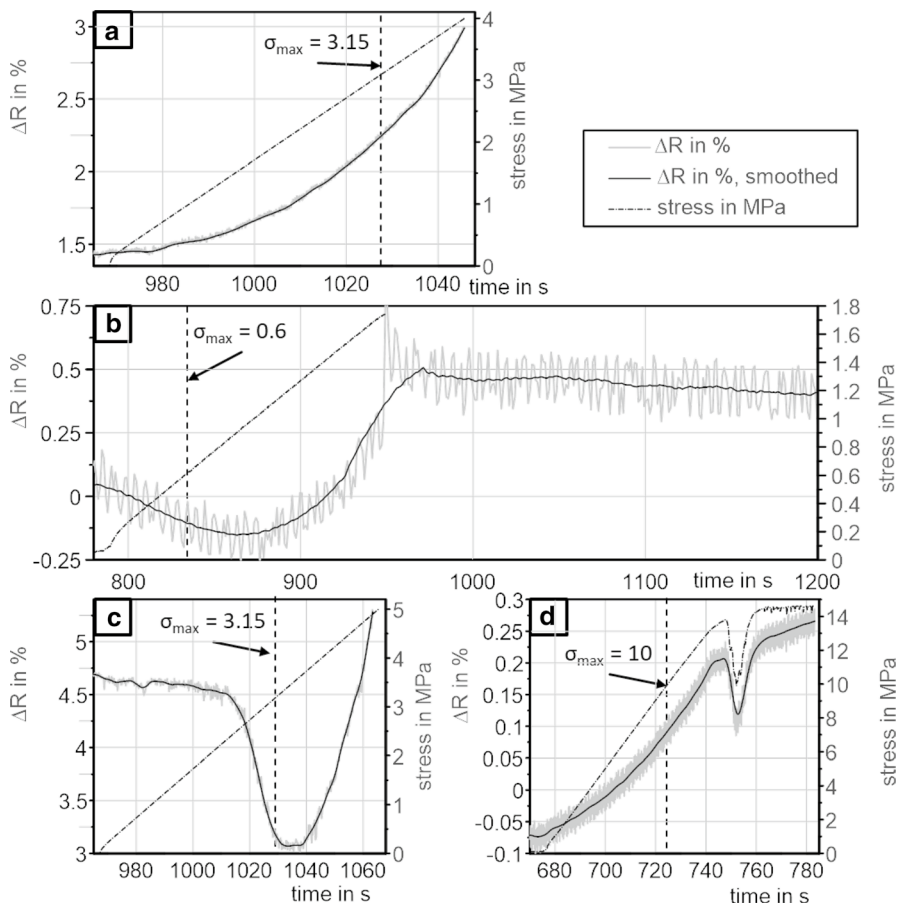


**Fig. 11** Piezoresistive reaction until failure from the first set of samples with **a** and **c** under compressive shear load, **b** under transversal tension load and **d** under tension load in finger joints

after the maximum load  $\sigma_{\max}$  during Phase I to IV, indicating that either the maximum strength of the material is reached, resulting in a plastic deformation or the tension/shear-based stresses became predominant in the sample. Figure 11d gives at least an example of pre-cracking (clearly audible) before failure in the finger-jointed specimen under tensile load.

## Conclusion

The experimental results from using electrically conductive adhesives in engineered timber were presented and discussed, focussing on the upscaling of earlier studies. The necessity of specimen design regarding the electrical contact and different specimen design for measurements of transversal tension, tension in finger joints, compression and shear are presented. All results clearly show the PR of the multi-functional adhesive bond line could be used to detect stresses. Further questions are discussed in the paper, including inverse PRs, signal drifting and behaviour until failure, coming up by evaluation of the tests.

A model to explain the results from the point of view of piezoresistive properties was designed. Further investigation is needed to include the restrictions of the three-dimensional strain analysis inside bond line and materials. The following conclusions can be drawn from the results:

1. It is possible to detect strains and the related stresses in glulam beams by means of the piezoresistive properties of the electrically conductive bond lines.
2. The PR turns positive prior to overloading and failure, even if the resistance was decreasing in the elastic regime.
3. In several measurements, a drift in electrical resistance could be measured but not traced back to one cause. Thus, the cause of the electrical drift needs to be investigated in detail.

Under the assumption of the model concept:

4. Electrically conductive adhesive bond lines in wood exhibit piezoresistive behaviour in accordance with the theory, showing negative PRs in compression and positive in tension.
5. In shear, the direction of measurement is crucial, decreasing the sensitivity if the electrical resistance is measured perpendicular to the shear field.
6. The results suggest that the piezoresistive adhesive bond line will measure the dominant stress state at the measurement point, thus overlapping stress states could lead to an increase or decrease in PR.

**Supplementary Information** The online version contains supplementary material available at <https://doi.org/10.1007/s00226-021-01305-6>.

**Funding** Open Access funding enabled and organized by Projekt DEAL. This work was supported by the German Government within the „Nachwachsende Rohstoffe“ program (FNR, BMEL) under Grant 22005018.

**Availability of data and material** Available upon request: [christoph.winkler@hnee.de](mailto:christoph.winkler@hnee.de).

## Declarations

**Conflict of interest** On behalf of all authors, the corresponding author states that there is no conflict of interest.

**Open Access** This article is licensed under a Creative Commons Attribution 4.0 International License, which permits use, sharing, adaptation, distribution and reproduction in any medium or format, as long as you give appropriate credit to the original author(s) and the source, provide a link to the Creative Commons licence, and indicate if changes were made. The images or other third party material in this article are included in the article's Creative Commons licence, unless indicated otherwise in a credit line to the material. If material is not included in the article's Creative Commons licence and your intended use is not permitted by statutory regulation or exceeds the permitted use, you will need to obtain permission directly from the copyright holder. To view a copy of this licence, visit <http://creativecommons.org/licenses/by/4.0/>.

## References

- Abu-Abdeen M, Aboud AI, Ramzy GH (2016) Effect of Temperature on creep behavior of poly(vinyl chloride) loaded with single walled carbon nanotubes. *Int J Sci Eng App* 5:112–120. <https://doi.org/10.7753/IJSEA0503.1001>
- Balageas D, Fritzen C-P, Güemes A (eds) (2006) *Structural Health Monitoring*. Iste Publishing Company, London
- Kasal B, Tannert T (eds) (2010) *In Situ Assessment of Structural Timber. State of the Art Report of the RILEM*. Springer, Heidelberg
- Chung DDL (2010) *Functional Materials: Electrical, dielectric, electromagnetic, optical and magnetic applications. Engineering materials for technological needs, vol 2*. World Scientific, Singapore
- Chung DDL (2020) A critical review of piezoresistivity and its application in electrical-resistance-based strain sensing. *J Mater Sci* 55:15367–15396. <https://doi.org/10.1007/S10853-020-05099-Z>
- EN 338 (2016) *Structural timber - Strength classes*. European Committee for Standardization (CEN), Brussels
- Filon LNG (1903) On an approximate solution for the bending of a beam of rectangular cross-section under any system of load, with special reference to points of concentrated or discontinuous loading. *Phil Trans r Soc Lond A* 201:63–155. <https://doi.org/10.1098/rsta.1903.0014>
- Franke S, Franke B, Rautenstrauch K (2007) Strain analysis of wood components by close range photogrammetry. *Mater Struct* 40:37–46. <https://doi.org/10.1617/s11527-006-9152-6>
- Han S, Meng Q, Araby S, Liu T, Demiral M (2019) Mechanical and electrical properties of graphene and carbon nanotube reinforced epoxy adhesives: Experimental and numerical analysis. *Compos Part A-Appl S* 120:116–126. <https://doi.org/10.1016/j.compositesa.2019.02.027>
- Jahreis MG, Rautenstrauch K (2016) High-Efficient Joint System for Timber Engineering with Casted-in Connectors. In: Eberhardsteiner J, Winter W, Fadaei A (eds) *World Conference on Timber Engineering (WCTE 2016)*: Vienna, Austria, 22–25 August 2016. Vienna University of Technology, Vienna
- Kang I, Schulz MJ, Kim JH, Shanov V, Shi D (2006) A carbon nanotube strain sensor for structural health monitoring. *Smart Mater Struct* 15:737–748. <https://doi.org/10.1088/0964-1726/15/3/009>
- Kästner M, Jahreis MG, Hädicke W, Rautenstrauch K (2014) Development of Continuous Composite Joints on the Basis of Polymer Mortar with matched Properties. In: Salenikovich A (ed) *World Conference on Timber Engineering (WCTE 2014)*: Quebec City, Canada, 10–14 August 2014. Curran Associates Inc, Red Hook, NY

- Koch J, Simon A, Arndt RW (2016) Monitoring of moisture content of protected timber bridges. In: Eberhardsteiner J, Winter W, Fadaei A (eds) World Conference on Timber Engineering (WCTE 2016): Vienna, Austria, 22–25 August 2016. Vienna University of Technology, Vienna
- Köckritz T, Wehnert F, Pap J-S, Jansen I (2015) Increasing the Electrical Values of Polydimethylsiloxane by the Integration of Carbon Black and Carbon Nanotubes: a Comparison of the Effect of Different Nanoscale Fillers. *J Adhes Soc Jpn* 51:221–222. <https://doi.org/10.11618/adhesion.51.221>
- Kumpenza C, Matz P, Halbauer P, Grabner M, Steiner G, Feist F, Müller U (2018) Measuring Poisson's ratio: mechanical characterization of spruce wood by means of non-contact optical gauging techniques. *Wood Sci Technol* 52:1451–1471. <https://doi.org/10.1007/s00226-018-1045-7>
- Kurz JH (2015) Monitoring of timber structures. *J Civil Struct Health Monit* 5:97. <https://doi.org/10.1007/s13349-014-0075-6>
- Kurz JH, Boller C (2015) Some background of monitoring and NDT also useful for timber structures. *J Civil Struct Health Monit* 5:99–106. <https://doi.org/10.1007/s13349-015-0105-z>
- Mang HA, Hofstetter G (2013) *Mechanics of Materials (Festigkeitslehre)*, 4th edn. Springer Vieweg, Berlin, Heidelberg
- Masaebi N, Peighambaroust SJ, Ahadzadeh I (2018) Electrically conductive nanocomposite adhesives based on epoxy resin filled with silver coated nanocarbon black. *J Mater Sci Mater Electron* 29:11840–11851. <https://doi.org/10.1007/s10854-018-9284-9>
- Massoumi B, Hosseinzadeh M, Jaymand M (2015) Electrically conductive nanocomposite adhesives based on epoxy or chloroprene containing polyaniline, and carbon nanotubes. *J Mater Sci Mater Electron* 26:6057–6067. <https://doi.org/10.1007/s10854-015-3183-0>
- Mentrasti L, Molari L, Fabiani M (2021) Poisson's ratio bounds in orthotropic materials. Application to natural composites: wood, bamboo and *Arundo donax*. *Compos Part B-Eng* 209:108612. <https://doi.org/10.1016/j.compositesb.2021.108612>
- Myslicki S, Winkler C, Gelinski N, Schwarz U, Walther F (2017) Fatigue assessment of adhesive wood joints through physical measuring technologies. In: *Fatigue 2017: 7th International Conference on Durability and Fatigue*, pp 446–455
- Niemz P, Sonderegger WU (2017) *Wood Physics (Holzphysik - Physik des Holzes und der Holzwerkstoffe)*. Fachbuchverlag Leipzig (Carl Hanser), Munich
- Oppel M, Jahreis MG, Rautenstrauch K (2016) Numerical constitutive model for wood with specified density function. In: Eberhardsteiner J, Winter W, Fadaei A (eds) World Conference on Timber Engineering (WCTE 2016): Vienna, Austria, 22–25 August 2016. Vienna University of Technology, Vienna, pp 2424–2434
- Paredes-Madrid L, Matute A, Bareño JO, Parra Vargas CA, Gutierrez Velásquez EI (2017) Underlying Physics of Conductive Polymer Composites and Force Sensing Resistors (FSRs). A Study on Creep Response and Dynamic Loading. *Materials (Basel)* 10. <https://doi.org/10.3390/ma10111334>
- Santamaria A, Muñoz ME, Fernández M, Landa M (2013) Electrically conductive adhesives with a focus on adhesives that contain carbon nanotubes. *J Appl Polym Sci* 129:1643–1652. <https://doi.org/10.1002/app.39137>
- Tannert T, Müller A (2010) Structural health monitoring of timber bridges. In: Malo KA, Kleppe O, Dyken T (eds) In: *Proceedings international conference timber bridges (ICTB2010)*, pp 205–212
- Ting TCT, Chen T (2005) Poisson's ratio for anisotropic elastic materials can have no bounds. *Q JI Mech Appl Math* 58:73–82. [https://urldefense.proofpoint.com/v2/url?u=https-3A\\_\\_doi.org\\_10.1093\\_qjmamj\\_hbb021&d=DwlFaQ&c=vh6FgFnduejNhPPD0fl\\_yRaSfZy8CWbWnlf4XJhSsx8&r=7GjDei\\_PxQva2JNOFhbJQKIolTpKkGdW\\_4o9-CecCzX9fDPu7SrgsodpYCPByYz&m=YislG9yQzW2uLeNznmgMPv61ZefCIMDYHHMFESPNccU&s=WT2HENNuFS8G4kNM8ZpJ0nEV1gDQ8cmuxicKqGK9Gr8&e=](https://urldefense.proofpoint.com/v2/url?u=https-3A__doi.org_10.1093_qjmamj_hbb021&d=DwlFaQ&c=vh6FgFnduejNhPPD0fl_yRaSfZy8CWbWnlf4XJhSsx8&r=7GjDei_PxQva2JNOFhbJQKIolTpKkGdW_4o9-CecCzX9fDPu7SrgsodpYCPByYz&m=YislG9yQzW2uLeNznmgMPv61ZefCIMDYHHMFESPNccU&s=WT2HENNuFS8G4kNM8ZpJ0nEV1gDQ8cmuxicKqGK9Gr8&e=)
- Wang P, Ding T (2010) Creep of electrical resistance under uniaxial pressures for carbon black–silicone rubber composite. *J Mater Sci* 45:3595–3601. <https://doi.org/10.1007/s10853-010-4405-8>
- Wehnert F, Langer M, Kaspar J, Jansen I (2014) Design of multifunctional adhesives by the use of carbon nanoparticles. *J Adhesion Sci Technol* 29:1849–1859. <https://doi.org/10.1080/01694243.2015.1014536>
- Winkler C, Schwarz U (2016) Characterization of adhesively bonded wood structures by electrical modification of the bonding system. In: Eberhardsteiner J, Winter W, Fadaei A (eds) World Conference on Timber Engineering (WCTE 2016): Vienna, Austria, 22–25 August 2016. Vienna University of Technology, Vienna
- Winkler C, Schäfer J, Jäger C, Konnerth J, Schwarz U (2020) Influence of polymer/filler composition and processing on the properties of multifunctional adhesive wood bonds from polyurethane

- prepolymers II: electrical sensitivity in compression. *J Adhesion* 96:185–206. <https://doi.org/10.1080/00218464.2019.1652602>
- Winkler C, Schäfer J, Jager C, Konnerth J, Schwarz U (2020b) Influence of polymer/filler composition and processing on the properties of multifunctional adhesive wood bonds from polyurethane prepolymers II:electrical sensitivity in compression. *J Adhesion* 96:185–206.[https://urldefense.proofpoint.com/v2/url?u=https-3A\\_\\_doi.org\\_10.1080\\_00218464.2019.1652602&d=DwIFaQ&c=vh6FgFnduejNhPPD0fl\\_yRaSfZy8CWbWnIf4XJhSqx8&r=7GjDei\\_PxQva2JNOFHbJQKIolTpKkGdW\\_4o9-CecCzX9fDPu7SrgsodpYCPByYz6&m=YislG9yQzW2uLeNznmgMPv6lZefClMDYHHMFE5PNccU&s=rdHWeu\\_g4jzDZgLD2BqN6lcx5W0qIgC2ryPvk2i9oJA&e=](https://urldefense.proofpoint.com/v2/url?u=https-3A__doi.org_10.1080_00218464.2019.1652602&d=DwIFaQ&c=vh6FgFnduejNhPPD0fl_yRaSfZy8CWbWnIf4XJhSqx8&r=7GjDei_PxQva2JNOFHbJQKIolTpKkGdW_4o9-CecCzX9fDPu7SrgsodpYCPByYz6&m=YislG9yQzW2uLeNznmgMPv6lZefClMDYHHMFE5PNccU&s=rdHWeu_g4jzDZgLD2BqN6lcx5W0qIgC2ryPvk2i9oJA&e=)
- Zhao J, Dai K, Liu C, Zheng G, Wang B, Liu C, Chen J, Shen C (2013) A comparison between strain sensing behaviors of carbon black/polypropylene and carbon nanotubes/polypropylene electrically conductive composites. *Compos Part A-Appl S* 48:129–136. <https://doi.org/10.1016/j.compositesa.2013.01.004>

**Publisher's Note** Springer Nature remains neutral with regard to jurisdictional claims in published maps and institutional affiliations.



## Supplementary Information

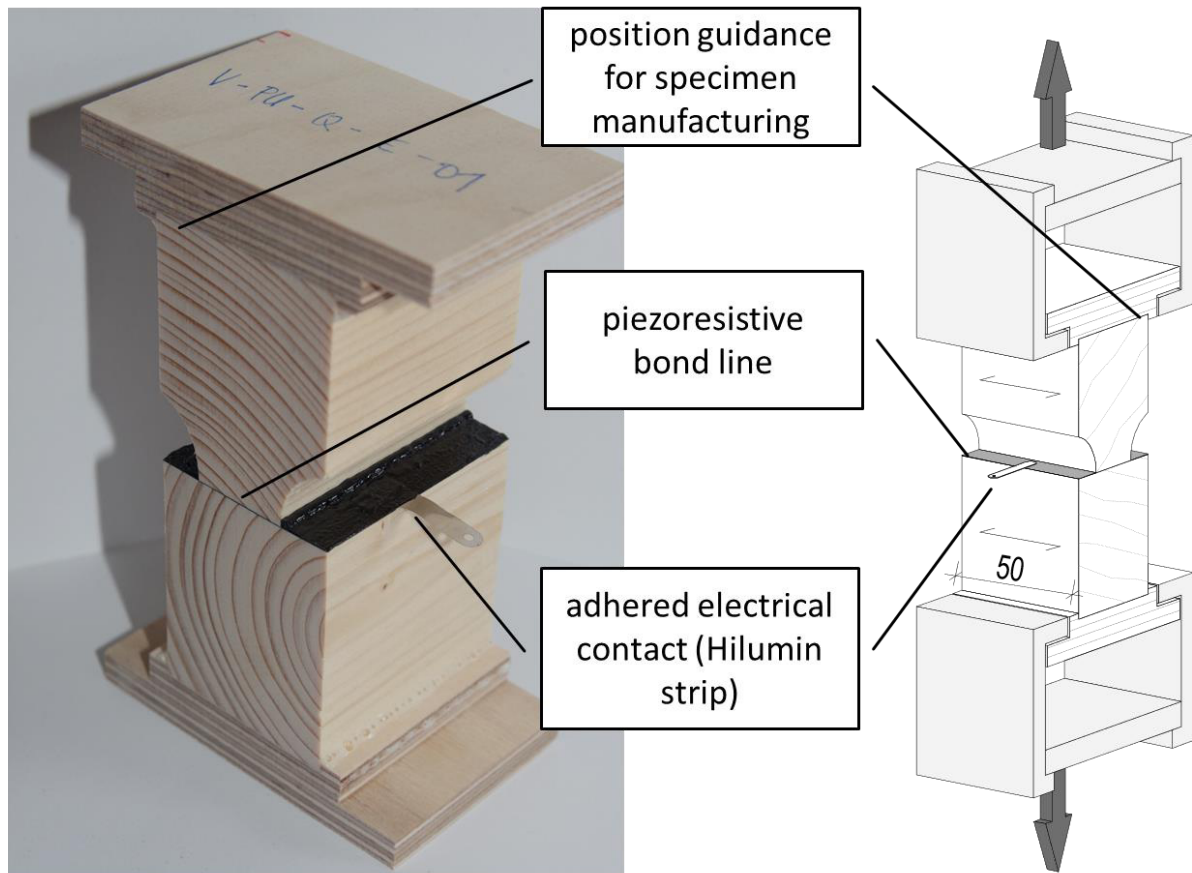


**Fig. 1** Details of specimen with piezoresistive bond line under transversal tension

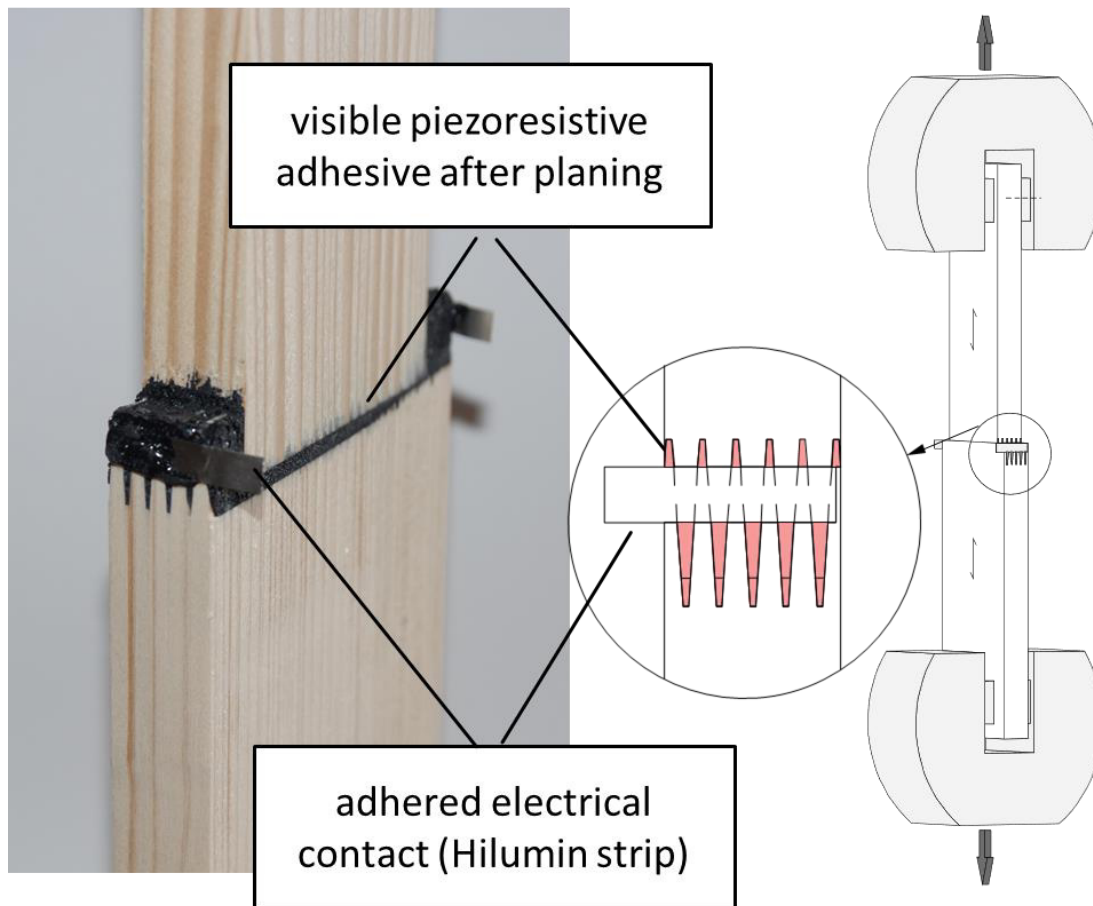


**Fig. 2:** Details of specimen with piezoresistive bond line in tapered finger joint under tension

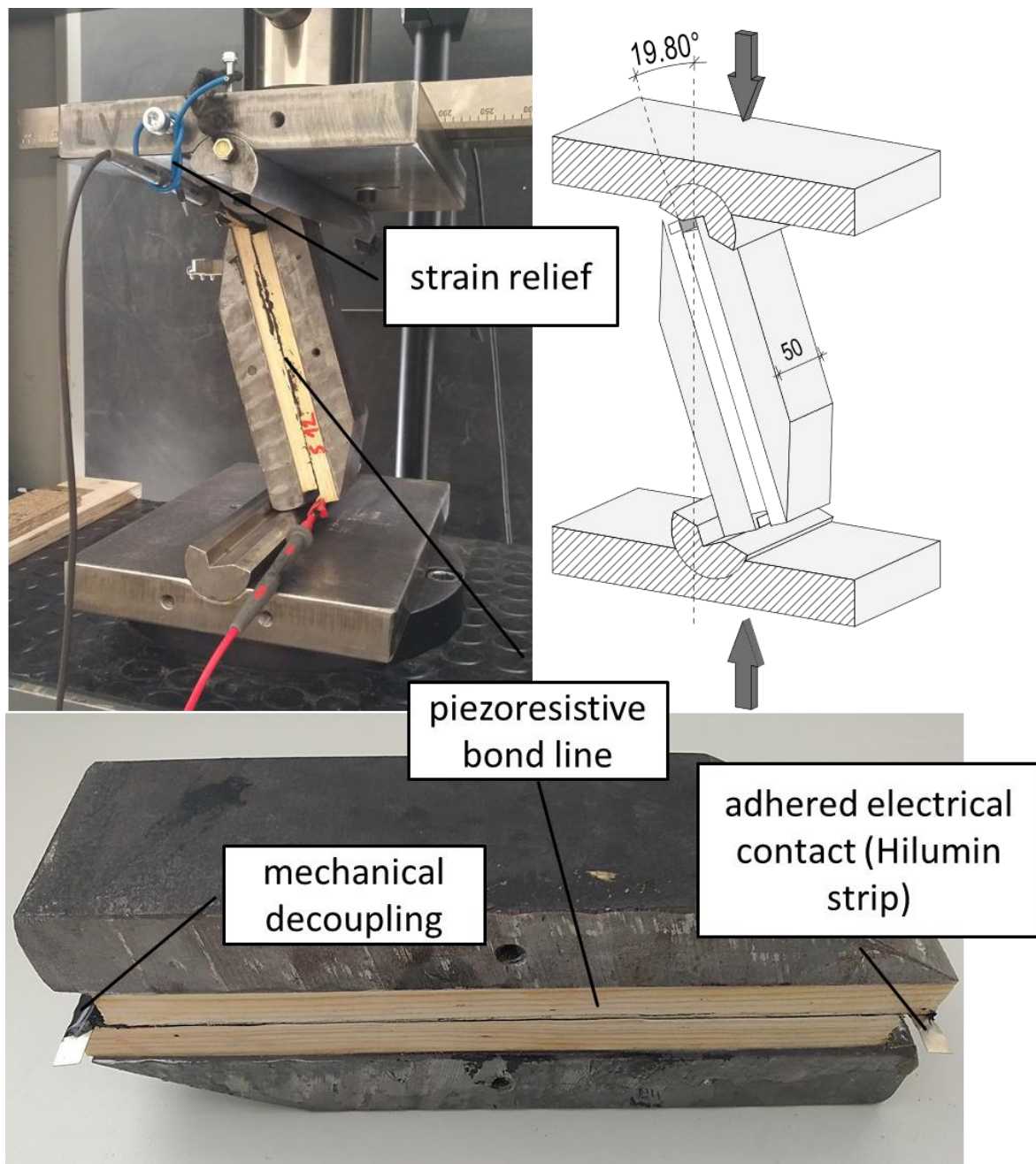


**Fig. 3:** Details of specimen with piezoresistive bond line under shear with compression

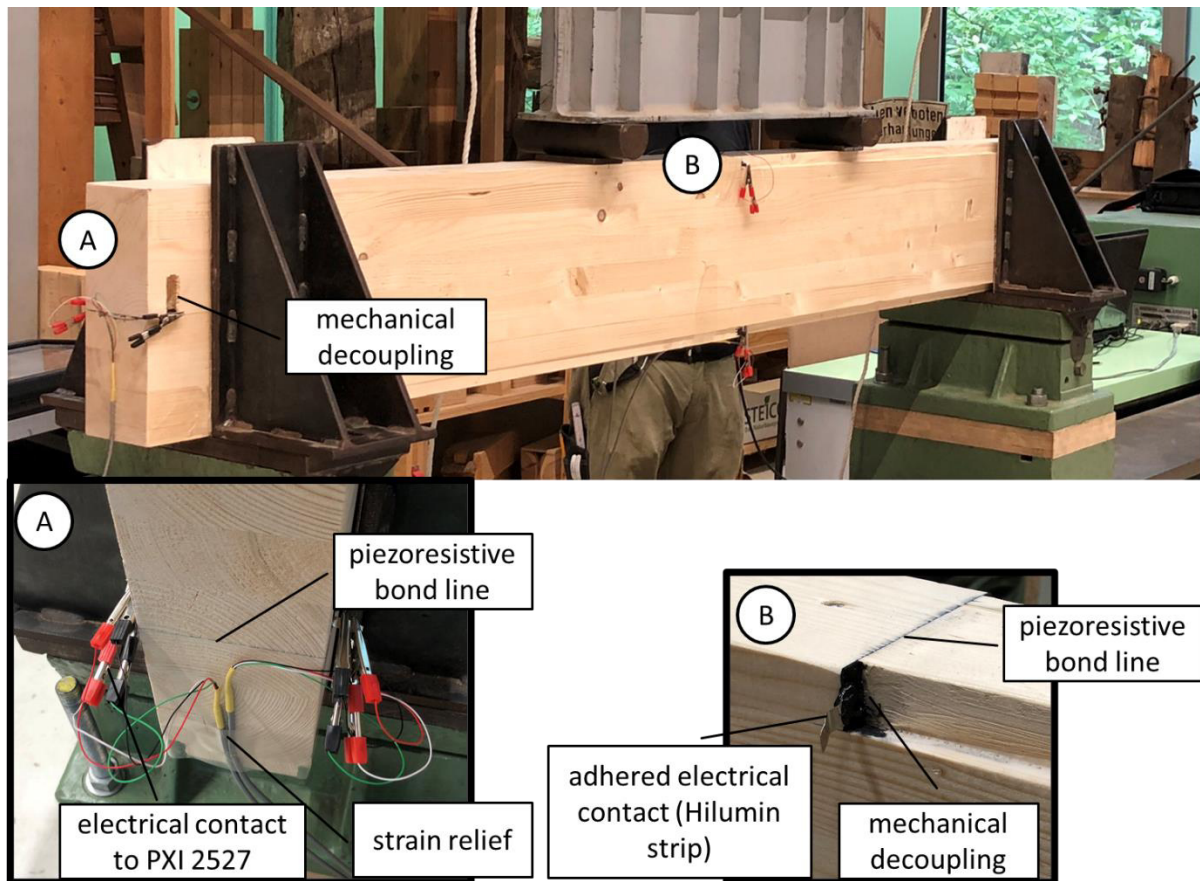


**Fig. 4:** Details of glulam beam with locally isolated piezoresistive bond lines strained in shear, bending tension and bending compression

## 5 MAIN FINDINGS AND DISCUSSION

At the beginning of this doctoral project, the term ‘multifunctional adhesive joint’ was preferentially used to indicate that the adhesive joint has additional functions. These new functionalities were shown in simplified laboratory tests in earlier work [32] in the area of strain, wood moisture, and fatigue measurements. Although the doctoral research solely concentrated on the measurement of stress/strains by means of an adhesive joint, various terms were used within the framework of its main investigations that were subject to a temporal and comprehensible development. These first need to be clarified to make the subsequent discussion of the hypotheses understandable.

The term piezoresistivity logically describes a change in resistivity due to a strain, which means that the change in resistance not only results from a change in the geometry, but also from a change in the specific resistivity  $\rho$  (see section 2.2.1), which is generally a fundamental material property. Otherwise, it would strictly be a resistive measurement [131]. On the other hand, piezoresistive polymers are usually characterized by the fractional change of resistance with strain [25], leading to the potential misunderstanding that piezoresistivity is a change of resistance with strain (which was defined as such in Paper IV). Additional confusion arises from the fact that piezoresistivity is sometimes defined in basic literature as a ‘change of resistance of semiconductors from mechanical stress’ [232]. While stress and strain are related by Hooke’s law, resistance is a measured value, and resistivity is a calculated property.

At the beginning of the thesis, however, the author was not yet aware of this difference as the previously mentioned studies of multifunctional bond lines attributed the effect to the change in the bond line dimensions (thickness and elongation) [34,35]. In Paper III, the term piezoresistivity was first introduced by describing polymers filled with electrically conductive particles as being piezoresistive. While the working mechanisms of piezoresistive polymers were described, the associated terms were not precisely defined. In Paper III and Paper IV, a change of resistance/impedance with a fractional change of stress was described and published, but the terms piezoresistivity, piezoresistive, and piezoresistive response were used in alignment with the use in other publications [31,128,132]. A delimitation of piezoresistivity and the term piezoresistive reaction was thus only made in Paper V. This delimitation was necessary as scientifically defined piezoresistivity does not account for shear strains in piezoresistive films such as piezoresistive adhesives, as explained in Paper V.

### 5.1 Piezoresistivity without reduction of bond strength

The first research question (RQ1) enquired whether the integration of ECF into wood adhesives impairs their bond strength, which is the main purpose of adhesives. According to the studies on piezoresistive polymers, the integration of an ECF network

would reliably add piezoresistive properties to the bond line (see section 2.2.1) if the filler concentration reaches the percolation threshold. On the other hand, filler integration is partly known for its detrimental effect on mechanical properties (see section 2.1.3). Thus, a decrease in filler concentration to reach the percolation threshold was one of the main driving research topics in the field of nanocomposites (see section 2.1.1). In contrast to adhesives in other industries, wood adhesives are designed to have better mechanical properties compared to wood, which mostly results in wood failure (see section 2.1.3).

Consequently, the resulting hypothesis H1 from RQ1 connected the decrease in bond strength to the aim of achieving piezoresistive properties, which in turn is connected to an unknown filler concentration to reach the percolation threshold:

*An addition of piezoresistive properties to the bond line in engineered timber – without reducing the strength of manufactured wood bonds – is possible by the integration of electrically conductive filler without reducing the strength of manufactured wood bonds*

In response to this dependency, the filler concentration necessary to achieve piezoresistive behaviour was investigated and the results were published in Paper III. The results show that piezoresistivity could be reached at a filler concentration of 2 wt% CB and 0.3 wt% CNTs (Paper III, figures 5–9). On the other hand, the reliability for reaching piezoresistivity increases with higher filler concentration, as shown by the relative fraction of samples with analysable signal quality. These findings are in agreement with the findings of other researchers who showed that higher concentrations of filler enhance the reproducibility of the piezoresistive sensitivity and are better suited for practical applications [125,134,135], due to the more stable network of interconnecting ECF particles and aggregates.

With higher filler concentrations being necessary for piezoresistive properties, in Paper II the TSS in a dry condition (EN 302-1, A1) was analysed concerning the filler concentration of CB and CNTs for 5 different 1C-PURs. The results showed no clear dependence of filler concentration and TSS among all 1C-PURs used (Paper II, figures 4–8). PU3 was the only polymer matrix that reacted according to the theory with decreasing shear strength although it also showed high WFP. As mentioned in section 3.2.1, the TTS does not indicate a decrease in mechanical strength of the adhesive itself if a high WFP is measured, as failure occurs outside the adhesive bond line.

Only PU2 showed a low WFP without filler, and also with increasing high filler concentration. The PU2 results showed that even at low filler concentration, the TSS exceeds the requirement of EN 302-1 in the A1 condition of 10 MPa, which the unfilled 1C-PUR did not reach (Paper II, figure 5). On the other hand, the TSS and low WFP stayed at this level without further increases or decreases resulting from increasing filler concentration.



Similar results at high WFP were reported in Paper I (Fig. 4) with the addition of 4 wt% of CB and the second combination of 2 wt% carbon nanofibers (CNF) together with 0.2 wt% CNTs to 1C-PUR as a nanocomposite matrix. Even at significantly lower TSS for both fillings, the WFP stayed at the same high level of 90–100 %.

Similar effects of filler on the TSS were reported by others. Clauss et al. [233] reported a significant increase of TSS with increasing content of chalk, together with an increase of 50–70% WFP for some testing conditions and a slight decrease for others. Other researchers have investigated the reinforcing effect of CNTs in wood adhesives such as soy protein-based adhesives [234,235], UF resins, and polyvinyl acetate glues (PVAc) [236] without the intention to use the piezoresistive properties, but with increasing filler concentration. Moya et al. [236] found an increase in TSS with increasing CNT concentration in most data sets. They assumed that the reduced significance of the reinforcing effect in PVAc results from remaining agglomerates. Afolabi et al. [234] showed an increase of TSS with increasing CNT concentration, followed by a decrease. Unfortunately, no WFP was reported, making the results difficult to compare. On the other hand, the authors showed that the shear mixing process resulted in remaining agglomerates. The observation is in line with the research of Han et al. [98], who also reported the same phenomenon for epoxy resins. Furthermore, crack initiation from remaining agglomerates has been identified as the major reason for the decreasing mechanical properties of nanocomposites [99]. Whether the wood failure was a result of microcracking in the bond line and therefore crack propagation into the wood adherend and wood failure, could not be evaluated from the data on TSS and WFP.

The TSS and WFP by the test standard EN 320-1 (A1) could thus not be used to understand the influence of ECF concentration on the mechanical properties of the cured adhesive. On the other hand, the results show that even at ECF concentrations of 6 wt% CB, a sufficient bond quality in dry conditions can be achieved that exceeds the requirement of 10 MPa. As a result, hypothesis H1 can be confirmed with the limitation of TSS in dry conditions (EN 302-1 (A1)).

## **5.2 Influence of process parameters**

Before the commencement of the research, bonded wood samples with electrically conductive bond lines were produced according to the guidelines of the datasheet of the commercial adhesives used. These are oriented towards achieving good bonding qualities, but not necessarily good piezoresistive properties. From research in other fields, it was expected that the process parameters for manufacturing can have an immense influence on the final properties (see section 2.3). It also became clear that not every process parameter could be investigated in detail within the scope of this thesis. This led to the derivation of the second research question (RQ2) regarding the main

influencing factors in the manufacturing process regarding the newly added properties, namely the decrease of electrical resistivity and increase of piezoresistive properties.

From the theoretical background it was concluded that, first of all, a low electrical resistance is necessary to achieve differentiation from the wood adherend as a parallel resistance (see section 2.4.2). Secondly, a high sensitivity and high stability (or low instability) characteristics are necessary, which in this thesis are summarised as piezoresistive properties (see section 2.2.2). As a result, the second hypothesis H2 was determined as follows:

*A decrease in electrical resistance and an increase in the piezoresistive properties of electrically conductive bond lines in wood can be achieved by the proper selection of ECF type and concentration, together with a suitable dispersion and assembly process.*

Two experiments were used to evaluate these influences, categorized according to the influence of adhesive ingredients (polymer, filler type, and concentration) and manufacturing variables (dispersion technique, adhesive application technique, glue spread, pressure, pressure time, and pressure temperature). The results were published in Paper II and Paper III.

Based on the results derived for the investigated variables, it could be concluded that the adhesive ingredients had a superior influence on the electrical (see the different scales for DC resistance in Paper II, Fig. 4-9) and piezoresistive properties compared to the manufacturing variables.

The influence of filler type and concentration is not a new insight concerning the state of the art in nanocomposites. CNTs are known for their lower intrinsic resistivity compared to CB [63] as well as their lower percolation threshold compared to CB due to their high aspect ratio [71,85,237,238]. The decrease in resistivity for combinations of ECF such as the one published in Paper I was previously found and simulated for fibrous and spherical fillers [84,85]. In Paper I, 0.2 wt% CNTs were added to 2 wt% CNFs, which combines two fibrous fillers of different sizes [239,240], resulting in an ECF network with more effective conducting paths than for other mixed ECF combinations. Furthermore, the finding that CB as a filler can result in higher sensitivities compared to MWNTs was shown in at least one other publication [128]. The same applies to higher ECF concentrations leading to higher stability of the piezoresistive response [125,134], which can be traced back to the lower amount of capacitive paths [135]. These findings are thus a confirmation of the state of the art.

In contrast, the type of adhesive/polymer in literature has mostly been viewed with respect to the final application and the non-electrical properties required — with adhesives in structural wood applications not yet being investigated in this context (see section 2.1.4). Paper II and Paper III presented the first results of choosing 1C-PUR as a matrix polymer concerning its electrical and piezoresistive properties. The effect of



foaming in 1C-PUR from CO<sub>2</sub>-formation has not been systematically investigated, but scanning electron microscopy (SEM) images (JSM-6460LV, JEOL [Germany] GmbH, Freising, Germany) of adhesive films from the same materials show that the electrically conductive paths are built around the foaming bubbles and the concentration of effective conductive paths is increased by the extent of foaming (see Fig. 11). As a result, it can be concluded that the effect of foaming is not necessarily detrimental to the DC resistance of foaming 1C-PUR and electrically conductive paths are built around these voids as proposed by Brunner [104].

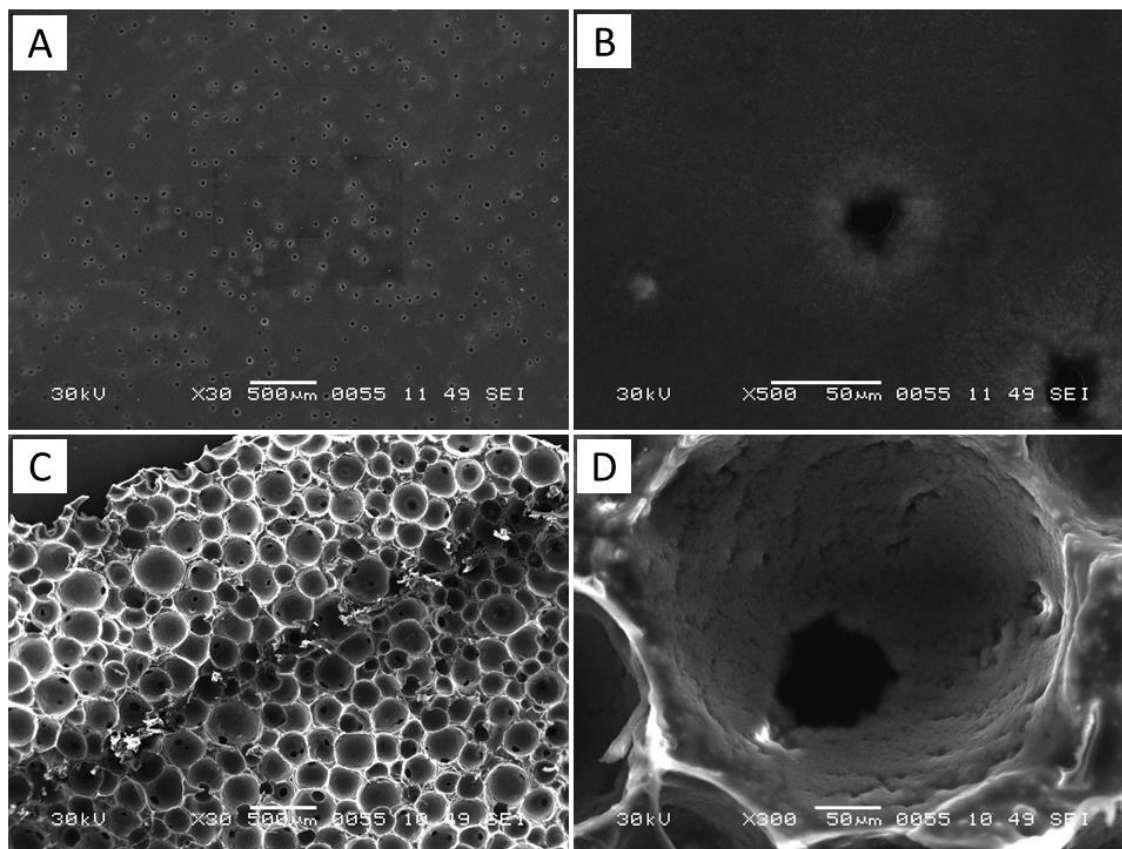


Fig. 11 Scanning electron microscope (SEM) images of polyurethane prepolymer (1C-PUR) filled with 3.5 wt% Ketjenblack EC-300J films with a thickness of 100  $\mu\text{m}$  (A,B) and 500  $\mu\text{m}$  (C,D), not coated. Bright locations show relative higher conductivity (© Westphalian University of Applied Sciences, [241])

Thus, even foaming 1C-PUR was found suitable for the production of piezoresistive adhesives.

In addition, the polymer formulation was shown to be of importance for achieving low instability properties as well as reliable sensitivity (see Paper III, Fig. 5-9). While it is known that different polymers require different dispersion techniques or even

functionalisation of the polymer or ECF (see section 2.3.1), differences between very similar polymers such as those in Paper II and Paper III were not previously reported. This is especially relevant, as one of the most important factors for the polymer matrix was proposed to be a low viscosity [63]. In the presented results, PU1 showed the best piezoresistive properties, but not the lowest viscosity. In contrast, the 1C-PUR with the lowest viscosity (PU2) exhibited inferior piezoresistive properties with high instabilities up to the highest processable filler concentration. In this regard, no clear correlation between the adhesive viscosity and the resulting piezoresistive properties could be identified.

Even though further analysis regarding the influence of formulation details was not possible due to the trade secrets of the manufacturing companies, the formulation of the adhesive (apart from viscosity) was found relevant for achieving proper piezoresistive properties in the cured bond line.

The last significant factor for producing piezoresistive adhesives from 1C-PUR was found in the dispersion technique. By using a dissolver for dispersion, significantly lower DC resistance and piezoresistive instability properties could be reached compared to the use of a 3-roll mill. In regard to the state of the art, this data suggests the presence of residues of agglomerates in the 1C-PUR due to the lower energy density from shear flow produced by the dissolver [158]. Remaining agglomerates from a not fully dispersed filler can result in a higher structured network of ECFs, thereby leading to lower resistance than a well-dispersed network of ECFs [161]. Another effect of agglomerate residues would be the introduction of defects and stress concentrations in the adhesive [98,99], which is supported by the significant decrease in TSS with the dissolver technique compared to the 3-roll mill (Paper II, Fig. 9). On the other hand, TTS does not indicate a decrease in mechanical strength of the adhesive itself, and a high wood failure percentage was measured in this context. Whether the wood failure occurred as a result of microcracking in the bondline and subsequent crack propagation into the wood adherend could not be evaluated by this method. Finally, the reported increase in stability parameters in Paper III (Fig. 11) supports a less dispersed network with agglomerate residues, which would result in fewer capacitive fractions in the resulting filler network. With less electrical energy stored in microcapacitors, a decrease in electrical drift is explainable. On the other hand, the increase of agglomerates and the fracturing of these remaining agglomerates under load has been identified as a disturbing influence on the electrical properties, leading to an increased resistance with load [242]. In the experimental data, this would result in higher baseline instability  $BI_{DC}$  and variability  $V_{c,DC}$ . It is important to note that all the interpretations are based on agglomerate residues. These are unlikely for the dispersion of the CB filler used, as was proposed by Köckritz et al. [243] who reported that only homogenization of Ketchenblack EC-300J in the adhesive matrix is necessary as it does not form strong agglomerates such as CNTs. Finally, the dispersion state of highly light-absorbing fillers

such as CB in high concentrations was not detectable as no analysing technique was available for such a highly filled nanocomposite. The only technique currently capable of this type of measurement would be the microscopy of thin sections down to 20  $\mu\text{m}$  or less. For the manufactured specimen, it was not possible to prepare microscopic specimens of this size. Thus, the reason for the better usability of the dissolver compared to a 3-roll-mill could not be explained, even if the advantages and effects were measurable in the properties of the cured adhesive bond lines.

From the current perspective, the influences of the assembly process on the DC resistance, published in Paper II, are – in contrast to the influence of ECF type, concentration, and dispersion technique – less reliable than the statistically significant differences suggest. At the time of the analysis, a decrease of resistance was theoretically – based on the calculation of resistance (equation IV) – attributed to a larger cross-section, a longer measuring length and/or a lower resistivity. Since the bond line thickness remained the only variable for the cross-section from theory, a change of adhesive penetration into the wood structure and, subsequently different bond line thicknesses, were discussed. Retrospectively, another influence could be identified. By attempting to find a method to measure the length-dependent DC resistance of the electrically conductive bond line, a high variation of resistance along the specimen was found. Fig. 12 gives the results derived from several specimens made from 1C-PUR with 2 wt% CNFs and 0.2 wt% CNTs and specimens with adhesives from 1C-PUR and 4 wt% CB. Due to the high variation along the length of the specimen, it cannot be excluded that the measured variations of DC resistance are partly accidental.

Due to this, it thus appears that no further discussion regarding the influences of the assembly process on the DC resistance is relevant. Since the differences of DC resistance with increasing filler concentration and the dispersion techniques are distinctly larger (see Paper II, Figs. 4–9), no doubts are given for their influence on the DC resistance compared to the assembly parameters.

The influence of the investigated manufacturing parameters on the piezoresistive properties was mainly measurable in the instability characteristics. Lower instability characteristics were found for longer press times and higher glue spread (Paper III, Fig. 11).

Press temperature was the only process parameter with a significant influence on the sensitivity, with higher press temperatures leading to less sensitivity. In the paper, the effect is explained by a decreasing porosity with higher temperatures due to coalescence/Ostwald ripening [244]. It was hypothesized that higher porosity leads to higher compressibility and therefore higher sensitivity. However, this hypothesis contrasts with the findings of Feng et al. [245], who found a decreasing sensitivity correlated with decreasing density of piezoresistive polyurethane foams.

In contrast to the resistance measurements, the piezoresistive measurements represent a relative change of resistance and are therefore less dependent on the bond

line cross-section, which was contacted to the measuring device by silver paste. Thus, smaller differences can be distinguished using this method.

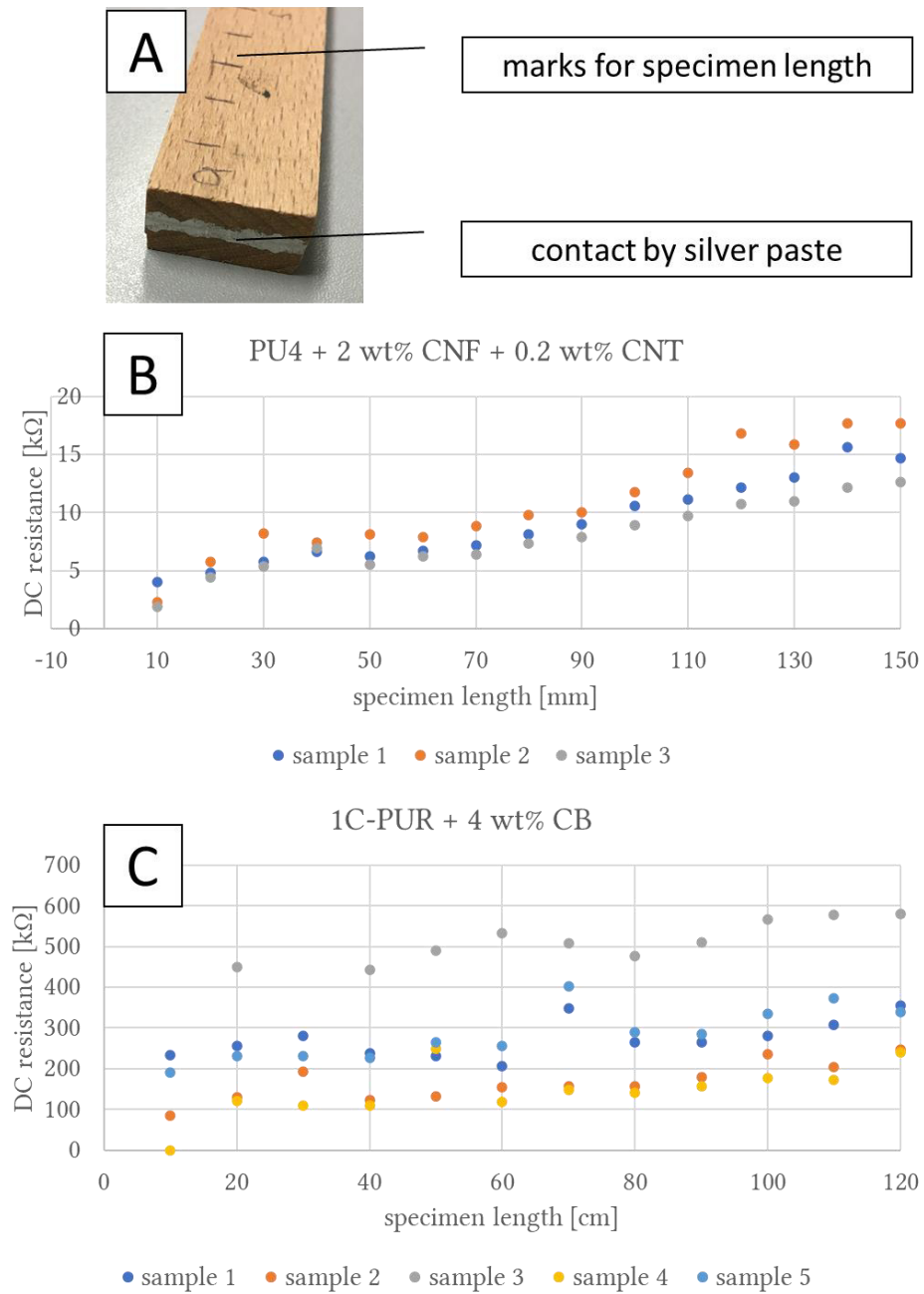


Fig. 12 Electrical resistance under direct current of specimen (A), dependent on the length of the bond line made from beechwood (*Fagus sylvatica*, L.) bonded with polyurethane prepolymer with (B) 2 wt% carbon nanofibers and 0.2 wt% carbon nanotubes added and (C) 4 wt% carbon black added (adapted from Winkler, Konopka [241])

This means that higher foaming would instantly decrease the sensitivity of piezoresistive bond lines with increased foaming. On the other hand, the experiments of Feng et al. [245] were compromised by the change on contact resistance from compression directly on the piezoresistive foam. The piezoresistive sensitivity from contact change on the microscopic level (see the experiments from Weiß [246]) is expected to increase together with the density, which is related to the contact area in foams. An additional explanation was subsequently found in the manuscript of Hu et al. [30] who showed that lower temperature can lead to higher electrical resistance and therefore higher sensitivity by increasing the ratio of tunnelling resistance to the overall resistance. A lower press temperature, which was presented in Paper II, did not support this hypothesis as no indication of a significantly higher DC resistance was found. Thus, the temperature effect still lacks a satisfactory explanation.

The results obtained are generally in agreement with the state of the art, with some minor additions. The large influence of ECF type and concentration together with the dispersion technique on the DC resistance and the piezoresistive properties, especially the stability related characteristics, are in agreement with hypothesis H2. As the investigated assembly process parameters only revealed a minor influence on the piezoresistive properties compared to the ingredients of the adhesive and the dispersion method, the DC resistance measurement must be retrospectively revised. In addition to the known state of the art, it was found that even similar polymer formulations can have an influence on the percolation threshold and the final piezoresistive properties of the cured adhesive. The fact that piezoresistive 1C-PUR can be produced by dispersion techniques such as the dissolver, which offers a low energy density compared to other dispersion techniques, offers further options for using traditional production methods of adhesive, making them easier to upscale.

### 5.3 Further improvement of piezoresistive properties

It is apparent that high piezoresistive sensitivity is a proper option to distinguish the piezoresistive reaction of the bond line from other disturbances. The high amplitude of the resistance change at low strain is also necessary to measure small changes in stress/strain. In response to this requirement, the third research question (RQ3) was regarding which further options – in addition to adhesive components and process parameters – exist to increase the piezoresistive sensitivity after manufacturing. In addition to lower ECF concentration, which has been discussed before, thermal postcuring of the bond line (see section 2.3.3) appeared to be a not yet investigated option. Therefore, the third derived hypothesis was:

*The sensitivity of piezoresistive wood bonds can be increased after manufacturing by thermal postcuring.*

Thermal postcuring was an assumed potential treatment for optimising the piezoresistive bond line analogous to other electrically conductive adhesives [171], where electrical conductivity and shear strength could be improved. Further, it was hypothesized in Paper I that by the variation of temperatures up to 95°C and postcuring times up to 48 hours, an improvement of mechanical properties was possible.

The micromechanical in situ testing of the bond line by nanoindentation revealed changes in mechanical properties (Paper I, Figs. 5–7). For pristine 1C-PUR and 1C-PUR filled with CNFs and CNTs, the stiffness (reduced modulus  $E_r$ ) and the hardness decreased for elongated postcuring, but not in a statistically significant manner (Paper I, Figs. 5–6). On the other hand, the creep factor of the bond line significantly increased at longer treatments of 48 hours (Paper I, Fig. 7). Thus, the bond line softens, which in turn is preferable for high piezoresistivity [131] as lower elastic moduli result in a higher strain at the same amount of stress [247] and higher strains result in a larger fractional change of the ECF network (see section 2.2.1). In contrast, 1C-PUR filled with CB showed no change in stiffness and hardness but a reduced creep factor (Paper I, Figs. 5–7).

To confirm hypothesis H2, the DC resistance and piezoresistive properties of the set of postcured samples were tested with the methods presented in Paper II and Paper III. The data showed that postcuring results in a significant improvement of the bond line properties by a decreased value and variation in DC resistance (Paper II, Fig. 10) and piezoresistive instability properties (Paper III, Fig. 12, resistance creep, variability, baseline instability). On the other hand, the sensitivity could not be influenced.

This means that the data either did not support the assumption that a decreasing stiffness of the adhesive bond line ( $E_r$ , shown in Paper I) results in an increased sensitivity of the piezoresistive adhesive bond line ( $S_{c,DC}$ , shown in Paper III) or that the effect is minor in relation to the variance of the data. Despite the potential lack of influence of the mechanical properties on the sensitivity, the data show a clear improvement in the piezoresistive stability (Paper III, Fig. 12). Therefore, the correlation of the significantly different creep factor ( $C_{IT}$ , measured by nanoindentation in Paper I) with the drift of electrical resistance under load ( $D_{c,DC}$ , presented in Paper III) was evaluated. Electrical drifts are partly attributed to the material creep in the polymer matrix [143]. Based on the visualised data in Fig. 13, no distinct correlation could be found due to the high variation of the values.

From the resulting properties of postcured piezoresistive bond lines, it can thus be concluded that a thermal treatment after curing can support a reduction in the variability (less production variation) and instability of the piezoresistive properties of the bond line from 1C-PUR, but no change in the piezoresistive sensitivity of the cured bondline between two wood adherends can be expected. Thus, hypothesis H2 must be rejected for postcuring as a method to increase the sensitivity of piezoresistive bond lines from 1C-PUR in wood. Based on the dataset and the method, no general conclusion can be drawn concerning the effect of thermal postcuring on the piezoresistive

properties of other nanocomposites, which – to the best knowledge of the author – were not investigated by others.

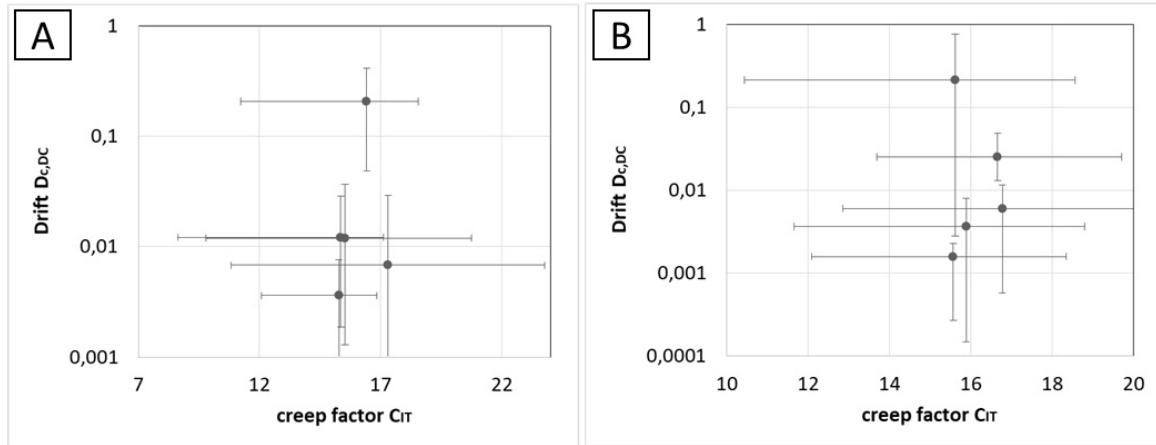


Fig. 13 Drift of electrical resistance under load  $D_{c,DC}$  over the mechanical creep factor  $C_{IT}$  for polyurethane, filled with 4 wt% carbon black (A) and 2 wt% carbon nanofibers with added 0.2 wt% carbon nanotubes (B)

#### 5.4 Improvements by impedance spectroscopy

Most of the test series under investigation in this doctorate included at least one sample that did not show piezoresistive behaviour of the DC resistance at all, as illustrated, for example, in Paper III, Fig. 4. Thus, no reliable manufacturing of piezoresistive wood bonds was possible, even if the piezoresistive properties of nanocomposites could be transferred to wood bonds. The reason for the lack of ability to measure the piezoresistive reaction was found in the high relative standard deviations of DC resistance – even after signal smoothing – which was one order of magnitude higher than the expectable sensitivity. As the mechanisms of piezoresistivity (see section 2.2.1) are potentially measurable in different frequency ranges (see section 3.2.5), impedance spectroscopy was investigated as an alternative measurement technique and compared with measurements based on DC resistance. H4 was defined as the working hypothesis:

*The signal quality of piezoresistive bond lines is frequency dependent and offers higher reliability than resistance measurements based on direct current.*

The investigations for hypothesis H4 are summarized in Paper IV. By comparing a set of specimens under shear load, it was found that the signal-to-noise ratio (SNR) [248] – a ratio of sensitivity to signal noise – could be optimised at certain frequencies (Paper IV, Fig. 7). At the optimal frequency in the experiment, the mean SNR at 447 kHz was calculated as being four times higher than with a DC resistance measurement (see Paper

IV, Table 1). Several samples showed piezoresistivity under alternating current, while the same samples only showed noise under direct current (19 out of 43). As a consequence, frequency domain measurements were shown to enhance the reliability and usability of piezoresistive wood bonds. In other words, all samples exhibit measurable piezoresistivity with impedance spectroscopic measurements, while no piezoresistivity was measured with DC resistance as an indicating value. Thus, hypothesis H4 could be accepted. Beyond the answer to H2, the separation of impedance  $Z$  into  $\text{Re}(Z)$  and  $\text{Im}(Z)$  revealed  $\text{Re}(Z)$  as the indicating value with higher piezoresistive amplitude, which confirmed that the piezoresistive reaction is grounded on the change in conductive paths rather than capacitive paths (effects I to III in section 2.2.1). This finding was in line with that of other researchers, as filler concentrations above the percolation threshold were used and thus the overall capacitive paths in the nanocomposite are lower [135].

A similar advantage of piezoresistive measurements with AC resistance over DC resistance was found by others [249,250], but different optimal frequencies were found for the same material composition (silicone rubber/CB). As different test setups were used, these results support the present analysis that the test setup (including cables, measuring device, contact electrodes, etc.) influences the optimal frequency as well as the specific optimal frequency of the measurement [227,228]. Thus, the optimal frequency of 447 kHz determined for piezoresistive measurements of wood bonds from 1C-PUR filled with 4 wt% CB is not a fundamental value but rather a strong indication that impedance measurements can offer more reliability compared to DC resistance as a leading measuring characteristic. Additionally, the presented method of comparative analysis by the SNR used offers a fast and reliable method to qualitatively compare the signal quality in different setups and measuring techniques with a large amount of data such as frequency domain measurements with lots of frequencies and, as far as known, this has not been used prior to this study.

## 5.5 Distinguishing stress by piezoresistive reactions

In previous studies, it was shown that the direction of resistance change depends on the strain in the measuring direction of a specimen in 3-point bending [32]. In the bending tension, the bond line gave an increasing resistance, while the bond line in the bending compression gave a decreasing resistance. Based on the current state of knowledge, the effect was attributed to the change in the bond line dimensions (thickness and elongation) [34,35]. Tests on lap-joint tensile shear specimens showed a piezoresistive reaction similar to the bond lines in bending tension (increasing resistance with increasing strain). In contrast to bending tension, the relative resistance change of the bond line in the lap shear sample was at least 2 decades higher in the elastic range (7.5 % compared to 0.07 %) [32]. Bearing engineered wood, especially GLT and CLT, in mind



for future applications these preliminary results needed to be transferred to engineered wood with larger dimensions to prove their reliability. This led to the fourth research question (RQ4), which asked whether different stresses in engineered wood are generally distinguishable by the piezoresistive reaction and what the nature of the piezoresistive reaction to shear stress is. Thus, H4 was specified as:

*The kind of stress in dry engineered wood (tension, compression, shear) can be distinguished by the direction (positive, negative) and extent (sensitivity) of the piezoresistive reaction in the piezoresistive bond line.*

In Paper V, several upscaled specimens with different joint geometries under tension, compression, and shear load were evaluated concerning their piezoresistive reaction. The results in Table 2 from Paper V clearly confirm hypothesis H5, as the varied stresses in the upscaled specimen result in differing sensitivities ( $S_{DC}$ ) and directions of the piezoresistive reaction (PR). Additionally, a model-based explanation for the differences in sensitivity extent and PR direction was found, which could also explain inverse piezoresistive reactions with increasing stress and within similar specimens (Paper V, Fig. 7). The proposed model is in agreement with recent experiments by Bregar et al. [251]. Using the example of a single-lap specimen bonded by a CNT-filled epoxy adhesive, he and his team demonstrated that stresses in the bond line can overlap similar to the used approach by the author (see Paper V, Fig. 9) and, depending on the dominating stress, the direction of resistance change can invert prior to failure (see Paper V, Fig. 11). Nonetheless, there are differences in the results of Bregar's team due to the materials used. First of all, the adherend is electrically conductive and used as a contact electrode to the bond line. Therefore, the change of resistance and resistivity is measured perpendicular to the bond line, making the change in contact resistance of adhesive and adherend an additional source for the measured piezoresistive reaction, especially as they used a two-probe method for DC resistance measurement [131]. Secondly, the strength of the aluminium adherend and epoxy adhesive is higher than the wood adherend and 1C-PUR adhesive. Thus, it is unlikely for wood adhesives to measure the failure in the bond line as opposed to in the penetration zone of the adhesive as shown in earlier studies [36]. Finally, the stress/strain distribution in Bregar's specimen is easier to analyze as aluminium exhibits neither anisotropy nor heterogeneity, which emphasizes the additional results from the proposed material model in Paper V (Fig. 7).

Further, with the material model presented in Paper V (Fig. 7) it was for the first time possible to show that the stress and strain-based resistance changes in the previously reported measurements on electrically conductive wood adhesives [32,34,35,252] is at least partly a change in the specific resistivity of the adhesive bond line and not only in resistance (see also the introduction to section 5).

## 6 CONCLUSION

This thesis focussed on the influence of manufacturing parameters and the properties of the involved materials (wood adherend, adhesive, ECF) on the mechanical, electrical, and piezoresistive properties of bond lines in engineered wood.

In the earlier sections of this thesis, piezoresistive measurements by DC resistance of electrically conductive wood bonds showed partly unexpected piezoresistive reactions or none at all. This made the manufacturing of piezoresistive bond lines unreliable. At present, it is possible to reliably transfer the piezoresistive properties of an electrically conductive adhesive on the microscale to engineered wood specimens on the macroscale. Some significant influences from the specific manufacturing process of electrically conductive adhesives and engineered wood were identified and material-based explanations were found to explain inverse and absent piezoresistivity. Additionally, some options such as thermal postcuring and frequency domain measurements were identified to optimise the use of piezoresistive bond lines in engineered wood.

It could successfully be shown that hypothesis H1 applies to the restricted case of a dry wood bond and that the dry bond strength (EN 302-1 (A1)) is not reduced by introducing piezoresistive properties into the cured adhesive.

Several variables from the material selection and process could be identified that can be used to decrease the electrical resistance and increase the piezoresistive properties of piezoresistive wood bonds. Therefore, hypothesis H2 could be accepted. In addition, it must also be stated that the selection of ECF type, concentration, and the dispersion technique have – according to the state of the art – a major influence on the process parameters. Compared to the theoretical background, a new finding is the influence of polymer formulation and the possibility of using foaming 1C-PUR as an adhesive matrix.

Hypothesis H3 had to be rejected as no increase in piezoresistive sensitivity could be found for postcured specimens under a transversal compressive load. Nonetheless, postcuring of piezoresistive wood bonds from 1C-PUR were not previously investigated and showed a reduction in piezoresistive instability characteristics in terms of value and variance.

For the first time in known literature, through the investigation of piezoresistive wood bonds with impedance spectroscopy, hypothesis H4 could be accepted. The data revealed an optimum frequency with at least four times higher SNR compared to the DC resistance measurements.

Hypothesis H5 could also be accepted, as different stresses in engineered wood could be distinguished by the direction and extent of the piezoresistive reaction. Further, a material based model was developed, which can explain qualitative differences in piezoresistive sensitivity due to superpositioning of micro strains in the adhesive nanocomposite. Thus, the piezoresistive sensitivity and direction of resistance change

will be influenced by the anisotropic properties of the adherend and the direction of measurement to the direction of the main microstrain. By considering these behaviours, shear stresses in bond lines are measurable. As far as known, these findings regarding the influence of anisotropic adherends are new for piezoresistive nanocomposites.

## 7 POTENTIAL FOR FUTURE RESEARCH AND DEVELOPMENT

The results in this thesis constitute the first step towards a more comprehensive objective, namely the addition of new functionalities to wood adhesives. In this context, the cured adhesive bond line is supposed to become multifunctional, combining the bond performance of the joint with electrical and piezoresistive properties. With multifunctional bond lines acting as measuring elements, engineered wood could potentially be produced with additional integrated features, thereby extending its applicability and the possibilities for use.

Despite the novel findings presented in this work, some questions could not be answered by means of the methods used and new questions also arose during the investigation. Furthermore, the general verification that piezoresistivity is possible in wood bonds opens new areas of research on the overall topic of multifunctional bond lines for engineered wood.

These potential areas are structured according to the following topics:

### Optimisation

The investigated material and manufacturing parameters mostly affected only the stability-related piezoresistive properties without changing the sensitivity. Only the curing temperature and lower concentrations of filler were able to increase the sensitivity at the cost of stability. Thus, a decrease of filler concentration without impairing the stability is of interest, especially as with lower filler concentration, fewer agglomerates are expected. The influence of agglomerates on mechanical properties are expected from theory but could not be proved in the thesis due to a lack of appropriate and reliable analysing techniques for the remaining agglomerates in highly filled black nanocomposites. However, under dry conditions, the TSS was not found to degrade the bond strength, while degradation under wet conditions or delamination, which are more difficult to surpass, was not tested. Thus, the objective of decreasing the necessary filler concentration to reach a percolation threshold still needs to be accomplished. From the literature, several promising methods were added to the general use of higher aspect fillers and other dispersion techniques. Example methods include the double percolation threshold by using polymer blends [66] or the use of segregated structures [66,105]. In addition, the short overview of preliminary tests on filler combinations in Paper I supports the method from literature (see section 2.1.2) whereby combinations of ECF types can decrease the percolation threshold of nanocomposites by maintaining their processability.

On the other hand, lower filler concentrations would be more greatly influenced by liquid processing with the possibility of reagglomeration or the formation of flocculated structures. Combined impedance spectroscopy with rheometric measurements to

analyse the restructuring of ECFs during liquid processing and curing could therefore be of interest in future applications.

Further, another aspect lies in the mechanical properties of the adhesive matrix that is used, as this influences the piezoresistive reaction [131]. Adhesives with higher stiffness after curing would offer a different behaviour until the point of wood failure than ductile adhesives such as 1C-PUR. Especially their long-term behaviour would be a critical parameter, as mentioned under section 2.1.4. Unfortunately, the ageing of cured wood adhesives is not well investigated. Some information regarding aged wood adhesives is available for caseins, UF, and PRF [114,253,254], but it does not support an understanding of the changes in microstructure or – in the case of an integrated electrically conductive network – the resistivity of the nanocomposite. In the literature, a change in impedance spectra with time after crosslinking was reported by Huang et al. [155], who also reported the influence of the dispersion method used on this change. A change of DC resistance after curing of the adhesive was also observed in the main investigations, which were reported as drift in Paper IV and Paper V.

#### Reliability/Long-term stability

Whether the drift depends on the ageing of the adhesive polymer or other parameters is a research question for which several explanations have been given in the literature and the author's own work. While drift was explained in Paper III using the literature supported material creep, in Paper IV the cause was already differentiated into drift by mechanical creep from strain hysteresis and electrically induced drift. Paper V introduced several new possible influences on the resistance drift but could not isolate the underlying causes. Thus, an understanding of the resistance drift in electrically conductive wood bonds is necessary for reliability and long-term stability. In addition to the published discussions, the following aspects need attention in this evaluation. Resistance creep can be caused by an incorrect supply voltage of the measuring setup [230], the exponential resistance drift from the capacitance in the measuring line [255], and the difference between insulating and dielectric materials. While polyurethane (PU) is treated as an insulating material for nanocomposites by other researchers [67], PU contains a large number of polar groups that can be oriented in electrical fields. Together with the flexibility of their polymer chains, high dielectric constants can be expected. This polar group mobility results in a frequency and temperature-dependent dielectric loss, making the dielectric loss prone to electrical-mechanical hysteresis that changes the electrical properties over time [256].

On the other hand, PU offers the possibility to engineer their polymer structure, as an increasing amount of hard segments in PU changes their dielectric properties [257].

Another topic for research and development (R&D) related to long term stability and reliability is the electrical contact of the instrument and adhesive bond line. The contact electrode is the most exposed part of the measuring line and can induce noise and

instability in the measurement. In this work, short-term stability of the contact was achieved under laboratory conditions, but for monitoring lasting several years, other solutions need to be developed. The contact between electrically conductive adhesives and electrodes and their instability are one of the main problems of electrically conductive adhesives, which was also defined by Petrie [86].

#### Development of feasible measuring techniques

In the results from Paper IV, impedance spectroscopy was proven to be an option to enhance the usability of the piezoresistive bond lines by frequency-dependent sensitivities. In addition, impedance spectroscopy offers more potential that has not yet been investigated. For example, it should be examined whether the necessary linearity of signals for sensors can be drawn from additional parameters such as the critical frequency shift [137]. Furthermore, the state of the art suggests that impedance spectroscopy provides the *‘possibility to separate effects having linearly independent dispersions and dominating in different frequency ranges’* [258]. It is further stated that *‘for sensors, decisive improvements of measurement accuracy can be reached and multifunctional sensors can be realized, which allow measurements of more than one measurement quantity at the same time and same state of a material or a device’* [258]. This makes further research on impedance spectroscopy for piezoresistive wood bonds interesting, as strain and wood moisture are interacting measuring variables.

#### Distinguishing between the measured variables

Even though the influence of moisture on the resulting signal was not investigated in this work, it remains one of the main research issues in the overall topic of multifunctional bond lines for engineered wood. Wood swells and shrinks orthotropically with increasing/decreasing WMC below the fibre saturation point. Additionally, the wood adherend changes its electrical properties with wood moisture, which at least influences the resistance of the electrical layered composite of two adherends and one electrically conductive bond line. Thus, the measured electrical resistance is not only influenced by the strain of the engineered wood but also by the strain from swelling/shrinkage and the resistivity of the wood adherend.

Additionally, the influence of combined stress and moisture uptake in the cured adhesive bond line [259], which can alter the conductivity [86] and the influence of moisture on the mechanical properties of IC-PUR, must be considered.

In contrast to this relatively large number of influences, the thesis only showed a small piezoresistive sensitivity. Although several approaches can help to distinguish the measurement of strain and moisture, these were not investigated in detail. Besides the differentiation by impedance spectroscopy mentioned, a spatially divided application of electrically adhesive areas can be used to measure WMC and strain at different locations [252]. In this case, the adhesive would only be used as a coupling medium to locally measure the WMC [32].

### Electrical properties of wood

As mentioned in section 2.4.2, neither the piezoelectric effect nor the influence of the passive electrical properties of wood was treated or considered in this thesis.

Nonetheless, there are interactions between the electric and piezoelectric properties of wood, and the piezoresistive effect of electrically conductive adhesives is realistic. For example, the piezoelectric properties of wood are a possible factor for noise and resistance drift, as potentials are created by strain in the adherend. Over and above these assumptions, a comprehensive study is needed to model and experimentally prove the electrical properties of the layered composite made up of wood and nanocomposite adhesives.

## REFERENCES

- [1] Rug W. 100 Jahre Hetzer-Patent. Bautechnik 2006;83(8):533–40.  
<https://doi.org/10.1002/bate.200610046>.
- [2] Brandt, Katarina. Active centenarian that changed the industry. Wood magazine 2019(3).
- [3] Teischinger A. Opportunities and limits of timber in construction: Möglichkeiten und Grenzen von Holz im Bauwesen. Österreichische Ingenieur- und Architekten-Zeitschrift 2017;162(1-12):1–6.
- [4] The Athena Institute. Minnesota Demolition Survey: Phase Two Report; 2004.
- [5] Roos A, Woxblom L, McCluskey D. The influence of architects and structural engineers on timber in construction – perceptions and roles. Silva Fenn. 2010;44(5). <https://doi.org/10.14214/sf.126>.
- [6] Winter S, Kreuzinger H. The Bad Reichenhall ice-arena collapse and the necessary consequences for wide span timber structures. In: 10th World Conference on Timber Engineering 2008. Red Hook, NY: Curran; 2009, 1978-1985.
- [7] Ramage MH, Burr ridge H, Busse-Wicher M, Fereday G, Reynolds T, Shah DU et al. The wood from the trees: The use of timber in construction. Renewable Sustainable Energy Rev 2017;68:333–59. <https://doi.org/10.1016/j.rser.2016.09.107>.
- [8] Schneider K-J, Albert A, Goris A, Akkermann J. Bautabellen für Ingenieure: Mit Berechnungshinweisen und Beispielen. 24th ed. Köln: Reguvis; 2020.
- [9] Dietsch P, Tannert T. Assessing the integrity of glued-laminated timber elements. Constr Build Mater 2015;101:1259–70.  
<https://doi.org/10.1016/j.conbuildmat.2015.06.064>.
- [10] Kasal B, Tannert T (eds.). In Situ Assessment of Structural Timber. Heidelberg: Springer; 2010.
- [11] Kurz JH. Monitoring of timber structures. J Civ Struct Health Monit 2015;5(2):97.  
<https://doi.org/10.1007/s13349-014-0075-6>.
- [12] DeStefano J, Anthony R, Nehil T, Lynch J. TFEC 3-2019: Guide to Structural Evaluation of Existing Timber Structures. East Greenwich, USA; 2019.
- [13] Tannert T, Müller A. Structural health monitoring of timber bridges. In: Malo KA, Kleppe O, Dyken T, editors. Proceedings: International Conference Timber Bridges (ICTB2010); 2010, p. 205–212.
- [14] Heiduschke A, Trümper W, Haller P, Cherif C. Monitoring of timber structures with carbon fibre sensors: Monitoring von Holzkonstruktionen mittels Carbonfaser-Sensoren. Bauingenieur 2008;83(11):468–72.
- [15] Norberg P. Monitoring wood moisture content using the WETCORR method: Part 1: Background and theoretical considerations. Holz Roh Werkst 1999;57:448–53.
- [16] Arndt RW, Koch J, Simon A, Jahreis MG. ProTimB - Monitoring of structurally protected timber bridges. In: ASNT - The American Society for Nondestructive



- Testing, editor. NDE/NDT Structural Materials Technology for Highways and Bridges (SMT); 2018.
- [17] Palma P, Steiger R. Structural health monitoring of timber structures – Review of available methods and case studies. *Constr Build Mater* 2020;248:118528. <https://doi.org/10.1016/j.conbuildmat.2020.118528>.
  - [18] Marzi T. Nanostructured materials for protection and reinforcement of timber structures: A review and future challenges. *Constr Build Mater* 2015;97:119–30. <https://doi.org/10.1016/j.conbuildmat.2015.07.016>.
  - [19] Wipf T, Phares BM, Ritter M. Literature Review and Assessment of Nanotechnology for Sensing of Timber Transportation Structures; 2012.
  - [20] Brischke C, Rapp AO, Bayerbach R. Measurement system for long-term recording of wood moisture content with internal conductively glued electrodes. *Build Environ* 2007;181–99. <https://doi.org/10.1016/j.buildenv.2007.10.002>.
  - [21] Alamusu, Hu N, Fukunaga H, Atobe S, Liu Y, Li J. Piezoresistive strain sensors made from carbon nanotubes based polymer nanocomposites. *Sensors (Basel)* 2011;11(11):10691–723. <https://doi.org/10.3390/s111110691>.
  - [22] Wichmann, Malte H. G., Buschhorn ST, Böger L, Adelung R, Schulte K. Direction sensitive bending sensors based on multi-wall carbon nanotube/epoxy nanocomposites. *Nanotechnology* 2008;19(47):475503. <https://doi.org/10.1088/0957-4484/19/47/475503>.
  - [23] Loyola BR, Zhao Y, Loh KJ, La Saponara V. The electrical response of carbon nanotube-based thin film sensors subjected to mechanical and environmental effects. *Smart Mater. Struct.* 2013;22(2):25010. <https://doi.org/10.1088/0964-1726/22/2/025010>.
  - [24] Sanli A, Benchirouf A, Müller C, Kanoun O. Piezoresistive performance characterization of strain sensitive multi-walled carbon nanotube-epoxy nanocomposites. *Sens Actuators, A* 2017;254(254):61–8. <https://doi.org/10.1016/j.sna.2016.12.011>.
  - [25] Bautista-Quijano JR, Avilés F, Cauich-Rodriguez JV. Sensing of large strain using multiwall carbon nanotube/segmented polyurethane composites. *J. Appl. Polym. Sci.* 2013;130(1):375–82. <https://doi.org/10.1002/app.39177>.
  - [26] Zhang R, Baxendale M, Peijs T. Universal resistivity/strain dependence of carbon nanotube/polymer composites. *Phys. Rev. B* 2007;76(19):195433. <https://doi.org/10.1103/PhysRevB.76.195433>.
  - [27] Dharap P, Li Z, Nagarajaiah S, Barrera EV. Nanotube film based on single-wall carbon nanotubes for strain sensing. *Nanotechnology* 2004;15(3):379–82. <https://doi.org/10.1088/0957-4484/15/3/026>.
  - [28] Zhang W, Suhr J, Koratkar N. Carbon nanotube/polycarbonate composites as multifunctional strain sensors. *J Nanosci Nanotechnol* 2006;6(4):960–4. <https://doi.org/10.1166/jnn.2006.171>.
  - [29] Kang I, Schulz MJ, Kim JH, Shanov V, Shi D. A carbon nanotube strain sensor for structural health monitoring. *Smart Mater. Struct.* 2006;15(3):737–48. <https://doi.org/10.1088/0964-1726/15/3/009>.

- [30] Hu N, Karube Y, Arai M, Watanabe T, Yan C, Li Y et al. Investigation on sensitivity of a polymer/carbon nanotube composite strain sensor. *Carbon* 2010;48(3):680–7. <https://doi.org/10.1016/j.carbon.2009.10.012>.
- [31] Miao Y, Yang Q, Chen L, Sammynaiken R, Zhang WJ. Modelling of piezoresistive response of carbon nanotube network based films under in-plane straining by percolation theory. *Appl. Phys. Lett.* 2012;101. <https://doi.org/10.1063/1.4742893>.
- [32] Winkler C, Schwarz U. Multifunctional Wood-Adhesives for Structural Health Monitoring Purposes. In: Aicher S, Reinhardt H-W, Garrecht H, editors. *Materials and Joints in Timber Structures: Recent developments of technology*. Dordrecht: Springer; 2014, p. 381–394.
- [33] Winkler C, Schwarz U. Effect of electrical conductive loading on the bonding strength of glue laminated timber. In: *EURADH - 11th European Adhesion Conference*; 2016, p. 90–93.
- [34] Winkler C, Schwarz U. Wood Adhesives for Non-Destructive Structural Monitoring. In: *DGZfP, editor. 19th World Conference on Non-Destructive Testing 2016*; 2016, p. 1–8.
- [35] Winkler C, Schwarz U. Characterization of adhesively bonded wood structures by electrical modification of the bonding system. In: Eberhardsteiner J, Winter W, Fadaei A, editors. *World Conference on Timber Engineering (WCTE 2016)*: Vienna, Austria, 22-25 August 2016. Vienna: Vienna University of Technology; 2016.
- [36] Myslicki S, Winkler C, Gelinski N, Schwarz U, Walther F. Fatigue assessment of adhesive wood joints through physical measuring technologies. In: *Fatigue 2017: 7th International Conference on Durability and Fatigue*, p. 446–455.
- [37] Das TK, Prusty S. Review on Conducting Polymers and Their Applications. *Polymer-Plastics Technology and Engineering* 2012;51(14):1487–500. <https://doi.org/10.1080/03602559.2012.710697>.
- [38] Kovacs JZ, Velagala BS, Schulte K, Bauhofer W. Two percolation thresholds in carbon nanotube epoxy composites. *Compos Sci Technol* 2007;67(5):922–8. <https://doi.org/10.1016/j.compscitech.2006.02.037>.
- [39] Gilg RG. *Ruß für leitfähige Kunststoffe*. In: Mair HJ, Roth S, editors. *Elektrisch leitende Kunststoffe*, 2nd ed. München: Hanser; 1989.
- [40] Bauhofer W, Kovacs JZ. A review and analysis of electrical percolation in carbon nanotube polymer composites. *Compos Sci Technol* 2009(69):1486–98. <https://doi.org/10.1016/j.compscitech.2008.06.018>.
- [41] Sahimi M. *Applications of percolation theory*. London, Bristol, Pa: Taylor & Francis; 1994.
- [42] Stauffer D, Aharony A. *Introduction to Percolation Theory*. 2nd ed. Boca Raton: Taylor & Francis Group; 2014.
- [43] Sumfleth J, Buschhorn ST, Schulte K. Comparison of rheological and electrical percolation phenomena in carbon black and carbon nanotube filled epoxy polymers. *J Mater Sci* 2011;46(3):659–69. <https://doi.org/10.1007/s10853-010-4788-6>.

- [44] Kota AK, Cipriano BH, Duesterberg MK, Gershon AL, Powell D, Raghavan SR et al. Electrical and Rheological Percolation in Polystyrene/MWCNT Nanocomposites. *Macromolecules* 2007;40:7400–6. <https://doi.org/10.1021/ma0711792>.
- [45] Gelves GA, Lin B, Sundararaj U, Haber JA. Electrical and rheological percolation of polymer nanocomposites prepared with functionalized copper nanowires. *Nanotechnology* 2008;19:215712. <https://doi.org/10.1088/0957-4484/19/21/215712>.
- [46] Mutiso RM, Winey KI. Electrical properties of polymer nanocomposites containing rod-like nanofillers. *Prog Polym Sci* 2015;40:63–84. <https://doi.org/10.1016/j.progpolymsci.2014.06.002>.
- [47] Hu N, Masuda Z, Yan C, Yamamoto G, Fukunaga H, Hashida T. The electrical properties of polymer nanocomposites with carbon nanotube fillers. *Nanotechnology* 2008;19:215701. <https://doi.org/10.1088/0957-4484/19/21/215701>.
- [48] Foygel M, Morris RD, Anez D, French S, Sobolev VL. Theoretical and computational studies of carbon nanotube composites and suspensions: Electrical and thermal conductivity. *Phys. Rev. B* 2005;71(10). <https://doi.org/10.1103/PhysRevB.71.104201>.
- [49] Coleman JN, Curran S, Dalton AB, Davey AP, McCarthy B, Blau W et al. Percolation-dominated conductivity in a conjugated-polymer-carbon-nanotube composite. *Phys. Rev. B* 1998;58(12):R7492 - R7495.
- [50] Balberg I. A comprehensive picture of the electrical phenomena in carbon black-polymer composites. *Carbon* 2002;40:139–43.
- [51] Rubin Z, Sunshine SA, Heaney MB, Bloom I, Balberg I. Critical behavior of the electrical transport properties in a tunneling-percolation system. *Phys. Rev. B* 1999;59(19):12196–9. <https://doi.org/10.1103/PhysRevB.59.12196>.
- [52] Bokobza L. Rubber Nanocomposites: New Developments, New Opportunities: 3. In: Karger-Kocsis J, Fakirov S, editors. *Nano- and micromechanics of polymer blends and composites*. München: Hanser; 2009.
- [53] Thostenson ET, Chou T-W. Processing-structure-multi-functional property relationship in carbon nanotube/epoxy composites. *Carbon* 2006;44:3022–9. <https://doi.org/10.1016/j.carbon.2006.05.014>.
- [54] Schulte K, Gojny FH, Wichmann, Malte H. G., Sumfleth J, Fiedler B. Polymer Nanocomposites: chances, risks and potential to improve the mechanical and physical properties. *Materialwissenschaft und Werkstofftechnik* 2006;37(9):698–703. <https://doi.org/10.1002/mawe.200600054>.
- [55] Wehnert F, Heinrich J, Jansen I. Multifunctional adhesives by integration of Carbon Nanotubes. In: EURADH - 9th European Adhesion Conference; 2012, p. 1–8.
- [56] Prasse T. Elektrisch leitfähige Funktions- und Strukturverbundstoffe auf der Basis von Kohlenstoff-Nanopartikeln und -fasern [Dissertation]: Technische Universität Hamburg-Harburg; 2001.
- [57] Yuen S-M, Ma C-CM, Wu H-H, Kuan H-C, Chen W-J, Liao S-H et al. Preparation and Thermal, Electrical, and Morphological Properties of Multiwalled Carbon

- Nanotube and Epoxy Composites. *J. Appl. Polym. Sci.* 2007;103:1272–8. <https://doi.org/10.1002/app.25140>.
- [58] Choi H-J, Kim MS, Ahn D, Yeo SY, Lee S. Electrical percolation threshold of carbon black in a polymer matrix and its application to antistatic fibre. *Sci Rep*;9(1):6338. <https://doi.org/10.1038/s41598-019-42495-1>.
  - [59] Khare R, Bose S. Carbon Nanotube Based Composites- A Review. *JMMCE* 2005;04(01):31–46. <https://doi.org/10.4236/jmmce.2005.41004>.
  - [60] Treacy MMJ, Ebbesen TW, Gibson JM. Exceptionally high Young's modulus observed for individual carbon nanotubes. *Nature* 1996;381(6584):678–80. <https://doi.org/10.1038/381678a0>.
  - [61] Khodabakhshi S, Fulvio PF, Andreoli E. Carbon black reborn: Structure and chemistry for renewable energy harnessing. *Carbon* 2020;162:604–49. <https://doi.org/10.1016/j.carbon.2020.02.058>.
  - [62] European commission. Commission recommendation on the definition of nanomaterial(2011/696/EU): Official Journal of the European Union; 2011.
  - [63] Gulrez SK, Ali Mohsin ME, Shaikh H, Anis A, Pulose AM, Yadav MK et al. A review on electrically conductive polypropylene and polyethylene. *Polym Compos* 2014;35(5):900–14. <https://doi.org/10.1002/pc.22734>.
  - [64] Badrul F, Halim KAA, Salleh MAAM, Omar MF, Osman AF, Zakaria MS. Current advancement in electrically conductive polymer composites for electronic interconnect applications: A short review. *IOP Conf. Ser.: Mater. Sci. Eng.* 2019;701:12039. <https://doi.org/10.1088/1757-899X/701/1/012039>.
  - [65] Bhattacharya SK, Chaklader ACD. Review on Metal-Filled Plastics. Part1. Electrical Conductivity. *Polymer-Plastics Technology and Engineering* 1982;19(1):21–51. <https://doi.org/10.1080/03602558208067726>.
  - [66] Li Y, Huang X, Zeng L, Li R, Tian H, Fu X et al. A review of the electrical and mechanical properties of carbon nanofiller-reinforced polymer composites. *J Mater Sci* 2019;54(2):1036–76. <https://doi.org/10.1007/s10853-018-3006-9>.
  - [67] Gurunathan T, Rao CRK, Narayan R, Raju KVS. Polyurethane conductive blends and composites: Synthesis and applications perspective. *J Mater Sci* 2013;48(1):67–80. <https://doi.org/10.1007/s10853-012-6658-x>.
  - [68] Battermann A. Conductive bonding - Joining technology that's fit for the future. *Adhes Adhes Sealants* 2012;3:40–3.
  - [69] Wu H, Wu X, Ge M, Zhang G, Wang Y, Jiang J. Effect analysis of filler sizes on percolation threshold of isotropical conductive adhesives. *CNT-NET 07 Special Issue with regular papers* 2007;67(6):1116–20. <https://doi.org/10.1016/j.compscitech.2006.05.017>.
  - [70] Kim C-H, Choi J-H, Kweon J-H. Defect detection in adhesive joints using the impedance method. *Compos Struct* 2015;120:183–8. <https://doi.org/10.1016/j.compstruct.2014.09.045>.
  - [71] Hwang S-H, Bang DS, Yoon KH, Park Y-B. *Smart Materials and Structures Based on Carbon Nanotube Composites*. London: INTECH Open Access Publisher; 2011.

- [72] Donnet JB, Bansal RC, Wang MJ. Carbon Black. Science and Technology. 2nd ed. Dekker; 1993.
- [73] van Bellinghen C, Probst N, Grivei E. Meeting application requirements with conductive carbon black. *J Vinyl Add Tech* 2006;12(1):14–8. <https://doi.org/10.1002/vnl.20061>.
- [74] Marinho B, Ghislandi M, Tkalya E, Koning CE, With G de. Electrical conductivity of compacts of graphene, multi-wall carbon nanotubes, carbon black, and graphite powder. *Powder Technol* 2012;221:351–8. <https://doi.org/10.1016/j.powtec.2012.01.024>.
- [75] Klüppel M. A fractal approach to structure analysis and micro-mechanical modeling of elastomer materials. Hannover Gottfried Wilhelm Leibniz Universität Hannover; 2007.
- [76] Liu D, Ji L, Ding Y, Weng X, Yang F, Zhang X. Mesoporous carbon black as a metal-free electrocatalyst for highly effective determination of chromium(VI). *J Electroanal Chem* 2017;803:58–64. <https://doi.org/10.1016/j.jelechem.2017.09.017>.
- [77] Krupa I, Prokes J, Krivka I, Spitalsky Z. Electrically Conductive Polymeric Composites and Nanocomposites. In: Boudenne A, Ibos L, Candau Y, Thomas S, editors. *Handbook of Multiphase Polymer Systems*, 1st ed. s.l.: Wiley; 2011, p. 425–478.
- [78] Xanthos M (ed.). *Functional fillers for plastics*. 2nd ed. Weinheim: Wiley-VCH; 2010.
- [79] Nichols G, Byard S, Bloxham MJ, Botterill J, Dawson NJ, Dennis A et al. A review of the terms agglomerate and aggregate with a recommendation for nomenclature used in powder and particle characterization. *J Pharm Sci* 2002;91(10):2103–9. <https://doi.org/10.1002/jps.10191>.
- [80] Walter D. Primary Particles - Agglomerates - Aggregates. In: Deutsche Forschungsgemeinschaft, editor. *Nanomaterials*. Weinheim, Germany: Wiley-VCH Verlag GmbH & Co. KGaA; 2013, p. 9–24.
- [81] Hopmann C, Fragner J, Haase S. Development of electrically conductive plastic compounds based on filler combinations. *Journal of Plastics Technology* 2014;2(10):50–67.
- [82] Qiao W, Bao H, Li X, Jin S, Gu Z. Research on electrical conductive adhesives filled with mixed filler. *Int J Adhes Adhes* 2014;48:159–63. <https://doi.org/10.1016/j.ijadhadh.2013.07.001>.
- [83] Lopes PE, Moura D, Hilliou L, Krause B, Pötschke P, Figueiredo H et al. Mixed Carbon Nanomaterial/Epoxy Resin for Electrically Conductive Adhesives. *J. Compos. Sci.* 2020;4(3):105. <https://doi.org/10.3390/jcs4030105>.
- [84] Ma P-C, Liu M-Y, Zhang H, Wang S-Q, Wang R, Wang K et al. Enhanced electrical conductivity of nanocomposites containing hybrid fillers of carbon nanotubes and carbon black. *ACS Appl Mater Interfaces* 2009;1(5):1090–6. <https://doi.org/10.1021/am9000503>.
- [85] Sun Y, Bao H-D, Guo Z-X, Yu J. Modeling of the Electrical Percolation of Mixed Carbon Fillers in Polymer-Based Composites. *Macromolecules* 2009;42(1):459–63. <https://doi.org/10.1021/ma8023188>.

- [86] Petrie EM. Electrically and Thermally Conductive Adhesives Formulation Strategies: <https://adhesives.specialchem.com>, participated: 18.05.2018.
- [87] Shenoy AV. Rheology of Filled Polymer Systems. Dordrecht: Kluwer Academic Publishers; Springer Netherlands; 1999.
- [88] Xanthos M. Modification of Polymer Properties with Functional Fillers. In: Xanthos M, editor. Functional fillers for plastics, 2nd ed. Weinheim: Wiley-VCH; 2010, p. 19–42.
- [89] Gojny FH, Nastalczyk J, Roslaniec Z, Schulte K. Surface modified multi-walled carbon nanotubes in CNT/epoxy-composites. Chem Phys Lett 2003;370(5-6):820–4. [https://doi.org/10.1016/S0009-2614\(03\)00187-8](https://doi.org/10.1016/S0009-2614(03)00187-8).
- [90] Mair HJ, Roth S (eds.). Elektrisch leitende Kunststoffe. 2nd ed. München: Hanser; 1989.
- [91] Hartwig A, Pütz D, Sebald M. Nanokomposite – Potenziale für die Klebtechnik. Adhäsion - Kleben & Dichten 2003;47(1-2):16–20. <https://doi.org/10.1007/BF03243980>.
- [92] Novák I, Krupa I, Chodák I. Relation between electrical and mechanical properties in polyurethane/carbon black adhesives. J Mater Sci Lett 2002;21(13):1039–41. <https://doi.org/10.1023/A:1016073010528>.
- [93] Meincke O, Kaempfer D, Weickmann H, Friedrich C, Vathauer M, Warth H. Mechanical properties and electrical conductivity of carbon-nanotube filled polyamide-6 and its blends with acrylonitrile/butadiene/styrene. Polymer 2004;45(3):739–48. <https://doi.org/10.1016/j.polymer.2003.12.013>.
- [94] Wehnert F, Langer M, Kaspar J, Jansen I. Design of multifunctional adhesives by the use of carbon nanoparticles. J Adhes Sci Technol 2014;29(17):1849–59. <https://doi.org/10.1080/01694243.2015.1014536>.
- [95] Dal Lago E, Cagnin E, Boaretti C, Roso M, Lorenzetti A, Modesti M. Influence of Different Carbon-Based Fillers on Electrical and Mechanical Properties of a PC/ABS Blend. Polymers 2019;12(1). <https://doi.org/10.3390/polym12010029>.
- [96] Gindl-Altmutter W, Fürst C, Mahendran Ar, Obersriebnig M, Emsenhuber G, Kluge M et al. Electrically conductive kraft lignin-based carbon filler for polymers. Carbon 2015;89:161–8. <https://doi.org/10.1016/j.carbon.2015.03.042>.
- [97] Tjong SC. Deformation Mechanisms of Functionalized Carbon Nanotube Reinforced Polymer Nanocomposites. In: Karger-Kocsis J, Fakirov S, editors. Nano- and micromechanics of polymer blends and composites. München: Hanser; 2009, p. 341–375.
- [98] Han S, Meng Q, Araby S, Liu T, Demiral M. Mechanical and electrical properties of graphene and carbon nanotube reinforced epoxy adhesives: Experimental and numerical analysis. Composites, Part A 2019;120:116–26. <https://doi.org/10.1016/j.compositesa.2019.02.027>.
- [99] Atif R, Inam F. Reasons and remedies for the agglomeration of multilayered graphene and carbon nanotubes in polymers. Beilstein J. Nanotechnol. 2016;7:1174–96. <https://doi.org/10.3762/bjnano.7.109>.

- [100] Robertson CG, Hardman NJ. Nature of Carbon Black Reinforcement of Rubber: Perspective on the Original Polymer Nanocomposite. *Polymers* 2021;13(4):538. <https://doi.org/10.3390/polym13040538>.
- [101] Brüninghoff H. Reinforcement / rehabilitation of glulam structures: Ertüchtigung von BS-Holz-Tragwerken. In: 13. Internationales Holzbau-Forum 2007, 5.-7. December 2007, p. 1–19.
- [102] Fischer A, Risi W, Richter K. Zustandsbeurteilung von Klebfugen wetterbeanspruchter Holzbrücken. Sonderdruck aus *bmH* 2014:1–8.
- [103] Estes RH. The Effect of Porosity on Mechanical, Electrical and Thermal Characteristics of Conductive Die-Attach Adhesives. *Solid State Technology* 1984;37:191–7.
- [104] Brunner H. Leitungsmechanismus und Funktionsverhalten elektrisch leitender Klebungen am Beispiel eines Leistungstransistors [Dissertation]. Düsseldorf: Technische Universität München; 1987.
- [105] Pang H, Xu L, Yan D-X, Li Z-M. Conductive polymer composites with segregated structures. *Prog Polym Sci* 2014;39(11):1908–33. <https://doi.org/10.1016/j.progpolymsci.2014.07.007>.
- [106] Stapf G, Aicher S, Zisi N. Curing Behaviour of Structural Wood Adhesives - Parallel Plate Rheometer Results. In: Forest Products Society, editor. The International Conference on Wood Adhesives; 2013.
- [107] Muszynski L, Hansen E, Fernando S, Schwarzmann G, Rainer J. Insights into the Global Cross-Laminated Timber Industry. *BioProducts Business* 2017;2(8):77–92.
- [108] Grøstad K, Bredeisen R. EPI for Glued Laminated Timber. In: Aicher S, Reinhardt H-W, Garrecht H, editors. *Materials and Joints in Timber Structures: Recent developments of technology*. Dordrecht: Springer; 2014, p. 355–364.
- [109] Müller U, Veigel S, Follrich J, Gindl W. Performance of one component polyurethane in comparison to other wood adhesives. In: ICWA 2009 - International Conference on Wood Adhesives.
- [110] Pizzi A. Melamine-Formaldehyde Adhesives. In: Pizzi A, editor. *Handbook of adhesive technology*, 2nd ed. New York, NY: Dekker; 2003.
- [111] Pizzi A, Ibeh CC. Phenol-Formaldehydes. In: Dodiuk H, editor. *Handbook of thermoset plastics*, 3rd ed. Amsterdam: Elsevier; 2014, p. 13–44.
- [112] Broughton J, Hutchinson A. Adhesive systems for structural connections in timber. *Int J Adhes Adhes* 2001;21(3):177–86. [https://doi.org/10.1016/S0143-7496\(00\)00049-X](https://doi.org/10.1016/S0143-7496(00)00049-X).
- [113] Petrie EM. *Epoxy adhesive formulations: Epoxy properties and characteristics ; techniques for improving epoxy strength, flexibility, and durability ; testing and quality control guidelines*. New York, NY: McGraw-Hill; 2006.
- [114] Raknes E. Durability of structural wood adhesives after 30 years ageing. *Holz Roh Werkst* 1997;55(2-4):83–90. <https://doi.org/10.1007/BF02990523>.
- [115] Hass P, Wittel FK, Mendoza M, Herrmann HJ, Niemz P. Adhesive penetration in beech wood: Part I: Experiments. *Wood Sci Technol* 2012;46(1-3):243–56. <https://doi.org/10.1007/s00226-011-0410-6>.

- [116] Bitomsky P, Krieger A, Nies C, Zimmer B, Possart W, Hartwig A. Polyurethane adhesives: influence of curing on dynamics and property changes with time. In: EURADH - 11th European Adhesion Conference; 2016.
- [117] Chung DDL. Functional Materials: Electrical, dielectric, electromagnetic, optical and magnetic applications. Singapore: World Scientific; 2010.
- [118] Lim AS, Melrose ZR, Thostenson ET, Chou T-W. Damage sensing of adhesively-bonded hybrid composite/steel joints using carbon nanotubes. CNT-NET 07 Special Issue with regular papers 2011;71(9):1183–9. <https://doi.org/10.1016/j.compscitech.2010.10.009>.
- [119] Mactabi R, Rosca ID, Hoa SV. Monitoring the integrity of adhesive joints during fatigue loading using carbon nanotubes. CNT-NET 07 Special Issue with regular papers 2013;78:1–9. <https://doi.org/10.1016/j.compscitech.2013.01.020>.
- [120] Kang M-H, Choi J-H, Kweon J-H. Fatigue life evaluation and crack detection of the adhesive joint with carbon nanotubes. Compos Struct 2014;108:417–22. <https://doi.org/10.1016/j.compstruct.2013.09.046>.
- [121] Boutar Y, Naïmi S, Mezlini S, da Silva LF, Ben Sik Ali M. Characterization of aluminium one-component polyurethane adhesive joints as a function of bond thickness for the automotive industry: Fracture analysis and behavior. Eng Fract Mech 2017;177:45–60. <https://doi.org/10.1016/j.engfracmech.2017.03.044>.
- [122] Khoramishad H, Zarifpour D. Fracture response of adhesive joints reinforced with aligned multi-walled carbon nanotubes using an external electric field. Theor Appl Fract Mech 2018;98:220–9. <https://doi.org/10.1016/j.tafmec.2018.10.007>.
- [123] Kang I, Heung Y, Kim JH, Lee JW, Gollapudi R, Subramaniam S et al. Introduction to carbon nanotube and nanofiber smart materials. Composites: Part B 2006;37:382–94. <https://doi.org/10.1016/j.compositesb.2006.02.011>.
- [124] Kanoun O, Müller C, Benchirouf A, Sanli A, Dinh TN, Al-Hamry A et al. Potential of Flexible Carbon Nanotube Films for High Performance Strain and Pressure Sensors. Sensors (Basel) 2014;14(6):10042–71. <https://doi.org/10.3390/s140610042>.
- [125] Pham GT, Park Y-B, Liang Z, Zhang C, Wang B. Processing and modeling of conductive thermoplastic/carbon nanotube films for strain sensing. Composites, Part B 2008;39(1):209–16. <https://doi.org/10.1016/j.compositesb.2007.02.024>.
- [126] Hu N, Karube Y, Yan C, Masuda Z, Fukunaga H. Tunneling effect in a polymer/carbon nanotube nanocomposite strain sensor. Acta Mater 2008;56(13):2929–36. <https://doi.org/10.1016/j.actamat.2008.02.030>.
- [127] Park M, Kim H, Youngblood JP. Strain-dependent electrical resistance of multi-walled carbon nanotube/polymer composite films. Nanotechnology 2008;19(5):55705. <https://doi.org/10.1088/0957-4484/19/05/055705>.
- [128] Wichmann, Malte H. G., Buschhorn ST, Gehrman J, Schulte K. Piezoresistive response of epoxy composites with carbon nanoparticles under tensile load. Phys. Rev. B 2009;80(24). <https://doi.org/10.1103/PhysRevB.80.245437>.



- [129] Xia X, Wang Y, Zhong Z, Weng GJ. A frequency-dependent theory of electrical conductivity and dielectric permittivity for graphene-polymer nanocomposites. *Carbon* 2017;111:221–30. <https://doi.org/10.1016/j.carbon.2016.09.078>.
- [130] Elimat ZM, Hamideen MS, Schulte K, Wittich H, La Vega A de, Wichmann, Malte H. G. et al. Dielectric properties of epoxy/short carbon fiber composites. *J Mater Sci* 2010;45(19):5196–203. <https://doi.org/10.1007/s10853-010-4557-6>.
- [131] Chung DDL. A critical review of piezoresistivity and its application in electrical-resistance-based strain sensing. *J Mater Sci* 2020;55(32):15367–96. <https://doi.org/10.1007/S10853-020-05099-Z>.
- [132] Ferreira A, Martínez MT, Ansón-Casaos A, Gómez-Pineda LE, Vaz F, Lanceros-Mendez S. Relationship between electromechanical response and percolation threshold in carbon nanotube/poly(vinylidene fluoride) composites. *Carbon* 2013;61:568–76. <https://doi.org/10.1016/j.carbon.2013.05.038>.
- [133] Luheng W, Tianhuai D, Peng w. Influence of carbon black concentration on piezoresistivity for carbon-black-filled silicone rubber composite. *Carbon* 2009;47(14):3151–7. <https://doi.org/10.1016/j.carbon.2009.06.050>.
- [134] Vertuccio L, Vittoria V, Guadagno L, Santis F de. Strain and damage monitoring in carbon-nanotube-based composite under cyclic strain. *Composites, Part A* 2015;71:9–16. <https://doi.org/10.1016/j.compositesa.2015.01.001>.
- [135] Sanli A, Müller C, Kanoun O, Elibol C, Wagner MF-X. Piezoresistive characterization of multi-walled carbon nanotube-epoxy based flexible strain sensitive films by impedance spectroscopy. *CNT-NET 07 Special Issue with regular papers* 2016;122:18–26. <https://doi.org/10.1016/j.compscitech.2015.11.012>.
- [136] Flandin L, Hiltner A, Baer E. Interrelationships between electrical and mechanical properties of a carbon black-filled ethylene–octene elastomer. *Polymer* 2001;42(2):827–38. [https://doi.org/10.1016/S0032-3861\(00\)00324-4](https://doi.org/10.1016/S0032-3861(00)00324-4).
- [137] Sanli A, Kanoun O. Electrical impedance analysis of carbon nanotube/epoxy nanocomposite-based piezoresistive strain sensors under uniaxial cyclic static tensile loading. *J. Compos. Mater.* 2020;54(6):845–55. <https://doi.org/10.1177/0021998319870592>.
- [138] Zhang R, Deng H, Valenca R, Jin J, Fu Q, Bilotti E et al. Strain sensing behaviour of elastomeric composite films containing carbon nanotubes under cyclic loading. *CNT-NET 07 Special Issue with regular papers* 2013;74:1–5. <https://doi.org/10.1016/j.compscitech.2012.09.016>.
- [139] Zhao J, Dai K, Liu C, Zheng G, Wang B, Liu C et al. A comparison between strain sensing behaviors of carbon black/polypropylene and carbon nanotubes/polypropylene electrically conductive composites. *Composites, Part A* 2013;48:129–36. <https://doi.org/10.1016/j.compositesa.2013.01.004>.
- [140] Shui X, Chung DDL. A piezoresistive carbon filament polymer-matrix composite strain sensor. *Smart Mater. Struct.* 1996;5(2):243–6. <https://doi.org/10.1088/0964-1726/5/2/014>.
- [141] Ku-Herrera JJ, Avilés F. Cyclic tension and compression piezoresistivity of carbon nanotube/vinyl ester composites in the elastic and plastic regimes. *Carbon* 2012;50(7):2592–8. <https://doi.org/10.1016/j.carbon.2012.02.018>.

- [142] Ke K, Pötschke P, Wiegand N, Krause B, Voit B. Tuning the Network Structure in Poly(vinylidene fluoride)/Carbon Nanotube Nanocomposites Using Carbon Black: Toward Improvements of Conductivity and Piezoresistive Sensitivity. *ACS Appl Mater Interfaces* 2016;8(22):14190–9. <https://doi.org/10.1021/acsami.6b03451>.
- [143] Wang P, Ding T. Creep of electrical resistance under uniaxial pressures for carbon black–silicone rubber composite. *J Mater Sci* 2010;45(13):3595–601. <https://doi.org/10.1007/s10853-010-4405-8>.
- [144] Bilotti E, Zhang R, Deng H, Baxendale M, Peijs T. Fabrication and property prediction of conductive and strain sensing TPU/CNT nanocomposite fibres. *J. Mater. Chem.* 2010;20(42):9449. <https://doi.org/10.1039/c0jm01827a>.
- [145] McGrath MJ, Scanail CN. *Sensor Technologies*. Berkeley, CA: Apress; 2013.
- [146] Modern Dispersions. Insights on dispersion. [October 12, 2021]; Available from: <http://www.moderndispersions.com/dispersion.html>.
- [147] Gojny FH, Wichmann, Malte H. G., Köpke U, Fiedler B, Schulte K. Carbon nanotube-reinforced epoxy-composites: enhanced stiffness and fracture toughness at low nanotube content. *Compos Sci Technol* 2004;64:2363–71. <https://doi.org/10.1016/j.compscitech.2004.04.002>.
- [148] Pohl M, Hogeekamp S, Hoffmann NQ, Schuchmann HP. Dispergieren und Desagglomerieren von Nanopartikeln mit Ultraschall. *Chem Ing Tech* 2004;76(4):392–6. <https://doi.org/10.1002/cite.200403371>.
- [149] Moller, Björn, P. Herstellung, Charakterisierung und Weiterverarbeitung von Carbon Nanotube Dispersionen [Dissertation]. Stuttgart; 2013.
- [150] Hilding J, Grulke EA, George Zhang Z, Lockwood F. Dispersion of Carbon Nanotubes in Liquids. *J Dispersion Sci Technol* 2003;24(1):1–41. <https://doi.org/10.1081/DIS-120017941>.
- [151] Dresel A, Teipel U. Dispergierung und Eigenschaften von Carbon Nanotubes. *Chem Ing Tech* 2016;88(7):857–63. <https://doi.org/10.1002/cite.201500168>.
- [152] Chen H, Jacobs O, Wu W, Rüdiger G, Schädel B. Effect of dispersion method on tribological properties of carbon nanotube reinforced epoxy resin composites. *Polym Test* 2007;26(3):351–60. <https://doi.org/10.1016/j.polymertesting.2006.11.004>.
- [153] Huang YY, Ahir SV, Terentjev EM. Dispersion rheology of carbon nanotubes in a polymer matrix. *Phys. Rev. B* 2006;73(12). <https://doi.org/10.1103/PhysRevB.73.125422>.
- [154] Wehnert F, Pötschke P, Jansen I. Hotmelts with improved properties by integration of carbon nanotubes. *Int J Adhes Adhes* 2015;62:63–8. <https://doi.org/10.1016/j.ijadhadh.2015.06.014>.
- [155] Huang YY, Marshall JE, Gonzalez-Lopez C, Terentjev EM. Variation in Carbon Nanotube Polymer Composite Conductivity from the Effects of Processing, Dispersion, Aging and Sample Size. *Mater Express* 2011;1(4):315–28. <https://doi.org/10.1166/mex.2011.1033>.

- [156] Ma P-C, Siddiqui NA, Marom G, Kim J-K. Dispersion and functionalization of carbon nanotubes for polymer-based nanocomposites: A review. *Composites, Part A* 2010;41(10):1345–67. <https://doi.org/10.1016/j.compositesa.2010.07.003>.
- [157] Lu KL, Lago RM, Chen YK, Green M, Harris P, Tsang SC. Mechanical damage of carbon nanotubes by ultrasound. *Carbon* 1996;34(6):814–6. [https://doi.org/10.1016/0008-6223\(96\)89470-X](https://doi.org/10.1016/0008-6223(96)89470-X).
- [158] Schilde C, Mages-Sauter C, Kwade A, Schuchmann HP. Efficiency of different dispersing devices for dispersing nanosized silica and alumina. *Powder Technol* 2011;207(1-3):353–61. <https://doi.org/10.1016/j.powtec.2010.11.019>.
- [159] Datsyuk V, Kalyva M, Papagelis K, Parthenios J, Tasis D, Siokou A et al. Chemical oxidation of multiwalled carbon nanotubes. *Carbon* 2008;46(6):833–40. <https://doi.org/10.1016/j.carbon.2008.02.012>.
- [160] Díez-Pascual AM. Chemical Functionalization of Carbon Nanotubes with Polymers: A Brief Overview. *Macromol* 2021;1(2):64–83. <https://doi.org/10.3390/macromol1020006>.
- [161] Buschhorn ST, Wichmann, Malte H. G., Sumfleth J, Schulte K, Pegel S, Kasaliwal GR et al. Charakterisierung der Dispersionsgüte von Carbon Nanotubes in Polymer-Nanokompositen. *Chem Ing Tech* 2011;83(6):767–81. <https://doi.org/10.1002/cite.201100046>.
- [162] Al-Saleh MH, Sundararaj U. A review of vapor grown carbon nanofiber/polymer conductive composites. *Carbon* 2009;47(1):2–22. <https://doi.org/10.1016/j.carbon.2008.09.039>.
- [163] Heintz SC. Über die Auswirkung von Scherbelastung auf das rheologische und elektrische Verhalten von Kohlenstoffnanoröhrchen / Epoxid Suspensionen [Dissertation]. Hamburg: Technische Universität Hamburg-Harburg; 2012.
- [164] Schüler R, Petermann J, Schulte K, Wentzel H-P. Agglomeration and Electrical Percolation Behavior of Carbon Black Dispersed in Epoxy Resin. *J. Appl. Polym. Sci.* 1997;63:1741–6.
- [165] Zhang R, Dowden A, Deng H, Baxendale M, Peijs T. Conductive network formation in the melt of carbon nanotube/thermoplastic polyurethane composite. *Compos Sci Technol* 2009;69(10):1499–504. <https://doi.org/10.1016/j.compscitech.2008.11.039>.
- [166] Wu G, Asai S, Zhang C, Miura T, Sumita M. A delay of percolation time in carbon-black-filled conductive polymer composites. *J. Appl. Phys.* 2000;88(3):1480. <https://doi.org/10.1063/1.373843>.
- [167] Skipa T, Lellinger D, Böhm W, Saphiannikova M, Alig I. Influence of shear deformation on carbon nanotube networks in polycarbonate melts: Interplay between build-up and destruction of agglomerates. *Polymer* 2010;51(1):201–10. <https://doi.org/10.1016/j.polymer.2009.11.047>.
- [168] Alig I, Skipa T, Engel M, Lellinger D, Pegel S, Pötschke P. Electrical conductivity recovery in carbon nanotube–polymer composites after transient shear. *phys. stat. sol. (b)* 2007;244(11):4223–6. <https://doi.org/10.1002/pssb.200776138>.

- [169] Buschhorn ST, Wichmann, Malte H. G., Gehrman J, Böger L, Schulte K. Direction sensitive deformation sensing with CNT/epoxy nanocomposites. In: International Committee on Composite Materials, editor. ICCM-17; 2009.
- [170] Hernández-López S, Viguera-Santiago E, Mayorga-Rojas M, Reyes-Contreras D. Thickness effect on electric resistivity on polystyrene and carbon black- based composites. J Phys Conf Ser 2009;167:12059. <https://doi.org/10.1088/1742-6596/167/1/012059>.
- [171] Ho L-N, Nishikawa H. Influence of post-curing and coupling agents on polyurethane based copper filled electrically conductive adhesives. J Mater Sci.: Mater Electron 2013;24(6):2077–81. <https://doi.org/10.1007/s10854-012-1059-0>.
- [172] Gupta VB, Drzal LT, Lee CY-C, Rich MJ. The temperature-dependence of some mechanical properties of a cured epoxy resin system. Polym. Eng. Sci. 1985;25(13):812–23. <https://doi.org/10.1002/pen.760251305>.
- [173] Richter K, Pizzi A, Despres A. Thermal stability of structural one-component polyurethane adhesives for wood—structure-property relationship. J. Appl. Polym. Sci. 2006;102(6):5698–707. <https://doi.org/10.1002/app.25084>.
- [174] Harrington JJ. Hierarchical modelling of softwood hygro-elastic properties. University of Canterbury. Mechanical Engineering; 2002.
- [175] Smith I, Landis E, Gong M. Fracture and Fatigue in Wood. West Sussex: Wiley-VCH; 2003.
- [176] Keylwerth R. Die anisotrope Elastizität des Holzes und der Lagenhölzer. VDI-Forschungsheft, Beilage zu Band 172 von Forschung auf dem Gebiete des Ingenieurwesens: Ausgabe B 1951(Band 430).
- [177] Baensch F. Damage evolution in wood and layered wood composites monitored in situ by acoustic emission, digital image correlation and synchrotron based tomographic microscopy [Dissertation]: ETH Zürich; 2015.
- [178] Schniewind AP (ed.). Concise encyclopedia of wood & wood-based materials. Oxford: Pergamon Press; 1989.
- [179] Niemz P, Sonderegger WU. Wood Physics (Holzphysik - Physik des Holzes und der Holzwerkstoffe). Munich: Fachbuchverlag Leipzig (Carl Hanser); 2017.
- [180] McKinley PE, Ching DJ, Kamke FA, Zauner M, Xiao X. Micro X-Ray computed tomography of adhesive bonds in wood. Wood and Fibre Science 2016(48):2–16.
- [181] Fengel D, Wegener G. Wood: Chemistry, Ultrastructure, Reactions. Berlin/New York: de Gruyter; 1983.
- [182] Schaumburg H. Sensoren. Wiesbaden: Vieweg+Teubner Verlag; 1992.
- [183] Katz AR, Miller DG. Effect of water storage on electrical resistance of wood. For Prod J 1963;XIII(7):255–9.
- [184] Skaar C. Wood-water relations. New York, Berlin: Springer-Vlg; 1988.
- [185] Tiitta M. Non-destructive methods for characterisation of wood material [Dissertation]. Kuopio: University of Kuopio.
- [186] Zelinka SL, Stone DS, Rammer DR. Equivalent circuit modeling of wood at 12% moisture content. Wood Fiber Sci 2007;39(4):556–65.
- [187] Torgovnikov GI. Dielectric properties of wood and wood-based materials. Berlin Heidelberg: Springer; 2012.

- [188] Stamm AJ. Wood and Cellulose Science. New York: The Ronald Press Company; 1964.
- [189] Robert J. Ross. Wood handbook - Wood as an engineering material. Madison, WI: Centennial ed. General technical report FPL; 2010.
- [190] Vermaas HF. A Summary of Literature References of Factors Affecting Moisture Content Determination with D.C. Resistance Measurements. South African Forestry Journal 1975;95(1):35–6. <https://doi.org/10.1080/00382167.1975.9629777>.
- [191] Wheat DL, Kallivokas LF, Garza C. Forward and Inverse Modeling of Piezoelectric Effects in Wood; 2006; Available from: [http://www.ewpa.com/Archive/2006/aug/Paper\\_277.pdf](http://www.ewpa.com/Archive/2006/aug/Paper_277.pdf).
- [192] Nakai T, Yamamoto H, Nakao T, Hamatake M. Mechanical behavior of the crystalline region of wood and the piezo response of wood in tension tests. Wood Sci Technol 2005;39(2):163–8.
- [193] Niemz P, Lühmann A, Wagner J. Orientierende Untersuchungen zur Ermittlung ausgewählter piezoelektrischer Konstanten an Holz. Holz Roh Werkst 1992;50:484.
- [194] Fukada E. Piezoelectricity as a fundamental property of wood. Wood Sci Technol 1968;2(4):299–307. <https://doi.org/10.1007/BF00350276>.
- [195] Ross RJ, Kan J, Wang X, Blankenburg J, Stockhausen JI, Pellerin RF. Wood and Wood-Based Materials as Sensors—A Review of the Piezoelectric Effect in Wood: General Technical Report FPL–GTR–212. Madison Wisconsin; 2012.
- [196] Tichý J, Erhart J, Kittinger E, Přivratská J. Fundamentals of Piezoelectric Sensorics. Berlin Heidelberg: Springer Berlin Heidelberg; 2010.
- [197] Sun J, Guo H, Schädli GN, Tu K, Schär S, Schwarze FW et al. Enhanced mechanical energy conversion with selectively decayed wood. Sci. Adv. 2021;7(11):eabd9138. <https://doi.org/10.1126/sciadv.abd9138>.
- [198] Fortino S, Hradil P, Metelli G. Moisture-induced stresses in large glulam beams. Case study: Vihantasalmi Bridge. Wood Material Science & Engineering 2019;14(5):366–80. <https://doi.org/10.1080/17480272.2019.1638828>.
- [199] Dietsch P, Franke S, Franke B, Gamper A, Winter S. Methods to determine wood moisture content and their applicability in monitoring concepts. J Civ Struct Health Monit 2015;5(2):115–27. <https://doi.org/10.1007/s13349-014-0082-7>.
- [200] Angst V, Malo KA. The effect of climate variations on glulam—an experimental study. Holz Roh Werkst 2012;70(5):603–13. <https://doi.org/10.1007/s00107-012-0594-y>.
- [201] Hoadley RB. Understanding Wood: A Craftsman's Guide to Wood Technology. Taunton Press; 1990.
- [202] Kollmann F. Technologie des Holzes und der Holzwerkstoffe. Berlin: Springer; 1982.
- [203] Gereke T. Moisture-induced stresses in cross-laminated wood panels [Dissertation]: ETH Zürich; 2009.
- [204] Wimmer R, Kläusler O, Niemz P. Water sorption mechanisms of commercial wood adhesive films. Wood Science and Technology, 47(4), 763–775. Wood Sci Technol 2013;47(4):763–75. <https://doi.org/10.1007/S00226-013-0538-7>.

- [205] Konnerth J, Stöckel F, Müller U, Gindl W. Elastic properties of adhesive polymers. III. Adhesive polymer films under dry and wet conditions characterized by means of nanoindentation. *J. Appl. Polym. Sci.* 2010;53:n/a-n/a. <https://doi.org/10.1002/app.32342>.
- [206] Klaesler O, Clauß S, Lübke L, Trachsel J, Niemz P. Influence of moisture on stress-strain behaviour of adhesives used for structural bonding of wood. *Int J Adhes Adhes* 2013;44:57–65. <https://doi.org/10.1016/j.ijadhadh.2013.01.015>.
- [207] Bockel S, Harling S, Grönquist P, Niemz P, Pichelin F, Weiland G et al. Characterization of wood-adhesive bonds in wet conditions by means of nanoindentation and tensile shear strength. *Holz Roh Werkst* 2020;78(3):449–59. <https://doi.org/10.1007/s00107-020-01520-1>.
- [208] Clerc G, Lüthi T, Niemz P, van de Kuilen JWG. Reaction kinetics investigation in relation to the influence of humidity on fatigue behavior of wood lap joints. *Holzforschung*, 0(0). *Holzforschung* 2020;74(9):865–80. <https://doi.org/10.1515/HF-2019-0136>.
- [209] Clerc G, Brülisauer M, Affolter S, Volkmer T, Pichelin F, Niemz P. Characterization of the ageing process of one-component polyurethane moisture curing wood adhesive. *Int J Adhes Adhes* 2017;72:130–8. <https://doi.org/10.1016/j.ijadhadh.2016.09.008>.
- [210] Blaß HJ, Frese M. Schadensanalyse von Hallentragwerken aus Holz; 2010.
- [211] Frese M, Grün A-K, Blaß HJ. Schäden an Hallentragwerken aus Holz Beschreibung - Ursachen - Vermeidung. Karlsruhe; 2015.
- [212] EN 302-1: Adhesives for load-bearing timber structures. Test methods. Determination of longitudinal tensile shear strength (April 2013).
- [213] Konnerth J, Gindl W, Harm M, Müller U. Comparing dry bond strength of spruce and beech wood glued with different adhesives by means of scarf- and lap joint testing method. *Eur J Wood Wood Prod* 2006;64(4):269–71. <https://doi.org/10.1007/s00107-006-0104-1>.
- [214] Konnerth J, Gindl W. Observation of the influence of temperature on the mechanical properties of wood adhesives by nanoindentation. *Holzforschung* 2008;62(6):71. <https://doi.org/10.1515/HF.2008.108>.
- [215] Konnerth J, Jäger A, Eberhardsteiner J, Müller U, Gindl W. Elastic properties of adhesive polymers. II. Polymer films and bond lines by means of nanoindentation. *J. Appl. Polym. Sci.* 2006;102(2):1234–9. <https://doi.org/10.1002/app.24427>.
- [216] Viljugrein T. Rheological methods to simulate adhesive properties for the wood working industry. In: Forest Products Society, editor. The International Conference on Wood Adhesives; 2013.
- [217] Kollmann F. Rheologie und Strukturfestigkeit von Holz. *Holz Roh Werkst* 1961;19(3):73–80. <https://doi.org/10.1007/BF02609517>.
- [218] Winkler C, Schwarz U, Senge B. Materialwissenschaftliche Analyse des Abbindeverhaltens von Holzklebstoffen am Beispiel von 1K-PUR. *Chem Ing Tech* 2020;92(6):759–68. <https://doi.org/10.1002/cite.201900171>.

- [219] Winkler C, Senge B, Schwarz U. Rheology of Industrial and Electrical Modified Structural Wood Adhesives after Production and Storage. In: Forest Products Society, editor. International Conference on Wood Adhesives; 2017.
- [220] Winkler C, Rodriguez Agudo JA, Schwarz U, Schäffler M. Process-Oriented Rheology of Packaging Adhesives. *Adhes Adhes Sealants* 2021;18(2):19–24. <https://doi.org/10.1007/s35784-021-0359-2>.
- [221] Department of Defence. MIL-STD-883E: Test Method Standard Microcircuits.
- [222] Small DJ. Reliability Considerations of Electrically Conductive Adhesives: Technical Paper (Loctite Electronics); 1999.
- [223] Schäfer J. Konzeption einer reproduzierbaren impedanzspektroskopischen Vermessungstechnik leitfähiger Klebstofffugen in quasistatisch belasteten Holzbauteilen [Bachelor-Thesis]. Eberswalde: Hochschule für nachhaltige Entwicklung Eberswalde; 2020.
- [224] Mühl T. Einführung in die elektrische Messtechnik. Teubner; 2006.
- [225] Funke K. Jump relaxation in solid electrolytes. *Prog Solid State Chem* 1993;22(2):111–95. [https://doi.org/10.1016/0079-6786\(93\)90002-9](https://doi.org/10.1016/0079-6786(93)90002-9).
- [226] Macdonald JR. Impedance spectroscopy. *Ann Biomed Eng* 1992;20(3):289–305. <https://doi.org/10.1007/BF02368532>.
- [227] Joffe EB, Lock K-S. Grounds for grounding: A circuit-to-system handbook. Hoboken, New Jersey, Piscataway, New Jersey: Wiley IEEE Press; IEEE Xplore; 2010.
- [228] Bulst M. Impedance Spectroscopy Basics: Choosing the Instrumentation. In: Gruden R, Schweiger B, Pliquet U, Carminati M, Büschel P, Strunz W et al., editors. Advanced School on Impedance Spectroscopy (ASIS). Chair for Measurement and Sensor Technology; 2017, p. 199–217.
- [229] Strunz W. Consistency Check of Impedance Spectra. In: Gruden R, Schweiger B, Pliquet U, Carminati M, Büschel P, Strunz W et al., editors. Advanced School on Impedance Spectroscopy (ASIS). Chair for Measurement and Sensor Technology; 2017, p. 127–155.
- [230] Paredes-Madrid L, Matute A, Bareño JO, Parra Vargas CA, Gutierrez Velásquez EI. Underlying Physics of Conductive Polymer Composites and Force Sensing Resistors (FSRs). A Study on Creep Response and Dynamic Loading. *Materials (Basel)* 2017;10(11). <https://doi.org/10.3390/ma10111334>.
- [231] Heimann M. Einsatz von Carbon Nanotubes in Aufbau- und Verbindungsstrukturen. Templin: Verlag Detert; 2010.
- [232] Park W-T. Piezoresistivity. In: Bhushan B, editor. Encyclopedia of Nanotechnology. Dordrecht: Springer; 2012, p. 2111–2117.
- [233] Clauß S, Allenspach K, Gabriel J, Niemz P. Improving the thermal stability of one-component polyurethane adhesives by adding filler material. *Wood Sci Technol* 2011;45(2):383–8. <https://doi.org/10.1007/s00226-010-0321-y>.
- [234] Afolabi AS, Sadare OO, Daramola MO. Effect of dispersion method and CNT loading on the quality and performance of nanocomposite soy protein/CNTs adhesive for wood application. *Adv Nat Sci.: Nanosci Nanotechnol* 2016;7(3):35005. <https://doi.org/10.1088/2043-6262/7/3/035005>.

- [235] Sadare OO, Daramola MO, Afolabi AS. Synthesis and performance evaluation of nanocomposite soy protein isolate/carbon nanotube (SPI/CNTs) adhesive for wood applications. *Int J Adhes Adhes* 2020;100:102605. <https://doi.org/10.1016/j.ijadhadh.2020.102605>.
- [236] Moya R, Rodríguez-Zúñiga A, Vega-Baudrit J. Effects of Adding Multiwall Carbon Nanotubes on Performance of Polyvinyl Acetate and Urea-Formaldehyde Adhesives in Tropical Timber Species. *J Nanomater* 2015;Vlome 2015(Article ID 895650):15 pages. <https://doi.org/10.1155/2015/895650>.
- [237] Khan T, Irfan MS, Ali M, Dong Y, Ramakrishna S, Umer R. Insights to low electrical percolation thresholds of carbon-based polypropylene nanocomposites. *Carbon* 2021;176:602–31. <https://doi.org/10.1016/j.carbon.2021.01.158>.
- [238] Sandler J, Kirk JE, Kinloch IA, Shaffer M, Windle AH. Ultra-low electrical percolation threshold in carbon-nanotube-epoxy composites. *Polymer* 2003;44(19):5893–9. [https://doi.org/10.1016/S0032-3861\(03\)00539-1](https://doi.org/10.1016/S0032-3861(03)00539-1).
- [239] Carbon Nanofibers PR-25-XT-HHT, information on <https://www.sigmaaldrich.com/DE/de/product/aldrich/719803?context=product>. [October 05, 2021].
- [240] Carbon Nanotubes NC 7000, information on <https://www.nanocyl.com/download/tds-nc7000/>. [October 05, 2021].
- [241] Winkler C, Konopka S. Zwischenbericht 2020 zum Projekt SmartTimbA: available by request (ulrich.schwarz@hnee.de); 2020.
- [242] Vadlamani VK, Chalivendra VB, Shukla A, Yang S. Sensing of damage in carbon nanotubes and carbon black-embedded epoxy under tensile loading. *Polym Compos* 2012;33(10):1809–15. <https://doi.org/10.1002/pc.22326>.
- [243] Köckritz T, Wehnert F, Pap J-S, Jansen I. Increasing the Electrical Values of Polydimethylsiloxane by the Integration of Carbon Black and Carbon Nanotubes: A Comparison of the Effect of Different Nanoscale Fillers. *J Adhes Soc Jpn* 2015;51(s1):221–2. <https://doi.org/10.11618/adhesion.51.221>.
- [244] Lerche D, Sobisch T. Direct and Accelerated Characterization of Formulation Stability. *J Dispersion Sci Technol* 2011;32(12):1799–811. <https://doi.org/10.1080/01932691.2011.616365>.
- [245] Feng D, Liu P, Wang Q. Exploiting the piezoresistivity and EMI shielding of polyetherimide/carbon nanotube foams by tailoring their porous morphology and segregated CNT networks. *Composites, Part A* 2019;124:105463. <https://doi.org/10.1016/j.compositesa.2019.05.031>.
- [246] Weiß K. Ein ortsauflösendes taktiles Sensorsystem für Mehrfinger-Greifer [Dissertation]: Universität Fridericiana zu Karlsruhe (TH).
- [247] Gere JM, Timoshenko SP. *Mechanics of Materials*. Boston: PWS-KENT Publishing Company; 1984.
- [248] Carminati M. *Advances in High-Resolution Microscale Impedance Sensors*. *J Sens* 2017;2017:1–15. <https://doi.org/10.1155/2017/7638389>.
- [249] Mei H, Zhang C, Wang R, Feng J, Zhang T. Impedance characteristics of surface pressure-sensitive carbon black/silicone rubber composites. *Sens Actuators, A* 2015;233:118–24. <https://doi.org/10.1016/j.sna.2015.06.009>.



- [250] Wang S-L, Wang P, Ding T-H. Piezoresistivity of silicone-rubber/carbon black composites excited by Ac electrical field. *J. Appl. Polym. Sci.* 2009;113(1):337–41. <https://doi.org/10.1002/app.29685>.
- [251] Bregar T, An D, Gharavian S, Burda M, Durazo-Cardenas I, Thakur VK et al. Carbon nanotube embedded adhesives for real-time monitoring of adhesion failure in high performance adhesively bonded joints. *Sci Rep* 2020;10(1):16833. <https://doi.org/10.1038/s41598-020-74076-y>.
- [252] Winkler C, Schwarz U. SHM capabilities of modified wood adhesives for timber structures. In: *ASNT - The American Society for Nondestructive Testing*, editor. *ASNT's 23rd Annual Research Symposium*; 2014.
- [253] Konnerth J, Müller U, Gindl W, Buksnowitz C. Reliability of wood adhesive bonds in a 50 year old glider construction. *Eur J Wood Wood Prod* 2012;70(1-3):381–4. <https://doi.org/10.1007/s00107-011-0536-0>.
- [254] Muller U, Müller H, Teischinger A. Durability of wood adhesives in 50 year old aircraft and glider constructions. *Wood Research - Drevarsky Vyskum* 2004;49(3):25–33.
- [255] Caneba GT, Axland J. Electrical And Thermal Coatings From A Single-Walled Carbon Nanotube (SWCNT)/Polymer Composite. *JMMCE* 2004;03(02):73–80. <https://doi.org/10.4236/jmmce.2004.32008>.
- [256] Szycher M. *Szycher's handbook of polyurethanes*. 2nd ed. Boca Raton, FL: CRC Press; 2013.
- [257] Xiang D, Liu M, Chen G, Zhang T, Liu L, Liang Y. Optimization of mechanical and dielectric properties of poly(urethane–urea)-based dielectric elastomers via the control of microstructure. *RSC Adv.* 2017;7(88):55610–9. <https://doi.org/10.1039/C7RA11309A>.
- [258] Kanoun O. Impedance spectroscopy advances and future trends: A comprehensive review. In: Kanoun O, editor. *Impedance Spectroscopy: Advanced Applications: Battery Research, Bioimpedance, System Design*. de Gruyter; 2019, p. 1–21.
- [259] Adams RD, Brearley T, Liu L. Adhesives and joints under the combined attack of moisture and stress. In: *EURADH - 9th European Adhesion Conference*; 2012.

## ADDITIONAL PUBLICATIONS AND OTHER CONTRIBUTIONS

### Peer-reviewed paper

**Winkler C**, Schwarz U, Senge B. Materialwissenschaftliche Analyse des Abbindeverhaltens von Holzklebstoffen am Beispiel von 1K-PUR. Chemie Ingenieur Technik 2020;92(6):759–68. <https://doi.org/10.1002/cite.201900171>

### Conference contributions

**Winkler C**, Schwarz U. Einfluss der elektrisch leitfähigen Füllstoffe auf die Klebfestigkeit von Schichtholzverbünden. In: 3. Kooperationsforum: Kleben von Holz und Holzwerkstoffen; Würzburg; 21./22.06.2017.

Myslicki, S, **Winkler, C**, Gelinski N, Schwarz U, Walther F. Fatigue assessment of adhesive wood joints through physical measuring technologies. In: Fatigue 2017: 7th International Conference on Durability and Fatigue, p. 446–455.

**Winkler C**, Gibcke J, Senge B, Schwarz U. Multifunctional adhesives for engineered timber: Structure changes during fluid processing and storage. In: Abstract book: International Workshop on Impedance Spectroscopy, IWIS 2017 September 26-29, 2017. Chemnitz: Chair for Measurement and Sensor Technology, Technische Universität Chemnitz; 2017.

**Winkler C**, Senge B, Schwarz U. Rheology of Industrial and Electrical Modified Structural Wood Adhesives after Production and Storage. In: Forest Products Society, editor. International Conference on Wood Adhesives; 2017.

**Winkler C**, Schwarz U, Konnerth J. Effect of a thermal postcure on the micro- and macromechanical properties of polyurethane bonded wood. In: EURADH 2018 - 11th European Adhesion Conference; 2018, Lissabon. 5.-7.9.2018.

**Winkler C**, Konnerth J, Gibcke J, Schwarz U. Influence of polymer/filler composition and processing on the properties of multifunctional adhesive wood bonds from polyurethane prepolymers I: Mechanical properties. In: da Silva, Lucas F. M., editor. 5th International Conference on Structural Adhesive Bonding (AB2019); 2019, Porto. 11.-12.07.2019.

**Winkler C**, Konnerth J, Gibcke J, Schwarz U. Influence of polymer/filler composition and processing on the properties of multifunctional adhesive wood bonds from polyurethane prepolymers II: Electrical properties. In: da Silva, Lucas F. M., editor. 5th International Conference on Structural Adhesive Bonding (AB2019); 2019, Porto. 11.-12.07.2019.

**Winkler C**, Schwarz U (2021) Challenges of applying impedance spectroscopy to characterize electrical conductive wood adhesives. In: IWIS 2021 - 14th International Workshop on Impedance Spectroscopy, pp 146–149

**Winkler C**, Steinhäuser D, Schwarz U et al. (2021) Piezoresistive adhesives in timber constructions. In: EURADH 2021 - 11th European Adhesion Conference

**Winkler C**, Teischinger A, Simon A et al. (2021) Challenges for the use of piezoresistive adhesives in anisotropic materials like timber. In: EURADH 2021 - 11th European Adhesion Conference

#### Other publications

Agudo JR, **Winkler C**, Schäffler M (2020) Ein rheologischer Multi-Task Versuch für die Charakterisierung in der Klebstoff-Anwendungstechnik. Application Report C92IA060DE-A.

**Winkler C**, Agudo JR, Schäffler M (2020) Rheologische Charakterisierung der Vernetzung feuchtereaktiver Polyurethan-Prepolymere. Application Report C92IA053DE-A.

**Winkler C**, Schwarz U, Koch K-U. Sensorische Klebstoffe für die Bauwerksüberwachung im Ingenieurholzbau. bmH bauen mit Holz 2021;01/2021(01):28–32.

**Winkler C**, Rodriguez Agudo JA, Schwarz U, Schäffler M. Process-Oriented Rheology of Packaging Adhesives. Adhes Adhes Sealants 2021;18(2):19–24. <https://doi.org/10.1007/s35784-021-0359-2>.

#### Supervised theses associated with thesis

Horber J. Die elektrischen Eigenschaften des Holzes: Einflüsse auf die elektrischen Messgrößen und die sensorische und messtechnische Darstellung [Diplomarbeit]: Hochschule für nachhaltige Entwicklung Eberswalde; 2018.

Gibcke J. Herstellung von leitfähigen 1-komponentigen Polyurethan – Klebstoffmischungen [Bachelorarbeit]. Eberswalde: Hochschule für nachhaltige Entwicklung Eberswalde; 2018.

Schäfer J. Konzeption einer reproduzierbaren impedanzspektroskopischen Vermessungstechnik leitfähiger Klebstofffugen in quasistatisch belasteten

Holzbauteilen [Bachelorarbeit]. Eberswalde: Hochschule für nachhaltige Entwicklung Eberswalde; 2020.

Schwartpaul T. Untersuchung von Maßnahmen zur Verbesserung der geometrischen Bestimmtheit von elektrisch leitfähigen Klebefugen an Holz und Holzwerkstoffen [Bachelorarbeit]. Eberswalde: Hochschule für nachhaltige Entwicklung Eberswalde; 2020.

Haase S. Messung mechanischer Spannungen in Holz durch elektrisch leitfähige Polyurethan-Klebstofffugen [Bachelorarbeit]. Eberswalde: Hochschule für nachhaltige Entwicklung Eberswalde; 2020.

Steinhäuser D. Entwicklung sensitiver Klebefugen auf Epoxidharzbasis zur Herstellung und Sanierung von Brettschichtholzträgern [Masterarbeit]. Erfurt: Fachhochschule Erfurt; 2020.

Fuchs M. Darstellung von Feuchte- und Dehnungsänderungen an multifunktional verklebtem Holz mittels Impedanzspektroskopie [Bachelorarbeit]. Eberswalde: Hochschule für nachhaltige Entwicklung Eberswalde; 2021.

Vierheilig R. Entwicklung eines Versuchsstandes zur Analyse des Langzeitverhaltens elektrisch leitfähiger Holzklebstoffe unter freier Bewitterung [Bachelorarbeit]. Eberswalde: Hochschule für nachhaltige Entwicklung Eberswalde; 2021.

## NOMENCLATURE

1C-PUR	one-component polyurethane prepolymer
20/65	standard climate of 20 °C and 65 % relative humidity
AC	alternating current
CB	carbon black
C <sub>IT</sub>	creep factor from measurements by nanoindentation
CLT	cross-laminated timber
CNT	carbon nanotube
CNF	carbon nanofiber
DC	direct current
D <sub>c,DC</sub>	DC resistance drift under load
DEA	dielectric analysis
DMM	digital multimeter
DUT	device under test
DWNT	double wall carbon nanotubes
ECA	electrically conductive adhesive
ECF	electrically conductive filler
EIS	electrochemical impedance spectroscopy
EP	epoxy resin
EPI	emulsion-polymer-isocyanates
E <sub>r</sub>	reduced elastic modulus from measurements by nanoindentation
GF	gauge factor
GLT	glued laminated timber
H	hypothesis
MUF	melamine-urea-formaldehyde resin
MWNT	multiwall carbon nanotubes
PRF	phenol-resorcin-formaldehyde resin
PVAc	polyvinyl acetate glue
PU	polyurethane
R&D	research and development
rH	relative humidity
RQ	research question
SHM	structural health monitoring
SNR	signal-to-noise ratio
TSS	tensile shear strength
UF	urea-formaldehyde resin
VOC	volatile organic compound
WFP	wood failure percentage
WMC	wood moisture content

## **LIST OF TABLES**

Table 1	Dispersion techniques and criteria for their use in producing nanocomposites...17
---------	---

## LIST OF FIGURES

Fig. 1	Illustrations of highly structured carbon black and multi-walled nanotubes with a high aspect ratio according to electron micrographs. (a) Ketjenblack® EC-600JD (Akzonobel) with a specific surface area of 1,400 m <sup>2</sup> /g, and (b) Nanocyl® 7000 (Nanocyl Belgium) with an aspect ratio of 10–1,000 m/m. The images were reproduced and adapted from [74] together with the terms of particle morphology used in subsequent sections of the text. ....	7
Fig. 2	Scheme of a network of carbon black aggregates together with the changes in electrical resistance and capacity from which piezoresistivity originates in nanocomposites.....	13
Fig. 3	Overview of the manufacturing steps of a piezoresistive bond line with the assigned influencing parameters shear rate, temperature, pressure, and time.....	16
Fig. 4	Effect of carbon black aggregate dispersion and homogenisation inside an insulating polymeric matrix with (a) no dispersion and low homogenisation, (b) low dispersion and high homogenisation, (c) high dispersion and low homogenisation, and (d) high dispersion and high homogenisation. The X-direction gives a percolation threshold at lower filler concentration, while the Y-direction gives less mechanical degradation by fewer agglomerates.....	18
Fig. 5	Scheme of the hierarchical structure of coniferous wood with features leading to heterogenous density. The original design was taken from Harrington [174] and slightly changed and extended by Teischinger [3]. ....	21
Fig. 6	Polar diagram of Young's modulus of solid wood and different plywood structures according to Keylwerth [176], modified by Baensch [177]. ....	22
Fig. 7	Cross-section of an electrically conductive bond line between two adherends from beech ( <i>Fagus sylvatica</i> L.) (a) and pine ( <i>Pinus sylvestris</i> L.) (b).....	23
Fig. 8	Example of a moisture gradient resulting from internal stresses in the drying stage and the subsequent potential for crack growth [201]. ....	25
Fig. 9	(a) Alternating voltage waveform for an applied potential and the resulting sinusoidal current under the influence of ohmic resistance, capacity, and inductivity, and (b) complex representation of impedance in vector format. ....	31
Fig. 10	Plateau and dispersive regimes of the real part in impedance spectroscopic measurements of electrically conductive adhesives. ....	32

Fig. 11	Scanning electron microscope (SEM) images of polyurethan prepolymer (1C-PUR) filled with 3.5 wt% Ketjenblack EC-300J films with a thickness of 100 $\mu\text{m}$ (A,B) and 500 $\mu\text{m}$ (C,D), not coated. Bright locations show relative higher conductivity (© Westphalian University of Applied Sciences, [241]) .....	46
Fig. 12	Electrical resistance under direct current of specimen (A), dependent on the length of the bond line made from beechwood ( <i>Fagus sylvatica</i> , L.) bonded with polyurethane prepolymer with (B) 2 wt% carbon nanofibers and 0.2 wt% carbon nanotubes added and (C) 4 wt% carbon black added (adapted from Winkler, Konopka [241]).....	49
Fig. 13	Drift of electrical resistance under load $D_{e,DC}$ over the mechanical creep factor $C_{IT}$ for polyurethane, filled with 4 wt% carbon black (A) and 2 wt% carbon nanofibers with added 0.2 wt% carbon nanotubes (B) .....	52